Bioinspired Strategies to Develop Dual-Functional Polymer-Based Antibacterial Coatings for Biomedical Applications

by

Adel S M Imbia

A thesis submitted in partial fulfillment of the requirements for the degree of

Doctor of Philosophy
in
Chemical Engineering

Department of Chemical and Materials Engineering
University of Alberta

Abstract

Biofilm, the accumulation of macromolecules or microorganisms on medical devices, has become a persistent problem in the medical field. Eradicating biofilm on the implantable device surface, especially biofouling in biological fluids, is a significant challenge. The surface becomes rapidly coated with proteins and other host molecules upon medical device insertion, providing a platform for bacterial attachment and subsequent biofilm formation. This can lead to antibiotic treatment or implant removal. A single-function coating strategy for bacteria killing or cell resistance is insufficient to combat biofilm for a long time. Therefore, developing strategies to endow the surface of medical devices with bactericidal and antifouling properties is highly desirable for preparing stable coatings for antibacterial activities. The nature-inspired coating technique, proposed as an innovative strategy, offers versatile adhesion on various substrates, coating simplicity under mild conditions, biocompatibility, and robust reactivity to bind polymer coatings covalently, enabling long-term use of the material. In this thesis work, the use of natural-inspired dual-function coatings using polyphenol chemistry of tannic acid (TA) and polydopamine (PDA) is explored as a novel approach to functionalize surfaces covalently with zwitterionic polymers, glycopolymers, and bactericidal agents for biomedical applications.

In the first project, a natural polyphenol tannic acid is used to functionalize surfaces with a zwitterionic polymer via robust covalent bonds in a straightforward method for flaunt resistance. Tannic acid was also used as a reducing agent to generate silver nanoparticles (AgNPs) for developing surfaces with bacteria-killing properties. To enhance the antifouling property and biocompatibility of the coating, the bioinspired zwitterionic 2-methacryloyloxyethyl phosphorylcholine (MPC) was copolymerized with 2-aminoethyl methacrylamide hydrochloride (AEMA) using conventional free radical polymerization. Through a Michael addition reaction,

the oxidized polyphenol groups of tannic acid enabled the co-deposition of the amino-containing copolymer with tannic acid. Subsequently, the resulting tannic acid/polymer-coated surfaces containing catechol groups generated silver nanoparticles (AgNPs) via the in-situ reduction of silver ions to impart antibacterial properties to the surface. The dual-function coatings demonstrated their effectiveness by showing antibacterial properties against E. coli and S. aureus and remarkably decreasing the adhesion of BSA protein. The as-prepared coating is potentially valuable for biomedical applications, providing a promising solution to the persistent problem of biofilm accumulation on medical devices.

The second project aims to develop a facile method by covalently grafting copolymers containing aldehyde to the amine groups of self-polymerized dopamine (PDA). Reversible addition-fragmentation chain transfer (RAFT) polymerization was used to copolymerize either zwitterionic 2-methacryloyloxyethyl phosphorylcholine monomer (MPC) or cationic 2-(methacryloyloxy)ethyl trimethylammonium monomer (META) with 4-formyl phenyl methacrylate monomer (FPMA). The two resulting copolymers [poly(MPC-*st*-FPMA) and poly(META-*st*-FPMA)] are denoted as MPF and MTF, respectively. MPF and MTF were then covalently grafted to the amino groups of polydopamine-coated surfaces by the dip-coating method. PDA/MPF/MTF-coated surfaces exhibited excellent antibacterial properties against *S. aureus* and *E. coli* and antifouling properties against bovine serum albumin (BSA) protein. The facile surface modification strategy discussed here is expected to be helpful in biomedical applications.

The third project developed a simple and environmentally friendly method to fabricate bifunctional metal-phenolic network-based coatings for biomedical applications using coordination chemistry between copper ions (Cu^{+2}) and glycopolymer-containing dopamine

methacrylamide (DMA). The monomers GAEMA and DMA were first synthesized and then copolymerized by free radical polymerization to obtain the statistical copolymer poly(GAEMA-*stat*-DMA) named GADMA. The GADMA copolymer and copper ions were deposited on the glass surfaces in a one-pot step to form a coordination complex of Cu^{+2} with catechol and amide groups, which imparted stability to the coating. The GADMA-Cu coating was hydrophilic and significantly reduced bovine serum albumin (BSA) protein adsorption even after shaking the coating in BSA solution for 30 h. Moreover, the coating exhibited strong antibacterial activity against *E. coli* and *S. aureus* and was biocompatible with 99% cell viability towards normal human fibroblast cells (HDFa). Thus, the developed coating could be very useful for medical devices.

Preface

This thesis is the original work of Adel S. Imbia under the supervision of Dr. Ravin Narain (Department of Chemical and Materials Engineering) at the University of Alberta.

Chapter 1 of the thesis briefly introduces previous studies exploring the antifouling and antibacterial coating strategies. It includes a part related to my contribution to the Click Chemistry in Hydrogels chapter in the book (Click Chemistry in Polymer Science: Designs to Applications) that will be published in the *Royal Society of Chemistry (RSC)*.

Chapter 2 in this thesis has been published as an article authorized by Adel S. Imbia, Artjima Ounkaew, Xiaohui Mao, Hongbo Zeng, Yang Liu, and Ravin Narain, Tannic Acid-Based Coatings Containing Zwitterionic Copolymers for Improved Antifouling and Antibacterial Properties in *Langmuir*, 2024, 40, 3549–3558. I was responsible for designing and performing the experiments and writing the manuscript for this project. Prof. Ravin Narain supervised the entire work and helped with the manuscript writing.

Chapter 3 of this thesis has been published in *Langmuir*, 2024, as Mussel-inspired Polymer-based Coating Technology for Antifouling and Antibacterial Properties**.** The publication was authorized by Adel S. Imbia, Artjima Ounkaew, Xiaohui Mao, Hongbo Zeng, Yang Liu, and Ravin Narain. I was responsible for synthesizing and characterizing monomers and polymers, analyzing experimental data, and composing the manuscript. Dr. Artjima Ounkaew helped with the biological experiments. Xiaohui Mao helped with surface characterization. Prof Ravin Narain provided expert insights and revised and edited the manuscript.

Chapter 4 of this thesis contains project 3 in my work, entitled Stable Antifouling and Antibacterial Coating Based on Assembly of Copper-Phenolic Networks. Adel S. Imbia, Artjima

Ounkaew, Hongbo Zeng, Yang Liu, and Ravin Narain authorized this project, which will be published shortly.

Chapter 5 provides a general conclusion, summarizing the major findings of this work and provides potential future studies to further improve the coating technology for antifouling and antibacterial surfaces specifically for biomedical technology.

.

Acknowledgments

I express my deepest gratitude to my supervisor, [Prof. Ravin Narain], for his guidance, support, and mentorship throughout my doctoral journey. His expertise, encouragement, and constructive feedback have been instrumental in shaping both my research and professional development. I am truly grateful for his dedication and belief in me. I am also profoundly grateful to my wife for her love, understanding, and patience during the highs and lows of this journey. Her support and encouragement have been my source of strength and motivation. I also thank my research group colleagues for their collaboration and exchange. Their insights and discussions have enriched my research experience and contributed to the success of my doctoral work. I am grateful for the cooperation of [Prof. Hongbo Zeng and Prof. Yang Liu] for their contributions, guidance, and willingness to share resources. Their expertise and collaboration have significantly enriched my research projects. Finally, I would like to acknowledge my colleague [Dr. Artjima Ounkaew] for her exceptional contributions, friendship, and support. Her dedication and enthusiasm have enriched my research experience and made a lasting impact on my academic journey. This thesis would not have been possible without these individuals' support, encouragement, and contributions; for that, I am profoundly grateful.

List of Contents

List of Figures

List of Tables

List of Schemes

List of Abbreviations

Abbreviation	Name
HAIs	Hospital-associated infections
LBL	Layer-by-layer
PDA	Polydopamine
TA	Tannic acid
PEG	Poly(ethylene glycol)
EO	Ethylene oxide
EPS	Exopolysaccharide
PDMS	Polydimethylsiloxane
PHEMA	Poly(2-hydroxyethyl methacrylate)
PAAm	Poly(acrylamide)
PMOXA	Poly(2- methyl-2-oxazoline)
PMPC	Poly(2-methacryloyloxyethylphosphorylcholine)
CMC	*o*-Carboxymethyl chitosan
PES	Polyethersulfone
LAEMA	2-Lactobionamidoethyl methacrylamide
GMA	Glycidyl methacrylate
BA	Isobornyl acrylate
GAEMA	2-Gluconamidoethyl methacrylamide
GAPMA	3-Gluconamidopropyl methacrylamide
QAC	Quaternary ammonium compounds
PAA	Poly(acrylic acid)

PDDA	Poly(dimethyldiallylammonium chloride)
ATRP	Atom transfer radical polymerization
RAFT	Reversible addition−fragmentation chain-transfer polymerization
SARA SI-ATRP	Surface-initiated atom-transfer radical polymerization
Q-PEI-MA	Qatarized polyethyleneimine methacrylate
PEGDMA	Polyethylene glycol dimethacrylate
MRSA	Methicillin-resistant *Staphylococcus aureus*
VRE	Vancomycin-resistant *Enterococcus faecalis*
SI-ARGET-ATRP	Surface-initiated activators regenerated by electron transfer atom-transfer radical polymerization
BSA	Bovine serum albumin
DMA	Dopamine methacrylamide
DMAEMA	2-(Dimethylamino)-ethyl methacrylate
GA	Gallic acid
DOPA	L-3,4-Dihydroxyphenylalanine
CB	Carboxylbetaine
SBMA	*N*-(3-sulfopropyl)-*N*-(methacryloxyethyl)-*N,N*-dimethylammonium betaine
PLYS	Polylysine
PNIPAM	Poly(N-isopropyl acrylamide)
AgNPs	Silver nanoparticles
AEMA	2-Aminoethyl methacrylamide hydrochloride

ACVA	4,4′-Azobis(4-cyano valeric acid)
BCA	Bicinchoninic acid
WCA	Water contact angle
^{1}H NMR	Proton nuclear magnetic resonance
GPC	Gel permeation chromatography
ATR-FTIR	Attenuated total reflectance Fourier transform infrared spectroscopy.
FESEM	Field Emission scanning electron microscopy
AFM	Atomic force microscopy
EDX	Bruker energy dispersive X-ray
DMEM	Dulbecco's Modified Eagle Medium
OD	Optical density
MTT	Thiazolyl blue tetrazolium bromide
MW	Molecular weight
META	2-(methacryloyloxy)ethyl trimethylammonium
E. Coli	*Escherichia coli*
eV	Electron volt
LB	Luria-Bertani broth
DMF	Dimethylformamide
CFU	Colony forming unit
$AgNO_3$	Silver nitrate
CuNPs	Copper nanoparticles
$Cu(SO_4)_2.5H_2O$	Copper sulfate pentahydrate

D_2O	Deuterium oxide
PP	Polypropylene
RMS	Root-mean-square
MRC-5	Normal human lung fibroblast cells
CTA	2-(1-carboxymethylethylsulfanylthiocarbonylsulfanyl) -2-methyl propionic acid
FPMA	4-formyl phenyl methacrylate
DA	Dopamine hydrochloride
PBS	Phosphate buffer solution
PDI	Polydispersity
DMSO-d6	Deuterated dimethyl sulfoxide
TS	Tryptic soy
S. aureus	*Staphylococcus aureus*
MPNs	Metal-phenolic networks
SDS	Sodium dodecyl sulfate
HDFa	Normal human fibroblast cells

List of Publications

1) **Adel S. Imbia**, Artjima Ounkaew, Xiaohui Mao, Hongbo Zeng, Yang Liu, and Ravin Narain, "Tannic Acid-Based Coatings Containing Zwitterionic Copolymers for Improved Antifouling and Antibacterial Properties", *Langmuir,* **2024,** *40* (7), pp 3549-3558

2) **Adel S. Imbia**, Artjima Ounkaew, Xiaohui Mao, Hongbo Zeng, Yang Liu, and Ravin Narain, "Mussel-inspired Polymer-based Coating Technology for Antifouling and Antibacterial Properties", *Langmuir*, **2024**.

3) **Adel S. Imbia**, Artjima Ounkaew, Hongbo Zeng, Yang Liu, and Ravin Narain, "Stable Antifouling and Antibacterial Coating Based on Assembly of Copper-Phenolic Networks", will be submitted in **2024**.

Chapter 1: General Introduction

1.1. General Introduction.

In the United States, hospital-associated infections (HAIs) are estimated to infect at least 2 million individuals and result in 23,000 deaths every year, costing USD 55 to 70 billion.[1] As the population of elderly people increases, the use of implantable medical devices is expected to increase worldwide annually. For example, the number of knee arthroplasty procedures is estimated to reach 1.26 million by 2030 in the United States alone.[2] HAIs often arise from biofilm formation on implantable devices such as biosensors, orthopedic implants, vascular stents, wound dressings, ocular devices, urinary catheters, dental implants, endotracheal tubes, and hospital textiles.[3,4] Upon medical device insertion, the surface becomes rapidly coated with proteins and other host molecules. This layer of adsorbed proteins can work as a platform for bacterial attachment and subsequent biofilm formation, which usually requires antibiotic treatment and negatively impacts the economy.[5,6] Even worse, the bacteria and other cells associated with forming biofilm matrix become significantly more antibiotic-resistant and often necessitate device removal, which increases the risk of patient mortality.[7–9] This developed antibiotic-resistant bacteria highlighted the need to fight biofilm by designing functional polymeric devices or coatings with antifouling and antibacterial properties as a potential solution to this global health issue. Because rendering bulk materials with antibacterial properties is impractical, the coating strategy has gained a lot of interest in endowing the device surface with dual-functional (antifouling and bactericidal) properties to prevent HAIs.[10,11] Polymer-based coatings are cheap, biocompatible, nontoxic, and can be easily modified, leading to tunable antibacterial functions while preserving the properties of bulk materials.[11] Various techniques have been widely used for polymeric coatings, such as sol-gel coatings,[12] layer-by-layer (LBL) assembly,[13] dip-coatings,[14] spin-coatings,[15] spray coatings,[16,17] plasma polymerization,[18] and

surface grafting.[19] Among these techniques, the dip-coating method has gained significant attention for surface functionalization due to its simplicity and suitability for polymer deposition at ambient conditions. However, the physical interactions between the polymeric layer and surface make it challenging to fabricate stable coatings. Hence, the fabrication of dual-functional coating with long-term stability via a robust approach is significant for modifying medical device surfaces. Owing to the complexity of biofilm, it is essential to inspire methods derived from biological systems and nature. Fortunately, researchers have developed an antibacterial strategy by mimicking the mussel adhesive proteins that inspired polydopamine (PDA) coatings because of their strong adhesive properties on various materials, including organic and inorganic substances.[20] Tannic acid (TA) coating is another promising way to endow the surface of materials with better coating adhesion and stability on all materials, including organic, inorganic, hydrophobic, hydrophilic, particles, and planner ones.[21–23] The oxidized catechol groups on polydopamine and tannic acid were used to reduce metals, like silver ions (Ag^{+}) and copper ions (Cu^{2+}), to form metal nanoparticles (AgNPs and CuNPs) *in situ*.[24–27] The abundance of catechol groups on TA and PDA also facilitated the coordination interactions between the hydroxyl groups and copper ions. It contributed to the formation of stable synergistic antibacterial and antifouling coatings.[28,29] Mussel- and plant-inspired coatings were developed based on the high reactivity of their catechol groups to promote selective covalent functionalization with polymers containing nucleophiles like amino and thiol groups in aqueous conditions and without additional initiators.[30–33] These bioinspired coatings are also biocompatible and universal and can be easily prepared for all organic and inorganic surfaces, making them powerful tools for surface modification. Hydrophilic polymers, such as zwitterionic polymers and poly(ethylene glycol) (PEG) polymers, are two common hydrophilic polymers employed for endowing surfaces with

antifouling properties. However, several researchers have demonstrated that PEG coatings can be susceptible to oxidative degradation and enzymatic cleavage over time, limiting their long-term antifouling durability, particularly in harsh conditions such as biological environments. PEG cleavage resulted in ethylene oxide (EO) subunits, which were finally converted into aldehyde-terminated chains, making them more attractive to the adsorption of amine-containing proteins.[34–36] PEG coatings are incompatible with some substrates and often require additional surface modifications, which can be costly when PEG is applied to larger substrates.[37,38] More importantly, PEG coatings show limited protein resistance at the temperature of the biological environment because PEG polymer may form a hydration layer via hydrogen bonds and easily lose its hydration layer, limiting their antifouling properties over long-term applications.[39] Therefore, zwitterionic polymers have been used as an alternative to PEG polymers due to their amphoteric nature, allowing them to form electrostatic interactions with water, which are much stronger than hydrogen bonds.[40] Zwitterionic polymers have been recognized as the next generation of promising antifouling materials because of the simplicity of synthesis and polymerization and the abundance of raw materials.[34] While such coatings can significantly reduce the adsorption of foulants, it is highly promising to fabricate synergistic coatings to repel and kill foulants for biomedical applications.

Polymer-based dual-functional coatings are expected to improve the comprehensive antibacterial function compared to the coatings function by either antifouling or bactericidal properties. However, bacteria can potentially adhere to and colonize surfaces due to the accumulation of dead bacteria and other debris on the coating surface, reducing the contact-active bactericidal efficacy.[41] Furthermore, the fast release rate of the release-killing agent may cause rapid depletion of bactericidal. In contrast, the high concentration of bactericidal agents will promote

cytotoxicity in an *in vivo* environment.[42] Hence, a dual-functional coatings strategy that can overcome the disadvantages of conventional strategies by killing bacteria and resisting foulants is needed. Considering all these facts, this thesis intends to develop hydrophilic polymer-based coatings with dual-functionality and high stability for potential biomedical applications.

1.2 Pathogenesis of Bacterial Biofilm Infection.

Biofilm is bacterial colonies enclosed in an extracellular polymeric substance matrix (EPS) and attached to foreign surfaces in a living organism. The initial adhesion of planktonic bacteria to the device surface commonly begins with nonspecific and reversible interactions such as hydrophobic and van der Waal's forces. The bacteria cells then undergo specific covalent binding and irreversible attachments. The adhered bacteria multiply and produce an extracellular polymeric substance matrix, followed by exopolysaccharide (EPS) colonization, which initiates biofilm formation (mature biofilm) on the surface. In the last step, some bacteria detach from mature biofilm and disperse again to start a new cycle of biofilm formation. In biomedical devices, after implanting the device in the body, molecules like proteins and polysaccharides immediately adhere to the device surface, forming a thin layer of conditioning film, which works as a platform for bacteria attachment and biofilm formation (**Scheme 1.1).**[43–45] Biological factors like extreme temperature, high pH, limited nutrients, high salt, and antimicrobial agent concentration can trigger biofilm development.[46–48] In addition to biological conditions, biofilm formation can be influenced by the hydrophobicity and charge of the device surface that affect the interactions between bacteria and the surface. Since the bacteria cells are often hydrophobic and negatively charged, hydrophobic and positively charged surfaces are more prone to colonization than those with high hydrophilicity and negative charges. These interactions are proposed to be through hydrophobic-hydrophobic interactions or by electrostatic force

attraction.[49,50] As a result, it is practical in biomedical applications to use an antifouling coating strategy to inhibit protein adsorption and bacteria cell adhesion and a bactericidal coating strategy to kill the bacteria.

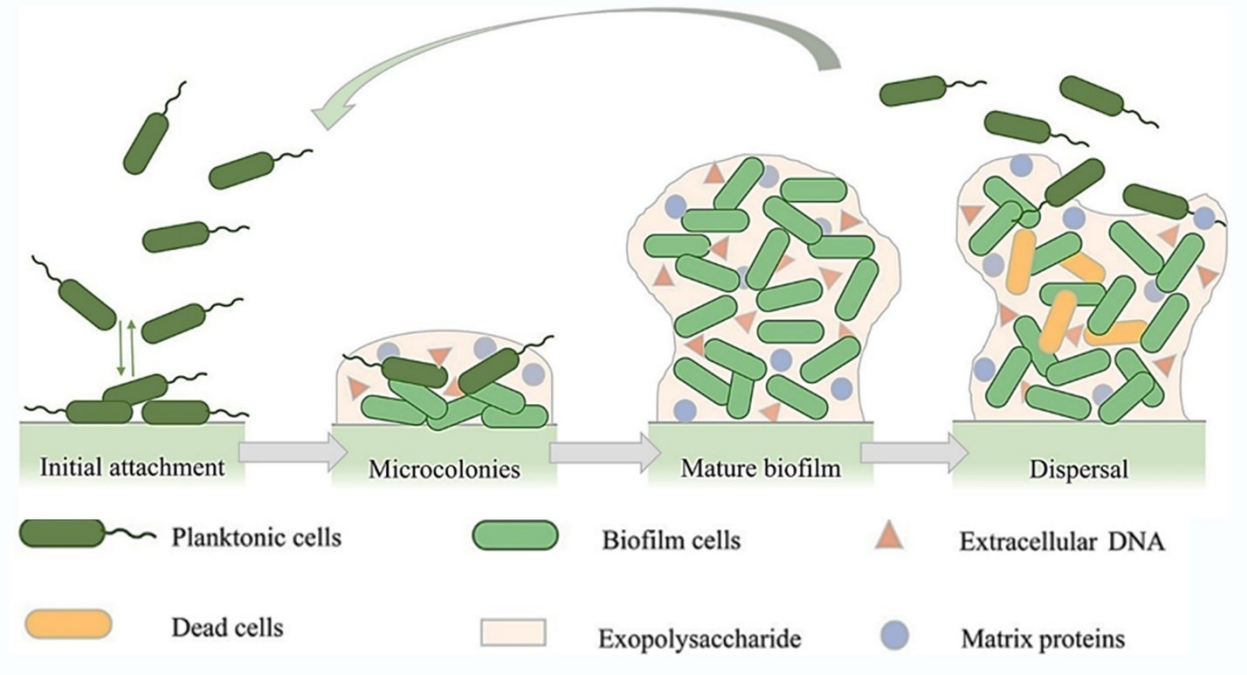

Scheme 1.1. Stages of biofilm formation reprinted with permission from ref.[51]

1.3. Strategies for Antifouling and Bactericidal Coatings.

1.3.1. Antifouling Coating Strategies.

The polymer-based coating strategies for medical device surfaces can be either fouling-resistant or fouling-release, depending on the modification of surface chemistry, topography, and architecture. The antifouling ability of the former is related to high interfacial energy surfaces. These coatings are commonly prepared from hydrophilic or zwitterionic polymers, inhibiting the nonspecific interactions of proteins and bacteria by forming a water layer as a physical barrier between the surface and foulants. Foulants can also be inhibited by steric repulsive forces that arise from the arrangement of polymer confirmations when the foulants approach the surface, which is an entropically unfavorable condition. On the other hand, hydrophobic polymers are

usually used to design coatings with low surface energy to promote detachment of weakly foulant-surface interaction if the coating is subjected to hydrodynamic shear force.[52–54]

1.3.1.1 Fouling-Release Strategy (Superhydrophobic Coating).

Inspired by the superhydrophobic hierarchical structure of the lotus leaf surface, efficient fouling-release coatings are often fabricated from fluoropolymers and silicones because they mostly meet the strategy requirements to release the weakly polar interactions. For example, a low surface energy containing fluoroalkylated acrylic acid oligomers reduced the *S. mutans* adhesion on substrate for dental application.[55] However, fluorine-based polymers proved susceptible to shear-induced damage, resulting in irreversible interactions with foulants. Additionally, the low solubility of these polymers makes them hard to process and attach to surfaces, which limits their application in the biomedical field.[56,57] Similarly, silicone-based coatings, like polydimethylsiloxane (PDMS) coatings and their derivatives, with poor mechanical properties and long reaction times under high temperatures, are seen as obstacles in biomedical applications.[58]

1.3.1.2. Fouling-Resistant Strategy (Hydrophilic, Zwitterionic, and Glycopolymer Coatings).

The most promising hydrophilic polymers for resisting foulants include polyethylene glycol (PEG),[59] poly(2-hydroxyethyl methacrylate) (PHEMA),[60] poly(acrylamide) (PAAm),[61] and poly(2- methyl-2-oxazoline) (PMOXA).[62] They typically consist of polar groups that can form hydrogen bonds with the surrounding water molecules in an aqueous environment, inhibiting the adsorption of proteins and bacteria. Among hydrophilic polymers, polyethylene glycol (PEG) and its derivatives are promising biocompatible candidates for medical device coatings. PEG polymer comprises repeat units (-CH2-CH2-O-), and each oxygen atom interacts with one water

molecule via hydrogen bonds. However, the oxidative degradation and enzymatic cleavage in biological conditions reduced its antifouling efficacy and caused concern for its stability during long-term applications.[34–36] Zwitterionic polymers have been used as an antifouling alternative to the PEG polymer.

Zwitterionic polymers, characterized by an equal number of positively and negatively charged groups, can form a strong hydration layer through ionic interactions with water, making them highly hydrophilic and antifouling candidates. Zwitterionic polymers can be classified into polybetaines and poly ampholytes according to the position of positively and negatively charged groups on the monomer subunits. While polybetaines carry the cationic and anionic groups on the same monomer unit, polyampholytes bear their oppositely charged groups on different monomer subunits. All polybetaines carry the same positive moiety (quaternary ammonium group). However, their negative groups can be phosphonate, carboxylate, or sulfonate. Therefore, polybetaines can be further classified into phosphonate-betaines (PB), carboxylate-betaines (CB), and sulfonate-betaines (SB) **(Figure 1.1)**.[63] Poly(2-methacryloyloxyethylphosphorylcholine) (PMPC), poly(carboxybetainemethacrylate) (PCBMA), poly(sulfobetainemethacrylate) (PSBMA), and poly(N-(3-aminopropyl)methacrylamide hydrochloride-co-acrylic acid (AMP-AA) are the most common examples of PB, CB, SB, and polyampholyte, respectively.[64] Zwitterionic groups are close to each other and interact via strong electrostatic forces, giving rise to many distinctive properties of zwitterionic polymers. For example, zwitterionic polymers have an anti-polyelectrolyte effect owing to the change in their confirmations from a collapsed state in the absence of salt to a stretched state in the presence of salt.[65] Another distinctive property is their ability to form a maximum electrostatically induced hydration layer and avoid favorable interaction with proteins.

Zwitterionic polymers are also pH-responsive and can change from a cationic state to anionic, zwitterionic polymers depending on the pH of the environment.[66,67] Recently, Poly(2-methacryloyloxyethylphosphorylcholine) (PMPC), which is biologically inspired by phosphorylcholine headgroups of phospholipids in cell membranes, has been demonstrated to bind strongly to water molecules, forming a hydration layer that prevents nonspecific protein and cell fouling on medical devices.[68] Thus, it is ideal to introduce the biocompatible layer of PMPC coatings onto target surfaces.

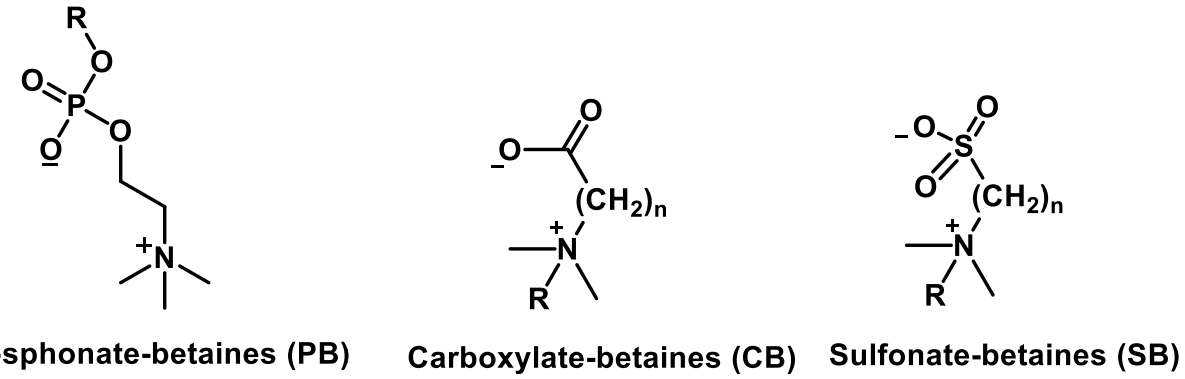

Figure 1.1. Chemical structures of zwitterionic functional groups: phosphonate-betaines (PB), carboxylate-betaines (CB), and sulfonate-betaines (SB).

It is well known that polysaccharides have been demonstrated as promising hydrophilic antifouling agents to replace synthetic polymers owing to their biocompatibility, renewability, and non-toxicity. One of the first polysaccharides explored for antifouling coating is hyaluronic acid (HA). Morra and Cassineli reported that covalently bound HA with a first layer of poly(ethyleneimine) coatings has shown good non-fouling properties with a significant reduction in bacterial adhesion compared to the uncoated glass slides.[69] Chitosan and its derivatives are another option that replaced the synthetic polymers and have been studied extensively as antibacterial and antifouling coatings. Wang et al. fabricated CMC-Ag-PU composite coating to endow polyethersulfone (PES) membranes with dual-functional antibacterial and antifouling

properties using a mussel-inspired method. *o*-Carboxymethyl chitosan (CMC) was modified by catechol using a straightforward step, which was achieved by linking the oxidized catechol with amino groups on CMC. A catechol-modified chitosan layer coated the substrates and then loaded by AgNPs via *in situ* reduction. The CMC-Ag-PU coating was finally formed after immersing the substrates in polyurethane containing PEG solution, which significantly reduced the adhesion of *E. coli and S. aureus* compared to pristine PES membrane.[70]

Glycopolymers are also an alternative to hydrophilic polymers and exhibit excellent antifouling behavior. Their structures contain many hydroxyl groups; therefore, their antifouling property mimics the hydrophilic carbohydrate-containing polymers (polysaccharides) by preventing bacterial adhesion and protein adsorption to surfaces.[71,72] As a result, synthetic glycopolymers containing pendant saccharides have been used to design antifouling coatings. Cheng et al. designed a glycosylated coating with antibacterial adhesion and antifouling properties fabricated by grafting amphiphilic terpolymer-containing glycopolymer onto the amine-modified substrate. The terpolymer was composed of 2-lactobionamidoethyl methacrylamide (LAEMA), glycidyl methacrylate (GMA), and isobornyl acrylate (BA). GMA facilitated the covalent attachment with the surface, LAEMA enhanced the surface hydrophilicity, while BA, with a particular stereochemical structure, provided antibacterial adhesion functionality. The control coating fabricated by copolymer containing only LAEMA and without the hydrophobic BA, segment showed the lowest water contact angle and the highest cell viability, confirming the hydrophilicity and biocompatibility of LAEMA.[73] Another group prepared glycopolymers-co-dopamine methacrylamide-based coating using the one-pot method. Silver nanoparticles were then generated by *in situ* reduction of silver ions, taking advantage of oxidized catechol groups on the surface. The formation of AgNPs promoted the bactericidal property while the

glycopolymer increased the antifouling and antifogging functionalities, suggesting that this transparent coating may have potential ocular application.[74]

While glycopolymers can be easily functionalized by functional monomers, synthesis of these glycopolymers is primarily time-consuming and requires multiple steps to protect and deprotect the hydroxyl groups on saccharides. In addition, the copper catalyst employed in glycopolymer synthesis via copper(I) catalyzed azide-alkyne cycloaddition may lead to cytotoxicity in *vivo* applications. Therefore, preparing glycopolymers using a simple method without protecting groups would be ideal. Narain group prepared stable glycol monomers containing stable amide linkages, such as 2-gluconamidoethyl methacrylamide (GAEMA) and 3-gluconamidopropyl methacrylamide (GAPMA), by introducing methacrylamide groups into carbon 1 (anomeric carbon) of the sugar (**Figure 1.2**).[75]

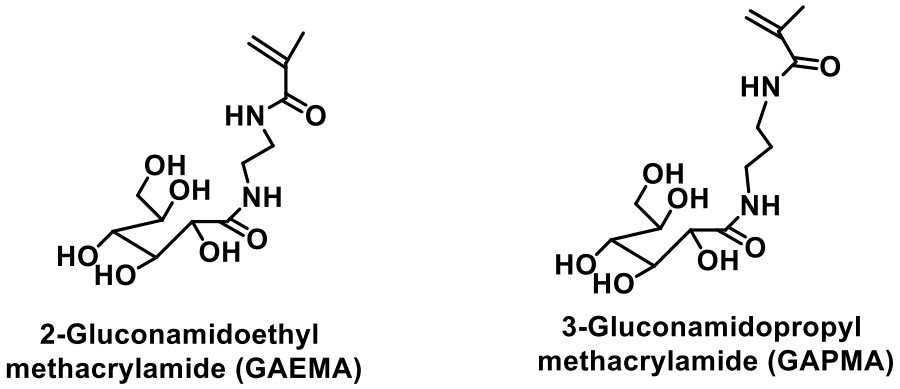

Figure 1.2. Chemical structures for GAEMA and GAPMA glycopolymers

1.3.2. Bactericidal Coating Strategies.

The most common bactericidal strategies for killing bacteria on medical device surfaces are (i) contact-active strategies or (ii) release-killing strategies.

1.3.2.1. Contact-Active Strategies.

Contact-killing coatings mainly contain non-leaching bactericidal moieties lethal to bacteria upon contact.[76,77] Many contact-active coatings rely on cationic biocides, including

nonpolymeric quaternary ammonium compounds (QAC),[78] antimicrobial peptides,[79] and antimicrobial cationic polymers.[80,81] Among them, bactericidal polymers have attracted significant attention in the biomedical field due to their ability to maintain bactericidal activity over time, making them promising candidates for long-term applications. Additionally, unlike antibiotics, they may not present pathways for the development of bacterial resistance.[82] The general mechanism of cationic polymeric coatings involves the electrostatic attraction between the positively charged polymers and the negatively charged bacterial cell membranes. Subsequently, as the cationic polymers interact with bacterial cell membrane, the hydrophobic groups on polymers begin to insert into the cell wall and disrupt it, resulting in the death of microbes.[83] Generally, the cationic and hydrophobic groups are essential for the bactericidal efficacy of antimicrobial cationic polymers. For cationic groups, several types of cationic polymers, including naturally derived polymers like chitosan[84] and cellulose[85] or synthetic cationic polymers that bear ammonium ions, sulfonium ions, or phosphonium ions.[86,87] However, the research mainly focused on ammonium-based cationic polymers because of the simplicity of synthetic methods. For the hydrophobic groups of cationic polymers, the lengths of hydrophobic alkyl chains often affect the bactericidal efficacy of cationic polymers. Tiller et al. designed a poly(4-vinyl-N-alkylpyridinium bromide) coated glass slides to kill airborne bacteria on contact. The QA-polymer coatings designed with different lengths of alkyl chains showed a distinctive reduction in viable bacteria. While chains containing 3 to 6 carbon atoms showed significant effectiveness, those containing 10 to 16 carbon atoms exhibited no bactericidal activity.[88] 2-(methacryloyloxy)ethyl trimethylammonium chloride polymer (META), a cationic polymer with 2 carbon atoms alkyl group, was frequently used for fabricating antibacterial coatings owing to its bactericidal and fungicidal activities against a broad spectrum of microbial.[89] META

monomer is commercially available and can easily be polymerized using free radicals and well-defined polymerizations.[90,91] Therefore, META polymer is highly desirable for constructing antibacterial coating based on contact-active mechanism.

1.3.2.2. Release-Killing Strategies.

Release-killing agents provide a first line of defense against bacterial adhesion and biofilm formation on medical devices. These agents can kill the bacteria on the surface and planktonic bacteria in suspension near the surface before they can colonize the surface. Common release-based agents for coating include metal nanoparticles,[92] antibiotics,[93] nitrogen oxide,[94] antibacterial enzymes,[95] and peptides.[96] Among these agents, metal nanoparticles have been widely used for creating antibacterial coatings due to their distinct bactericidal properties, attributed to their high surface-to-volume ratio, against various microorganisms.[97] When metal nanoparticles are incorporated into polymeric coatings, it is crucial to design the polymer matrices to ensure that the release kinetics and stability are appropriate for the intended application, whether short-term or long-term. The release rate in the antibacterial polymer coatings depends on the cross-linking degree between the bactericidal agent and the polymer coating. A fast release is expected if the agent is loaded on the polymeric coating with fewer interactions. For instance, Meng et al. prepared AgNPs-modified silk fabrics with 2-8 layers of poly(acrylic acid) (PAA)/poly(dimethyl diallyl ammonium chloride) (PDDA). Based on their experimental data of the growth curve assay, the more significant the number of layers, the more extended the release profile of silver ions is to achieve a sustainable antimicrobial effect. They suggested that the 2-layer coating had low-density loading of AgNPs and fewer protection layers to slow down the release profile.[98] An example of a biomedical application that requires the short-term release of an antibacterial agent is preventing infections associated with internal

fixation devices during the early period after orthopedic implant insertion.[99] On the other hand, bactericidal agents with slow release rates are widely used in the coating of most medical implants, where these implants are responsible for a significant number of device-associated infections annually. Silver and copper nanoparticles are the most commonly bactericidal agents employed in constructing stable polymeric-based coatings for medical devices. The general mechanism of metal nanoparticles in many studies is related to the enhanced release of metal ions from nanoparticle surfaces because the specific area increases as the particle size decreases, allowing for more interactions between the particle and the surrounding bacteria.[58]

While coatings function by either antifouling or bactericidal properties, which can significantly reduce the adhesion of foulants or kill the bacteria, the antifouling coatings are usually unstable and will degrade over time, which may promote the proliferation of any attached bacteria. On the other hand, using coatings based on bactericidal activity alone will cause the loss of antimicrobial activity over time due to the depletion of the active species and the adhesion of dead bacteria.[100] Hence, there is a need to integrate antifouling and bactericidal properties in a single synergistic coating to increase the probability of inhibiting bacterial colonization.[101] However, achieving an ideal coating with high stability and long-term durability is still challenging in many applications. Thus, we need stable and durable antifouling coatings that can be cost-effective and universally applied to various surfaces**.**

1.4. Universal Bifunctional Polymer-based Antibacterial Coating Techniques.

Grafting the hydrophilic and zwitterionic polymer brushes on medical devices via stable covalent bonds is a common strategy to prevent biofilm formation. The well-known controllable grafting methods are usually classified into “grafting to” and “grafting from.” “Grafting to” means preformed functional polymers are grafted to a preliminary treated surface via a chemical bond,

while “grafting from” refers to the grafting reaction that can proceed by polymerizing the monomer from the surface. Although the two methods can produce high-grafting density, they suffer from susceptibility toward degradation and need complicated and expensive protocols. Also, the process of pre-activation for hydrophobic and inert surfaces requires the use of harsh conditions and multiple chemical steps. These covalent strategies are also problematic when translated to larger surface areas easily and facilely. Therefore, there is a need to develop universal coatings that can be formed by versatile, efficient, and simple methods that avoid direct and specific chemical interactions between the coating and the substrate. The most common universal coatings technologies include layer-by-layer (LbL) assembly, mussel-inspired deposition, and polyphenolic (e.g., tannic acid) deposition.

For the layer-by-layer assembly (LbL) method, neutral polymers or polyelectrolytes with opposite charges are deposited on charged surfaces, and after multiple cycles, multilayer films are formed. The four main driving forces for constructing multilayer films using LbL assembly are electrostatic interaction, hydrogen bonding, covalent interaction, and coordination interaction. Although the versatility of this technique and the ability to generate stable multilayer-coatings through consecutive covalent interactions, it involves multiple steps and requires polymer functionalization for crosslinking, making it a time-consuming and labor-intensive method. These problems may be overcome by using surface-independent polydopamine and tannic acid coatings.

1.5. Chemistry of Dopamine.

In 2007, Messersmith and coworkers reported a simple and versatile strategy for surface modification inspired by the polydopamine adhesive ability of mussels.[102] A few years later, Caruso and his team found that natural polyphenols (e.g., tannic acid) can also form films on

various substrates.[103] After the seminal discovery by Messersmith and Caruso, researchers have been paying more attention to functionalizing surfaces via dopamine and tannic acid chemistries. It has been reported that dopamine under oxidative conditions can be self-polymerized to form a thin film layer in a one-step method. Hong et al. proposed that this polydopamine was formed through non-covalent self-assembly and covalent polymerization (**Figure 1.3)**.[104] The residual quinone, catechol, and amino groups of (PDA) can covalently bind with other molecules containing thiol, amine, or aldehyde groups via Michael addition and Schiff-base reactions to facilitate the secondary immobilization.[105] Additionally, the quinone groups of the polydopamine film can reduce the metal ions in situ to generate metal nanoparticles. PDA also serves as a linker for initiators for atom transfer radical polymerization (ATRP) and reversible addition−fragmentation chain-transfer polymerization (RAFT) techniques. By connecting polydopamine coating with these initiators, various polymer chains can be grafted onto the PDA-modified surfaces via ATRP or RAFT polymerization. Based on recent studies, polydopamine-assisted deposition of a combination of fouling-resistance polymer and cationic polymer or metal ions in fabricating universal multifunctional coatings using the following approaches: spontaneous deposition of dopamine and polymers, post-modification of PDA-coated surface, direct modification of dopamine with polymers, and polymerization of initiated surfaces.[106]

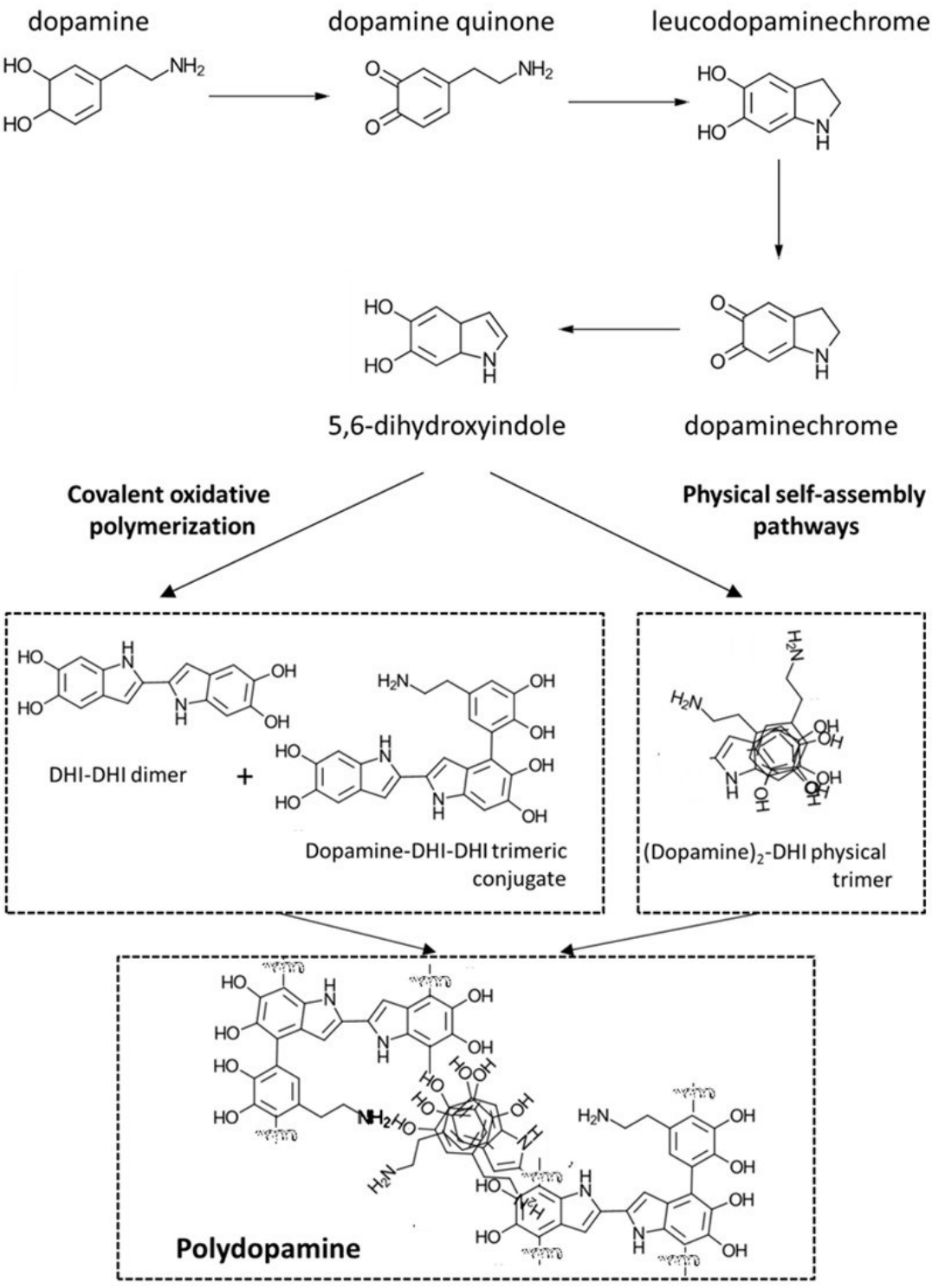

Figure 1.3. Self-polymerization of dopamine via two mechanisms: polymerization through covalent bonds (left) and polymerization through non-covalent bonds (right). Reprinted with permission from ref.[104]

1.6. Universal Antibacterial Coatings Based on Polydopamine.

Based on dopamine chemistry, several universal coatings with antifouling and bactericidal properties have been prepared. Generally, these coatings can be prepared either by the "grafting from" method based on crosslinking polydopamine with initiators for polymerization or by "grafting to" based on the conjugating polydopamine with functional polymers. For the "grafting from" method, the substrates are usually coated first with PDA film. This is then immersed in the ATRP initiator aqueous solution for PDA/initiator crosslinking, followed by growing the functionalized polymers from the modified surface. In the normal SI-ATRP, the polymerization reaction requires a high toxic transition metal catalyst concentration. This limitation can be avoided by limiting the catalyst concentration to the parts per million level (ppm). Zhou *et al*. prepared antibacterial and antibiofilm coating for cylindrical catheters via supplemental activator and reducing agent surface-initiated atom-transfer radical polymerization (SARA SI-ATRP). In their study, the ATRP initiator (α-bromoisobutyryl bromide, BiBB) was grafted onto the reactive sites of PDA film. Three different monomers [3-acrylamidopropyl trimethylammonium chloride (AMPTMA), quaternized polyethyleneimine methacrylate (Q-PEI-MA), and polyethylene glycol methacrylate (PEGDMA)] were then heated and polymerized for coating fabrication in the presence of copper wire to stabilize the Cu^{I} species *in situ* at low oxygen levels. Coating 1 containing AMPTMA/PEGDMA exhibited good antibiofilm and antimicrobial effect (2.21 log reduction) against methicillin-resistant Staphylococcus aureus (MRSA) due to its high hydrophilic properties and positive charge density. Coating 2 consisting of AMPTMA/PEGDMA/Q-PEI-MA had significant efficacy (1.5 log reduction) against vancomycin-resistant *Enterococcus faecalis* (VRE) (**Figure 1.4)**.[107] In another study, the authors developed a universal method for efficient fabrication of compatible blood coatings via

polydopamine-assisted surface-initiated activators regenerated by electron transfer atom-transfer radical polymerization of zwitterions (PDA-SI-ARGET-ATRP) and without deoxygenation. The PDA-adhesive film was first deposited on material-independent substrates, such as stainless steel, glass, PP, PET, PDMS, PC, and PTFE, followed by covalent immobilization of 3-trimethoxysilyl propyl 2-bromo-2-methylpropionate (SiBr, ATRP initiator). Finally, Zwitterionic polymer brushes are prepared by immersing the PDA/SiBr-coated substrates in zwitterionic monomer solutions containing $CuBr_2$ and reducing agent (ascorbic acid) to change the catalysts from Cu(II) to Cu(I) in aqueous solution under atmospheric conditions. The as-prepared zwitterionic polymer brushes showed ultralow biofouling against bovine serum albumin (BSA) and extreme blood compatibility.[108] Although the SI-ATRP strategy can prepare zwitterionic polymer coatings with high density and large thickness, the approach involves multistep, resulting in a high-cost and time-consuming process.

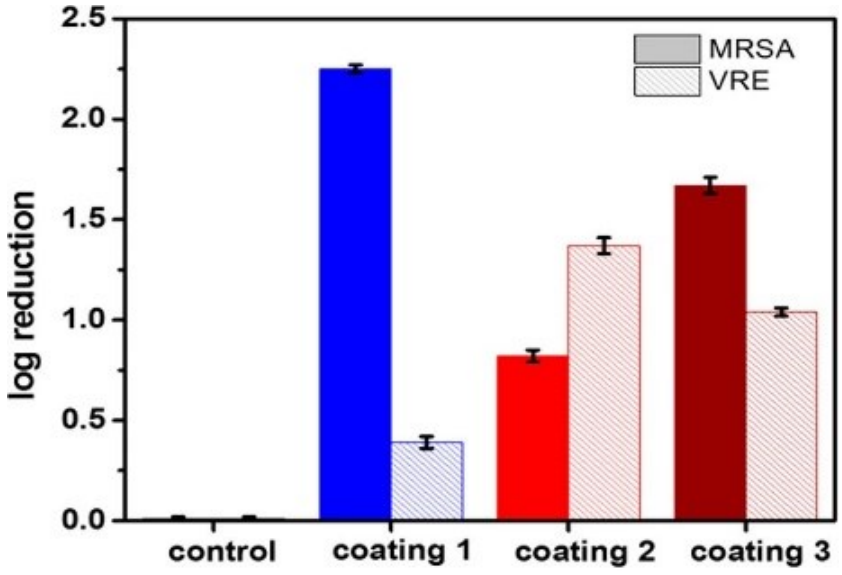

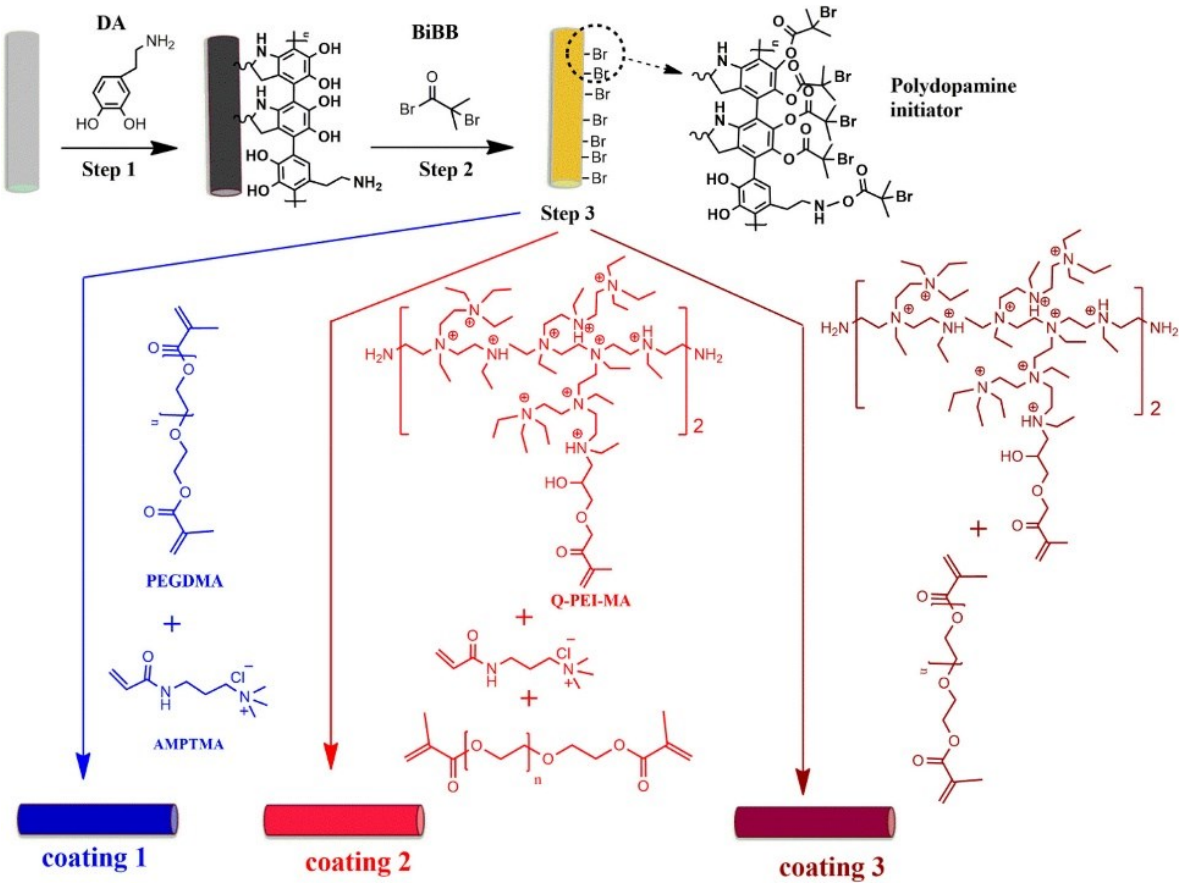

Figure 1.4. *In vitro* antibacterial activity of PDMS catheter control and coatings 1, 2, and 3 against MRSA and VRE (top). Coating steps using the SARA SI-ATRP technique for fabricating three different coatings (bottom). Reprinted with permission from ref.[107]

For the "grafting to" method, it is highly convenient and feasible to endow the surfaces with antifouling and bactericidal functions because of its simplicity in coating fabrication. The first report published by Messersmith's group in 2003, where the monomethoxy terminated PEG polymer covalently conjugated onto PDA coating, was the first idea for the "grafting to" approach using mussel-inspired coating chemistry.[109] Following this strategy, tethering zwitterionic polymers directly with dopamine-containing catechol groups is highly desirable because of its adhesive property to a wide range of substrates in a one-step method. Chen's

group successfully synthesized a novel bio-inspired terpolymer by conventional free radical polymerization. The terpolymer consists of three monomer components [MPC for antifouling, dopamine methacrylamide (DMA) for anchoring, and 2-(dimethylamino)-ethyl methacrylate (DMAEMA) for the potential contact killing. The silicon wafers and pristine PDMS substrates were immersed in terpolymer solution, followed by quaternization of the terpolymer coating by 1-bromoheptane, and finally resulted in P(DMA-co-MPC-co-DMAEMA^{+}) coating. The coating was successfully killed and resisted the adhesion of *E. coli* and *S. aureus*.[110] Similarly, released-based bactericidal coatings were prepared for wound dressing applications as they can kill the bacteria in deeper skin tissue layers. Liu *et al.* recently reported a coating decorated with Ag NPs for wound healing application. A one-step co-deposition of PDA and PEI was carried out via the polymerization of dopamine and the simultaneous reaction of the formed PDA with PEI through Schiff-base coupling and Michael addition reactions (**Scheme 1.2**). Anionic gallic acid stabilized Ag NPs (GA@AgNPs) were then anchored through Michael addition (between the carboxyl of GA and imine of PEI) and hydrogen bonding with PEI, resulting in a negatively charged GA@AgNPs/PDA−PEI coating. The GA@AgNPs/PDA−PEI surface had nonfouling and bactericidal properties against *E. coli*, *S. aureus*, and Methicillin-resistant *S. aureus* (MRSA). Their coating followed the synergistic strategy "repel-kill-release" due to the presence of a high density of anionic carboxyl groups on the outer GA@AgNP layer, contact killing and ion-mediated killing of GA@ AgNPs, and sustained release of Ag^{+}, respectively.[111] To increase the binding affinity of dopamine-modified zwitterionic polymer, Sun *et al.* fabricated a coating for biosensing applications by conjugating poly(carboxy betaine) (PCB) with L-3,4-dihydroxyphenylalanine (DOPA) groups via a simple "grafting to" deposition. The catechol groups facilitated the strong adhesion of the coating on the paper-based sensor surface, and pCB

provided the antifouling functionality while the covalent immobilization of bovine serum albumin antibody (anti-BSA) and fibrinogen antibody (anti-Fg) onto the pCB-coated surface via 1-ethyl-3-(3-(dimethylamino)propyl)-carbodiimide and N-hydroxysuccinimide (EDC/NHS) chemistry facilitated the detection of antigens.[112]

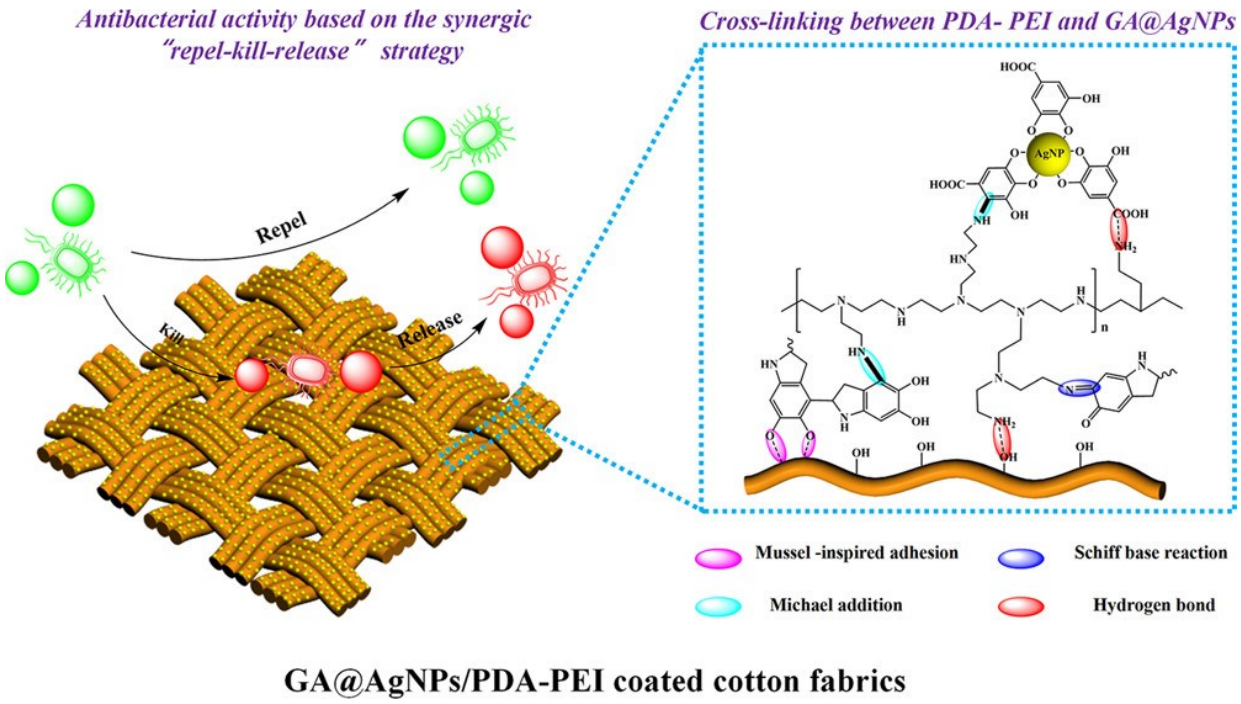

Scheme 1.2. Schematic routes represented the cross-linking interactions of GA@AgNPs/PDA–PEI-coated cotton fabrics and their antibacterial strategies. Reprinted with permission from ref.[111]

1.7. Chemistry of Tannic Acid (TA).

Polyphenol compounds (tannic acid) have gradually become a research focus for surface modification owing to their unique adhesive capability, water solubility, and low price. TA, a plant-derived compound, is commonly classified as gallotannin and commercially extracted from the gallnuts found on oak and sumac trees. TA, or penta-*m*-digalloyl glucose, has a chemical structure composed of a central glucose molecule containing two functional groups of 2,3,4-tri

hydroxyphenyl (esterified gallic acid) on each hydroxyl group of the sugar moiety (**Figure 1.5).**[113] The high number of dihydroxyphenols (catechol) and trihydroxyphenols (pyrogallol) in the TA structure leads to the formation of colorless and uniform coating of TA on a wide range of substrates that can actively inhibit the adhesion of bacteria and microbes.[114] Under oxidative conditions, these phenolic groups, like dopamine, work as active functional sites to fabricate antifouling and bactericidal surfaces via spontaneous or sequential modifications such as metal coordination, boronate ester complexation, and covalent and non-covalent interactions.[115]

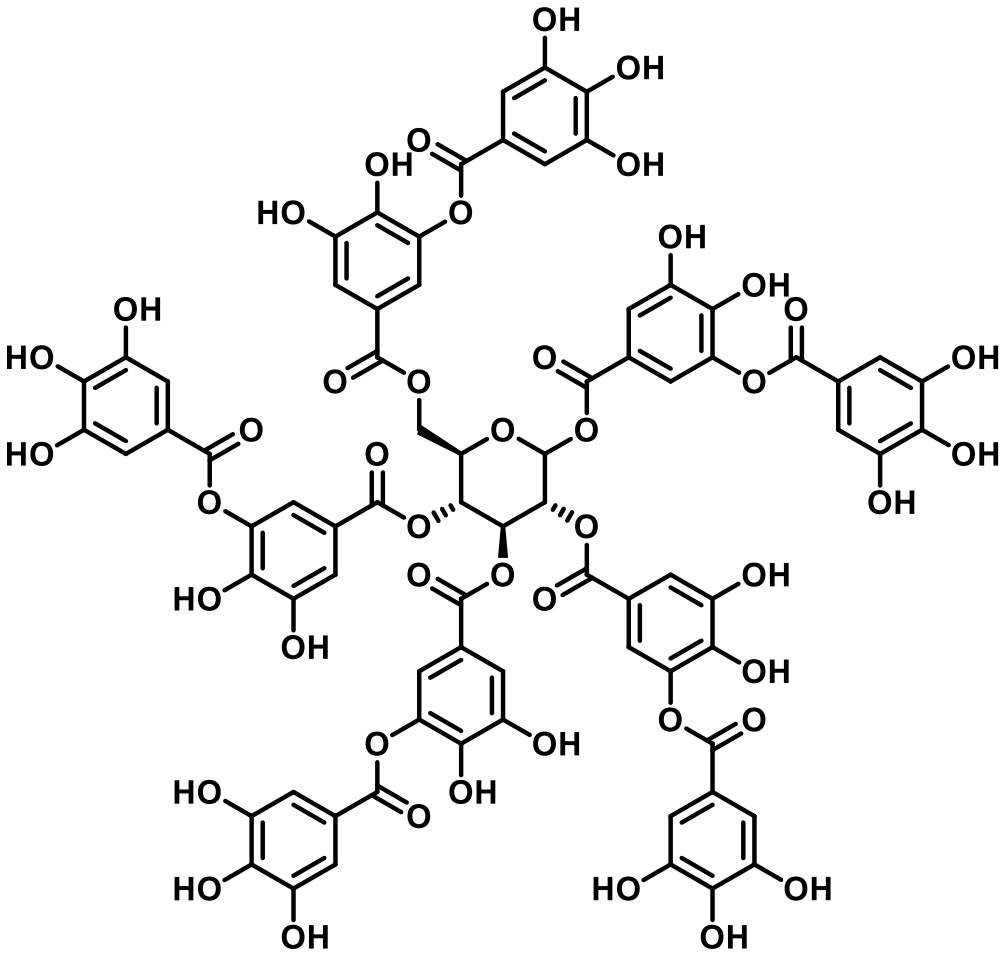

Figure 1.5. Chemical structure of tannic acid

1.8. TA-Assisted Universal Dual-Functional Coatings.

Inspired by the inherent adhesive affinity of plant polyphenols, TA can be anchored onto a wide range of substrates via multiple non-covalent interactions, such as electrostatic interactions, hydrogen bonding, hydrophobic attractions, or van der Waals interactions, making it an ideal candidate to fabricate polymer-based coatings. Functional polymers can be deposited to TA-driven surfaces through several methods, including the co-deposition process in which the functional polymers and tannic acid are simultaneously deposited onto the surface. Polymers can also be deposited onto the TA-coted surface via covalent or noncovalent interactions. Polymer-modified tannic acid is another technique that can be directly deposited onto the substrates. Polymer chains are grown from pre-initiated TA-coated surfaces via "grafting from" polymerization.

1.8.1. Grafting Polymer Chains From TA-coted Surfaces.

Researchers have explored "grafting from" polymerization to grow polymers from TA-based coatings to achieve ideal antibacterial coatings since this method provides better polymer brush density than the "grafting to" method. Kang and co-workers have synthesized TA-based initiator primer by partial modification of TA with alkyl bromide to facilitate the initiator anchoring through the remaining trihydroxy phenyls of TA onto stainless steel, titanium oxide, polystyrene dish, silicon wafer, and glass slide via tridentate coordination complexes. The bromide-TA served as initiating sites for the post-modification of surface-initiated atom transfer radical polymerization (SI-ATRP) of 2-(methacryloyloxy)ethyl trimethylammonium chloride (META), 2-methacryloyloxyethyl phosphorylcholine (MPC), and *N*-(3-sulfopropyl)-*N*-(methacryloxyethyl)-*N, N*-dimethylammonium betaine (SBMA). The cationic polymer-grafted stainless steel [SS-g-P(META)] exhibited bactericidal function against Gram-negative

Pseudomonas sp. And Gram-positive *Staphylococcus aureus* (*S. aureus*), while the zwitterionic coatings [SS-g-P(MPC) and SS-g-P(SPMA)] resisted the adhesion of bacteria. However, the drawback of this strategy is the requirement of a high concentration of catalysts (CuBr and $CuBr_2$) to allow for a redox cycling mechanism.[116] To overcome this limitation, Jeong *et al*. introduced an activator regenerated by electron transfer polymerization (ARGET) ATRP under air conditions and in the presence of the reducing agent (ascorbic acid), which acts as a chemical reservoir to regenerate active Cu(I) species from inactive Cu(II) species. Their coating was versatile for designing coatings with antifouling properties since the zwitterionic polymer can be initiated from various initiating substrates ("grafting from" process). The substrates were first treated with TA and Fe^{III} ions to deposit the TA-metal complex via coordination bonds, followed by functionalizing the TA-based coating with an aryl azide-based initiator (ABI) under photoreaction to generate ATRP initiating sites. The polymerization of MPC was then carried out to develop a hydrophilic MPC polymer brush layer on the surface.[117]

1.8.2. Deposition of Polymer-Modified TA Coating.

The high number of reactive phenolic groups in tannic acid facilitates various chemical modifications, including (a) electrophilic and nucleophilic substitution reactions. (b) TA can form phenoxy radicals, which participate in oxygen-carbon and carbon-carbon coupling reactions. (c) TA can also be oxidized into α-hydroxy-ortho-quinones, which act as nucleophiles, electrophiles, and (hetero) dienes and dienophiles in Diels–Alder reactions **(Figure 1.6)**.[115]

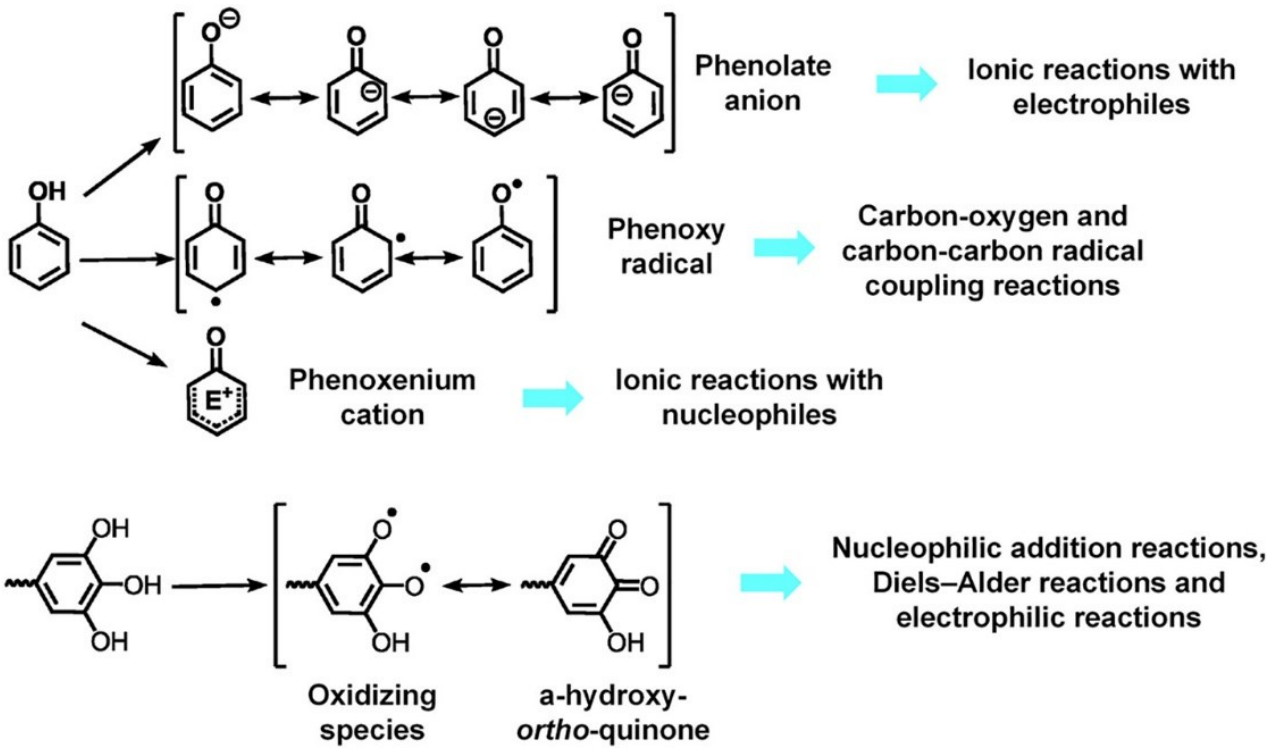

Figure 1.6. Mechanism routes of phenol modification. Reprinted with permission from ref.[115]

Direct modification of TA with zwitterionic polymer was used to prepare multifunctional coatings that could be used in *in vivo* applications; Teo and co-workers used catalyst-free reversible addition−fragmentation chain transfer (RAFT) polymerization and copper-free azide−alkyne cycloaddition to functionalize TA with zwitterionic polymer and lysine, respectively, to prepare the coating p(MPC)-TA-p(Lys)). As shown in **Figure 1.7**, TA was quickly modified by RAFT agent (CTA) and azide in a one-pot reaction to form the "clickable" macro-CTA (CTA-TA-N3). The authors found that their coating was stable against protein adsorption, bacterial adhesion, and microalgal attachment after 30 days of exposure to seawater.[118]

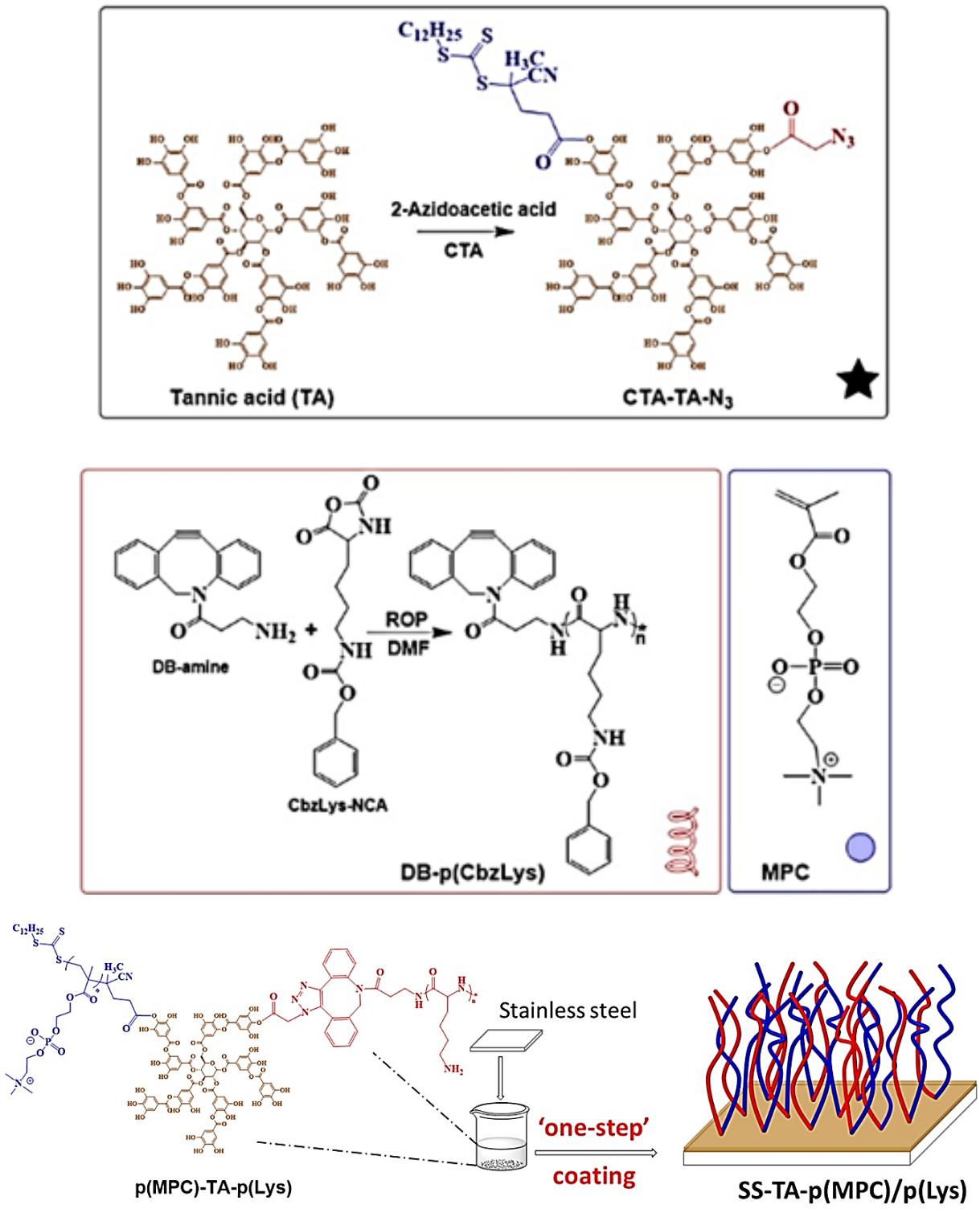

Figure 1.7. Synthetic route of polymer-modified tannic acid [p(MPC)-TA-p(Lys)] (top). One-step deposition of polymer-modified TA on stainless steel substrate (bottom). Reprinted with permission from ref.[118]

For long-term application of TA-driven coatings, pH-responsive polymers have been incorporated into the TA to develop a coating with a self-release/self-cleaning strategy. Lowering the pH induced by bacteria growth is an external trigger for releasing antibacterial agents. For example, pH-responsive poly(2-diisopropylaminoethyl methacrylate)-b-poly(2-methacryloyloxyethyl phosphorylcholine) (PDPA-b-PMPC) and cationic polylysine (PLYS) chains were simultaneously conjugated with TA to design the PLYS-TA-PDPA-b-PMPC. Using a one-pot strategy, the TA-derived polymer was coated on the stainless-steel substrate for antifouling and antimicrobial applications. Since the bacterial infection lowers the pH to less than 6, the protonation of the PDPA (pK_a=7.3) occurred at pH=5.5, resulting in swelling and improving the antifouling ability. In contrast, after raising the pH to 7.4, the antimicrobial resumed. The coating, after aging for 30 days in filtered seawater, showed similar antimicrobial and antifouling as the freshly coated substrate.[119]

1.8.3. Post-Deposition of Functional Polymer onto TA-coated Surfaces.

The high number of tri-hydroxyphenyl groups facilitates the adhesion of TA to the substrates via non-covalent interactions. The remaining oxidized quinone of catechol motifs can bind covalently with polymers containing amine or thiol groups via a Michael addition or Schiff-base reaction to form a selective and stable layer**.**

Stable and antifouling surfaces were developed by a simple dip-coating process and based on the crosslinking between zwitterionic polymer containing quaternary polyethyleneimine (PEI-S) with pre-formed TA/Fe^{+3} complex in its oxidized state via Schiff-base reaction or Michael-type addition (**Figure 1.8a)**. These coatings contain TA/Fe^{+3} (M-TA) complex that can be disassembled in acidic conditions and oxidized in basic environments. For long-term applications, the stability of the polymeric-coated polyethersulfone (PES) membranes was

investigated by measuring the water contact angle (WCA) after immersing the PES membranes coated by (M-TA), (M-TA/PEI), and (M-TA/PEI-S) in acidic and alkaline solutions for 12. As shown in **Figure 1.8b**, the WCA for the sample M-TA increased significantly in both the acidic and alkaline solutions; however, in the case of (M-TA/PEI) and (M-TA/PEI-S), there was no significant change observed in the respective figures. The as-prepared surface could effectively resist protein adsorption, bacteria attachment, and platelet adhesion. This universal coating could also be applied to various materials, including polyvinylidene fluoride (PVDF) and polystyrene (PS) membranes, as well as the 3D-polyvinyl chloride (PVC) surface (yellow duck toy).[120]

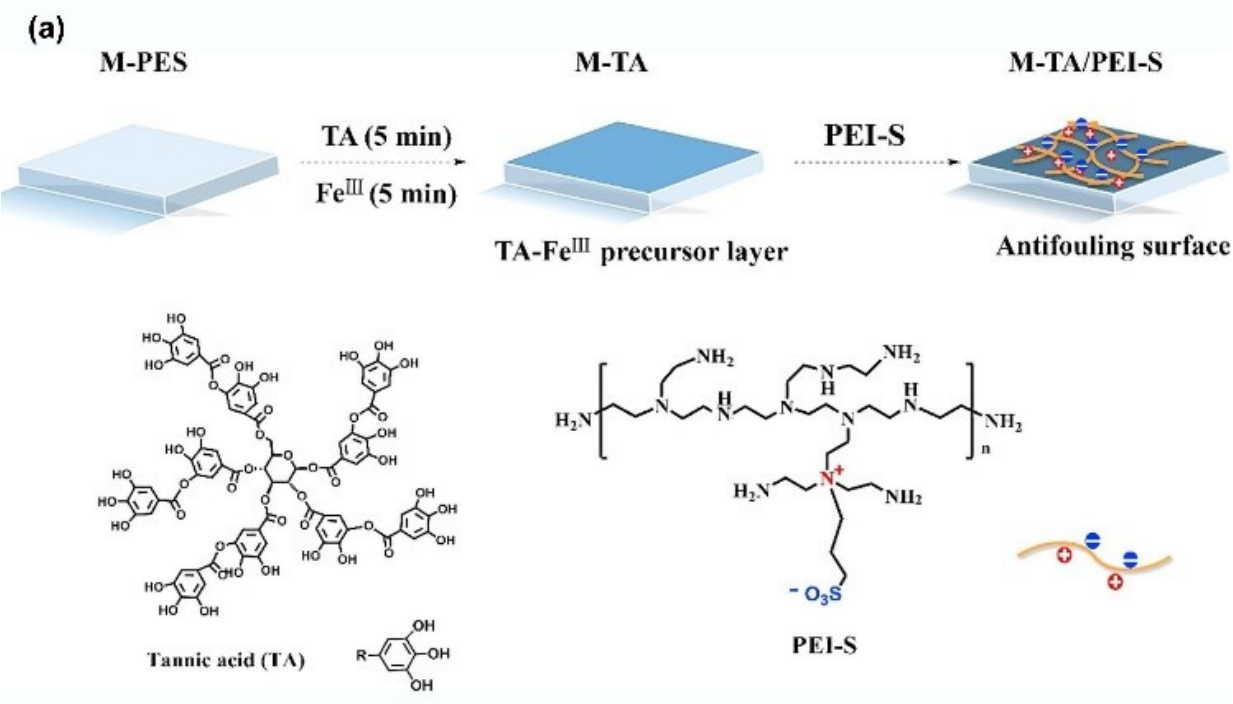

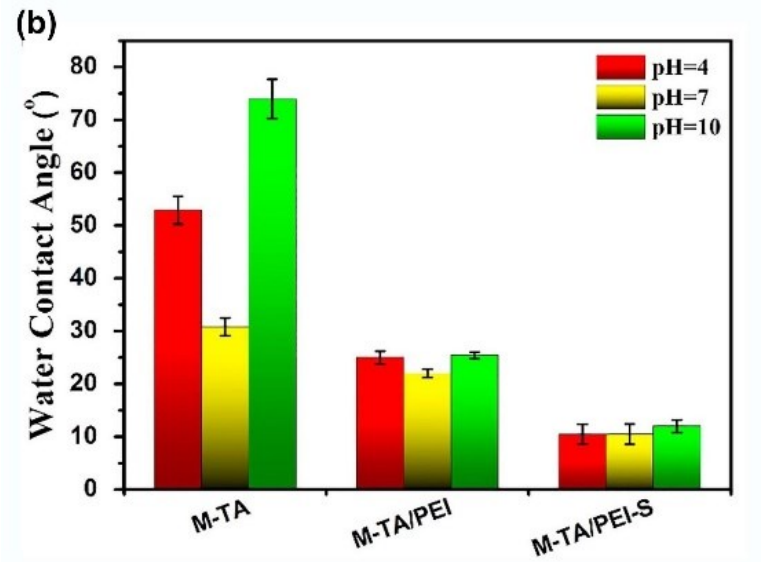

Figure 1.8. a) Grafting of zwitterionic-modified cationic polyethylene (PEI-S) onto metal-TA complex coating via dip-coating. b) WCA measurements were taken for three different samples at different pH values, and the M-TA/PEI-S coating showed low WCA values in all media. Reprinted with permission from ref.[120]

Similarly, Xie et al. proposed integrating zwitterionic polymer and *in situ* formation of silver nanoparticles (AgNPs) into membrane surface by universal, one-step, and environmentally friendly methods. This approach aims to endow the TA-coated membrane with simultaneous antifouling and antibacterial functions. The polymer-based membrane showed antibacterial activity even after being cocultured with the bacteria over 96 h.[121] Temperature-responsive and antibacterial tannic acid-based coatings have also been developed to overcome the limitations of conventional coatings via an "on-demand" killing strategy. One of the investigations developed a smart, TA-based surface with a switchable function between bacteria killing and bacteria releasing based on near-infrared photothermal activation and thermal responsiveness for potential applications in the health sector. This study involved the deposition of TA-Fe3+ complexes onto the bare Au surface (Au-TA/Fe) and then grafting of poly(N-

isopropylacrylamide) (PNIPAM) polymer to form the coating (Au-TA/Fe-PNIPAM) through Schiff base reaction or Michael addition. The Au-TA/Fe-PNIPAM surface showed that 90% of the attached *E. coli* on the surface after being killed photothermally, were released when the temperature decreased to 4 ºC. However, the Au-TA/Fe surface released only 5% of the attached bacteria. Moreover, no significant change in killing and release abilities was observed after two attach-kill-release cycles. The switchable coating was also highly stable, and the coated substrate, after aging for 10 days in PBS, showed a similar antibacterial efficacy as the freshly coated substrate.[122]

1.8.4. Grafting of TA and Polymer in One Step Process.

Tannic acid-assisted co-deposition allows for precise control over the thickness of the coating, leading to tailored material properties. TA-driven co-deposition can simplify the coating procedure by integrating the deposition and functionality in one step. A coating on the titanium surface was fabricated via simultaneous and successive deposition of a polyphenol tannic acid (TA) and four-armed poly (ethylene glycol) (PEG_{10k}-4− OH) to obtain the modified surfaces (Ti-TA/PEG) and (Ti-TA-PEG), respectively. The (Ti-TA/PEG) process is rapid and yields a uniform coating with a tunable thickness compared to the (Ti-TA-PEG) coating. Due to the formation of hydrogen bonds between hydroxyphenyl groups on TA as hydrogen-bond donors and hydroxyl groups on PEG as proton acceptors, both (Ti-TA/PEG) and (Ti-TA-PEG) coatings showed good antifouling properties against proteins adsorption and bacteria and platelet adhesion. Moreover, the former had better fouling resistance than (Ti-TA-PEG) coating, which could be attributed to the higher thickness of the former as illustrated by ellipsometry measurements.[123] In another study, a coating based on tannic acid and thermo-responsive microgel was fabricated for the multifunctional antibacterial property. The TA/Fe^{+3} complex as

an adhesive layer was simultaneously deposited with poly (N-isopropylacrylamide-co-sulfobetain methacrylate) [poly (NIPAM-co-SBMA)] microgels on a silicon wafer. This coating killed about 94.3% of *E. coli* and 93.6% of *S. aureus* after 24h of incubation. Due to its zwitterionic and thermos-responsive polymer components, the coating reduced the adhesion of bacteria over 72h and released as high as 91.7% for *E. coli* and 94.4% for *S. aureus* by lowering the temperature. The authors suggested that their hemocompatible coating has promising applications in biomedical and industrial fields.[124]

1.9. Biomedical Applications of Polydopamine- and Tannic Acid-Based Coatings.

Recently, Tannic acid and dopamine coatings have been investigated for their potential biomedical applications, particularly in developing polymer-based coatings with integrated bactericidal and antifouling properties for medical devices. These coatings have shown promise in limiting biofilm formation and subsequent bacteria attachment. The simplicity and versatility of the coating processes make them attractive for surface modification in biomedical applications.[125] Therefore, a combination of tannic acid or polydopamine with hydrophilic polymers makes them a great potential to develop advanced coatings for medical devices such as wound dressings, implants, catheters, biosensors, etc. Tables 1.1 and 1.2 summarize the recent advances in tannic acid and dopamine-mediated surfaces in conjugation with hydrophilic polymers for various applications.

Table 1.1. Summary of the recent applications of dopamine-based coatings

Substrate	**Coating material**	**Coating method**	**Application**	**Refs.**
Polypropylene	Sulfobetaine methacrylate and glycidyl methacrylate p(SBMA- co-GMA)	SI-ATRP	Orientation-based	[126]

			immobilization of antibodies and the creation of a responsive immunoassay platform.	
Stainless steel	SBMA	SI-ATRP	Bioadhesion resistance against plasma protein, blood cells, mammalian cells, and bacteria.	[127]
Titanium	MPC	ATRP	Inhibition of platelet and fibrinogen adhesion for potential use in blood-contact devices like cardiovascular stents.	[128]

Porcine skin	Zwitterionic sulfobetaine modified catechol containing poly(amidoamine) polymers (CPAA-ZS).	Catechol/$FeCl_3$ cross-linking	Wound healing	[129]
Electrospun poly (L - lactic) acid (PLLA) film	poly (sulfobetaine methacrylate) (pSBMA)-catechol	ATRP	Antifouling in complex media for biomedical application	[130]
poly(L)-lactide (PLLA) nanofibrous scaffold	Polydopamine (PDA)	combining electrospinning and post-in-situ polymerization.	Increased hydrophilicity, cell growth, proliferation, excellent oxidation resistance, and notable *in-vitro* elimination ability of ROS. *In vivo,* approved nanofibers have good histocompatibility, Antibacterial	[131]

			ability	
Commercial thin-film composite (TFC) membranes	Poly(Sulfobetaine methacrylate-b-[2-(Methacryloyloxy)ethyl]trimethylammonium chloride (SBMA-b-MTAC)	ARGET-ATRP	Antifouling and antimicrobial activities for biomedical applications.	[132]
Titanium screws	$(DOPA)_4$-bioactive peptides	Multivalent coordinative interactions	Improving clinical outcome of Ti-based implants in the osteoporotic condition	[133]
Glass substrate	hyaluronic acid–dopamine conjugate with silver-doped bioactive glass nanoparticles	LbL	Potential application for orthopedic implants	[134]
Glass, stainless steel, gold, and polyvinyl chloride (PVC)	Dopamine-modified hyaluronic acid/polyvinyl amine (HA-DN/PVAm)	LbL	Inhibition of the bacteria and tumor cell line growth	[135]

Table 1.2. Summary of the recent applications of tannic acid-based coatings

Substrate	Coating material	Coating method	Application	Refs.
Polyamide thin film composite forward osmosis (FO) membranes	TA/polyethylene imine/graphene oxide nanosheets	One-pot dip coating method	Antibacterial and antifouling coating for membrane filtration	[136]
PP membrane, fabric, and copper mesh)	TA/APTES/ODS or PEI or AgNPs	Dip coating method	Oil/water separation, dye adsorption, and reduction of 4-nitrophenol	[137]
Titanium surface	TA/PEG-4OH	One-pot dip coating method	Antifouling application	[138]
Silicon wafers	TA and benzalkonium chloride (BAC)/AgNPs	TA modification, then a one-step coating method	Antibacterial coating for preventing catheter-associated infections	[139]
Titanium (Ti), polystyrene (PS), silicon (Si), glass, and zinc	PEG-TA/V^{III+}	One-step co-deposition method	Antifouling and photothermal antibacterial properties, preventing biofilm formation	[140]

alloy				
Silicon (Si) wafers, glass slides, polycarbonate (PC), poly (methyl methacrylate) (PMMA), polystyrene (PS) sheets, and safety goggles	TA-PEI	One-step deposition process	Antifogging and antibacterial coating for optical devices	[141]
PVDF membrane coupon	TA-Cu-Fe	One-step codeposition method	Antibacterial function and algal inhibition application	[142]

1.10. Goal and Outline of the Project.

Antifouling and antibacterial coatings to combat medical device-associated infections are hot research topics. “Grafting to,” “grafting from,” and LBL are the most common methods for fabricating dual-functional antifouling and antibacterial applications. Although the grafting techniques can produce a high density of coatings, they are susceptible to degradation and need complicated and expensive protocols. Also, these surface-dependent grafting processes need a pre-activation for hydrophobic and inert surfaces, which is problematic when transferring the

coating to a larger scale. The LBL method is a universal and surface-independent coating technique that can deposit functional materials onto surfaces through non-covalent bonds. The process involves applying multiple steps to form a stable coating, making it time-consuming when upscaling is required for coating fabricating. Hence, achieving stable and cost-effective bifunctional coating using these methods is challenging.

The main objective of this thesis is to construct bifunctional coatings by combining the functional polymers with tannic acid, dopamine, and dopamine methacrylate via strong covalent bonds to enhance the mechanical stability of the coatings. Hydrophilic polymers and bactericidal agents have been exploited to prepare stable dual-functional coatings for biomedical applications. Three different projects have been developed in this thesis as follows:

First project: A simple dip-coating method using tannic acid chemistry was used to develop a superhydrophilic coating with antifouling and antibacterial properties. The copolymer [zwitterionic 2-methacryloyloxyethyl phosphorylcholine-random-2-aminoethyl methacrylamide hydrochloride] (MPC-co-AEMA) was randomly grafted to the tannic acid through Michael addition reaction and using one-step co-deposition. The remaining quinone groups on TA generated silver nanoparticles (AgNPs) *in situ*. The dual-functional coatings showed antibacterial properties against *E. coli* and *S. aureus* and remarkably decreased the adhesion of BSA protein. The resulting coating is potentially valuable for biomedical applications.

Second project: stable contact-killing coating was developed, which killed the bacteria even after immersion in PBS for 7 days, using a simple co-deposition process. Reversible addition-fragmentation chain transfer (RAFT) polymerization was used to copolymerize either zwitterionic 2-methacryloyloxyethyl phosphorylcholine monomer (MPC) or cationic 2-(methacryloyloxy)ethyl trimethylammonium monomer (META) with 4-formyl phenyl

methacrylate monomer (FPMA). The copolymers were then covalently grafted to the amino groups of polydopamine-coated surfaces and exhibited excellent antibacterial properties against *S. aureus* and *E. coli* and antifouling properties against bovine serum albumin (BSA) protein. The resulting coating is expected to be helpful in biomedical applications.

Third project: a stable dual-functional bactericidal coating was developed based on the copper ions-catechol complexation. The monomers GAEMA and DMA were first synthesized and then copolymerized by free radical polymerization to obtain the random GAEMA-DMA. This copolymer containing glycopolymer with fouling-resistance properties was incorporated with copper ions via metal-phenol networks (MPNs) to fabricate a coating with high antifouling properties and stability. The copper ions inhibited the bacterial cell adhesion and imparted stability to the coating, resulting in reduced protein adsorption even after 30 h of incubation in a BSA protein solution. MPNs interactions increased the antifouling durability of the bifunctional bactericidal coating, demonstrating the potential for its application in the biomedical field.

1.10. References.

(1) Li, B.; Webster, T. J. Bacteria Antibiotic Resistance: New Challenges and Opportunities for Implant-Associated Orthopedic Infections. *J. Orthop. Res.* **2018**, *36* (1), 22–32.

(2) Sloan, M.; Premkumar, A.; Sheth, N. P. Projected Volume of Primary Total Joint Arthroplasty in the u.s., 2014 to 2030. *J. Bone Jt. Surg. - Am. Vol.* **2018**, *100* (17), 1455–1460.

(3) Besser, M.; Terberger, J.; Weber, L.; Ghebremedhin, B.; Naumova, E. A.; Arnold, W. H.; Stuermer, E. K. Impact of Probiotics on Pathogen Survival in an Innovative Human Plasma Biofilm Model (HpBIOM). *J. Transl. Med.* **2019**, *17* (1), 1–9.

(4) Leslie, D. C.; Waterhouse, A.; Berthet, J. B.; Valentin, T. M.; Watters, A. L.; Jain, A.; Kim, P.; Hatton, B. D.; Nedder, A.; Donovan, K.; Super, E. H.; Howell, C.; Johnson, C. P.; Vu, T. L.; Bolgen, D. E.; Rifai, S.; Hansen, A. R.; Aizenberg, M.; Super, M.; Aizenberg, J.; Ingber, D. E. A Bioinspired Omniphobic Surface Coating on Medical Devices Prevents Thrombosis and Biofouling. *Nat. Biotechnol.* **2014**, *32* (11), 1134–1140.

(5) Wang, B.; Ye, Z.; Xu, Q.; Liu, H.; Lin, Q.; Chen, H.; Nan, K. Construction of a Temperature-Responsive Terpolymer Coating with Recyclable Bactericidal and Self-Cleaning Antimicrobial Properties. *Biomater. Sci.* **2016**, *4* (12), 1731–1741.

(6) Xu, L. C.; Siedlecki, C. A. Submicron-Textured Biomaterial Surface Reduces Staphylococcal Bacterial Adhesion and Biofilm Formation. *Acta Biomater.* **2012**, *8* (1), 72–81.

(7) Bryers, J. D. Medical Biofilms. *Biotechnol. Bioeng.* **2008**, *100* (1), 1–18.

(8) Levin, S. The Crisis in Antibiotic Resistance. *Infect. Dis. Clin. Pract.* **1993**, *2* (1), 53.

(9) Bagge, N.; Schuster, M.; Hentzer, M.; Ciofu, O.; Givskov, M.; Greenberg, E. P.; Høiby,

N. Pseudomonas Aeruginosa Biofilms Exposed to Imipenem Exhibit Changes in Global Gene Expression and β-Lactamase and Alginate Production. *Antimicrob. Agents Chemother.* **2004**, *48* (4), 1175–1187.

(10) Piddock, L. J. V. The Crisis of No New Antibiotics-What Is the Way Forward? *Lancet Infect. Dis.* **2012**, *12* (3), 249–253.

(11) Mitra, D.; Kang, E. T.; Neoh, K. G. Polymer-Based Coatings with Integrated Antifouling and Bactericidal Properties for Targeted Biomedical Applications. *ACS Appl. Polym. Mater.* **2021**, *3* (5), 2233–2263.

(12) Tan, J.; Liang, X.; Yang, J.; Zhou, S. Sol-Gel-Derived Hard Coatings from Tetraethoxysilane and Organoalkoxysilanes Bearing Zwitterionic and Isothiazolinone Groups and Their Antifouling Behaviors. *J. Mater. Chem. B* **2022**, *10* (3), 406–417.

(13) Vaterrodt, A.; Thallinger, B.; Daumann, K.; Koch, D.; Guebitz, G. M.; Ulbricht, M. Antifouling and Antibacterial Multifunctional Polyzwitterion/Enzyme Coating on Silicone Catheter Material Prepared by Electrostatic Layer-by-Layer Assembly. *Langmuir* **2016**, *32* (5), 1347–1359.

(14) Zhang, F.; Yang, L.; Hu, C.; Li, L.; Wang, J.; Luo, R.; Wang, Y. Phosphorylcholine- And Cation-Bearing Copolymer Coating with Superior Antibiofilm and Antithrombotic Properties for Blood-Contacting Devices. *J. Mater. Chem. B* **2020**, *8* (36), 8433–8443.

(15) Zhang, C.; Liu, S.; Tan, L.; Zhu, H.; Wang, Y. Star-Shaped Poly(2-Methyl-2-Oxazoline)-Based Films: Rapid Preparation and Effects of Polymer Architecture on Antifouling Properties. *J. Mater. Chem. B* **2015**, *3* (27), 5615–5628.

(16) Cortez, C.; Quinn, J. F.; Hao, X.; Gudipati, C. S.; Stenzel, M. H.; Davis, T. P.; Caruso, F. Multilayer Buildup and Biofouling Characteristics of PSS-b-PEG Containing Films.

Langmuir **2010**, *26* (12), 9720–9727.

(17) Zhu, X.; Jańczewski, D.; Guo, S.; Lee, S. S. C.; Parra Velandia, F. J.; Teo, S. L. M.; He, T.; Puniredd, S. R.; Julius Vancso, G. Polyion Multilayers with Precise Surface Charge Control for Antifouling. *ACS Appl. Mater. Interfaces* **2015**, *7* (1), 852–861.

(18) Liu, J.; Ye, L.; Sun, Y.; Hu, M.; Chen, F.; Wegner, S.; Mailänder, V.; Steffen, W.; Kappl, M.; Butt, H. J. Elastic Superhydrophobic and Photocatalytic Active Films Used as Blood Repellent Dressing. *Adv. Mater.* **2020**, *32* (11).

(19) Thompson, V. C.; Adamson, P. J.; Dilag, J.; Uswatte Uswatte Liyanage, D. B.; Srikantharajah, K.; Blok, A.; Ellis, A. V.; Gordon, D. L.; Köper, I. Biocompatible Anti-Microbial Coatings for Urinary Catheters. *RSC Adv.* **2016**, *6* (58), 53303–53309.

(20) Ryu, J. H.; Messersmith, P. B.; Lee, H. Polydopamine Surface Chemistry: A Decade of Discovery. *ACS Appl. Mater. Interfaces* **2018**, *10* (9), 7523–7540.

(21) Chandler, D. N T E R F a C E S a N D T H E D R I V I N G F O R C E O F H Y D R O P H O B I C a S S Em B L Y. *Nature* **2005**, *437*, 640–647.

(22) Oh, H.; Hoff, J. E.; Armstrong, G. S.; Haff, L. A. Hydrophobic Interaction in Tannin-Protein Complexes. *J. Agric. Food Chem.* **1980**, *28* (2), 394–398.

(23) Nigg, J. T. 基因的改变NIH Public Access. *Bone* **2008**, *23* (1), 1–7.

(24) Zhao, C.; Nguyen, N. S.; Li, X.; McCarthy, D.; Wang, H. Tannic Acid Coating and in Situ Deposition of Silver Nanoparticles to Improve the Antifouling Properties of an Ultrafiltration Membrane. *J. Appl. Polym. Sci.* **2019**, *136* (14), 1–10.

(25) Li, D.; Li, J.; Wang, S.; Wang, Q.; Teng, W. Dually Crosslinked Copper-Poly(Tannic Acid) Nanoparticles with Microenvironment-Responsiveness for Infected Wound Treatment. *Adv. Healthc. Mater.* **2023**, *12* (17), 1–18.

(26) Zhou, Y.; Wu, S.; Liu, F. High-Performance Polyimide Nanocomposites with Polydopamine-Coated Copper Nanoparticles and Nanowires for Electronic Applications. *Mater. Lett.* **2019**, *237*, 19–21.

(27) Liu, Y.; Han, Y.; Chen, R.; Zhang, H.; Liu, S.; Liang, F. In Situ Immobilization of Copper Nanoparticles on Polydopamine Coated Graphene Oxide for H2O2 Determination. *PLoS One* **2016**, *11* (7), 1–12.

(28) Li, J.; Li, J.; Wei, J.; Zhu, X.; Qiu, S.; Zhao, H. Copper Tannic Acid-Coordinated Metal-Organic Nanosheets for Synergistic Antimicrobial and Antifouling Coatings. *ACS Appl. Mater. Interfaces* **2021**, *13* (8), 10446–10456.

(29) Zhu, Z.; Gao, Q.; Long, Z.; Huo, Q.; Ge, Y.; Vianney, N.; Daliko, N. A.; Meng, Y.; Qu, J.; Chen, H.; Wang, B. Polydopamine/Poly(Sulfobetaine Methacrylate) Co-Deposition Coatings Triggered by CuSO4/H2O2 on Implants for Improved Surface Hemocompatibility and Antibacterial Activity. *Bioact. Mater.* **2021**, *6* (8), 2546–2556.

(30) Shahkaramipour, N.; Lai, C. K.; Venna, S. R.; Sun, H.; Cheng, C.; Lin, H. Membrane Surface Modification Using Thiol-Containing Zwitterionic Polymers via Bioadhesive Polydopamine. *Ind. Eng. Chem. Res.* **2018**, *57* (6), 2336–2345.

(31) Abouelmagd, S. A.; Meng, F.; Kim, B. K.; Hyun, H.; Yeo, Y. Tannic Acid-Mediated Surface Functionalization of Polymeric Nanoparticles. *ACS Biomater. Sci. Eng.* **2016**, *2* (12), 2294–2303.

(32) Zhang, M.; Cheng, C.; Guo, C.; Jin, L.; Liu, L.; Li, M.; Shang, L.; Liu, Y.; Ao, Y. Co-Depositing Bio-Inspired Tannic Acid-Aminopropyltriethoxysilane Coating onto Carbon Fiber for Excellent Interfacial Adhesion of Epoxy Composites. *Compos. Sci. Technol.* **2021**, *204* (October 2020), 108639.

(33) Alfieri, M. L.; Panzella, L.; Oscurato, S. L.; Salvatore, M.; Avolio, R.; Errico, M. E.; Maddalena, P.; Napolitano, A.; d'Ischia, M. The Chemistry of Polydopamine Film Formation: The Amine-Quinone Interplay. *Biomimetics* **2018**, *3* (3).

(34) Chen, S.; Li, L.; Zhao, C.; Zheng, J. Surface Hydration: Principles and Applications toward Low-Fouling/Nonfouling Biomaterials. *Polymer (Guildf).* **2010**, *51* (23), 5283–5293.

(35) Chen, S.; Cao, Z.; Jiang, S. Ultra-Low Fouling Peptide Surfaces Derived from Natural Amino Acids. *Biomaterials* **2009**, *30* (29), 5892–5896.

(36) Nguyen, A. T.; Baggerman, J.; Paulusse, J. M. J.; Zuilhof, H.; Van Rijn, C. J. M. Bioconjugation of Protein-Repellent Zwitterionic Polymer Brushes Grafted from Silicon Nitride. *Langmuir* **2012**, *28* (1), 604–610.

(37) Greene, G. W.; Martin, L. L.; Tabor, R. F.; Michalczyk, A.; Ackland, L. M.; Horn, R. Lubricin: A Versatile, Biological Anti-Adhesive with Properties Comparable to Polyethylene Glycol. *Biomaterials* **2015**, *53*, 127–136.

(38) Yi, L.; Xu, K.; Xia, G.; Li, J.; Li, W.; Cai, Y. New Protein-Resistant Surfaces of Amphiphilic Graft Copolymers Containing Hydrophilic Poly(Ethylene Glycol) and Low Surface Energy Fluorosiloxane Side-Chains. *Appl. Surf. Sci.* **2019**, *480* (February), 923–933.

(39) Leckband, D.; Sheth, S.; Halperin, A. Grafted Poly(Ethylene Oxide) Brushes as Nonfouling Surface Coatings. *J. Biomater. Sci. Polym. Ed.* **1999**, *10* (10), 1125–1147.

(40) Chen, S.; Zheng, J.; Li, L.; Jiang, S. Strong Resistance of Phosphorylcholine Self-Assembled Monolayers to Protein Adsorption: Insights into Nonfouling Properties of Zwitterionic Materials. *J. Am. Chem. Soc.* **2005**, *127* (41), 14473–14478.

(41) Riga, E. K.; Vöhringer, M.; Widyaya, V. T.; Lienkamp, K. Polymer-Based Surfaces Designed to Reduce Biofilm Formation: From Antimicrobial Polymers to Strategies for Long-Term Applications. *Macromol. Rapid Commun.* **2017**, *38* (20), 1–18.

(42) McBain, A. J.; Rickard, A. H.; Gilbert, P. Possible Implications of Biocide Accumulation in the Environment on the Prevalence of Bacterial Antibiotic Resistance. *J. Ind. Microbiol. Biotechnol.* **2002**, *29* (6), 326–330.

(43) Francolini, I.; Donelli, G. Prevention and Control of Biofilm-Based Medical-Device-Related Infections. *FEMS Immunol. Med. Microbiol.* **2010**, *59* (3), 227–238.

(44) Khatoon, Z.; McTiernan, C. D.; Suuronen, E. J.; Mah, T. F.; Alarcon, E. I. Bacterial Biofilm Formation on Implantable Devices and Approaches to Its Treatment and Prevention. *Heliyon* **2018**, *4* (12), e01067.

(45) Li, X.; Sun, L.; Zhang, P.; Wang, Y. Novel Approaches to Combat Medical Device-Associated Biofilms. *Coatings* **2021**, *11* (3), 1–31.

(46) Alotaibi, G. F. Factors Influencing Bacterial Biofilm Formation and Development. *Am. J. Biomed. Sci. Res.* **2021**, *12* (6), 617–626.

(47) Muhammad, M. H.; Idris, A. L.; Fan, X.; Guo, Y.; Yu, Y.; Jin, X.; Qiu, J.; Guan, X.; Huang, T. Beyond Risk: Bacterial Biofilms and Their Regulating Approaches. *Front. Microbiol.* **2020**, *11* (May), 1–20.

(48) Toyofuku, M.; Inaba, T.; Kiyokawa, T.; Obana, N.; Yawata, Y.; Nomura, N. Environmental Factors That Shape Biofilm Formation. *Biosci. Biotechnol. Biochem.* **2016**, *80* (1), 7–12.

(49) Cyanobacteria, C. The Relative Importance of Shear Forces and Surface Hydrophobicity on Biofilm Formation By.

(50) Guo, K.; Freguia, S.; Dennis, P. G.; Chen, X.; Donose, B. C.; Keller, J.; Gooding, J. J.; Rabaey, K. Effects of Surface Charge and Hydrophobicity on Anodic Biofilm Formation, Community Composition, and Current Generation in Bioelectrochemical Systems. *Environ. Sci. Technol.* **2013**, *47* (13), 7563–7570.

(51) Yin, R.; Cheng, J.; Wang, J.; Li, P.; Lin, J. Treatment of Pseudomonas Aeruginosa Infectious Biofilms: Challenges and Strategies. *Front. Microbiol.* **2022**, *13* (August), 1–16.

(52) Magin, C. M.; Cooper, S. P.; Brennan, A. B. Non-Toxic Antifouling Strategies. *Mater. Today* **2010**, *13* (4), 36–44.

(53) Thérien-Aubin, H.; Chen, L.; Ober, C. K. Fouling-Resistant Polymer Brush Coatings. *Polymer (Guildf).* **2011**, *52* (24), 5419–5425.

(54) Sakala, G. P.; Reches, M. Peptide-Based Approaches to Fight Biofouling. *Adv. Mater. Interfaces* **2018**, *5* (18), 1–26.

(55) Okada, A.; Nikaido, T.; Ikeda, M.; Okada, K.; Yamauchi, J.; Foxton, R. M.; Sawadda, H.; Tagami, J.; Matin, K. **疏油**-亲水 **原始**讨论构造文章. *Dent. Mater. J.* **2008**, *27* (4), 565–572.

(56) Lejars, M.; Margaillan, A.; Bressy, C. Fouling Release Coatings: A Nontoxic Alternative to Biocidal Antifouling Coatings. *Chem. Rev.* **2012**, *112* (8), 4347–4390.

(57) Selim, M. S.; Shenashen, M. A.; El-Safty, S. A.; Higazy, S. A.; Selim, M. M.; Isago, H.; Elmarakbi, A. Recent Progress in Marine Foul-Release Polymeric Nanocomposite Coatings. *Prog. Mater. Sci.* **2017**, *87*, 1–32.

(58) Maan, A. M. C.; Hofman, A. H.; de Vos, W. M.; Kamperman, M. Recent Developments and Practical Feasibility of Polymer-Based Antifouling Coatings. *Adv. Funct. Mater.*

2020, *30* (32).

(59) Faustino, C. M. C.; Lemos, S. M. C.; Monge, N.; Ribeiro, I. A. C. A Scope at Antifouling Strategies to Prevent Catheter-Associated Infections. *Adv. Colloid Interface Sci.* **2020**, *284*.

(60) Han, H.; Zhu, J.; Wu, D. Q.; Li, F. X.; Wang, X. L.; Yu, J. Y.; Qin, X. H. Inherent Guanidine Nanogels with Durable Antibacterial and Bacterially Antiadhesive Properties. *Adv. Funct. Mater.* **2019**, *29* (12), 1–17.

(61) Wu, G.; Li, C. C.; Jiang, X. H.; Yu, L. M. Highly Efficient Antifouling Property Based on Self-Generating Hydrogel Layer of Polyacrylamide Coatings. *J. Appl. Polym. Sci.* **2016**, *133* (42), 1–11.

(62) Serhan, M.; Sprowls, M.; Jackemeyer, D.; Long, M.; Perez, I. D.; Maret, W.; Tao, N.; Forzani, E. Total Iron Measurement in Human Serum with a Smartphone. *AIChE Annu. Meet. Conf. Proc.* **2019**, *2019-Novem*.

(63) Jiang, S.; Cao, Z. Ultralow-Fouling, Functionalizable, and Hydrolyzable Zwitterionic Materials and Their Derivatives for Biological Applications. *Adv. Mater.* **2010**, *22* (9), 920–932.

(64) He, M.; Gao, K.; Zhou, L.; Jiao, Z.; Wu, M.; Cao, J.; You, X.; Cai, Z.; Su, Y.; Jiang, Z. Zwitterionic Materials for Antifouling Membrane Surface Construction. *Acta Biomater.* **2016**, *40* (92), 142–152.

(65) Xiao, S.; Ren, B.; Huang, L.; Shen, M.; Zhang, Y.; Zhong, M.; Yang, J.; Zheng, J. Salt-Responsive Zwitterionic Polymer Brushes with Anti-Polyelectrolyte Property. *Curr. Opin. Chem. Eng.* **2018**, *19*, 86–93.

(66) Kawano, S.; Lie, J.; Ohgi, R.; Shizuma, M.; Muraoka, M. Modulating Polymeric

Amphiphiles Using Thermo- And PH-Responsive Copolymers with Cyclodextrin Pendant Groups through Molecular Recognition of the Lipophilic Dye. *Macromolecules* **2021**, *54* (11), 5229–5240.

(67) Quan, X.; Zhao, D.; Li, L.; Zhou, J. Understanding the Cellular Uptake of PH-Responsive Zwitterionic Gold Nanoparticles: A Computer Simulation Study. *Langmuir* **2017**, *33* (50), 14480–14489.

(68) Ueda, T.; Oshida, H.; Kurita, K.; Ishihara, K.; Nakabayashi, N. Preparation of 2-Methacryloyloxyethyl Phosphorylcholine Copolymers with Alkyl Methacrylates and Their Blood Compatibility. *Polym. J.* **1992**, *24* (11), 1259–1269.

(69) Morra, M.; Cassineli, C. Non-Fouling Properties of Polysaccharide-Coated Surfaces. *J. Biomater. Sci. Polym. Ed.* **1999**, *10* (10), 1107–1124.

(70) Wang, R.; Song, X.; Xiang, T.; Liu, Q.; Su, B.; Zhao, W.; Zhao, C. Mussel-Inspired Chitosan-Polyurethane Coatings for Improving the Antifouling and Antibacterial Properties of Polyethersulfone Membranes. *Carbohydr. Polym.* **2017**, *168*, 310–319.

(71) Ribeiro, J. P. M.; Mendonça, P. V.; Coelho, J. F. J.; Matyjaszewski, K.; Serra, A. C. Glycopolymer Brushes by Reversible Deactivation Radical Polymerization: Preparation, Applications, and Future Challenges. *Polymers (Basel).* **2020**, *12* (6).

(72) Yu, K.; Kizhakkedathu, J. N. Synthesis of Functional Polymer Brushes Containing Carbohydrate Residues in the Pyranose Form and Their Specific and Nonspecific Interactions with Proteins. *Biomacromolecules* **2010**, *11* (11), 3073–3085.

(73) Cheng, Q.; Peng, Y. Y.; Asha, A. B.; Zhang, L.; Li, J.; Shi, Z.; Cui, Z.; Narain, R. Construction of Antibacterial Adhesion Surfaces Based on Bioinspired Borneol-Containing Glycopolymers. *Biomater. Sci.* **2022**, *10* (7), 1787–1794.

(74) Feng, K.; Peng, L.; Yu, L.; Zheng, Y.; Chen, R.; Zhang, W.; Chen, G.; Chen, G. Universal Antifogging and Antimicrobial Thin Coating Based on Dopamine-Containing Glycopolymers. *ACS Appl. Mater. Interfaces* **2020**, *12* (24), 27632–27639.

(75) Matsumura, S.; Hlil, A. R.; Lepiller, C.; Gaudet, J.; Guay, D.; Shi, Z.; Holdcroft, S.; Hay, A. S. Stability and Utility of Pyridyl Disulfide Functionality in RAFT and Conventional Radical Polymerizations. *J. Polym. Sci. Part A Polym. Chem.* **2008**, *46* (April), 7207–7224.

(76) C., W. Molecular Mechanisms That Confer Antibacterial Drug Resistance. *Nature* **2000**, *406* (775–781), 775–781.

(77) Kohanski, M. A.; Dwyer, D. J.; Collins, J. J. How Antibiotics Kill Bacteria: From Targets to Networks. *Nat. Rev. Microbiol.* **2010**, *8* (6), 423–435.

(78) Jennings, M. C.; Minbiole, K. P. C.; Wuest, W. M. Quaternary Ammonium Compounds: An Antimicrobial Mainstay and Platform for Innovation to Address Bacterial Resistance. *ACS Infect. Dis.* **2016**, *1* (7), 288–303.

(79) Calabrese, D. R.; Wenning, B.; Finlay, J. A.; Callow, M. E.; Callow, J. A.; Fischer, D.; Ober, C. K. Amphiphilic Oligopeptides Grafted to PDMS-Based Diblock Copolymers for Use in Antifouling and Fouling Release Coatings. *Polym. Adv. Technol.* **2015**, *26* (7), 829–836.

(80) Palermo, E. F.; Vemparala, S.; Kuroda, K. Cationic Spacer Arm Design Strategy for Control of Antimicrobial Activity and Conformation of Amphiphilic Methacrylate Random Copolymers. *Biomacromolecules* **2012**, *13* (5), 1632–1641.

(81) Oda, Y.; Kanaoka, S.; Sato, T.; Aoshima, S.; Kuroda, K. Block versus Random Amphiphilic Copolymers as Antibacterial Agents. *Biomacromolecules* **2011**, *12* (10),

3581–3591.

(82) Yang, Y.; Cai, Z.; Huang, Z.; Tang, X.; Zhang, X. Antimicrobial Cationic Polymers: From Structural Design to Functional Control. *Polym. J.* **2018**, *50* (1), 33–44.

(83) Ganewatta, M. S.; Tang, C. Controlling Macromolecular Structures towards Effective Antimicrobial Polymers. *Polymer (Guildf).* **2015**, *63*, A1–A29.

(84) Narciso, F.; Cardoso, S.; Monge, N.; Lourenço, M.; Martin, V.; Duarte, N.; Santos, C.; Gomes, P.; Bettencourt, A.; Ribeiro, I. A. C. 3D-Printed Biosurfactant-Chitosan Antibacterial Coating for the Prevention of Silicone-Based Associated Infections. *Colloids Surfaces B Biointerfaces* **2023**, *230* (August), 0–2.

(85) Zhou, Y.; Jiang, Y.; Zhang, Y.; Tan, L. Improvement of Antibacterial and Antifouling Properties of a Cellulose Acetate Membrane by Surface Grafting Quaternary Ammonium Salt. *ACS Appl. Mater. Interfaces* **2022**, *14* (33), 38358–38369.

(86) Chang, H. I.; Yang, M. S.; Liang, M. The Synthesis, Characterization and Antibacterial Activity of Quaternized Poly(2,6-Dimethyl-1,4-Phenylene Oxide)s Modified with Ammonium and Phosphonium Salts. *React. Funct. Polym.* **2010**, *70* (12), 944–950.

(87) Xu, X.; Wang, Q.; Chang, Y.; Zhang, Y.; Peng, H.; Whittaker, A. K.; Fu, C. Antifouling and Antibacterial Surfaces Grafted with Sulfur-Containing Copolymers. *ACS Appl. Mater. Interfaces* **2022**, *14* (36), 41400–41411.

(88) Tiller, J. C.; Liao, C. J.; Lewis, K.; Klibanov, A. M. Designing Surfaces That Kill Bacteria on Contact. *Proc. Natl. Acad. Sci. U. S. A.* **2001**, *98* (11), 5981–5985.

(89) Shiga, T.; Mori, H.; Uemura, K.; Moriuchi, R.; Dohra, H.; Yamawaki-Ogata, A.; Narita, Y.; Saito, A.; Kotsuchibashi, Y. Evaluation of the Bactericidal and Fungicidal Activities of Poly([2-(Methacryloyloxy)Ethyl]Trimethyl Ammonium Chloride)(Poly (METAC))-

Based Materials. *Polymers (Basel).* **2018**, *10* (9), 1–9.

(90) Kobayashi, M.; Terada, M.; Terayama, Y.; Kikuchi, M.; Takahara, A. Direct Synthesis of Well-Defined Poly[{2-(Methacryloyloxy)Ethyl} Trimethylammonium Chloride] Brush via Surface-Initiated Atom Transfer Radical Polymerization in Fluoroalcohol. *Macromolecules* **2010**, *43* (20), 8409–8415.

(91) Xu, G.; Liu, P.; Pranantyo, D.; Xu, L.; Neoh, K. G.; Kang, E. T. Antifouling and Antimicrobial Coatings from Zwitterionic and Cationic Binary Polymer Brushes Assembled via "Click" Reactions. *Ind. Eng. Chem. Res.* **2017**, *56* (49), 14479–14488.

(92) Furno, F.; Morley, K. S.; Wong, B.; Sharp, B. L.; Arnold, P. L.; Howdle, S. M.; Bayston, R.; Brown, P. D.; Winship, P. D.; Reid, H. J. Silver Nanoparticles and Polymeric Medical Devices: A New Approach to Prevention of Infection? *J. Antimicrob. Chemother.* **2004**, *54* (6), 1019–1024.

(93) Tagar, S.; Qambrani, N. A. Bacteriological Quality Assessment of Poultry Chicken Meat and Meat Contact Surfaces for the Presence of Targeted Bacteria and Determination of Antibiotic Resistance of Salmonella Spp. in Pakistan. *Food Control* **2023**, *151* (April), 109786.

(94) Lu, Y.; Slomberg, D. L.; Schoenfisch, M. H. Nitric Oxide-Releasing Chitosan Oligosaccharides as Antibacterial Agents. *Biomaterials* **2014**, *35* (5), 1716–1724.

(95) El-Aziz, S. M. A.; Faraag, A. H. I.; Ibrahim, A. M.; Albrakati, A.; Bakkar, M. R. Tyrosinase Enzyme Purification and Immobilization from Pseudomonas Sp. EG22 Using Cellulose Coated Magnetic Nanoparticles: Characterization and Application in Melanin Production. *World J. Microbiol. Biotechnol.* **2024**, *40* (1), 1–18.

(96) Cao, M.; Zhao, W.; Wang, L.; Li, R.; Gong, H.; Zhang, Y.; Xu, H.; Lu, J. R. Graphene

Oxide-Assisted Accumulation and Layer-by-Layer Assembly of Antibacterial Peptide for Sustained Release Applications. *ACS Appl. Mater. Interfaces* **2018**, *10* (29), 24937–24946.

(97) Seil, J. T.; Webster, T. J. Antimicrobial Applications of Nanotechnology: Methods and Literature. *Int. J. Nanomedicine* **2012**, *7*, 2767–2781.

(98) Meng, M.; He, H.; Xiao, J.; Zhao, P.; Xie, J.; Lu, Z. Controllable in Situ Synthesis of Silver Nanoparticles on Multilayered Film-Coated Silk Fibers for Antibacterial Application. *J. Colloid Interface Sci.* **2016**, *461*, 369–375.

(99) Zimmerli, W. Clinical Presentation and Treatment of Orthopaedic Implant-Associated Infection. *J. Intern. Med.* **2014**, *276* (2), 111–119.

(100) Zhang, J.; Zhou, R.; Wang, H.; Jiang, X.; Wang, H.; Yan, S.; Yin, J.; Luan, S. Bacterial Activation of Surface-Tethered Antimicrobial Peptides for the Facile Construction of a Surface with Self-Defense. *Appl. Surf. Sci.* **2019**, *497* (April), 143480.

(101) Yu, Q.; Wu, Z.; Chen, H. Dual-Function Antibacterial Surfaces for Biomedical Applications. *Acta Biomater.* **2015**, *16* (1), 1–13.

(102) Alapján-, V. 済無No Title No Title No Title. **2016**, *318* (OCTOBER), 1–23.

(103) Ejima, H.; Richardson, J. J.; Liang, K.; Best, J. P.; Van Koeverden, M. P.; Such, G. K.; Cui, J.; Caruso, F. One-Step Assembly of Coordination Complexes. *Science (80-.).* **2013**, *341* (6142), 154–157.

(104) Salazar, P.; Martin, M.; Gonzalez, J. L. Polydopamine-Modified Surfaces in Biosensor Applications. *Polym. Sci. Res. Adv. Pract. Appl. Educ. Asp.* **2016**, *1* (July), 385–396.

(105) Li, S.; Scheiger, J. M.; Wang, Z.; Dong, Z.; Welle, A.; Trouillet, V.; Levkin, P. A. Substrate-Independent and Re-Writable Surface Patterning by Combining Polydopamine

Coatings, Silanization, and Thiol-Ene Reaction. *Adv. Funct. Mater.* **2021**, *31* (50).

(106) Asha, A. B.; Chen, Y.; Narain, R. Bioinspired Dopamine and Zwitterionic Polymers for Non-Fouling Surface Engineering. *Chem. Soc. Rev.* **2021**, *50* (20), 11668–11683.

(107) Zhou, C.; Wu, Y.; Thappeta, K. R. V.; Subramanian, J. T. L.; Pranantyo, D.; Kang, E. T.; Duan, H.; Kline, K.; Chan-Park, M. B. In Vivo Anti-Biofilm and Anti-Bacterial Non-Leachable Coating Thermally Polymerized on Cylindrical Catheter. *ACS Appl. Mater. Interfaces* **2017**, *9* (41), 36269–36280.

(108) Li, N.; Li, T.; Qiao, X. Y.; Li, R.; Yao, Y.; Gong, Y. K. Universal Strategy for Efficient Fabrication of Blood Compatible Surfaces via Polydopamine-Assisted Surface-Initiated Activators Regenerated by Electron Transfer Atom-Transfer Radical Polymerization of Zwitterions. *ACS Appl. Mater. Interfaces* **2020**, *12* (10), 12337–12344.

(109) Dalsin, J. L.; Hu, B. H.; Lee, B. P.; Messersmith, P. B. Mussel Adhesive Protein Mimetic Polymers for the Preparation of Nonfouling Surfaces. *J. Am. Chem. Soc.* **2003**, *125* (14), 4253–4258.

(110) Wang, B. L.; Jin, T. W.; Han, Y. M.; Shen, C. H.; Li, Q.; Lin, Q. K.; Chen, H. Bio-Inspired Terpolymers Containing Dopamine, Cations and MPC: A Versatile Platform to Construct a Recycle Antibacterial and Antifouling Surface. *J. Mater. Chem. B* **2015**, *3* (27), 5501–5510.

(111) Liu, G.; Xiang, J.; Xia, Q.; Li, K.; Yan, H.; Yu, L. Fabrication of Durably Antibacterial Cotton Fabrics by Robust and Uniform Immobilization of Silver Nanoparticles via Mussel-Inspired Polydopamine/Polyethyleneimine Coating. *Ind. Eng. Chem. Res.* **2020**, *59* (20), 9666–9678.

(112) Sun, F.; Wu, K.; Hung, H. C.; Zhang, P.; Che, X.; Smith, J.; Lin, X.; Li, B.; Jain, P.; Yu,

Q.; Jiang, S. Paper Sensor Coated with a Poly(Carboxybetaine)-Multiple DOPA Conjugate via Dip-Coating for Biosensing in Complex Media. *Anal. Chem.* **2017**, *89* (20), 10999–11004.

(113) Baldwin, A.; Booth, B. W. Biomedical Applications of Tannic Acid. *J. Biomater. Appl.* **2022**, *36* (8), 1503–1523.

(114) Xu, L. Q.; Pranantyo, D.; Neoh, K. G.; Kang, E. T.; Fu, G. D. Thiol Reactive Maleimido-Containing Tannic Acid for the Bioinspired Surface Anchoring and Post-Functionalization of Antifouling Coatings. *ACS Sustain. Chem. Eng.* **2016**, *4* (8), 4264–4272.

(115) Chen, C.; Yang, H.; Yang, X.; Ma, Q. Tannic Acid: A Crosslinker Leading to Versatile Functional Polymeric Networks: A Review. *RSC Adv.* **2022**, *12* (13), 7689–7711.

(116) Pranantyo, D.; Xu, L. Q.; Neoh, K. G.; Kang, E. T.; Ng, Y. X.; Teo, S. L. M. Tea Stains-Inspired Initiator Primer for Surface Grafting of Antifouling and Antimicrobial Polymer Brush Coatings. *Biomacromolecules* **2015**, *16* (3), 723–732.

(117) Jeong, W.; Kang, H.; Kim, E.; Jeong, J.; Hong, D. Surface-Initiated ARGET ATRP of Antifouling Zwitterionic Brushes Using Versatile and Uniform Initiator Film. *Langmuir* **2019**, *35* (41), 13268–13274.

(118) Xu, G.; Liu, P.; Pranantyo, D.; Neoh, K. G.; Kang, E. T.; Lay-Ming Teo, S. One-Step Anchoring of Tannic Acid-Scaffolded Bifunctional Coatings of Antifouling and Antimicrobial Polymer Brushes. *ACS Sustain. Chem. Eng.* **2019**, *7* (1), 1786–1795.

(119) Xu, G.; Neoh, K. G.; Kang, E. T.; Teo, S. L. M. Switchable Antimicrobial and Antifouling Coatings from Tannic Acid-Scaffolded Binary Polymer Brushes. *ACS Sustain. Chem. Eng.* **2020**, *8* (6), 2586–2595.

(120) Chen, S.; Xie, Y.; Xiao, T.; Zhao, W.; Li, J.; Zhao, C. Tannic Acid-Inspiration and Post-

Crosslinking of Zwitterionic Polymer as a Universal Approach towards Antifouling Surface. *Chem. Eng. J.* **2018**, *337* (October 2017), 122–132.

(121) Xie, Y.; Chen, S.; Zhang, X.; Shi, Z.; Wei, Z.; Bao, J.; Zhao, W.; Zhao, C. Engineering of Tannic Acid Inspired Antifouling and Antibacterial Membranes through Co-Deposition of Zwitterionic Polymers and Ag Nanoparticles. *Ind. Eng. Chem. Res.* **2019**, *58* (27), 11689–11697.

(122) Wang, Y.; Wei, T.; Qu, Y.; Zhou, Y.; Zheng, Y.; Huang, C.; Zhang, Y.; Yu, Q.; Chen, H. Smart, Photothermally Activated, Antibacterial Surfaces with Thermally Triggered Bacteria-Releasing Properties. *ACS Appl. Mater. Interfaces* **2020**, *12* (19), 21283–21291.

(123) Guo, L. L.; Cheng, Y. F.; Ren, X.; Gopinath, K.; Lu, Z. S.; Li, C. M.; Xu, L. Q. Simultaneous Deposition of Tannic Acid and Poly(Ethylene Glycol) to Construct the Antifouling Polymeric Coating on Titanium Surface. *Colloids Surfaces B Biointerfaces* **2021**, *200* (September 2020), 111592.

(124) Liu, Y.; Mao, S.; Zhu, L.; Chen, S.; Wu, C. Based on Tannic Acid and Thermoresponsive Microgels Design a Simple and High-Efficiency Multifunctional Antibacterial Coating. *Eur. Polym. J.* **2021**, *153* (May), 110498.

(125) Zhang, H.; Shen, X.; Fei, Z.; Fan, X.; Ma, L.; Wang, H.; Tian, C.; Zhang, B.; Luo, R.; Wang, Y.; Huang, S. Ag-Incorporated Polydopamine/Tannic Acid Coating on Titanium With Enhanced Cytocompatible and Antibacterial Properties. *Front. Bioeng. Biotechnol.* **2022**, *10* (March), 1–9.

(126) Zhao, J.; Mo, R.; Tian, L. M.; Song, L. J.; Luan, S. F.; Yin, J. H.; Ren, L. Q. Oriented Antibody Immobilization and Immunoassay Based on Boronic Acid-Containing Polymer Brush. *Chinese J. Polym. Sci. (English Ed.* **2018**, *36* (4), 472–478.

(127) Sin, M. C.; Sun, Y. M.; Chang, Y. Zwitterionic-Based Stainless Steel with Well-Defined Polysulfobetaine Brushes for General Bioadhesive Control. *ACS Appl. Mater. Interfaces* **2014**, *6* (2), 861–873.

(128) Ma, W.; Yang, P.; Li, J.; Li, S.; Li, P.; Zhao, Y.; Huang, N. Immobilization of Poly(MPC) Brushes onto Titanium Surface by Combining Dopamine Self-Polymerization and ATRP: Preparation, Characterization and Evaluation of Hemocompatibility in Vitro. *Appl. Surf. Sci.* **2015**, *349*, 445–451.

(129) Peng, B.; Lai, X.; Chen, L.; Lin, X.; Sun, C.; Liu, L.; Qi, S.; Chen, Y.; Leong, K. W. Scarless Wound Closure by a Mussel-Inspired Poly(Amidoamine) Tissue Adhesive with Tunable Degradability. *ACS Omega* **2017**, *2* (9), 6053–6062.

(130) Yang, W.; Sundaram, H. S.; Ella, J. R.; He, N.; Jiang, S. Low-Fouling Electrospun PLLA Films Modified with Zwitterionic Poly(Sulfobetaine Methacrylate)-Catechol Conjugates. *Acta Biomater.* **2016**, *40*, 92–99.

(131) Xiong, F.; Wei, S.; Sheng, H.; Han, X.; Jiang, W.; Zhang, Z.; Li, B.; Xuan, H.; Xue, Y.; Yuan, H. In Situ Polydopamine Functionalized Poly-L-Lactic Acid Nanofibers with near-Infrared-Triggered Antibacterial and Reactive Oxygen Species Scavenging Capability. *Int. J. Biol. Macromol.* **2022**, *201* (December 2021), 338–350.

(132) Ye, G.; Lee, J.; Perreault, F.; Elimelech, M. Controlled Architecture of Dual-Functional Block Copolymer Brushes on Thin-Film Composite Membranes for Integrated "Defending" and "Attacking" Strategies against Biofouling. *ACS Appl. Mater. Interfaces* **2015**, *7* (41), 23069–23079.

(133) Zhao, H.; Huang, Y.; Zhang, W.; Guo, Q.; Cui, W.; Sun, Z.; Eglin, D.; Liu, L.; Pan, G.; Shi, Q. Mussel-Inspired Peptide Coatings on Titanium Implant to Improve

Osseointegration in Osteoporotic Condition. *ACS Biomater. Sci. Eng.* **2018**, *4* (7), 2505–2515.

(134) Carvalho, A. L.; Vale, A. C.; Sousa, M. P.; Barbosa, A. M.; Torrado, E.; Mano, J. F.; Alves, N. M. Antibacterial Bioadhesive Layer-by-Layer Coatings for Orthopedic Applications. *J. Mater. Chem. B* **2016**, *4* (32), 5385–5393.

(135) Zhang, T. Di; Deng, X.; Wang, Y. F.; Wang, X. T.; Zhang, X.; Chen, L. L.; Cao, X.; Zhang, Y. Z.; Zhang, C. Y.; Zheng, X.; Yin, D. C. Layer-by-Layer Coating of Polyvinylamine and Dopamine-Modified Hyaluronic Acid Inhibits the Growth of Bacteria and Tumor Cell Lines on the Surface of Materials. *Appl. Surf. Sci.* **2020**, *530* (July), 147197.

(136) Hegab, H. M.; ElMekawy, A.; Barclay, T. G.; Michelmore, A.; Zou, L.; Saint, C. P.; Ginic-Markovic, M. Single-Step Assembly of Multifunctional Poly(Tannic Acid)-Graphene Oxide Coating to Reduce Biofouling of Forward Osmosis Membranes. *ACS Appl. Mater. Interfaces* **2016**, *8* (27), 17519–17528.

(137) Wang, Z.; Han, M.; Zhang, J.; He, F.; Xu, Z.; Ji, S.; Peng, S.; Li, Y. Designing Preferable Functional Materials Based on the Secondary Reactions of the Hierarchical Tannic Acid (TA)-Aminopropyltriethoxysilane (APTES) Coating. *Chem. Eng. J.* **2019**, *360* (September 2018), 299–312.

(138) Guo, L. L.; Cheng, Y. F.; Ren, X.; Gopinath, K.; Lu, Z. S.; Li, C. M.; Xu, L. Q. Simultaneous Deposition of Tannic Acid and Poly(Ethylene Glycol) to Construct the Antifouling Polymeric Coating on Titanium Surface. *Colloids Surfaces B Biointerfaces* **2021**, *200* (January), 111592.

(139) Liu, L.; Shi, H.; Yu, H.; Zhou, R.; Yin, J.; Luan, S. One-Step Hydrophobization of Tannic

Acid for Antibacterial Coating on Catheters to Prevent Catheter-Associated Infections. *Biomater. Sci.* **2019**, *7* (12), 5035–5043.

(140) Lu, Q.; Zou, F.; Chen, Z.; Gnanasekar, S.; Zhao, D.; Liu, Y.; Liu, H.; Zhang, Y.; Lu, Z.; Kang, E. T.; Xu, L.; Rao, X. A Bioactive Tannic Acid/Vanadium Ions Co-Deposited Coating on Various Surfaces for Antifouling, Photothermal Anti-Bacterial, and Antioxidant Effects. *Prog. Org. Coatings* **2024**, *186* (July 2023), 108010.

(141) Ren, J.; Kong, R.; Gao, Y.; Zhang, L.; Zhu, J. Bioinspired Adhesive Coatings from Polyethylenimine and Tannic Acid Complexes Exhibiting Antifogging, Self-Cleaning, and Antibacterial Capabilities. *J. Colloid Interface Sci.* **2021**, *602*, 406–414.

(142) Liu, J.; Yu, X.; Yang, E.; Li, T.; Yu, H.; Wang, Z.; Dong, B.; Fane, A. G. A Combined Tannic Acid-Copper-Iron Coating of Ultrafiltration Membrane for Enhanced Anti-Bacterial and Algal-Inhibition Performance. *J. Water Process Eng.* **2022**, *50* (September), 103250.

Chapter 2: Tannic Acid-Based Coatings Containing Zwitterionic Copolymers for Improved Antifouling and Antibacterial Properties

The content of this chapter was published in

The Journal of Langmuir

2.1. Introduction.

Biofilm, which is the attachment of bacteria and microorganisms to the surfaces of medical devices, has become a severe problem in the biomedical field.[1] Upon medical device insertion, the surface becomes rapidly coated with proteins and other host molecules. This layer of adsorbed proteins can work as a platform for bacterial attachment and subsequent biofilm formation, ultimately leading to device failure.[2] Hence, endowing a medical device surface with antifouling and antibacterial properties is crucial to combat the foulant attachments to medical devices. Recently, researchers have developed several surface modification technologies to combat biofilm formation, such as chemical coating,[3] surface grafting,[4] and surface topography modification.[5] Among all methods, the nature-inspired coating technique has been proposed as an innovative strategy to alternate other grafting methods owing to its versatile adhesion on various substrates, robust reactivity for chemical modification, coating simplicity under mild conditions, and biocompatibility. For example, *in situ* polymerization of dopamine under mildly alkaline conditions generated polydopamine coatings on different organic and inorganic surfaces through a simple dip coating process.[6] Moreover, the PDA-coated surfaces can covalently graft polymers with amine-containing molecules and reduce metal ions to metal nanoparticles.[7,8] However, the complex polymerization chemistry, which can be challenging for controlling coating uniformity, and the potential neurotoxicity of polydopamine may limit its applications in the biomedical sector.[9,10] Moreover, due to the relatively high dopamine price, the industrializing method was complex. Hence, a universal and low-cost approach toward antifouling surfaces was strongly required.

Tannic acid, a polyphenol compound, has gradually become a research focus for surface modification owing to its unique adhesive capability, water solubility, and low price. TA is also

an antibacterial and antioxidant agent and non-toxic at minimal concentrations, making it an ideal agent for fabricating coatings for biomedical applications.[11].[12].[13,14] Research has shown that tannic acid can be combined with zwitterionic polymers for fabricating surfaces on various substrates, such as polyvinylidene fluoride, polystyrene,[15] polyurethane, silicon wafer, glass slide, titanium dioxide,[16] polyurushiol,[17] and polyethersulfone membrane.[18] For example, Yeh and co-workers developed a one-pot coating method by depositing sulfobetaine methacrylate-aminoethyl methacrylate copolymer and self-polymerized pyrogallol on various surfaces to resist the protein and cell adhesions passively. Interestingly, their modified surfaces suppressed the attachment of L929 cells by about 99%.[19] The high antifouling performance for these coatings could be attributed to the ability of hydrophilic zwitterionic polymeric brushes to interact with water through strong electrostatic interactions and form a physical barrier to resist protein adsorption on the surface.[20]

The functional groups of TA have been investigated to oxidize under oxidative conditions into quinone groups, which can work as active sites for the co-deposition and post-modification coatings through several interactions such as metal coordination, boronate ester complexation, covalent and non-covalent interactions. For example, the tannic acid coating has been successfully used as a versatile platform for introducing functional materials via robust covalent crosslinking using a layer-by-layer technique (LBL). Xu and co-workers effectively resisted four different types of bacteria and Amphora coffeaeformis microalgae by taking advantage of the increased number of coating multilayers. They initially applied tannic acid chemistry to anchor the stainless-steel surface by TA, followed by covalently tethering parasin 1 peptide into TA-modified steel surface via Michael addition/Schiff base reaction between catechol groups of TA and amine-rich parasin 1.[21] In another study, stimuli-responsive, antibacterial tannic acid-based

coatings have been developed to overcome the limitations of conventional coatings via an "on-demand" killing strategy. The authors developed a smart, TA-based surface with a switchable function between bacteria killing and bacteria releasing based on near-infrared photothermal activation and thermal responsiveness for potential applications in the health sector. This study involved the deposition of TA-Fe3+ complexes onto the bare Au surface (Au-TA/Fe) and then grafting of poly(N-isopropylacrylamide) (PNIPAM) polymer to form the coating (Au-TA/Fe-PNIPAM) through Schiff base reaction or Michael addition. The Au-TA/Fe-PNIPAM surface showed that 90% of the attached *E. coli* on the surface after being killed photothermally were released when the temperature decreased to 4 ºC; however, the Au-TA/Fe surface released only 5% of attached bacteria. Moreover, no significant change in killing and release abilities was observed after two attach-kill-release cycles. The switchable coating was also highly stable, and after aging for 10 days in PBS, the coated substrate showed a similar antibacterial efficacy as the freshly coated substrate.[22] To prolong the application of TA-driven coatings, pH-responsive polymers have been incorporated into the TA to develop a coating with a self-release/self-cleaning strategy. Lowering the pH induced by bacteria growth is an external trigger for releasing antibacterial agents. For example, pH-responsive polymer [cationic polylysine – tannic acid - poly(2-diisopropylaminoethyl methacrylate)-b-poly(2-methacryloyloxyethyl phosphorylcholine)] (PLYS-TA-PDPA-b-PMPC) was coated on the stainless-steel substrate for antifouling and antimicrobial applications. Since the bacterial infection lowers the pH to less than 6, the protonation of the PDPA (pK_a=7.3) occurred at pH=5.5, resulting in swelling and improving the antifouling ability. In contrast, after raising the pH to 7.4, the antimicrobial resumed. After aging for 30 days in filtered seawater, the coating showed antimicrobial and antifouling properties similar to the freshly coated substrate.[23] To endow surfaces with

antibacterial activity, various bactericidal materials, such as antimicrobial peptides,[21] cationic polymers,[24,25,] and metallic nanoparticles,[26] have been introduced on surfaces via polyphenols chemistry. For instance, AgNPs-based coating can be generated within the reaction mixture from the redox reaction between oxidative tannic acid and reductive silver nitrate without additional reagents. These AgNPs-coated surfaces showed excellent antimicrobial properties against various microorganisms.[27,28] For this reason, the *in situ* generation of silver nanoparticles method is superior to other conventional techniques, such as electrochemical deposition, ion exchange, and plasma spraying, owing to its simplicity, where special equipment and energy sources are unnecessary. As a result, modification of medical devices with antifouling and bactericidal coatings is considered the first step to resist the initial adsorption of biofouling.[29]

Researchers have explored that a dip coating process to fabricate tannic acid-based coatings has the potential for scaling up at a pilot scale due to its simplicity. Jyske et al. reported that tannic acid-coated fiber networks at a pilot scale as substituents for plastics, surgical face masks, and food packaging prevented the infection of *S. aureus*, *E. coli,* and Enterovirus coxsackievirus. The authors also reported that their coatings must be developed to ensure a long-term antibacterial effect since the non-covalent bonds were the driving force between the TA and hand sheet substrate.[30] As a result, the durability of the zwitterionic polymer-based coating is a challenge during the large-scale application, even when the polymer was covalently linked to the TA.[31]

In this work, we report a simple one-pot dip-coating process for depositing TA and zwitterionic copolymers containing amine groups under oxidizing conditions to form covalent conjugation between the quinone and amino groups via the Michael addition reaction.[24] The unreacted catechol and pyrogallol groups on the as-prepared surface were used to reduce silver ions to generate AgNPs, resulting in a modified surface with antifouling and antibacterial properties

(Scheme 2.1). Three polymers with different molar ratios of MPC and AEMA [$pMPC_{100}$, $pMPC_{80}$-*st*-$AEMA_{20}$, and $pMPC_{90}$-*st*-$AEMA_{10}$] were synthesized using conventional free radical polymerization, and they are denoted as pMP, pMP8AE2, and pMP9AE1, respectively.

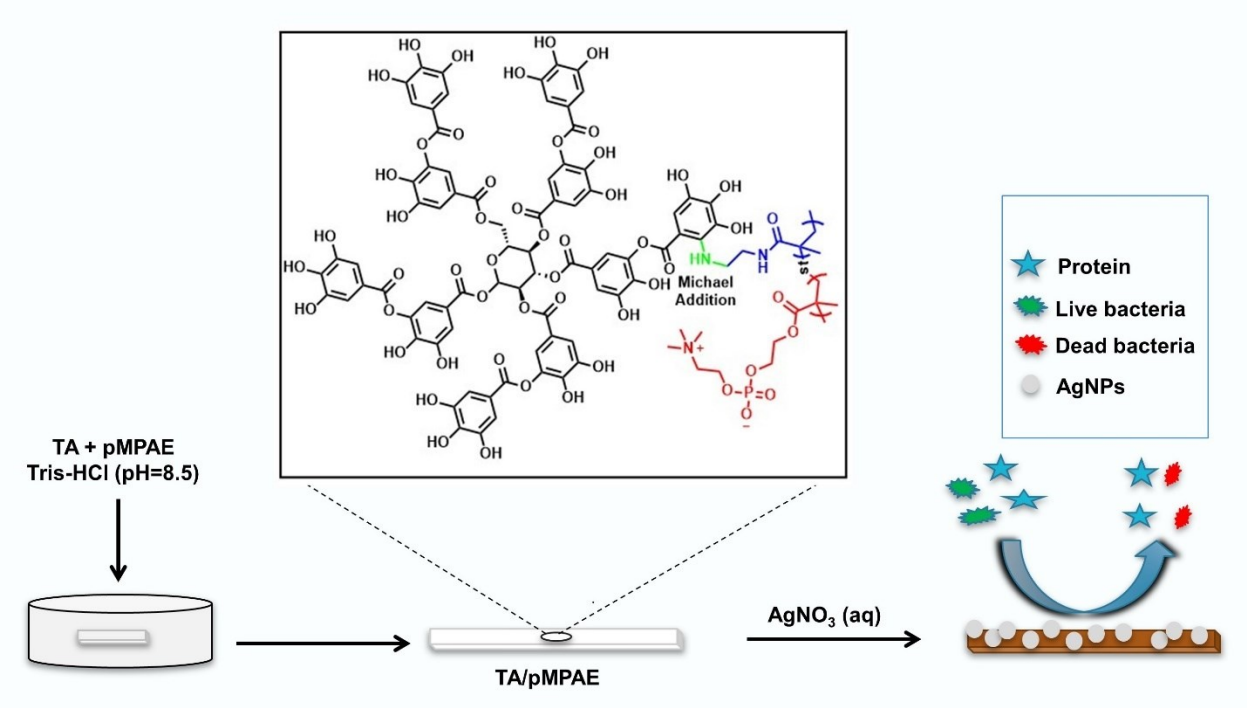

Scheme 2.1. Schematic showing the co-deposition of TA and poly(MPC-*st*-AEMA) onto glass surface followed by *in situ* generation of AgNPs. The polymer was covalently cross-linked to TA, and the coating showed antibacterial activity.

2.2. Experimental Section.

2.2.1. Materials. MPC monomer was acquired from Prof. Ishihara's lab (University of Tokyo, Japan). Azo-initiator [4,4′-Azobis(4-cyano valeric acid) (ACVA)], bovine serum albumin (BSA), Silver Nitrate ($AgNO_3$), and Tannic acid (TA) were obtained from Sigma-Aldrich. Micro BCA™ Protein Assay Kit was purchased from Fisher Scientific. *N,N*-dimethylformamide (DMF), Sodium dodecyl sulfate (SDS), Ethylene diamine (EDA), Isopropanol, Methacrylic anhydride, and Dimethyl sulfoxide (DMSO) were obtained from Caledon Laboratories Ltd. (Canada).

2.2.2. Synthesis of Zwitterionic Polymers. Free radical polymerization was used to synthesize homopolymer (pMP) and copolymers (pMP9AE1 and pMP8AE2) by combining MPC and AEMA monomers at molar ratios of (100/0, 90/10, and 80/20), respectively, using 4,4′-Azobis(4-cyano valeric acid) (ACVA) as an initiator.

2.2.2.1. Synthesis of pMP. In a 50-ml polymerization tube, MPC monomer (600 mg, 2.03 mmol) and ACVA (6.25 mg, 0.0223 mmol) were dissolved in a solvent mixture of DI water and DMF, and then the tube was sealed with a rubber septum. The reaction mixture was degassed under nitrogen for 30 min, and the reaction vessel was transferred to an oil bath and heated at 70 °C with continuous stirring. The polymerization reaction was allowed to continue for 24 h and stopped by quenching in liquid nitrogen. The crude homopolymer was then dialyzed against distilled water using a cellulose membrane (MWCO 12 kDa) for three days to remove the residual monomer and solvent. The purified polymer (pMP) was finally obtained by drying the resultant using lyophilization for three days.

2.2.2.2. Synthesis of pMP9AE1. MPC monomer (659 mg, 2.23 mmol), and AEMA monomer (41 mg, 0.25 mmol) were mixed in a tube of polymerization, and ACVA (6.95 mg, 0.0248 mmol) was dissolved in 0.5 mL of DMF and added to the mixture. Mixed solvents of DI water and DMSO were added to the reaction tube. The rest of the protocol steps were the same procedure indicated above. The structures and molecular weights of the synthesized polymers were characterized by ^{1}H NMR and Viscotek conventional gel permeation chromatography (GPC), respectively.

2.2.3. Surface Modification using Co-deposition of TA and Polymer. A solution of TA (2 mg/mL) and polymer (5 mg/mL) was prepared using 10 mM Tris-HCl buffer solution (pH 8.5) and then shaken by hand for 1 min. The glass substrates were soaked in the solution, followed by

shaking by a shaker for 10 h at RT. Finally, the modified glass coverslips were removed, washed gently with deionized water, and dried at RT to give the substrates (TA, TA/pMP, TA/pMP8AE2, and TA/pMP9AE1). The coated glass slides were immersed in a well plate containing silver nitrate solution (8 mg/mL). The well plate was kept in the dark at RT for 18 h. The *in situ* AgNPs-coated surfaces were rinsed thoroughly with diH2O before being air-dried to obtain the substrates (TA/Ag, TA/pMP/Ag, TA/pMP8AE2/Ag, and TA/pMP9AE1/Ag).

2.2.4. Surface Characterization. Attenuated total reflectance Fourier transform infrared (ATR-FTIR) spectroscopy using an Agilent Technologies Cary 600 Series FTIR spectrometer was utilized to investigate the chemical structures of the pristine propylene and TA/polymer-coated propylene surfaces. Atomic force microscopy (AFM) in PeakForce tapping mode and under dry conditions was employed to measure the morphology and roughness of the modified substrates. Zeiss Sigma Field Emission scanning electron microscopy (FESEM), operated in high vacuum and variable pressure modes, was used to observe silver nanoparticle morphology. Bruker energy dispersive X-ray (EDX) system with a resolution of 123 eV was used to collect EDX spectra of AgNPs-coated substrates. To investigate the hydrophilicity of the substrates, the water contact angle (WCA) of every modified surface and the control were measured using a contact angle goniometer equipped with a camera to capture the water droplets.

2.2.5. Protein Adsorption on Functionalized Substrates. Using a BCA protein assay kit, bovine serum albumin (BSA) was employed to evaluate the antifouling properties of bare and TA/polymer-modified glass slides.[32,33] Briefly, 0.5 mL of BSA solution was incubated on each sample for 2 h at 37 °C, followed by rinsing with DI water to remove the loose protein. Subsequently, a solution of SDS (2 mg/mL) was added to the control and modified surfaces before shaking the well plate for fifteen minutes using an ultrasonic cleaner to separate the

adsorbed BSA on each sample. The protein extracts were then transferred to a 96-well microplate with an equal volume of BCA reagent. The plate was then incubated at 37 °C for 2h before measuring the absorbance at 570 nm using a Tecan GENios Pro microplate reader. The concentration of adsorbed protein was calculated according to the standard curve. The experiment was conducted in triplicate for all the samples.

2.2.6. Antibacterial Properties of the AgNPs-coated Substrates. Having identified the protein-resistant property of our coatings, we next assessed the bacteria-killing activity of the bare glass and AgNPs-modified glass substrates against the gram-negative *E. coli* (ATCC 25922, USA) and gram-positive *S. aureus* (ATCC 25923, USA). For this, pre-mixed LB and TS agar powders were used to prepare nutrient-rich culture media following the instructions outlined by the manufacturer. Subsequently, *E. coli* and *S. aureus* single colonies were collected from LB and TS agar plates using a sterile pipette tip and then put into tubes containing 25 mL of autoclaved LB and TS buffer solutions. To allow an aerobic culture of bacteria, the tube caps were loosened before putting the tubes into a shaking incubator for 16 h at 37 °C. A centrifuge instrument set on 4000 revolutions per minute (rpm) and for 5 minutes was used to centrifuge the tubes containing cultured bacteria thrice by replacing the supernatants with fresh PBS media. After centrifuging the bacterial suspensions, the collected bacteria were dispersed in a volume of PBS solution to obtain bacterial populations with optical densities (OD_{600}) of 0.15, corresponding to about 8 x 10^9 cells/mL.

2.2.6.1. Inhibition Zone Test. A zone-of-inhibition test was first employed to investigate the antibacterial activity of AgNPs-loaded coatings against *E. coli* and *S. aureus*. Briefly, 30 µl of each bacteria suspension, with a concentration of 8×10^9 cells/mL, was spread onto sterile LB and TS agar plates using a plastic spreader. Afterward, the controls and AgNPs-modified

substrates were placed onto the agar plates and incubated at 37 °C. After 24 h of incubation, the presence of inhibition zones surrounding the substrates was observed and imaged using a digital camera.

2.2.6.2. Growth Curve Assay. The impact of silver-coated surfaces on the growth of *E. coli* and *S. aureus* bacteria, with a concentration of approximately 8 x 10^9 cells/mL, was investigated using the growth curve assay and following the methodology reported elsewhere.[34] (further details can be found in the Supplementary Information section).

2.2.7. In vitro Cell Viability Assay. The cell growth on the coating extracts was evaluated by placing the coating substrates in a well plate containing DMEM media (100 μL in each well) for 24 h. Each coating extract and fresh DMEM medium (as a control) were then incubated with the precultured normal human lung fibroblast cells (RMC-5) in a culture plate for 48 h and tested by MTT assay as per our published report protocol.[35]

2.3. Results and Discussion.

2.3.1. Synthesis of Copolymer, P(MPC-st-AEMA). 2-aminoethyl methacrylamide hydrochloride monomer (AEMA) was prepared as per the procedure reported previously by our group.[26] The ^{1}H NMR spectrum of AEMA was recorded using D_2O as a solvent to confirm the chemical structure (**Figure S2-1**). Subsequently, we used the conventional free-radical polymerization technique to synthesize the homopolymer (pMPC) and the statistical copolymers *p*(MPC_{80}-*st*-$AEMA_{20}$) and *p*(MPC_{90}-*st*-$AEMA_{10}$). **Figures (2.1a and 2.1b) show** the reaction routes for the as-prepared polymers, and **Figures S2-2 and S2-4** show their ^{1}H NMR spectra recorded on a Varian spectrometer using D_2O as a solvent. The molar ratios of AEMA content were calculated from the spectra to be 18% and 10% in the copolymers pMP8AE2 and pMP9AE1, respectively**.** These calculations were achieved by comparing the proportional

integral intensities of CH_2 signals appearing at 3.75 ppm in the MPC backbone and 3.10 ppm in the AEMA chain (**Table 2.1)**.

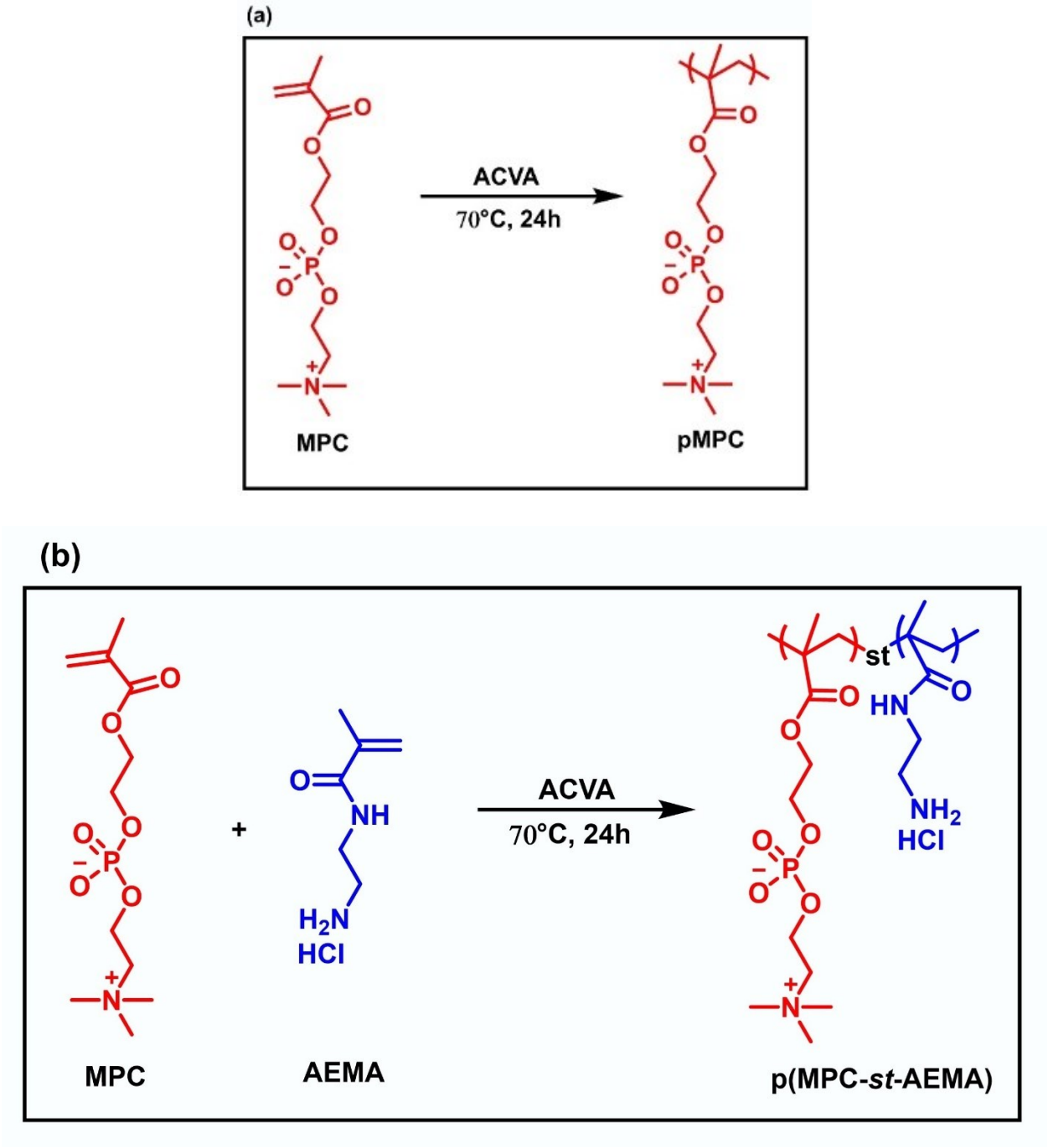

Figure 2.1. Synthetic route for the polymers (a) *p*MPC and (b) *p*(MPC-*st*-AEMA).

Table 2.1. Chemical Compositions and Molecular Weights of the Synthesized Polymers

	Composition of copolymer (mole %)		molecular weight	
polymer	MPC:AEMA[a]	MPC:AEMA[b]	M_n (10^4)	PDI
pMP	100:0	-	2.04	2.0
pMP8AE2	80:20	82:18	2.34	2.5
pMP9AE1	90:10	90:10	2.58	2.6

[a]Feed molar ratio. [b]Molar ratio calculated from ^{1}H NMR spectra. [c]Obtained by aqueous GPC.

2.3.2. Surface Characterization. To confirm the grafting of TA onto the pristine propylene (PP) surface, we conducted ATR-FTIR measurements as part of our study. Analysis of the ATR-FTIR spectra (**Figure 2.2)** revealed the presence of new peaks in the TA-coated PP surface, distinguishing it from the original PP substrate. The appearance of a broad peak between 3600 and 3100 cm^{-1} in the spectrum can be attributed to the stretching vibration of the −OH groups, resulting from the abundant presence of phenol groups in TA. The absorption peak at 1643 cm^{-1} indicates the stretching vibration of the C=O bond in the phenolic ester groups.[36] The frequency at 1554 cm^{-1} corresponds to the stretching vibration of the C=C bond in the aromatic ring.[37] The peak at 1518 cm^{-1} can be attributed to the in-plane bending of the hydroxyl group bonded to a carbon atom (C-O-H). The absorption at 1380 cm^{-1} represents the stretching vibration of the C-O bond.[38] After TA/pMP80AE20 coating on PP, the intensity of characteristic peaks of the PP surface slightly reduced. The absorption at 1280 cm^{-1} corresponds to the stretching vibration of the C-N bond. The absorption at 1145 cm^{-1} arises from the C-O-C bond in polymer and TA.[39] The peak observed at 1527 cm^{-1} is attributed to the bending of the secondary N-H bond,

indicating the occurrence of Michael's addition product.[40]

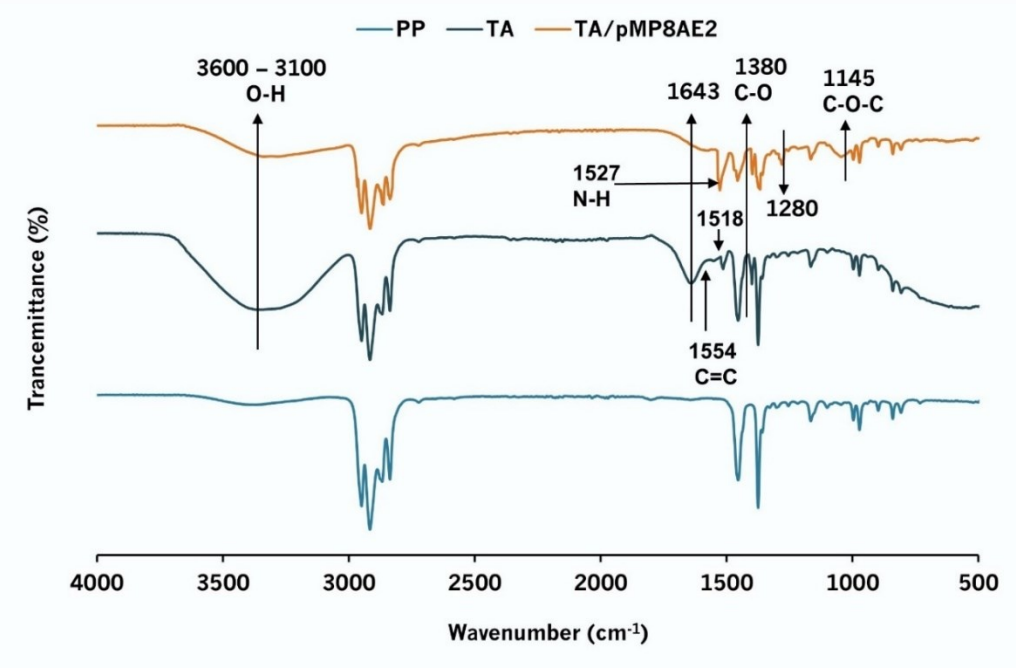

Figure 2.2. FTIR spectra for PP, PP/TA, and PP/TA/pMP8AE2

2.3.3. Surface Morphology. The surface morphologies of our coatings were determined using Atomic Force Microscopy (AFM) in noncontact tapping mode under dry conditions. The analysis was conducted to compare the surface characteristics of the control glass surface with that of TA/polymer-coated surfaces (**Figure 2.3**). The AFM images showed that the root-mean-square (RMS) roughness values ranged from 0.51 to 0.37 nm. These values may indicate the formation of uniform and smooth polymeric coating surfaces, which could be attributed to the hydrophilic state of the coatings[2] and the gradual covering of the whole substrates.[19] As shown in **Figure 2.**3, the control bare glass surface had a relatively low smooth surface, with an RMS roughness value of 1.25 nm. In contrast, the surface coated with TA was smoother, with an RMS value of 0.51 nm. The co-deposition of TA with zwitterionic polymers led to a decrease in the RMS (**Table S2-1**).[41] This indicates that the polymers were successfully bound with TA and grafted on the surfaces, forming highly smooth surfaces.

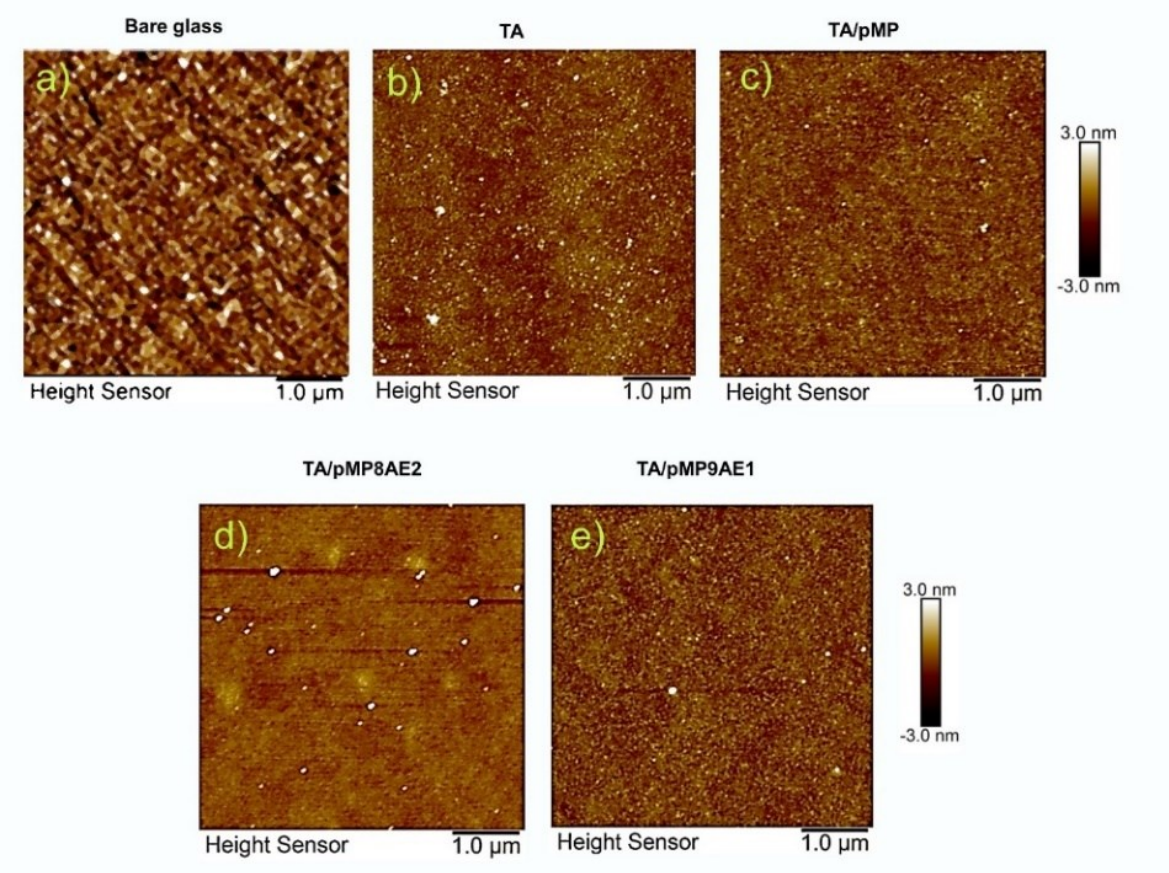

Figure 2.3. AFM images of (a, b) bare glass and TA-covered glass (as controls) and (c, d, e) polymer-covered glass.

Coatings with AgNPs were achieved by immersing all the modified surfaces in an aqueous solution of silver nitrate. After 18 hours of coating, the appearance of colorless TA/polymer-coated surfaces turned brown, as shown in **Figure S2-5**. This color change strongly indicated the in-situ generation of silver nanoparticles. The transformation in color is attributed to the presence of tannic acid (TA), which acts as a reducing agent, facilitating the reduction of silver ions to form silver nanoparticles (AgNPs).[18,42] Next, SEM and EDX techniques were used to examine the morphology and elemental composition of surfaces loaded with silver nanoparticles (AgNPs). The SEM images in Figure 2.4 provided visual evidence of the successful formation of AgNPs, displaying small particles of AgNPs in the samples.[43] Moreover, it was observed that

more nanoparticles with smaller diameters covered the TA/Ag and TA/pMP surfaces. These results are consistent with the percentages of silver from EDX, as shown in **Figure S2-6** and Table S2-2. The EDX results indicated that the control TA/Ag and TA/pMP coatings exhibited the highest percentages of the silver element compared to the surfaces covered with copolymers. This high silver content can be explained by many catechol groups on the TA layer that reduce silver ions into AgNPs.[44] By contrast, the amino groups on copolymer coatings can bind covalently with TA, resulting in fewer catechol groups and less amount of AgNPs on the surfaces. As expected, the EDX results for pMP8AE2/Ag coating, with the highest ratio of AEMA content, showed that this coating had the lowest percentage of AgNPs, which could be ascribed to the low number of catechol groups available to reduce silver ions.

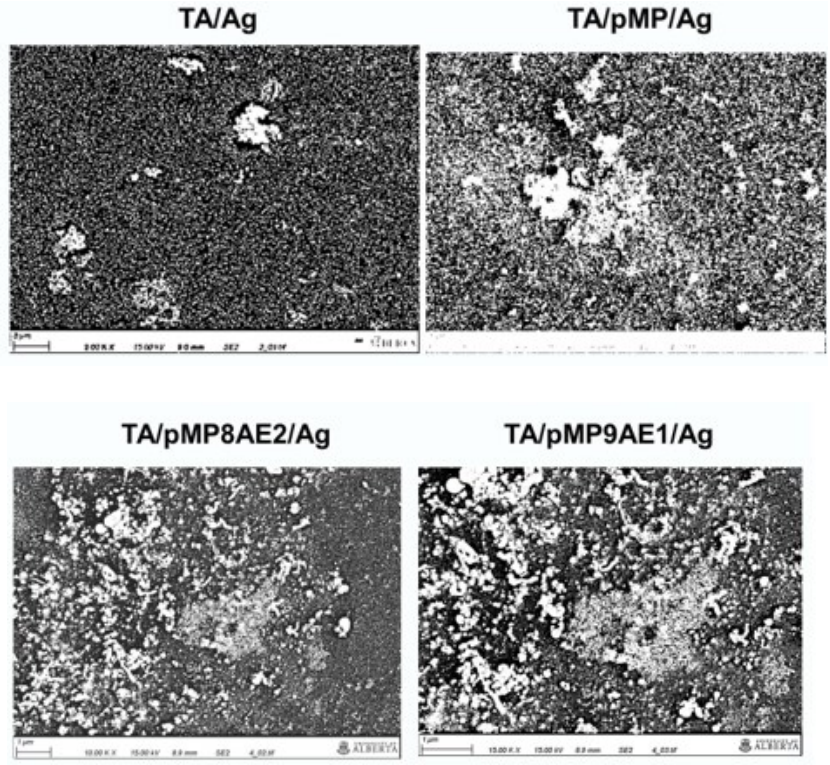

Figure 2.4. SEM images of AgNPs-loaded coatings [TA/Ag, TA/pMP/Ag, TA/pMP8AE2/Ag, and TA/pMP9AE1/Ag]

2.3.4. Surface Hydrophilicity. Surface wettability plays a crucial role in surface biocompatibility and antifouling ability. Zwitterionic polymers have gained recognition as promising materials for their potential as antifouling agents due to their ability to create hydration shells through electrostatic interactions, forming more compact and closely bound water layers.[45,46] The static water contact angles (WCAs) of the bare glass and polymer-coated glass surfaces were measured To assess the surface wettability (**Figure 2.5)**. The initial contact angle of the uncoated glass surface was measured to be 37 ± 0.5°. However, after applying a coating of tannic acid (TA), the contact angle significantly decreased to 13.9 ± 1.5°. More importantly, when TA was co-deposited with zwitterionic copolymers, there was a remarkable drop in the water contact angle (WCA) to less than 5°. This drop in WCA indicates a substantial improvement in the hydrophilicity of the surfaces. Among these coated surfaces, the TA/pMP9AE1 combination exhibited a low contact angle, in which the water droplet spread entirely on the glass slide. These findings are consistent with the protein adhesion assay results in **Figure 2.6**, demonstrating a remarkable antifouling performance of the TA/pMP9AE1-coated surface, achieving nearly 93% effectiveness.

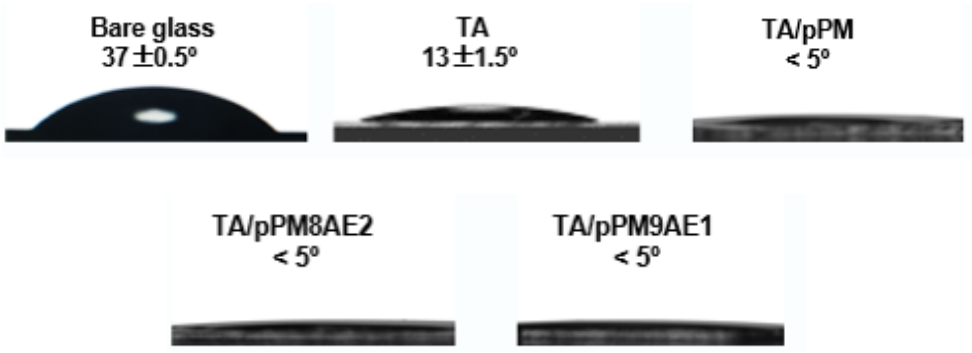

Figure 2.5. WCA for bare glass, TA, TA/pMP, TA/pMP8AE2, and TA/pMP9AE1

2.3.5. Protein Adsorption. To quantify the adsorbed protein on our coatings, we employed a BCA protein assay using BSA as a standard for protein quantification due to its enhanced non-

specific adhesion to a wide range of surfaces, which promotes bacterial adhesion.[20,47] We selected BSA as a versatile, non-specific adhesive protein because it can bind to surfaces with positive and negative charges. BSA is negatively charged at neutral pH and expected to be repelled by opposing surfaces; however, its adsorption on the negatively charged was observed where the predominant interactions are expected to be hydrogen bonding or hydrophobic interaction. While both negatively and positively charged surfaces proved to have a similar quantity of adsorbed BSA, the initial kinetic adsorption rate of BSA for positively charged surfaces is faster than for negatively charged surfaces.[48] As shown in **Figure 2.6**, the bare glass surface exhibited the most significant amount of adsorbed BSA by 2.9 μg/cm^2, consistent with its highest RMS value measured by AFM spectroscopy (**Table S2-1**). However, the surface antiadhesion performance significantly improved after polymer coating the surfaces. These polymer coatings showed variations in the amount of adsorbed protein depending on the molar ratio contents of the polymer. For example, the protein amounts adsorbed on pMP8AE2 (0.7 μg/cm^2) and pMP9AE1 (0.21 μg/cm^2) surfaces are lower than that on the pMP coating (1.28 μg/cm^2). This phenomenon can be explained by the pMP interacting with TA through noncovalent interactions, including phenol-phospholipid hydrogen bonding and cation-π interactions,[49]. At the same time, AEMA moieties may promote the grafting of copolymers on the surfaces via the Michael addition reaction, which may increase the grafting density and the stability of zwitterionic moieties on the coatings containing copolymers[50]. On the other hand, high AEMA content on pMP8AE2 coating may facilitate more electrostatic interactions between the cationic amino groups of AEMA and the anionic charges of BSA at pH 7.4, resulting in higher adsorbed protein compared to pMP9AE1 substrate. This is consistent with the study that demonstrated that high AEMA content increases the positive charges, so less AEMA (9:1) is

optimal for antifouling property over 8:2 content and the homopolymer.[51] Additionally, the pMP9AE1-coated surface with a higher content of zwitterionic polymer-containing positive and negative charged moieties may create a strong hydration layer on the top of the surface, resulting in more protein resistances.[19]

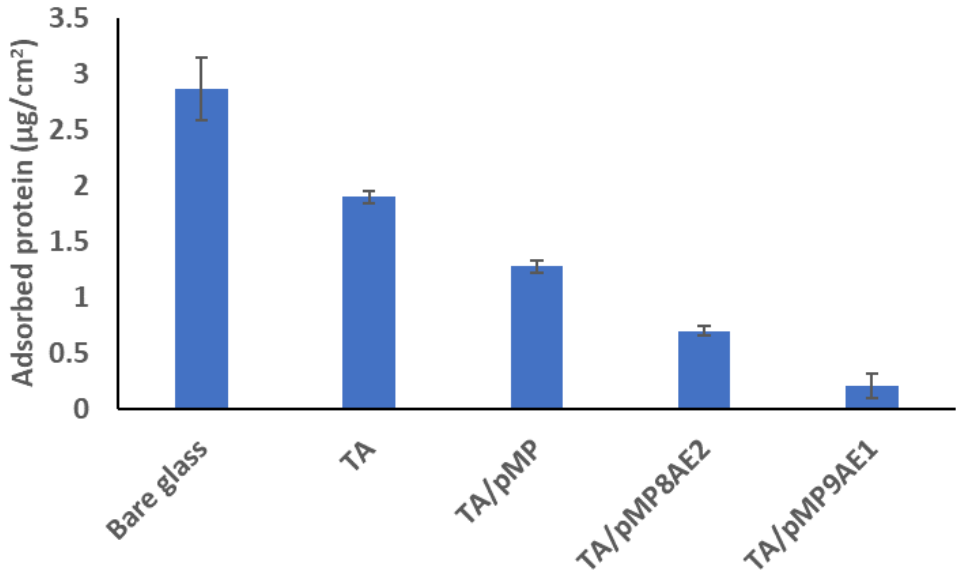

Figure 2.6. *In vitro* protein adsorption on glass, TA, TA/pMP, TA/pMP8AE2, and TA/pMP9AE1.

2.3.6. Antibacterial Activity of Coatings. The inhibitory effects for the controls (bare glass and glass/TA) and AgNPs-coated surfaces against *E. coli* and *S. aureus* were initially evaluated using the inhibition zone test. In brief, the control slides and AgNPs-loaded coatings were placed in direct contact with the agars containing the bacteria for up to 24 h. The images in **Figure 2.7** showed that all the samples coated with silver were surrounded by inhibition zones against *E. coli* and *S. aureus*, indicating the suppression of bacterial growth on these substrates. In contrast, the lack of antibacterial activity of the controls against both bacteria was qualitatively confirmed by the absence of bacterial inhibition zones around the bare glass and tannic acid surfaces.

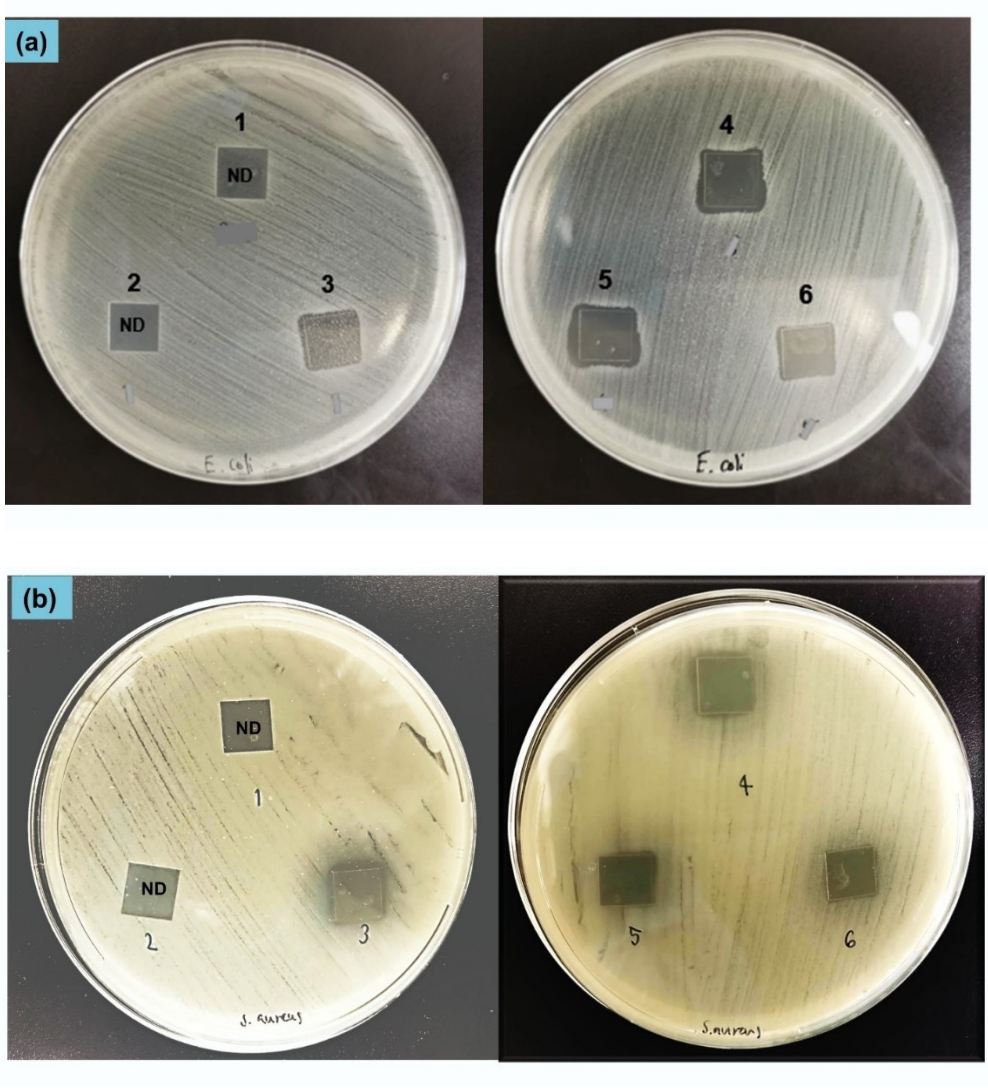

Figure 2.7. Photographs of the inhibition zones against (a) *E. coli* and (b) *S. aureus,* for (1) bare glass, (2) TA, (3) TA/Ag, (4) TA/pMP/Ag, (5) TA/pMP9AE1/Ag, and (6) TA/pMP8AE2/Ag.

To investigate the effect of AgNPs releases from the coatings, we further evaluated the growth of bacteria on the modified surfaces using the growth-inhibition test. As shown in Figure 2.8a, the growth rate of *E. coli* at 24 h of incubation of bare glass was measured to be high, with an OD value of 1.30. By contrast, *E.coli* growth on all AgNPs-modified surfaces exhibited only OD values of 0.05 during the initial six hours of incubation, indicating slow growth of the bacteria compared to bare glass, which could be attributed to the ability of a coating to release a relatively

large amount of silver.[35,52] There was a slight increase in growth rate at 24h, but the bacterial growth values were still less than that on the control. Figure S2-7 shows that the turbidity of bacterial suspensions of bare glass after 6h of incubation can be observed slightly more than the turbidity appearances of AgNPs-loaded surfaces. The higher the bacteria growth, the more visible the cloudy appearance of the turbidity. Moreover, it is worth noting that the TA/pMP9AE1/Ag surface demonstrated the lowest OD value of only 1.00, indicating relatively limited growth of *E. coli* on this surface. This OD value was lower than the observed growth value (1.15) on TA/pMP8AE2/Ag coating. One potential reason for the decreased *E. coli* growth on TA/pMP9AE1/Ag is the high content of released AgNPs; the explanation is consistent with EDX results in Table S2-2. Also, the decreased growth of *E. coli* on the TA/pMP9AE1/Ag coating can also be explained by the increased hydrophilicity imparted by the presence of a higher content of MPC moiety that prevents the adhesion of bacteria and the debris of dead bacteria, leading to better bactericidal activity. A similar phenomenon for *S. aureus* (Figure 2.8b) is that the OD values during the first ten hours of incubation on AgNPs-loaded surfaces were only 0.12. The figures moderately increased after 24 h of incubation, with the lowest OD value of 1.20 for TA/pMP9AE1/Ag coating, which was still lower than the growth rate observed for the bare glass surface (OD =1.44). Generally, The coatings release the bactericidal agent over a short time, making them suitable for short-term surgical applications, where a high-dose release is desirable during the early period of implant insertion.[53] The coatings were expected to diffuse the agent into the aqueous medium rapidly since the agent was loaded without any chemical interactions with the polymer matrix.[54] Moreover, AgNPs-loaded coatings exhibited antibacterial properties against gram-positive S. aureus for longer than the gram-negative *E. coli*. These findings were mainly due to the differences in bacterial cell wall structure. Gram-negative

bacteria have an additional outer membrane composed of lipopolysaccharides and proteins, compared with gram-positive bacteria.[52] The results align with the antibacterial properties marked in the inhibition zone assay and support the potential of using TA/pMP9AE1/Ag coating as an effective agent in preventing bacterial growth.

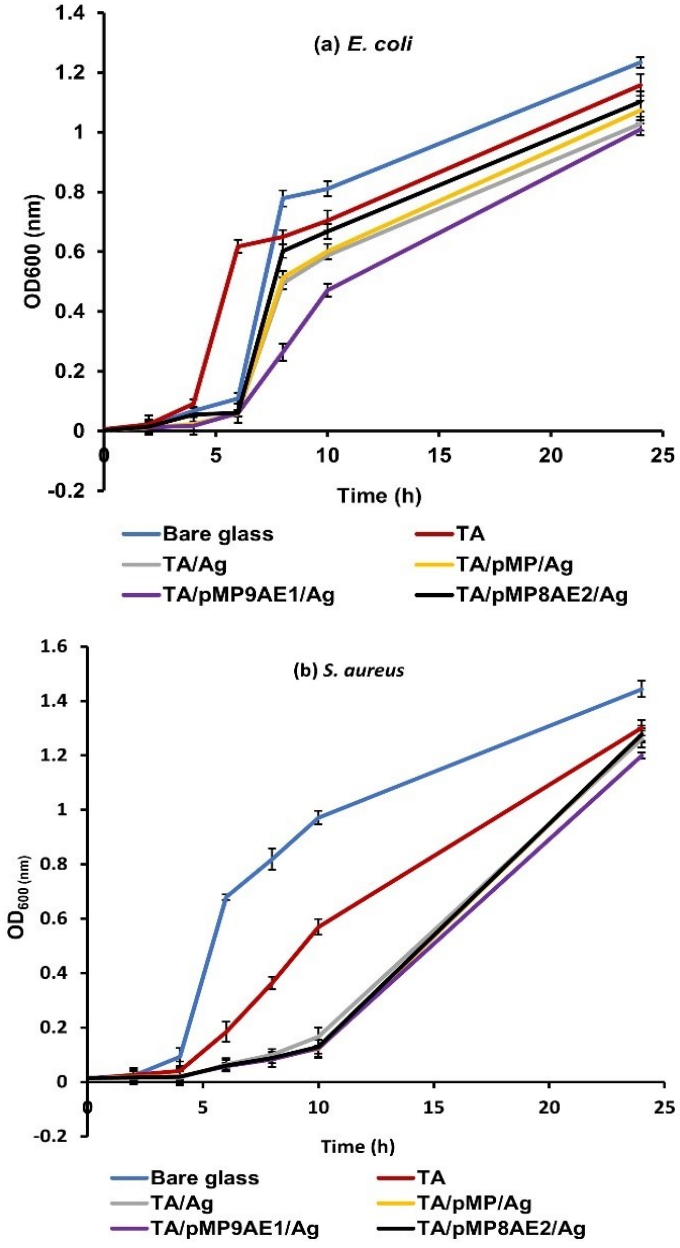

Figure 2.8. Growth curves of (a) *E. coli* and (b) *S. aureus* were treated with glass, TA-coated glass (controls), and AgNPs-coated surfaces.

2.3.7. Cell Cytotoxicity. The cytotoxic effect of the supernatants of silver-free and silver-coated surfaces on normal human lung fibroblast cells (MRC-5) was assessed via the MTT assay. To that end, MRC-5 cells at a density of 6 x 10^3 cells per well were incubated for 24 h with the culture media or coating extracts and then used to evaluate the cell viability. As shown in Figure 2.9a and as expected, the silver-free coatings showed no toxic activity on MRC-5 cells. TA/pMP, TA/pMP9AE1, and TA/pMP8AE2 coatings all promoted cell proliferation and exhibited favorable cell viability compared to the control. We also assessed the cell toxicity of AgNP-based coatings, as shown in Figure 2.9b. The control TA/AgNPs coating exhibited slightly lower cell viability, ~ 84%. This reduction in cell survival could be due to the high number of catechol groups on the surface, promoting the formation of AgNPs and, subsequently, making the surface slightly more toxic to the cells. These findings are consistent with the EDX results where the TA/AgNPs-grafted surface had the highest silver element. On the other hand, TA/polymer/AgNPs coatings were found to have less silver, which may contribute to the increased cell growth on these surfaces compared to TA/AgNPs coating. Our coatings generally showed negligible cytotoxicity to normal human lung fibroblast cells (MRC-5). According to ISO 10993-5, percentages of cell viability above 80% are considered non-cytotoxic, those within the range 80%–60% are considered weak, percentages falling between 60%–40% are regarded as moderate, and values below 40% are regarded as strong cytotoxic.[55] Based on *in vitro* data, our coatings demonstrate suitability for biomedical applications. However, *in vivo* studies are required to confirm their true potential.

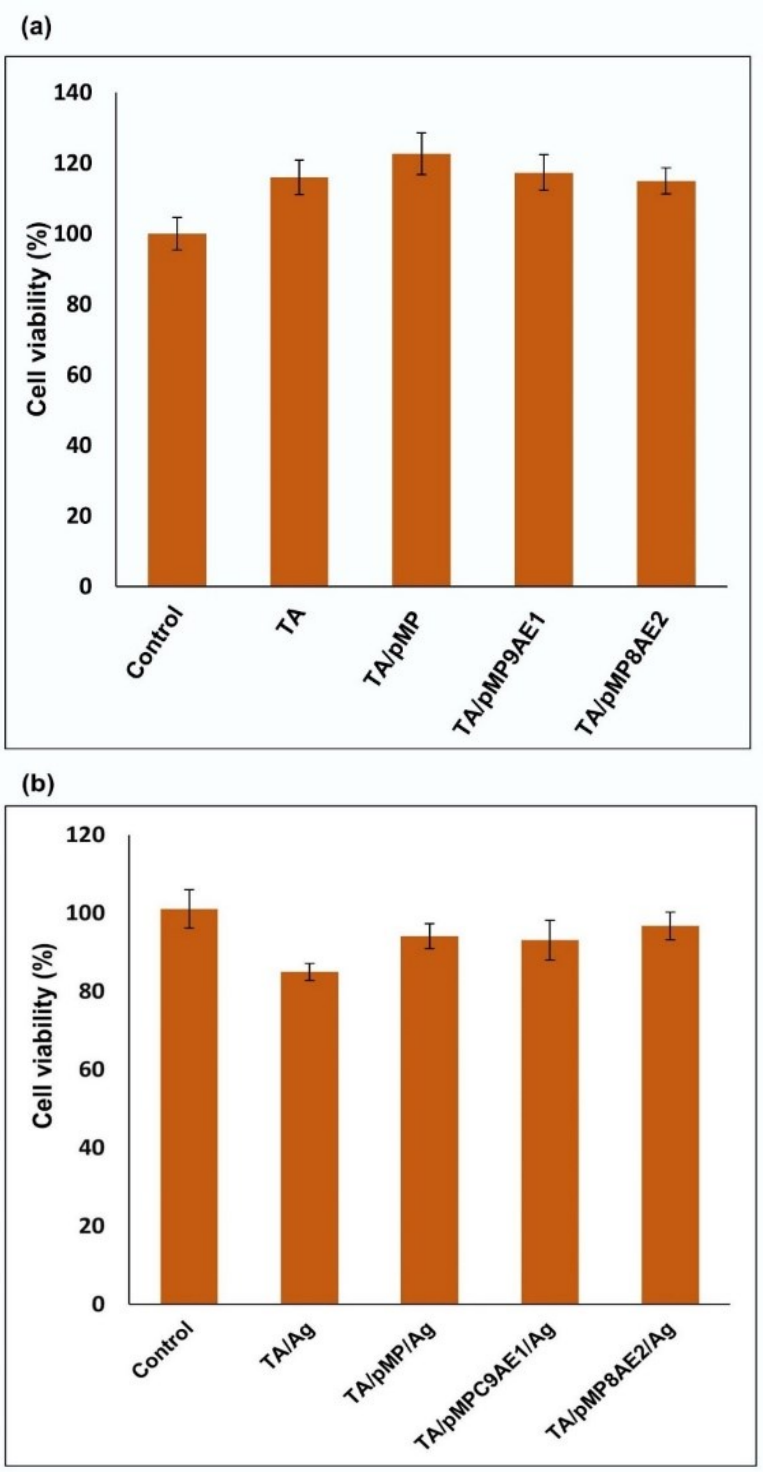

Figure 2.9. Cytotoxic effects of (a) TA, TA/pMP, TA/pMP9AE1, and TA/pMP8AE2 (b) control, TA/Ag, TA/pMP/Ag, TA/pMP9AE1/Ag, and TA/pMP8AE2/Ag coating extracts on MRC-5 cells.

2.4. Conclusion.

A dip-coating technique was employed for a uniform coating by simultaneously depositing TA and p(MPC-*st*-AEMA). The subsequent *in situ* reduction of silver ions enabled the formation of silver nanoparticles directly on the coated surface. In this process, the tannic acid (TA) covalently bonded to the copolymer and facilitated the binding of coating materials to the surfaces. The anti-adhesion property of the as-prepared coatings was challenged with bovine serum albumin protein (BSA), and the antibacterial effect was challenged with Gram-negative bacteria (*E. coli*) and Gram-positive bacteria (*S. aureus*). The resulting TA/pMP9AE1 coating, with silver nanoparticles embedded within the coating matrix, exhibited desired antifouling and antibacterial properties and reliable biocompatibility. Thus, the proposed surface modification is potentially useful as an effective and biocompatible antifouling coating for biomedical applications.

2.5. Supporting Information.

2.5.1. Synthesis and Characterization of Monomer [AEMA].

The monomer [AEMA] was synthesized following our previously published report.[56] The chemical structure was characterized by the ^{1}H NMR spectrum recorded on a Varian 500 MHz spectrometer in D_2O (**Figure S2-1**).

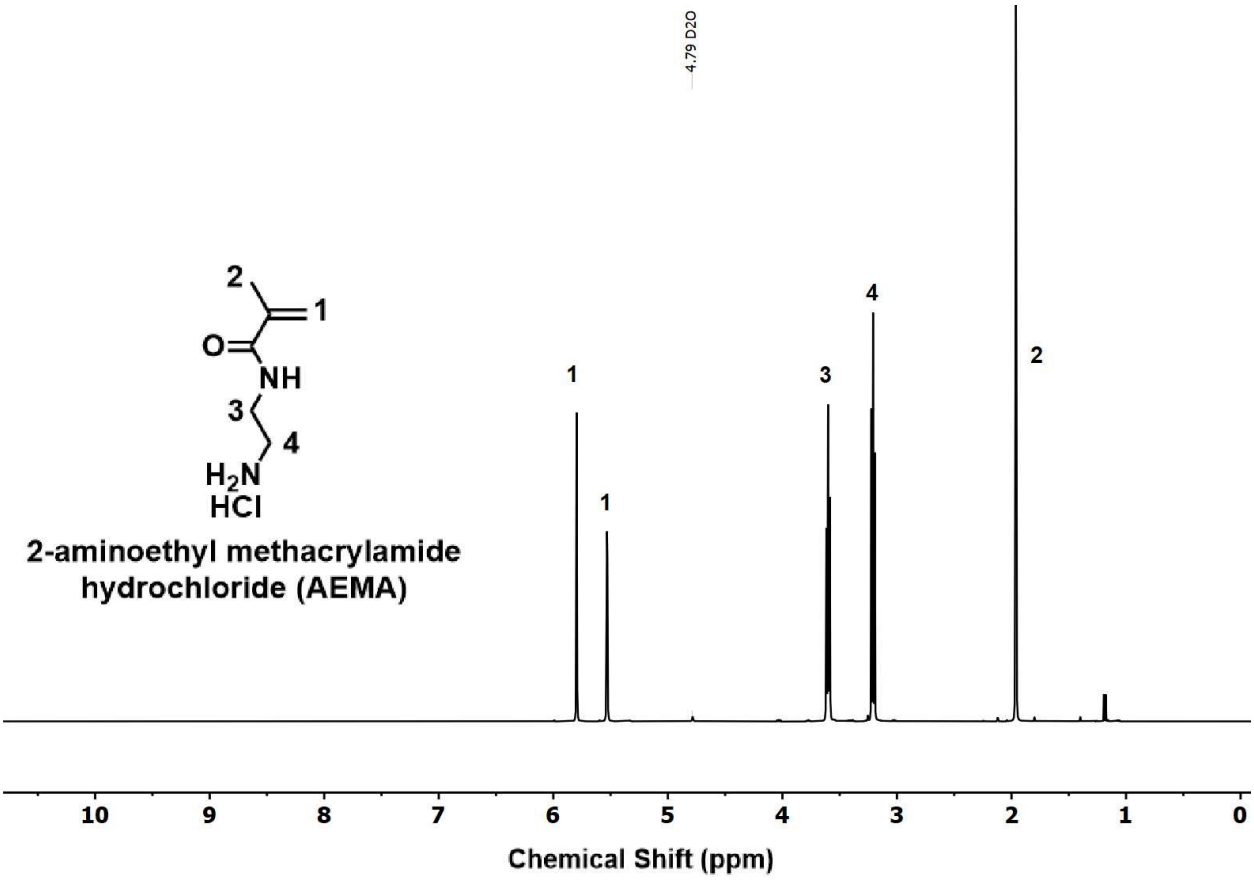

Figure S2-1: ^{1}H NMR spectrum of 2-aminoethyl methacrylamide hydrochloride monomer (AEMA).

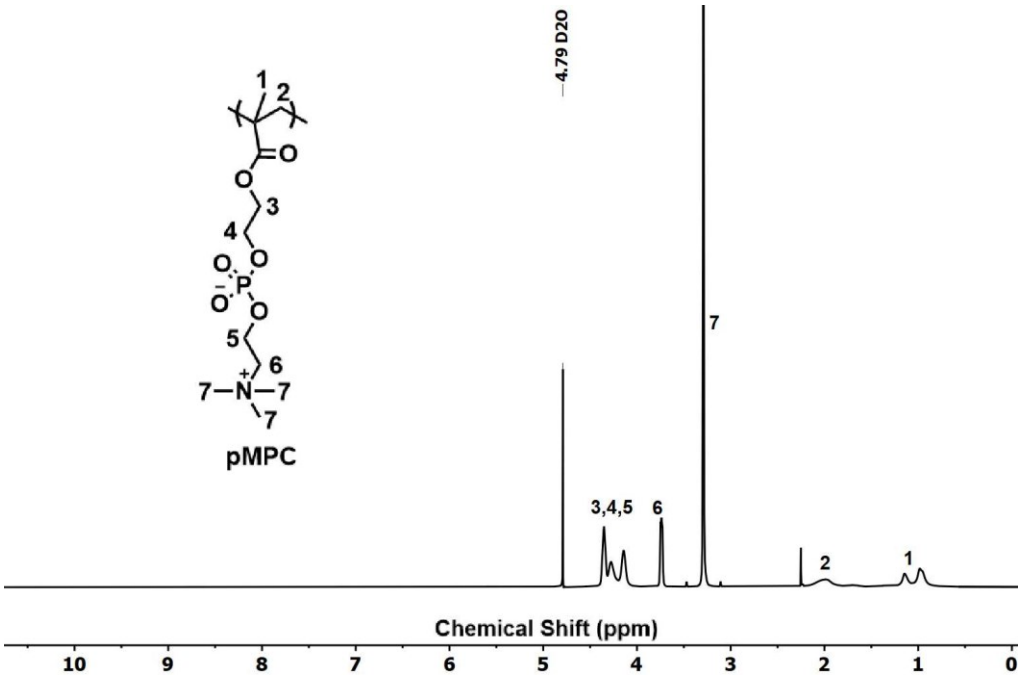

Figure S2-2: ^{1}H NMR spectrum of 2-methacryloyloxyethyl phosphorylcholine homopolymer (polyMPC) (500 MHz, D_2O).

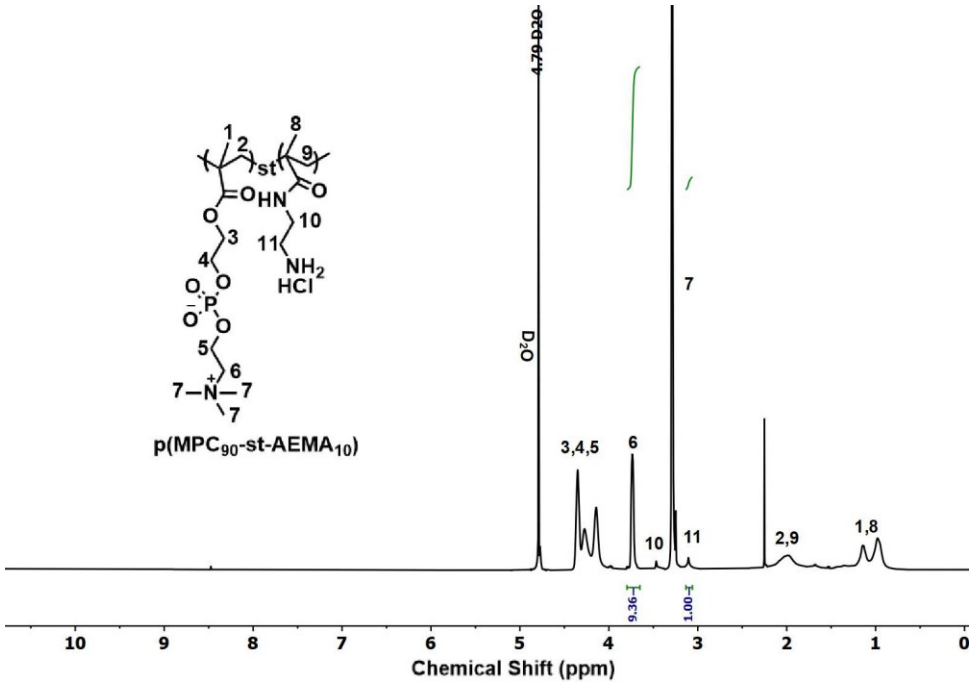

Figure S2-3: ^{1}H NMR spectrum of statistical copolymer p(MPC_{90}-*st*-$AEMA_{10}$) (500 MHz, D_2O).

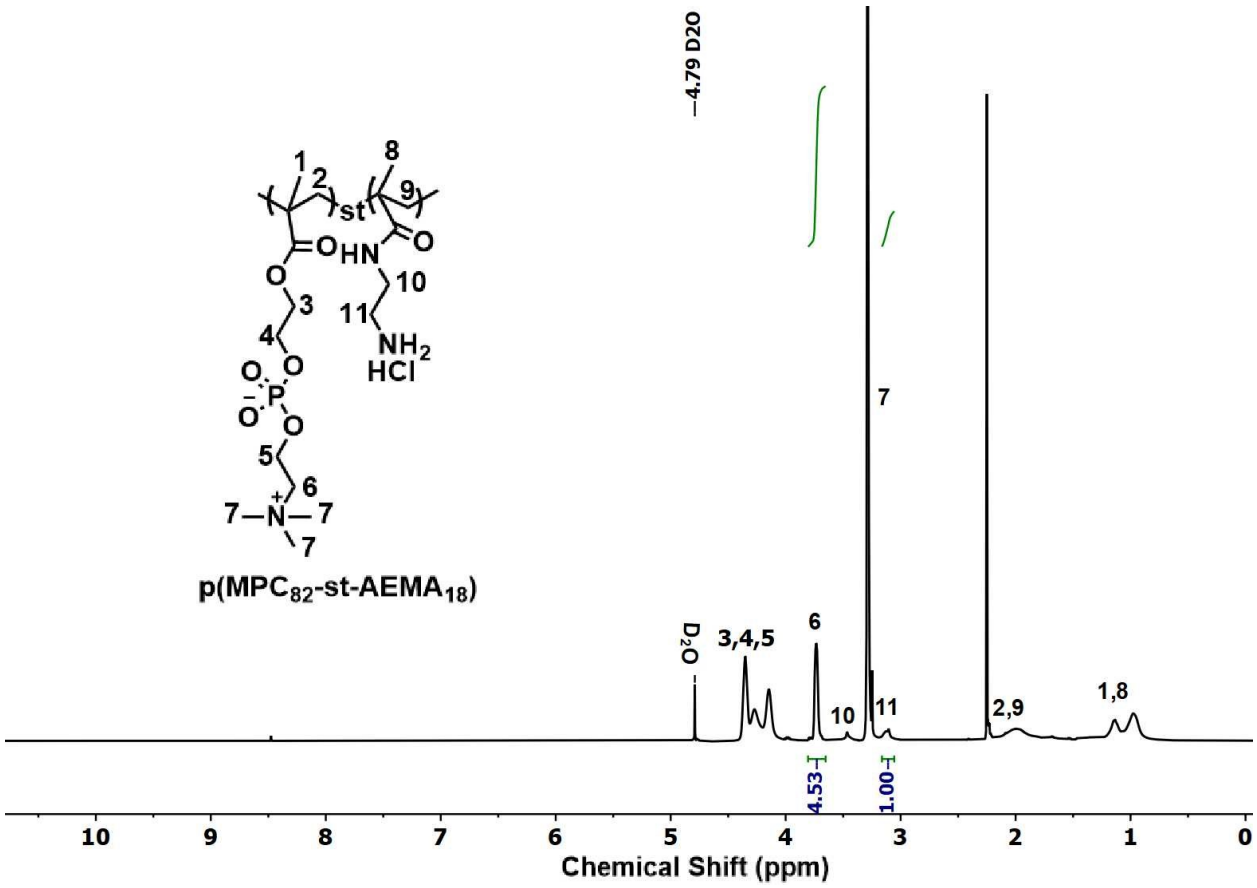

Figure S2-4: ^{1}H NMR spectra for statistical copolymer p(MPC$_{82}$-*st*-AEMA$_{18}$) (500 MHz, D_2O).

Sample	RMS Value (nm)
Bare glass	1.250
TA	0.510
TA/pMP	0.373
TA/pMP8AE2	0.303
TA/pMP9AE1	0.371

Table S2-1. Root-mean-square (RMS) in nanometer (nm) measurements using atomic force microscopy (AFM) for the bare glass, TA-coated glass, TA/pMP, TA/pMP8AE2, and TA/pMP9AE1.

Figure S2-5: photographic images for glass slides coated by TA, TA/pMP9AE1, and TA/pMP9AE1/Ag.

Sample	C (%)	O (%)	Na (%)	Mg (%)	Si (%)	Cl (%)	Ca (%)	Ag (%)
TA/Ag	2.80	13.29	2.41	0.68	9.48	-	2.33	69.01
TA/pMP/Ag	3.28	17.86	2.86	0.71	7.37	-	2.20	65.72
TA/pMP8AE2/Ag	9.61	28.18	6.37	1.52	23.03	0.77	5.61	24.91
TA/pMP9AE1/Ag	5.32	27.01	5.04	1.16	16.28	-	4.46	40.73

Table S2-2. Elemental composition percentages (%) of the surfaces (TA/Ag, TA/pMP/Ag, TA/pMP8AE2/Ag, and TA/pMP9AE1/Ag) were measured by Bruker energy dispersive X-ray spectroscopy (EDX).

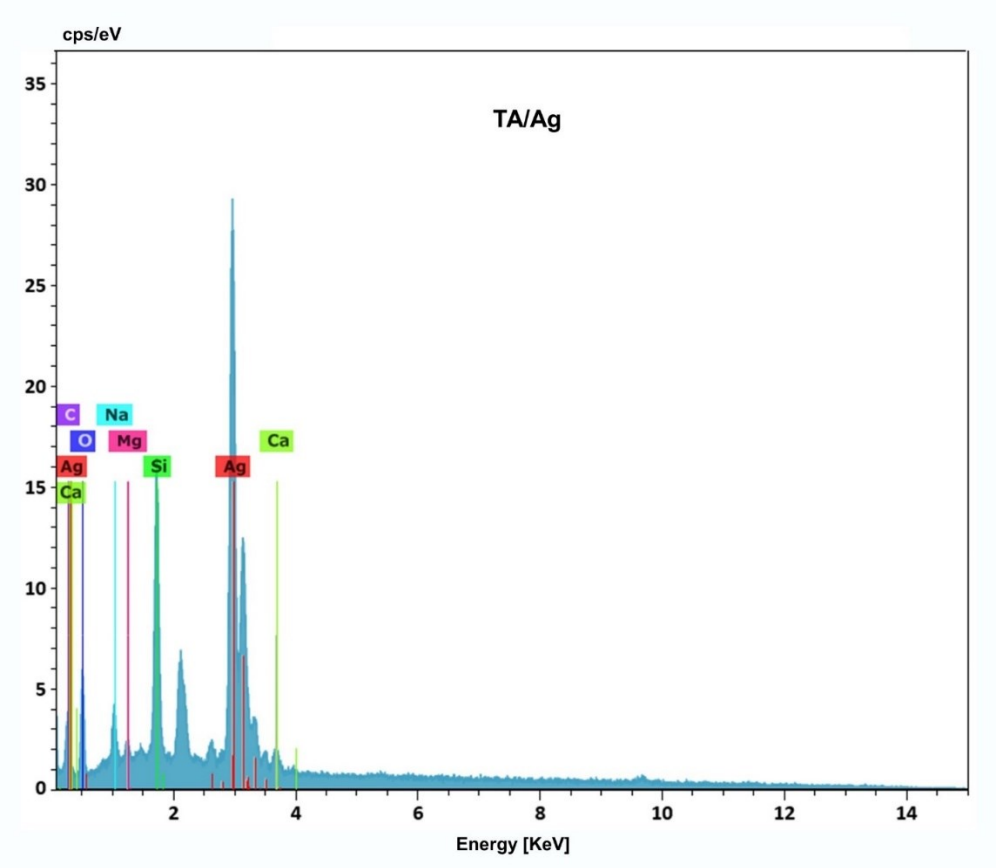
cps/eV
TA/Ag
C
Na
O
Mg
Ca
Ag
Si
Ag
Ca
Energy [KeV]

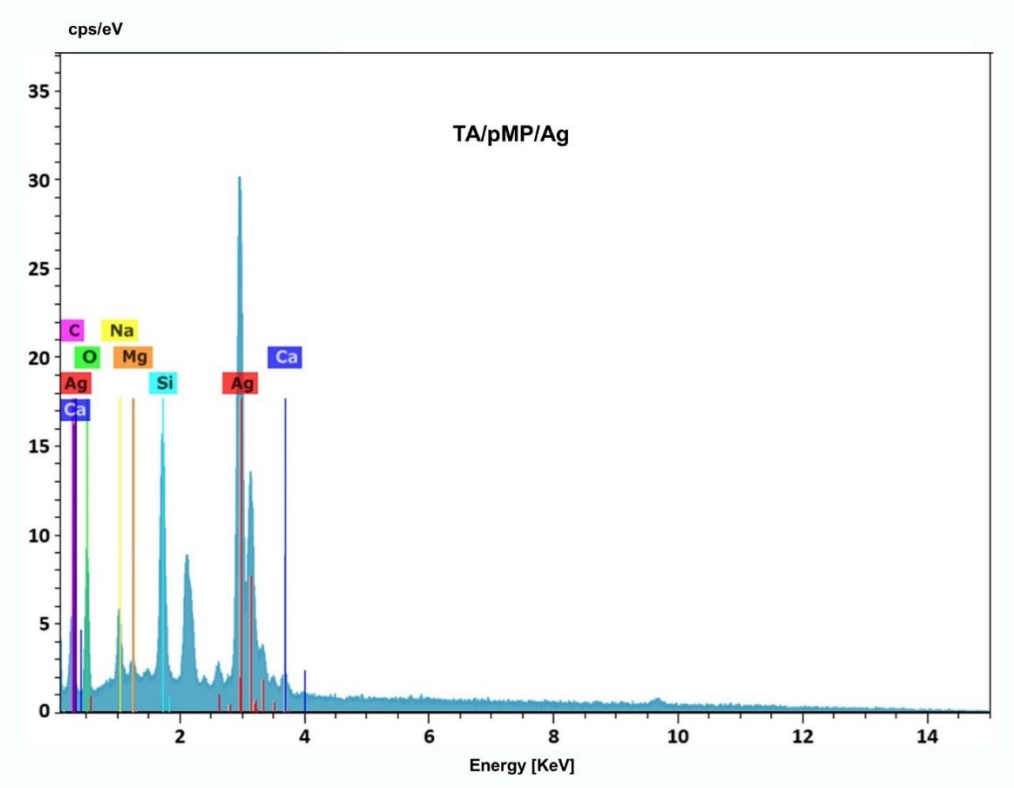
cps/eV
TA/pMP/Ag
C
Na
O
Mg
Ca
Ag
Si
Ag
Ca
Energy [KeV]

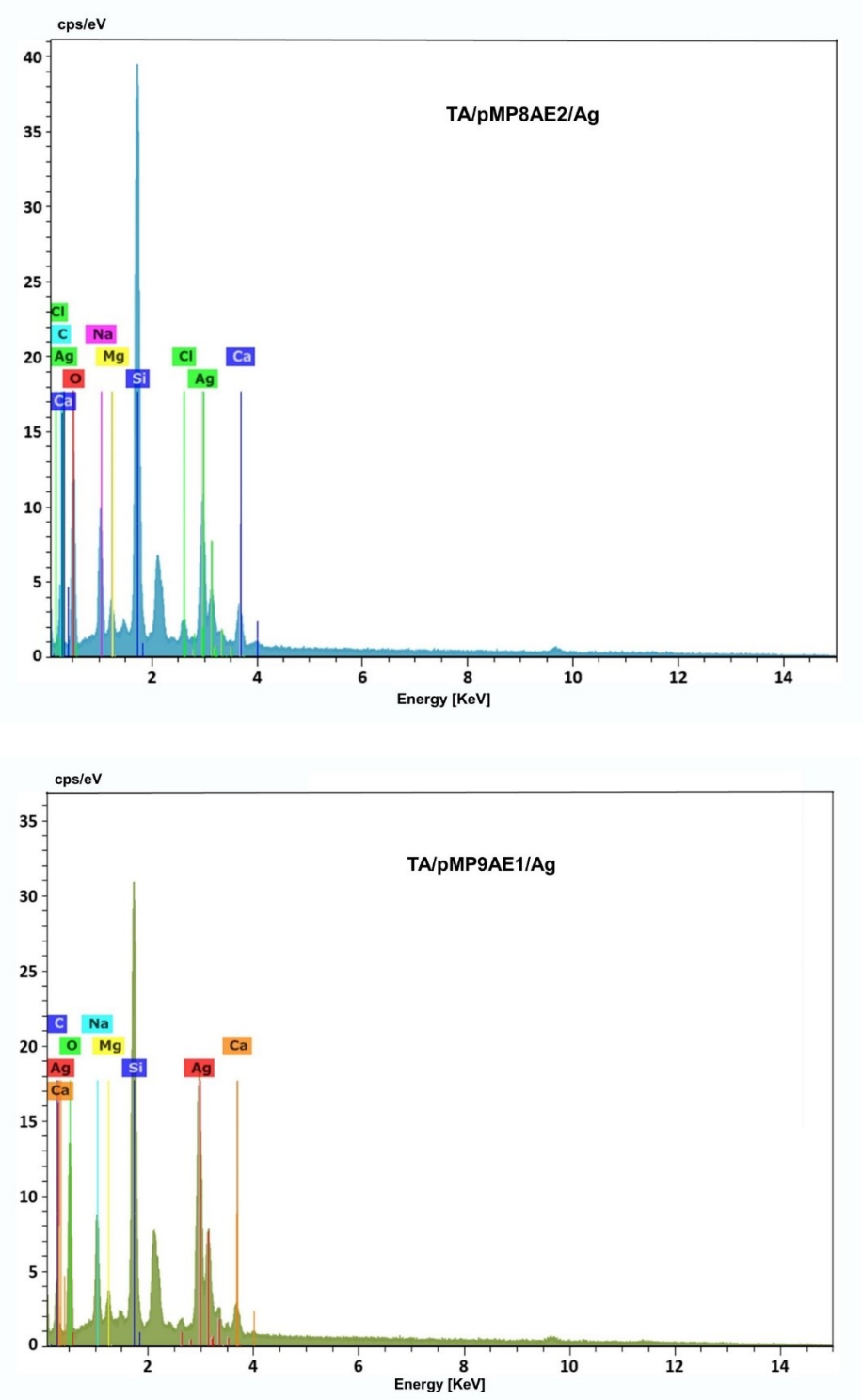

Figure S2-6: EDX spectra for TA/Ag, TA/pMP/Ag, TA/pMP8AE2/Ag, and TA/pMP9AE1/Ag surfaces. The y-axis represents the number of counts, and the x-axis represents the energy of X-rays.

2.5.2. Growth Inhibition Curve Assay.

Sterile culture tubes containing 3 mL of autoclaved LB (Luria-Bertani) or TSB (Tryptic Soy Broth) media were prepared. Every sample was immersed separately in the LB or TSB medium in each culture tube. Aliquot (10 µL) of *E. coli* or *S. aureus* bacterial suspension was inoculated in the above tubes before incubating at 37 °C and for up to 24h. The bacterial growth in each medium for every sample was obtained by measuring the optical density (OD) at a wavelength of 600 nm using a spectrophotometer (Aliquots at intervals of every two hours were taken). The growth graph was then conducted by plotting the average of triplicate OD measurements versus time.

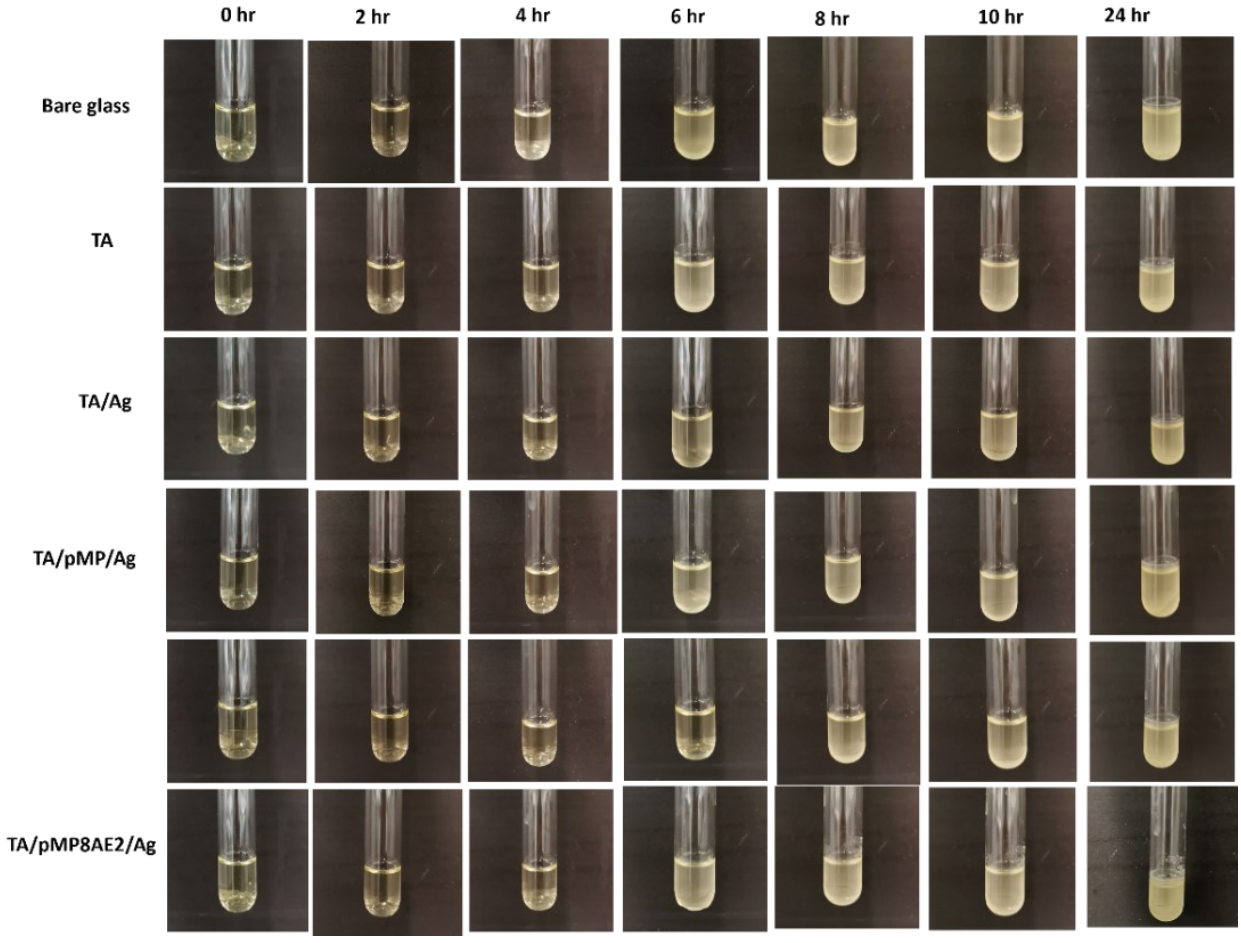

Figure S2-7. Pictures of *E. coli* sustentions cultured with glass and AgNPs-loaded surfaces at

2h,4h, 6h, 8h, 10h, and 24h.

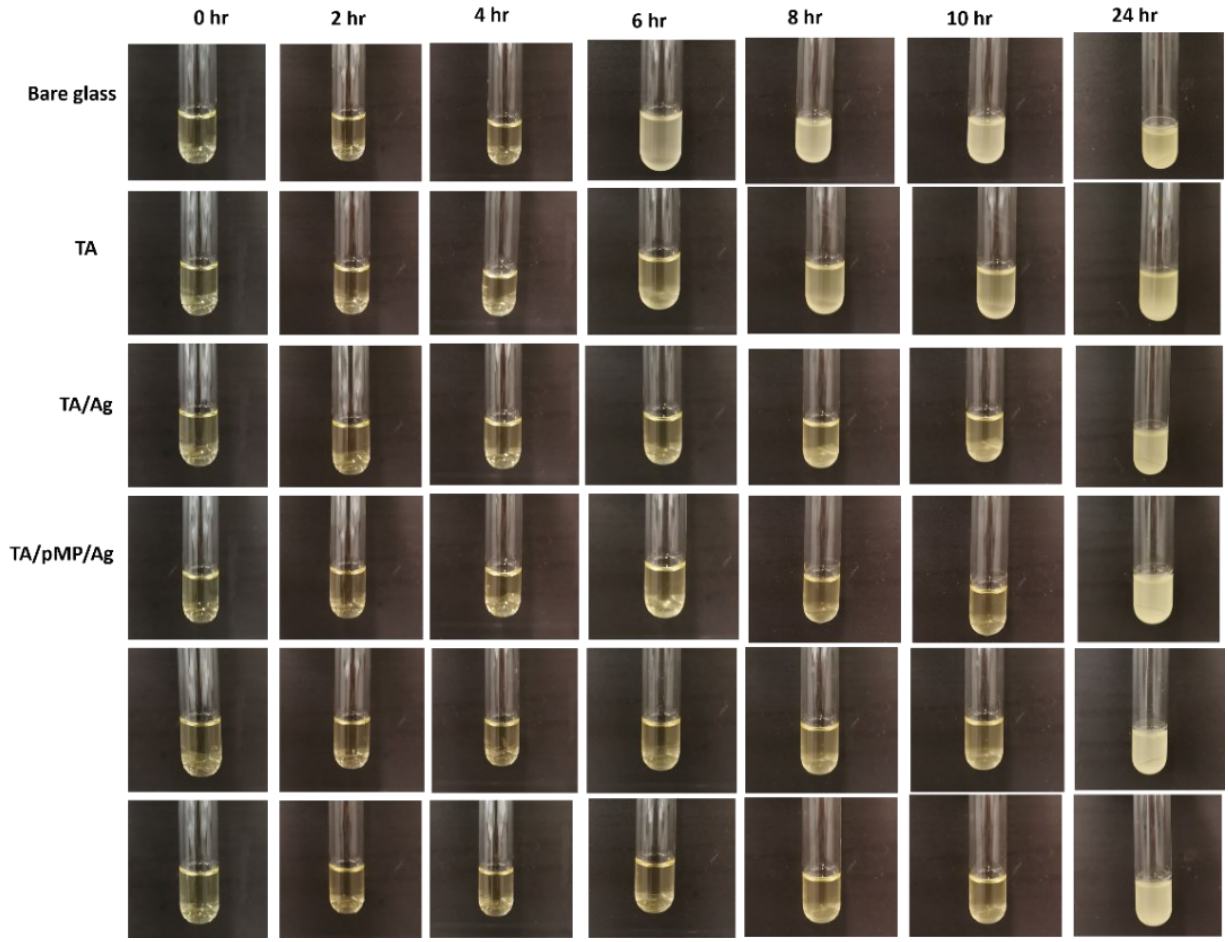

Figure S2-8. Pictures of *S. aureus* sustentions cultured with glass and AgNPs-loaded surfaces at 2h, 4h, 6h, 8h, 10h, and 24h**.**

2.6. References.

(1) Leslie, D. C.; Waterhouse, A.; Berthet, J. B.; Valentin, T. M.; Watters, A. L.; Jain, A.; Kim, P.; Hatton, B. D.; Nedder, A.; Donovan, K.; Super, E. H.; Howell, C.; Johnson, C. P.; Vu, T. L.; Bolgen, D. E.; Rifai, S.; Hansen, A. R.; Aizenberg, M.; Super, M.; Aizenberg, J.; Ingber, D. E. A Bioinspired Omniphobic Surface Coating on Medical Devices Prevents Thrombosis and Biofouling. *Nat. Biotechnol.* **2014**, *32* (11), 1134–1140.

(2) Wang, B.; Ye, Z.; Xu, Q.; Liu, H.; Lin, Q.; Chen, H.; Nan, K. Construction of a Temperature-Responsive Terpolymer Coating with Recyclable Bactericidal and Self-Cleaning Antimicrobial Properties. *Biomater. Sci.* **2016**, *4* (12), 1731–1741.

(3) Sagle, A. C.; Ju, H.; Freeman, B. D.; Sharma, M. M. PEG-Based Hydrogel Membrane Coatings. *Polymer (Guildf).* **2009**, *50* (3), 756–766.

(4) Elfarargy, R. G.; Sedki, M.; Samhan, F. A.; Hassan, R. Y. A.; El-Sherbiny, I. M. Surface Grafting of Polymeric Catheters and Stents to Prevent Biofilm Formation of Pathogenic Bacteria. *J. Genet. Eng. Biotechnol.* **2023**, *21* (1).

(5) Dundar Arisoy, F.; Kolewe, K. W.; Homyak, B.; Kurtz, I. S.; Schiffman, J. D.; Watkins, J. J. Bioinspired Photocatalytic Shark-Skin Surfaces with Antibacterial and Antifouling Activity via Nanoimprint Lithography. *ACS Appl. Mater. Interfaces* **2018**, *10* (23), 20055–20063.

(6) Knorr, D. B.; Tran, N. T.; Gaskell, K. J.; Orlicki, J. A.; Woicik, J. C.; Jaye, C.; Fischer, D. A.; Lenhart, J. L. Synthesis and Characterization of Aminopropyltriethoxysilane-Polydopamine Coatings. *Langmuir* **2016**, *32* (17), 4370–4381.

(7) Clodt, J. I.; Filiz, V.; Rangou, S.; Buhr, K.; Abetz, C.; Höche, D.; Hahn, J.; Jung, A.; Abetz, V. Double Stimuli-Responsive Isoporous Membranes via Post-Modification of Ph-

Sensitive Self-Assembled Diblock Copolymer Membranes. *Adv. Funct. Mater.* **2013**, *23* (6), 731–738.

(8) Lu, Z.; Xiao, J.; Wang, Y.; Meng, M. In Situ Synthesis of Silver Nanoparticles Uniformly Distributed on Polydopamine-Coated Silk Fibers for Antibacterial Application. *J. Colloid Interface Sci.* **2015**, *452*, 8–14.

(9) Kim, H. J.; Kim, D.; Yoon, H.; Choi, Y.; Yoon, J.; Lee, J. Polyphenol / Fe III Complex Coated Membranes Having Multifunctional Properties Prepared by a One-Step Fast Assembly. **2015**, 1–8.

(10) Rappold, P. M.; Cui, M.; Grima, J. C.; Fan, R. Z.; Mesy-bentley, K. L. De; Chen, L.; Zhuang, X.; Bowers, W. J.; Tieu, K. Dopamine Release Deficits in Vivo. *Nat. Commun.* **2014**.

(11) Liu, Y.; Mao, S.; Zhu, L.; Chen, S.; Wu, C. Based on Tannic Acid and Thermoresponsive Microgels Design a Simple and High-Efficiency Multifunctional Antibacterial Coating. *Eur. Polym. J.* **2021**, *153* (March), 110498.

(12) Barrett, D. G.; Sileika, T. S.; Messersmith, P. B. Precursors of Tannin-Inspired Nanocoatings †. **2014**, 7265–7268.

(13) Dong, G.; Liu, H.; Yu, X.; Zhang, X.; Lu, H.; Zhou, T. Antimicrobial and Anti-Biofilm Activity of Tannic Acid against Staphylococcus Aureus. *Nat. Prod. Res.* **2018**, *6419*, 1–4.

(14) Wang, P.; Liu, J.; Luo, X.; Xiong, P.; Gao, S.; Yan, J. Mg – Zn – Y – Nd Alloy with Antioxidant and Platelet-Repellent Functionalities for Vascular. **2019**, 7314–7325.

(15) Chen, S.; Xie, Y.; Xiao, T.; Zhao, W.; Li, J.; Zhao, C. Tannic Acid-Inspiration and Post-Crosslinking of Zwitterionic Polymer as a Universal Approach towards Antifouling Surface. *Chem. Eng. J.* **2018**, *337* (October 2017), 122–132.

(16) Ko, M. P.; Huang, C. J. A Versatile Approach to Antimicrobial Coatings via Metal-Phenolic Networks. *Colloids Surfaces B Biointerfaces* **2020**, *187* (November 2019), 110771.

(17) Antifouling, P.; Properties, A.; Xu, K.; Xie, H.; Sun, C.; Lin, W.; You, Z.; Zheng, G.; Zheng, X.; Xu, Y.; Chen, J.; Lin, F. Sustainable Coating Based on Zwitterionic Functionalized. **2023**.

(18) Xie, Y.; Chen, S.; Zhang, X.; Shi, Z.; Wei, Z.; Bao, J.; Zhao, W.; Zhao, C. Engineering of Tannic Acid Inspired Antifouling and Antibacterial Membranes through Co-Deposition of Zwitterionic Polymers and Ag Nanoparticles. *Ind. Eng. Chem. Res.* **2019**, *58* (27), 11689–11697.

(19) Yeh, S.; Wang, T.; Yusa, S.; Thissen, H.; Tsai, W. Conjugation of Polysulfobetaine via Poly (Pyrogallol) Coatings for Improving the Antifouling E Ffi Cacy of Biomaterials. **2021**, 6–13.

(20) Schleno, J. B. Zwitteration: Coating Surfaces with Zwitterionic Functionality to Reduce Nonspeci Fi c Adsorption. **2014**.

(21) Xu, G.; Pranantyo, D.; Zhang, B.; Xu, L.; Neoh, K.; Kang, E. RSC Advances Deposition of Parasin I Peptide for Antifouling and Antimicrobial Coatings †. **2016**, 14809–14818.

(22) Wang, Y.; Wei, T.; Qu, Y.; Zhou, Y.; Zheng, Y.; Huang, C.; Zhang, Y.; Yu, Q.; Chen, H. Smart, Photothermally Activated, Antibacterial Surfaces with Thermally Triggered Bacteria-Releasing Properties. *ACS Appl. Mater. Interfaces* **2020**, *12* (19), 21283–21291.

(23) Xu, G.; Neoh, K. G.; Kang, E. T.; Teo, S. L. M. Switchable Antimicrobial and Antifouling Coatings from Tannic Acid-Scaffolded Binary Polymer Brushes. *ACS Sustain. Chem. Eng.* **2020**, *8* (6), 2586–2595.

(24) Qiu, W.; Zhao, Z.; Du, Y.; Hu, M.; Xu, Z. Applied Surface Science Antimicrobial Membrane Surfaces via Efficient Polyethyleneimine Immobilization and Cationization. *Appl. Surf. Sci.* **2017**, *426*, 972–979.

(25) Ding, X.; Yang, C.; Lim, T. P.; Hsu, L. Y.; Engler, A. C.; Hedrick, J. L.; Yang, Y. Y. Antibacterial and Antifouling Catheter Coatings Using Surface Grafted PEG-b-Cationic Polycarbonate Diblock Copolymers. *Biomaterials* **2012**, *33* (28), 6593–6603.

(26) Cheng, Y. F.; Pranantyo, D.; Kasi, G.; Lu, Z. S.; Li, C. M.; Xu, L. Q. Amino-Containing Tannic Acid Derivative-Mediated Universal Coatings for Multifunctional Surface Modification. *Biomater. Sci.* **2020**, *8* (8), 2120–2128.

(27) Bu, Y.; Zhang, S.; Cai, Y.; Yang, Y.; Ma, S.; Huang, J.; Yang, H.; Ye, D.; Zhou, Y.; Xu, W.; Gu, S. Fabrication of Durable Antibacterial and Superhydrophobic Textiles via in Situ Synthesis of Silver Nanoparticle on Tannic Acid-Coated Viscose Textiles. *Cellulose* **2019**, *26* (3), 2109–2122.

(28) Zhan, F.; Yan, X.; Sheng, F.; Li, B. Facile in Situ Synthesis of Silver Nanoparticles on Tannic Acid/Zein Electrospun Membranes and Their Antibacterial, Catalytic and Antioxidant Activities. *Food Chem.* **2020**, *330* (June), 127172.

(29) Chen, S.; Yu, F.; Yu, Q.; He, Y.; Jiang, S. Strong Resistance of a Thin Crystalline Layer of Balanced Charged Groups to Protein Adsorption. **2006**, No. 18, 8186–8191.

(30) Jyske, T.; Liimatainen, J.; Tienaho, J.; Brännström, H.; Aoki, D.; Kuroda, K.; Reshamwala, D.; Kunnas, S.; Halmemies, E.; Nakayama, E.; Kilpeläinen, P.; Ora, A.; Kaseva, J.; Hellström, J.; Marjomäki, V. S.; Karonen, M.; Fukushima, K. Inspired by Nature: Fiber Networks Functionalized with Tannic Acid and Condensed Tannin-Rich Extracts of Norway Spruce Bark Show Antimicrobial Efficacy. *Front. Bioeng. Biotechnol.*

2023, *11* (April), 1–20.

(31) Maan, A. M. C.; Hofman, A. H.; de Vos, W. M.; Kamperman, M. Recent Developments and Practical Feasibility of Polymer-Based Antifouling Coatings. *Adv. Funct. Mater.* **2020**, *30* (32).

(32) Guo, J.; Sun, W.; Kim, J. P.; Lu, X.; Li, Q.; Lin, M.; Mrowczynski, O.; Rizk, E. B.; Cheng, J.; Qian, G.; Yang, J. Development of Tannin-Inspired Antimicrobial Bioadhesives. *Acta Biomater.* **2018**, *72*, 35–44.

(33) Wang, B. L.; Jin, T. W.; Han, Y. M.; Shen, C. H.; Li, Q.; Lin, Q. K.; Chen, H. Bio-Inspired Terpolymers Containing Dopamine, Cations and MPC: A Versatile Platform to Construct a Recycle Antibacterial and Antifouling Surface. *J. Mater. Chem. B* **2015**, *3* (27), 5501–5510.

(34) Huang, W.; Wang, J. Q.; Song, H. Y.; Zhang, Q.; Liu, G. F. Chemical Analysis and in Vitro Antimicrobial Effects and Mechanism of Action of Trachyspermum Copticum Essential Oil against Escherichia Coli. *Asian Pac. J. Trop. Med.* **2017**, *10* (7), 663–669.

(35) Asha, A. B.; Ounkaew, A.; Peng, Y. Y.; Gholipour, M. R.; Ishihara, K.; Liu, Y.; Narain, R. Bioinspired Antifouling and Antibacterial Polymer Coating with Intrinsic Self-Healing Property. *Biomater. Sci.* **2022**, *11* (1), 128–139.

(36) Cumberland, S. L.; Strouse, G. F. Analysis of the Nature of Oxyanion Adsorption on Gold Nanomaterial Surfaces. *Langmuir* **2002**, *18* (1), 269–276.

(37) Oulad, F.; Zinadini, S.; Zinatizadeh, A. A.; Derakhshan, A. A. Fabrication and Characterization of a Novel Tannic Acid Coated Boehmite/PES High-Performance Antifouling NF Membrane and Application for Licorice Dye Removal. *Chem. Eng. J.* **2020**, *397* (April), 125105.

(38) Costa, G. G.; Brito, C. C. S. M.; Terezo, A. J.; Cardoso, A. P.; Ionashiro, E. Y.; B. de Siqueira, A. Preparation, Characterization and Antioxidant Evaluation of Cu(II) and Zn(II) Tannates. *Open Chem. J.* **2018**, *5* (1), 158–171.

(39) Liu, C.; Wu, L.; Zhang, C.; Chen, W.; Luo, S. Surface Hydrophilic Modification of PVDF Membranes by Trace Amounts of Tannin and Polyethyleneimine. *Appl. Surf. Sci.* **2018**, *457* (June), 695–704.

(40) Hu, Z.; Berry, R. M.; Pelton, R.; Cranston, E. D. One-Pot Water-Based Hydrophobic Surface Modification of Cellulose Nanocrystals Using Plant Polyphenols. *ACS Sustain. Chem. Eng.* **2017**, *5* (6), 5018–5026.

(41) Guo, L. L.; Cheng, Y. F.; Ren, X.; Gopinath, K.; Lu, Z. S.; Li, C. M.; Xu, L. Q. Simultaneous Deposition of Tannic Acid and Poly(Ethylene Glycol) to Construct the Antifouling Polymeric Coating on Titanium Surface. *Colloids Surfaces B Biointerfaces* **2021**, *200* (January), 111592.

(42) Hanif, Z.; Khan, Z. A.; Siddiqui, M. F.; Tariq, M. Z.; Park, S.; Park, S. J. Tannic Acid-Mediated Rapid Layer-by-Layer Deposited Non-Leaching Silver Nanoparticles Hybridized Cellulose Membranes for Point-of-Use Water Disinfection. *Carbohydr. Polym.* **2020**, *231* (December 2019), 115746.

(43) Zhang, H.; Shen, X.; Fei, Z.; Fan, X.; Ma, L.; Wang, H.; Tian, C.; Zhang, B.; Luo, R.; Wang, Y.; Huang, S. Ag-Incorporated Polydopamine/Tannic Acid Coating on Titanium With Enhanced Cytocompatible and Antibacterial Properties. *Front. Bioeng. Biotechnol.* **2022**, *10* (March), 1–9.

(44) Zhao, A.; Zhang, N.; Li, Q.; Zhou, L.; Deng, H.; Li, Z.; Wang, Y.; Lv, E.; Li, Z.; Qiao, M.; Wang, J. Incorporation of Silver-Embedded Carbon Nanotubes Coated with Tannic

Acid into Polyamide Reverse Osmosis Membranes toward High Permeability, Antifouling, and Antibacterial Properties. *ACS Sustain. Chem. Eng.* **2021**, *9* (34), 11388–11402.

(45) Zhao, J.; Shi, Q.; Luan, S.; Song, L.; Yang, H.; Shi, H.; Jin, J.; Li, X.; Yin, J.; Stagnaro, P. Improved Biocompatibility and Antifouling Property of Polypropylene Non-Woven Fabric Membrane by Surface Grafting Zwitterionic Polymer. *J. Memb. Sci.* **2011**, *369* (1–2), 5–12.

(46) Choi, W.; Jin, J.; Park, S.; Kim, J. Y.; Lee, M. J.; Sun, H.; Kwon, J. S.; Lee, H.; Choi, S. H.; Hong, J. Quantitative Interpretation of Hydration Dynamics Enabled the Fabrication of a Zwitterionic Antifouling Surface. *ACS Appl. Mater. Interfaces* **2020**, *12* (7), 7951–7965.

(47) Sabaté del Río, J.; Henry, O. Y. F.; Jolly, P.; Ingber, D. E. An Antifouling Coating That Enables Affinity-Based Electrochemical Biosensing in Complex Biological Fluids. *Nat. Nanotechnol.* **2019**, *14* (12), 1143–1149.

(48) Phan, H. T. M.; Bartelt-Hunt, S.; Rodenhausen, K. B.; Schubert, M.; Bartz, J. C. Investigation of Bovine Serum Albumin (BSA) Attachment onto Self-Assembled Monolayers (SAMs) Using Combinatorial Quartz Crystal Microbalance with Dissipation (QCM-D) and Spectroscopic Ellipsometry (SE). *PLoS One* **2015**, *10* (10).

(49) Chang, C. C.; Kolewe, K. W.; Li, Y.; Kosif, I.; Freeman, B. D.; Carter, K. R.; Schiffman, J. D.; Emrick, T. Underwater Superoleophobic Surfaces Prepared from Polymer Zwitterion/Dopamine Composite Coatings. *Adv. Mater. Interfaces* **2016**, *3* (6), 1–9.

(50) Shahkaramipour, N.; Lai, C. K.; Venna, S. R.; Sun, H.; Cheng, C.; Lin, H. Membrane Surface Modification Using Thiol-Containing Zwitterionic Polymers via Bioadhesive Polydopamine. *Ind. Eng. Chem. Res.* **2018**, *57* (6), 2336–2345.

(51) Yeh, S. L.; Wang, T. C.; Yusa, S. I.; Thissen, H.; Tsai, W. B. Conjugation of Polysulfobetaine via Poly(Pyrogallol) Coatings for Improving the Antifouling Efficacy of Biomaterials. *ACS Omega* **2021**, *6* (5), 3517–3524.

(52) Lu, M. M.; Wang, Q. J.; Chang, Z. M.; Wang, Z.; Zheng, X.; Shao, D.; Dong, W. F.; Zhou, Y. M. Synergistic Bactericidal Activity of Chlorhexidineloaded, Silver-Decorated Mesoporous Silica Nanoparticles. *Int. J. Nanomedicine* **2017**, *12*, 3577–3589.

(53) Zimmerli, W. Clinical Presentation and Treatment of Orthopaedic Implant-Associated Infection. *J. Intern. Med.* **2014**, *276* (2), 111–119.

(54) Mitra, D.; Kang, E. T.; Neoh, K. G. Polymer-Based Coatings with Integrated Antifouling and Bactericidal Properties for Targeted Biomedical Applications. *ACS Appl. Polym. Mater.* **2021**, *3* (5), 2233–2263.

(55) López-García, J.; Lehocký, M.; Humpolíček, P.; Sáha, P. HaCaT Keratinocytes Response on Antimicrobial Atelocollagen Substrates: Extent of Cytotoxicity, Cell Viability and Proliferation. *J. Funct. Biomater.* **2014**, *5* (2), 43–57.

(56) Wu, D.; Wang, W.; Diaz-Dussan, D.; Peng, Y. Y.; Chen, Y.; Narain, R.; Hall, D. G. In Situ Forming, Dual-Crosslink Network, Self-Healing Hydrogel Enabled by a Bioorthogonal Nopoldiol-Benzoxaborolate Click Reaction with a Wide PH Range. *Chem. Mater.* **2019**.

Chapter 3: Mussel-inspired Polymer-based Coating Technology for Antifouling and Antibacterial Properties

The content of this chapter was published in

The Journal of Langmuir

3.1. Introduction.

Biofilm formation is a severe complication formed after implant-associated infections, creates a high risk to human health worldwide, and negatively impacts the economy.[1,2] The initial adhesion of protein and other substances to the surface of the device develops into a film that is prone to subsequent microbial attachment, resulting in biofilm formation.[3] Therefore, there is an urgent need for an alternative approach to creating durable antibacterial surfaces that can effectively prevent or eradicate infections related to implants. The coating method is one of the various strategies developed to tailor the inherent physical and chemical characteristics of surfaces. Currently, coating technology is dominated by two strategies according to their mechanisms: passively resisting biofouling (antifouling coatings),[4] and the other aims to actively kill bacteria (antibacterial coatings).[5] Although the passive antifouling strategy is widely used in coating chemistry, its ability to suppress bacteria attachments, especially in the case of proliferative fouling, is limited.[6] On the other hand, when the bactericidal coating method is used to kill the bacteria, the increased dead and accumulated bacteria could provide binding sites for subsequent biofilm forming, ultimately leading to the loss of the antibacterial property. Therefore, modification of coatings with a combination of zwitterionic polymers and unrealizable quaternary ammonium compounds provides a promising strategy to reduce implant-associated infections.[7]

Hydrophilic polymers, such as zwitterionic polymers and poly(ethylene glycol) (PEG) polymers, are two common hydrophilic polymers employed for antifouling surface fabrication.[8] However, several researchers have demonstrated that PEG polymers may form a hydration layer via hydrogen bonds, and they are prone to oxidize under biological conditions, which limits their antifouling properties over long-term applications.[9,10] Therefore, zwitterionic polymers have

been used as an alternative to PEG polymers due to their amphoteric nature, which allows them to form strong electrostatic interactions with water.[11,12] Niu and coworkers reported that catechol containing dopamine methacrylamide (DMA) and the zwitterionic monomer 2-methacryloyloxyethylphosphorylcholine (MPC) copolymers were grafted on stainless steel meshes and silicon wafers via ozone activation. The poly MPC-grafted surfaces effectively resisted protein adsorption and showed promising antifouling properties.[13] However, these anti-fouling coatings are unable to kill the approaching bacteria. Therefore, bactericides, such as antibacterial peptides, antibiotics, carbon nanotubes, quaternary ammonium salts, and metal nanoparticles, have been widely coated on surfaces for bacteria killing. Among them, coatings bearing ammonium salts were determined to be successful materials for killing bacteria due to their ability to kill bacteria even at low concentrations.[14–18] The potential mechanism of these agents is that polymers bearing positive charge groups, like poly(META), can interact with the negatively charged phospholipids on bacterial membranes. Then, the hydrophobic tail penetrates the membrane and disrupts it, resulting in cell death.[19–21] Farah et al. prepared coatings with antimicrobial ability based on quaternary ammonium polymers. They prepared Quaternary ammonium-based Polydiethylaminoethyl methacrylate (QA-PDEAEM) in the first method by alkylation of DEAEM monomer followed by free radical polymerization and vice versa in the second method. Their QA-polymers coated well-plate showed distinctive antibacterial activity against four representative Gram-positive and Gram-negative bacteria after 6 days of incubation.[22]

Recently, a mussel-inspired dopamine strategy has increasingly been used for coating multi-functionalities based on the self-polymerization of dopamine under mild conditions, giving rise to the formation of polydopamine. Hong et al. proposed that this polydopamine was formed

through two pathways: non-covalent self-assembly and covalent polymerization.[23] The residual quinone, catechol, and amino groups of (PDA) give rise to secondary modification.[24] The quinone and catechol groups could react with nucleophilic amino and thiol groups via the Michael addition and Schiff base reactions under basic conditions. For example, Qiu et al. modified a membrane surface by co-deposition of dopamine/polyethyleneimine (PEI), and then they obtained an N-alkylated PEI-coated membrane with antimicrobial properties.[25] The membrane surface modification was also achieved by Michael's addition reaction between a thiol-containing zwitterionic polymer and an intermediate polydopamine layer.[26] Moreover, Zhang et al. prepared a biocatalytic membrane based on polydopamine (PDA) coating to facilitate enzyme immobilization with the aim of applications in food, pharmaceutical, and water treatment. Glutaraldehyde (GA) was grafted on the PDA-coated membrane by the reaction between aldehyde groups of GA and hydroxy/amino groups of PDA, which was regarded as an active site for further covalently binding enzymes.[27] Herein, we employ glass slides as a model for inorganic surfaces and propose a facile strategy to construct antimicrobial polycationic-zwitterionic coatings by firstly depositing polydopamine, then followed by grafting the copolymers poly(MPC-*st*-FPMA) and poly(META-*st*-FPMA) which are donated as MPF and MTF, respectively (**Scheme 3.1**). The antimicrobial and antifouling properties of the resultant coatings were evaluated.

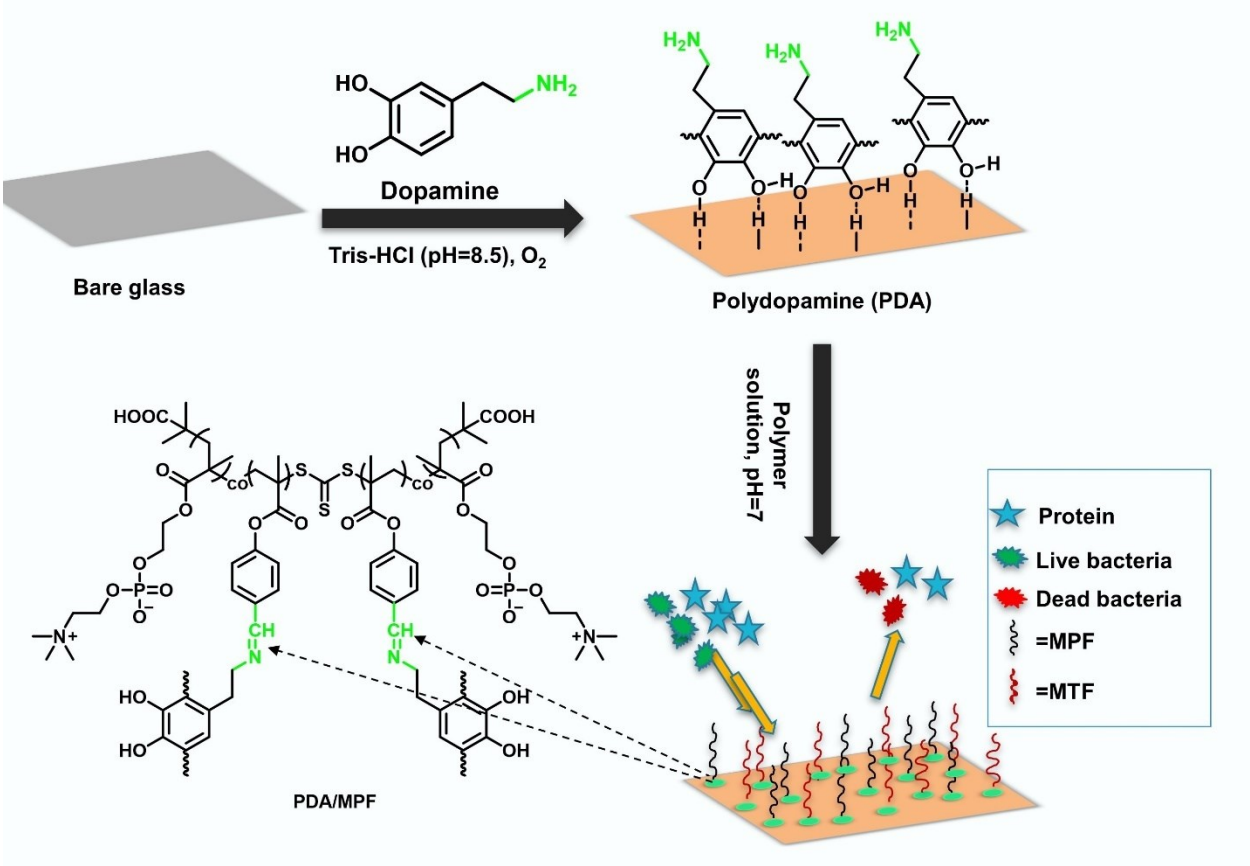

Scheme 3.1. Schematic illustrates the grafting of MPF copolymer containing aldehyde to the amino groups of PDA-coated substrate, resulting in protein-resistant bacteria-killing.

3.2. Experimental Section.

3.2.1. Materials. 4,4′-Azobis(4-cyano valeric acid), bovine serum albumin, 2-(methacryloyloxy)ethyl trimethylammonium chloride, dopamine hydrochloride, 4-hydroxybenzaldehyde, triethylamine, thiazolyl blue tetrazolium bromide, and methacryloyl chloride were purchased from Sigma-Aldrich. Micro BCATM Protein Assay Kit was purchased from Fisher Scientific. Organic solvents were obtained from Caledon Laboratories Ltd.

3.2.2. Synthesis of Random Polymers (MPF and MTF).

2-(1-carboxy methylethylsulfanylthiocarbonylsulfanyl)-2-methyl propionic acid (CTA) and 4-formyl phenyl methacrylate (FPMA) were initially synthesized as previously reported,[28,29] and their compositions were confirmed by ^{1}H NMR. The MPF and MTF copolymers were obtained by RAFT polymerization using CTA as a chain transfer agent and ACVA as an initiator (**Figures 3.1 and 3.2**). Typically, the reactants of the two copolymers [FPMA (180 mg, 0.9473 mmol), MPC (1.12 g, 3.7966 mmol), CTA (29.85 mg, 0.106 mmol), and ACVA (5.97 mg, 0.0213 mmol)] and [FPMA (242 mg, 1.2736 mmol), META (1058 mg, 5.0938 mmol), CTA (40.81 mg, 0.1447 mmol), and ACVA (8.11 mg, 0.02894 mmol)] were put in polymerization tubes containing methanol, DI water, and DMF. The reaction mixtures were stirred to dissolve the reactants and then degassed under nitrogen for 30 min. The polymerization reactions were carried out in an oil bath while stirring at 70 °C for 20 h. After that, dialysis was performed against diH_2O, followed by lyophilization to obtain the copolymers. The random polymers (MPF and MTF) were characterized by ^{1}H NMR spectroscopy to analyze the chemical composition and gel permeation chromatography (GPC) to measure the average molecular weights as indicated in the literature.[30]

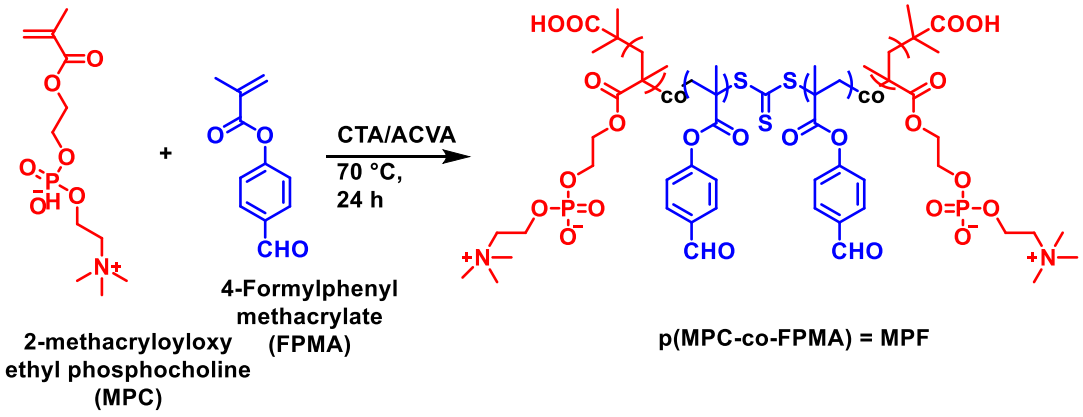

Figure 3.1. Reaction scheme of RAFT polymerization between MPC and FPMA

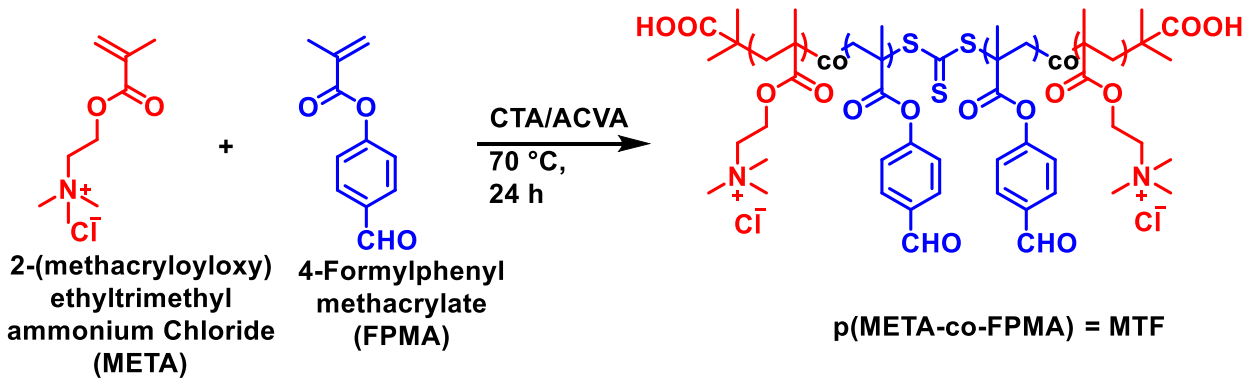

Figure 3.2. Reaction scheme of RAFT polymerization between META and FPMA.

3.2.3. Deposition of Polydopamine and Copolymers onto the Glass Slides. The slides were placed in diH_2O and sonicated for 20 minutes, followed by rinsing the slides with ethanol for at least 10 minutes. The surfaces were then dried by exposure to the air. Dopamine hydrochloride (DA) was dissolved in Tris-HCl, pH 8.5, to prepare a dopamine solution with a 2 mg/mL concentration. The slides were immersed into a 24-well plate containing 500 µl of DA solutions. After shaking the plate for 8 h at room temperature, the PDA-modified surfaces were removed and washed carefully with DI water. Three concentrations of MPF and MTF solutions were prepared to graft the polymers on polydopamine coatings (see **Table 3.1**). The same protocol as in the polydopamine layer was used for the post-coating of copolymers to afford the samples (control PDA-, PDA/MPF-, PDA/MPF/MTF-, and PDA/MTF-coated glass surfaces).

Table 3.1. Weight ratios of MPF and MTF polymers applied to PDA-coatings.

Sample	MPF (wt%)	MTF (wt%)
PDA/MPF	100	0
PDA/MPF/MTF	50	50
PDA/MTF	0	100

3.2.4. Surface Characterization. The chemical interactions of polydopamine and polymers with polypropylene (PP) surfaces were investigated by collecting ATR-FTIR (Attenuated total reflectance Fourier transform infrared) spectra for the pristine PP, PP/PDA, and PP/PDA/PMPF-PMTF substrates. The surface morphology and roughness of the modified substrates were characterized by atomic force microscopy (AFM) in dry conditions. The wettability of surfaces was evaluated by measuring the water contact angle (WCA) in the air using a goniometer. 10 µl of DI water was dropped on each surface, and the average of WCA in three different locations was calculated.

3.2.5. Protein Adsorption Assay. All sample substrates (each with a surface area of 1 x 1 cm^2) were stained with bovine serum albumin (BSA) to investigate protein adsorption on the polymer-coated surfaces and bare glass. Following the previous study protocol, the BCA protein assay kit determined how much protein was absorbed on the sample surfaces.[31]

3.2.6. Bacterial Adhesion Assays. *S. aureus* (Gram-positive) and *E. coli* (Gram-negative) were used as typical bacteria to evaluate the antibacterial properties of zwitterionic and cationic polymers coated glass substrates. A colony forming units (CFU) assay was carried out to study the antibacterial adhesion activity.[32,33] In brief, *S. aureus* and *E. coli* were collected as single bacteria colonies from TS and LB agar plates, inoculated in 25 mL of TS broth and LB broth, respectively, and cultured for 16h at 37 °C. The cells were centrifuged at 4000 rpm for 5 minutes and resuspended thrice in a sterile PBS solution. Next, the bacterial cells were dispersed in 1 mL PBS buffer solution and then adjusted to an optical density of 0.15 readout at 670 nm (OD 670), corresponding to about ($8x10^9$ cells/mL). The bacteria suspension was diluted in PBS to obtain a cell concentration of about ($1x10^7$ cells/mL). 100 µl bacterial solution ($1x10^7$ cells/mL) was dropped onto surfaces and co-cultured for 3h at 37 °C. The bare glass and modified surface

samples were washed gently three times with PBS to ensure the non-adherent bacteria were removed. Then, Surfaces were sonicated in 10 mL PBS solution to remove the attached bacteria onto substrates. Subsequently, dilutions were carried out for each bacteria suspension, and 10 µL from each dilution was cultivated in triplicate on TS and LB agar plates. Colony forming units (CFU) were observed after spreading the bacteria onto agar plates and incubating them for 24 h at 37 °C. The viable bacteria colonies were counted, and the number of attached bacteria was calculated using the equation (N/N0)x100, where N0 and N are the numbers of bacterial colonies on the bare glass and modified substrate, respectively.

3.2.7. Stability and Durability of the Coatings. The stability and durability of the bare glass and polymer-coated substrates were assayed by subjecting the surfaces to phosphate-buffered saline (PBS) solution (pH=7.4) and shaking for 7 days. The bacterial adhesion activity of aged substrates against *S. aureus* and *E. coli* was evaluated using CFU assay.

3.2.8. Cell Viability Assay (MTT). The MTT assay was performed to investigate the cytotoxicity of the modified surfaces using normal human lung fibroblast cells (MRC-5). Briefly, to prepare the coating extracts, 100 µl of Dulbecco's modified Eagle's medium (DMEM) [1% sodium pyruvate, 10% FBS, and 1% penicillin/streptomycin] was placed separately in each well of the culture plate. Every coating substrate was immersed in the medium solution, followed by shaking the samples for 24h. After collecting the extracts, MRC-5 cells with a density of $6x10^3$ cells/well were seeded onto each well of the cell culture plate containing 100 µl of DMEM medium and incubated at 37 °C for 24 h. Afterward, the old media were replaced by fresh DMEM medium (as a positive control) or media of coating extracts and incubated for another 24h. Next, following the supplier protocol (Micro BCA Protein Assay Kit, Thermo Fisher Scientific), twenty microliters of MTT dye solution (5 mg/mL in sterilized PBS) were added to

each well, followed by incubation for 4h. After removing the media, 100 µl of isopropanol/DMSO solution was added as a lysis buffer. The absorbance measurements were then taken for every sample, and the number was expressed as percentages of the control.

3.3. Results and Discussion.

3.3.1. Synthesis of MPF and MTF Copolymers. A difunctional reversible addition-fragmentation transfer agent (CTA), S,S'-bis (α,α'-dimethylacetic acid) trithiocarbonate, was prepared from Carbon disulfide, chloroform, acetone, and tetrabutylammonium chloride, similar to the protocol described elsewhere.[28] as a chain transfer agent, this CTA has been demonstrated to give excellent control of molecular weight (MW) with narrow polydispersity index PDI for methyl methacrylate polymers. It was also used in the synthesis of water-soluble and temperature-sensitive polymers**.**[34] For this purpose, we used this CTA to facilitate the copolymerization of FPMA with either MPC or META. FPMA was prepared from 4-hydroxybenzaldehyde and methacryloyl chloride (**FIgure S3-1**) following the procedure in the previous report.[29] Proton nuclear magnetic resonance spectra (^{1}H NMR) of CTA and FPMA were recorded with a Varian spectrometer at 500 MHz; DMSO-d_6 was used as a solvent (**Figures S3-1 and S3-2**). The (MPC-st-FPMA) and (META-st-FPMA) were synthesized via RAFT polymerization of FPMA with either MPC or META and a targeted degree of polymerization of 130. **Figures 3.1 and 3.2** show the synthesis routes for MPF and MTF, respectively. The FPMA mole contents within the MPF and MTF copolymer chains were determined using ^{1}H NMR analysis (**Figures S3-3 and S3-4**). By comparing the integral of the distinctive peak for FPMA (δ 8.12-7.50 ppm) with the characteristic peak integrals for MPC (δ 3.72 ppm) and META (δ 3.86 ppm), the calculated FPMA mole contents were found to be 17% and 18% for MPF and MTF, respectively. These values align closely with the intended designed

ratio of the copolymers **Table 3.2**. The number (M_n) and weight (M_w) average molecular weights of MPF and MTF were determined by aqueous GPC and summarized in **Table 3.2**.

Table 3.2. Characteristics of the Copolymers (MPF) and (MTF).

Composition (mole %)							**Molecular weight**	
	in feed			Calculated from ^{1}H NMR			Calculated from GPC	
Polymer	MPC	META	FPMA	MPC	META	FPMA	M_n x 10^4 (Da)	PDI
MPF	80	0	20	83	0	17	4.23	1.05
MTF	0	80	20	0	82	18	2.93	1.12

3.3.2. Surface Characterization.

3.3.2.1. Surface Composition.

The deposit of PDA and polymers was confirmed by conducting attenuated total reflectance Fourier transform infrared (ATR-FTIR) spectroscopy for the surfaces (PP, PP/PDA, PP/PDA/PMPF-PMTF, PP/PDA/MTF, and PP/PDA/MPF) **(Figure 3.3).** Polypropylene surface (PP) is a material that can be used as a substrate for FTIR analysis.[35,36] As shown in **Figure 3.3**, polypropylene spectra displayed asymmetric and symmetric stretching peaks at 2950 and 2867 cm^{-1} for the CH_3 group and at 2923 and 2836 cm^{-1} for the CH_2 group, while the two intensive peaks at 1454 and 1375 cm^{-1} were assigned to the C–H bending vibration of CH_2 and CH_3 groups, respectively.[37] The intensities of these peaks are slightly reduced on the spectra of polymer-coated PP substrates, confirming the deposition of polydopamine and polymer coatings on the PP surfaces. In all PDA and PDA/polymer coatings, the broad peaks between 3200 and

3600 cm^{-1} were assigned to the stretching vibration of N–H and O–H, which mainly originates from the polydopamine. In contrast, the broad peak at 500 to 900 cm^{-1} could be attributed to the fingerprint area for the catechol stretching vibration.[38] Looking at the spectra of copolymer substrates, new peaks were observed compared to the pristine PP and PP/PDA spectra. The peak at 1650 cm^{-1} was observed on the spectra of PP/PDA/MPF-MTF, PP/PDA/MTF, and PP/PDA/MPF surfaces. This peak is assigned to the C=N vibration of the Schiff base (reaction of PDA with the polymers MPF and MTF). Moreover, the band at 1275 cm^{-1} on the spectra of PP/PDA/MPF-MTF and PP/PDA/MPF was attributed to the absorption of the P=O group on MPF chains, which was absent in the PP/PDA and PP/PDA/MTF spectra.[35,39] The signal at 1720 cm^{-1} was assigned to C=O aldehyde in PP/PDA/MPF and PP/PDA/MTF spectra. The overlapping broad peak at 3200 to 3600 cm^{-1} on the PP/PDA/MTF spectrum can be assigned to the adsorption of O–H and $–N^{+}(CH_3)_3$ groups.[40] The absorption peak at 1626 cm^{-1} in the PP/PDA/MPF-MTF spectrum was attributed to N–H stretching. All these results confirmed that the polydopamine and two polymers (MPF and MTF) were successfully deposited on PP surfaces.

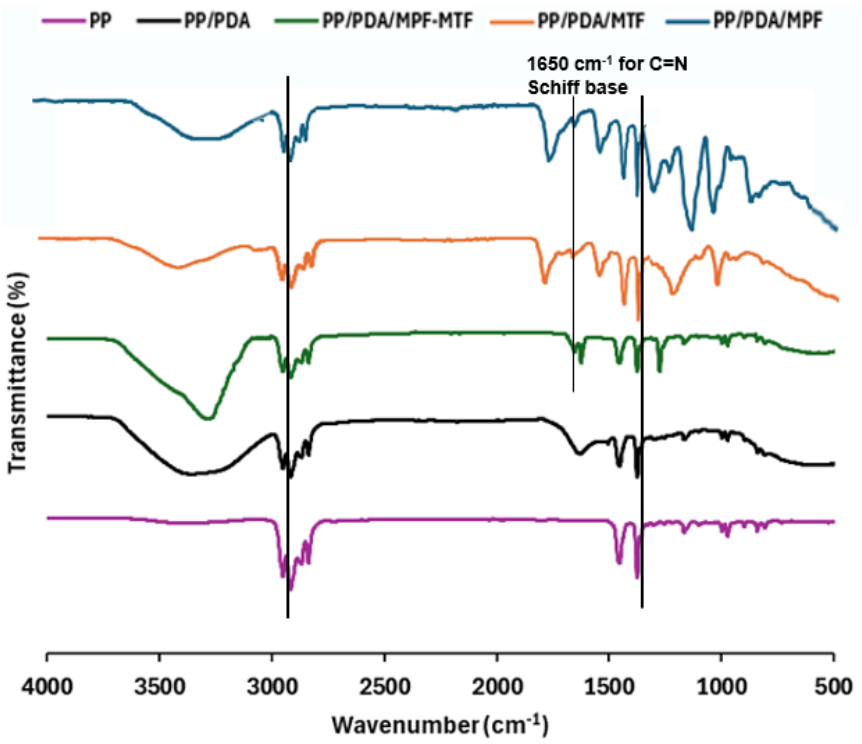

Figure 3.3. FTIR of PP, PP/PDA, PP/PDA/MPF/MTF PP/PDA/MTF, and PP/PDA/MPF substrates

3.3.2.2. Morphologies of Modified Surfaces.

The bare and functionalized glass surface morphologies were investigated using atomic force microscopy (AFM) (**Figure 3.4**). The bare glass was relatively smooth, with an RMS of 1.22 nm. However, the root mean square (RMS) roughness of the PDA (polydopamine) coated surface is measured to be 3.96 nm, indicating that the surface is rougher than the control glass surface. In this case, the increased roughness is primarily attributed to the deposition of self-polymerized large PDA aggregates on the surface, which leads to uneven surface morphology.[41] Introducing MPF and MTF copolymers onto the PDA-coated surface led to homogeneous and smoother surfaces with lower RMS values than polydopamine coating. In particular, the PDA-MPF surface showed the lowest RMS roughness with a value of 1.27 nm. These observations suggest that the

MPF and MTF were successfully grafted onto the PDA-coated surfaces. This decrease in roughness can be ascribed to the contribution of copolymers to form more uniform and even surfaces, thereby confirming their adequate coverage over the PDA aggregates layer**.**

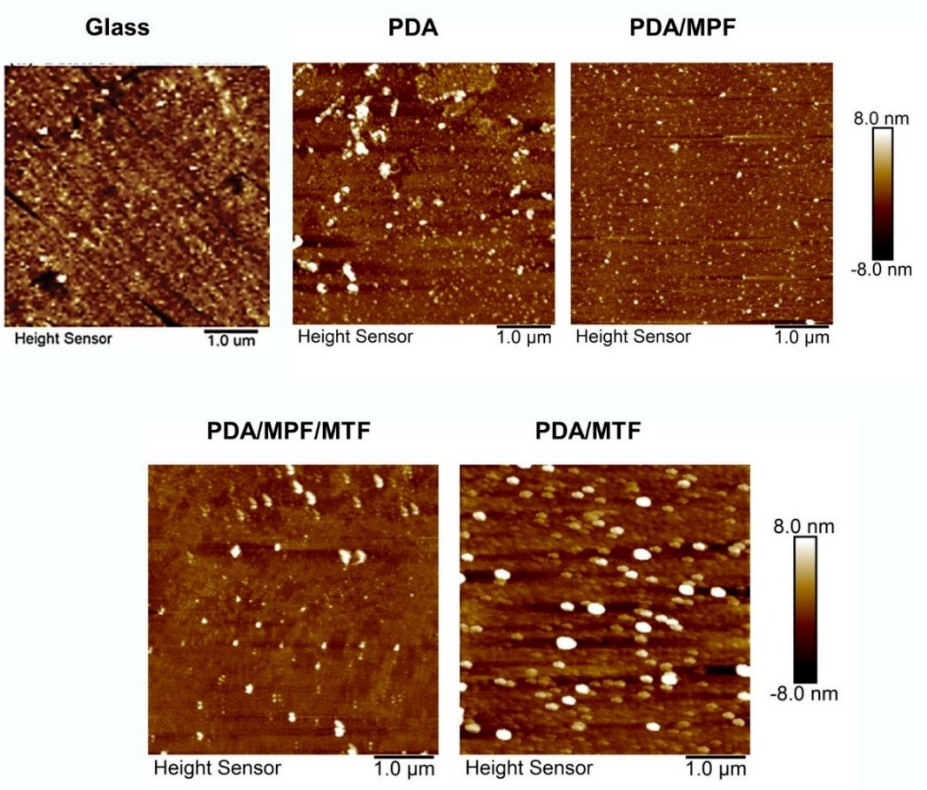

Figure 3.4. AFM images of bare glass-, PDA-, PDA/MPF-, PDA/MPF/MTF-, and PDA/MTF-coated surfaces.

3.3.2.3. Surface Hydrophilicity.

The hydrophilicity of biomaterials is an important characteristic that can impact protein adsorption and other surface interactions. The static water contact angle (WCA) was measured to evaluate the hydrophilicity of bare glass and the coated surfaces. As shown in **Figure 3.5**, the pristine glass slide had a WCA of 37.5 ± 0.7° (n = 3), indicating its moderate hydrophilicity. The PDA-coated surface exhibited a higher WCA of 41.1 ± 1.4°, suggesting low hydrophilicity and a

weak affinity for water compared to the glass control. In contrast, all polymer-modified surfaces showed lower water contact angles than the bare glass and PDA-coated surface. The PDA/MPF-coated surface demonstrated the lowest WCA of 14.3 ± 1°, suggesting that dense zwitterionic polymeric coating contributes to more surface hydration. The zwitterionic polymer content likely enhances the interaction with water, leading to a more effective surface hydration layer.[42] When the zwitterionic polymer content on the surface was decreased, there was a slight increase in the water contact angle, indicating that the presence of MPF polymer on the PDA surface contributes to a more robust interaction with water than the cationic groups of the MTF polymer brushes.[43]

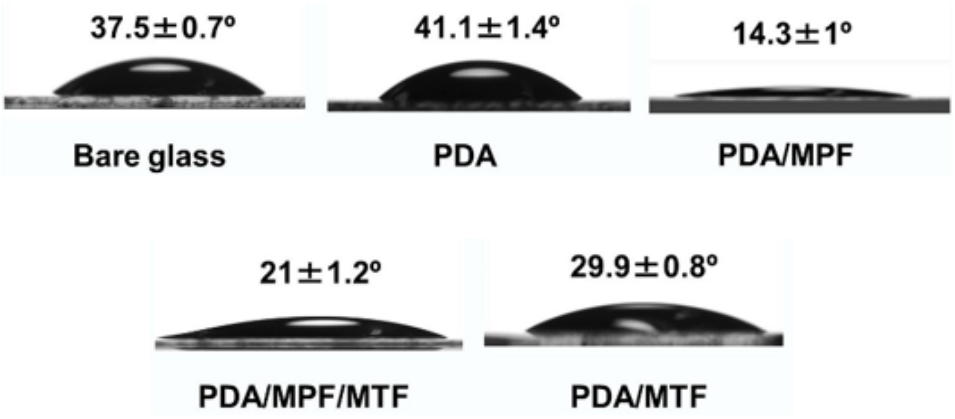

Figure 3.5. WCA images of bare glass, PDA, PDA/MPF, PDA/MPF/MTF, and PDA/MTF surfaces.

3.3.3. Protein Adsorption.

The adsorption of BSA (bovine serum albumin) on our coatings was measured using the BCA assay. As shown in **Figure 3.6**, the bare glass and PDA-coated surfaces showed the highest percentage of protein adsorption due to their hydrophobic interactions with BSA protein and their hydrophobicity, confirmed by their relatively high contact angles, as shown in Figure 3.5. This lack of protein suppression could also be attributed to the increase in surface roughness

caused by the PDA coating.[44] After introducing the polymer coating, the substrates became more hydrophilic, leading to less adsorbed protein. However, some protein was adsorbed onto the coatings containing MTF polymer. This amount of the adsorbed protein is due to the electrostatic interactions between the positively charged MTF polymer and the negatively charged BSA protein.[45] The PDA/MPF surface showed the lowest percentage of adsorbed protein (3 %), which can be attributed to the ability of the zwitterionic polymer to form a strong hydration layer on the surface. This layer can prevent the non-specific adsorption of proteins.[46] The small amount of BSA adsorbed onto the MPF coating could be attributed to surface roughness and the formation of covalent bonds between the aldehyde groups of MPF copolymer and amino groups of BSA.[47] Generally, it has been demonstrated that the protein adhesive layer is a platform for bacterial attachments and subsequent infections. Bacterial infections usually induce weak acidic conditions in the biological environment. These acidic environments could cleave the Schiff base linkage between the PDA and MPF or MTF copolymers. Such irreversible covalent bonds can facilitate the removal of both live and dead bacteria electrostatically attached to the polymer layer and release the adsorbed protein.[47]

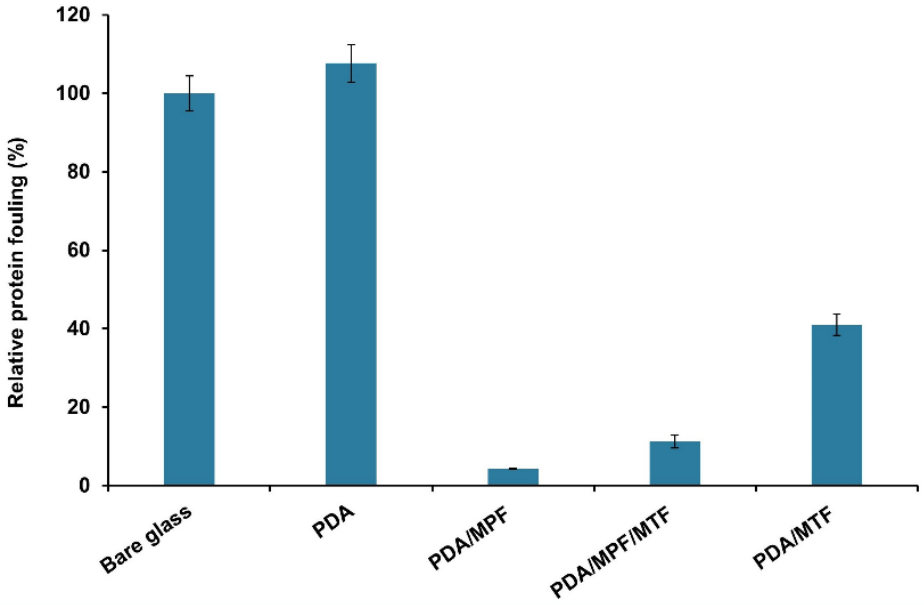

Figure 3.6. Relative protein adsorption onto bare glass, PDA, PDA/MPF, PDA/MPF/MTF, and PDA/MTF.

3.3.4. Antibacterial Performance of Polymer Coatings.

To examine the antiadhesion property of our surfaces against bacteria cells, we utilized CFU assay to determine the survival rates of *S. aureus* and *E. coli* seeded on the substrates for 3h with a concentration of $1x10^7$ cells per mL. As shown in **Figure 3.7(a, b),** all coatings containing MTF content showed low percentages of *viable S. aureus and E. coli* cells. In detail, Figures 3.7a (top) and 3.7b (top) show the antibacterial performance against S. aureus. Massive bacterial colonies of *S. aureus* were observed on the bare glass and PDA substrates, indicating the high accumulation and adherence of bacteria, which the large surface roughness can ascribe. The number of viable *S. aureus* adhered to the zwitterionic-coated substrate (PDA/MPF) was relatively low, showing 36 % of adhered bacteria compared to bare glass. By contrast, the figures for the PDA/MPF/MTF- and PDA/MTF-coated substrates significantly decreased to 19.20 % and 6.8 %, respectively. Meanwhile, a similar trend of the bactericidal ability of our coatings was

observed against *E. coli* [**Figure 3.7a** (bottom) and 7b (bottom)]. For example, the *E. coli* survival rate on PDA/MTF coating was the lowest by only 1.2%. This decrease in bacterial viability can be ascribed to the fact that by introducing the cationic MTF polymer, which has a simultaneous contact-killing action, to the coatings, the surface biocidal activity significantly increased along with the increase of the cationic component.[48] To compare the antibacterial effect of the PDA/MTF and PDA/MPF/MTF substrates, the biocidal activity depends on the density of cationic quaternary ammonium moieties in META brushes, which is a commonly used biocide with a permanent and pH-independent positive charge. Therefore, PDA/MTF coating, fabricated at a high density of MTF content, may result in a coating with a high proportion of ammonium cationic groups and is expected to be more effective at killing bacteria than PDA/MPF/MTF coating where the MTF density is less.[49,50] Moreover, it has been reported that coatings with high roughness can decrease bacterial adhesion by reducing the contact area between the bacteria and the surface.[51] As shown in **Figure 3.4**, the PDA/MTF coating surface was relatively rough and had large aggregates due to the successive deposition of polydopamine and MTF polymer. This relatively high level of roughness may provide physical protection against the adhesion of bacteria cells.

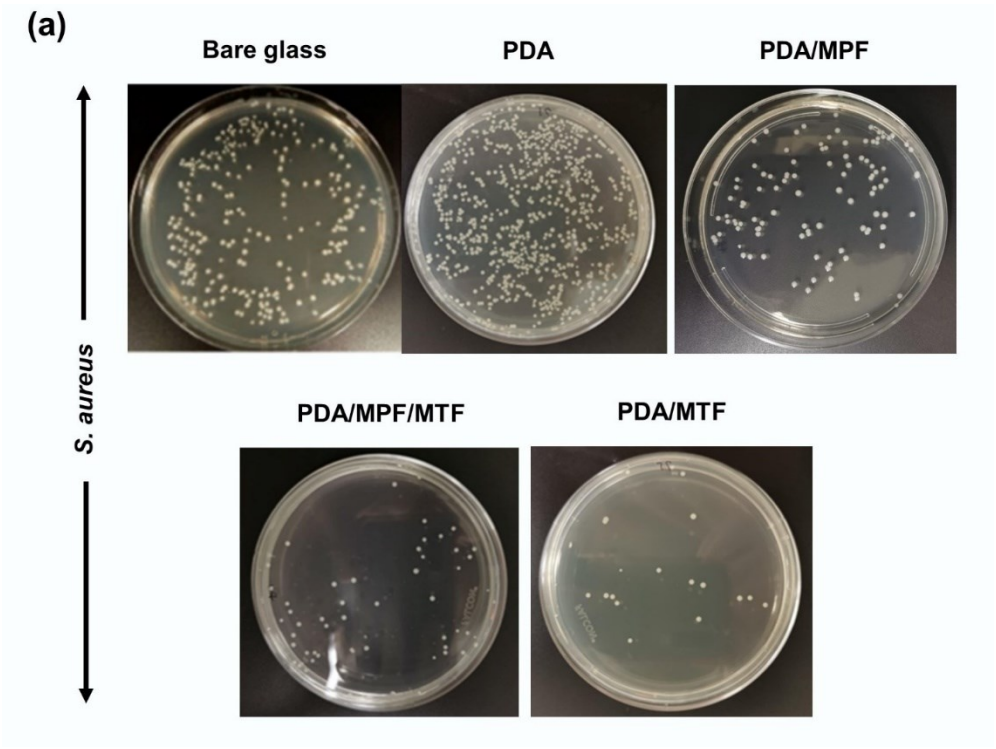
(a)
Bare glass
PDA
PDA/MPF
S. aureus
PDA/MPF/MTF
PDA/MTF

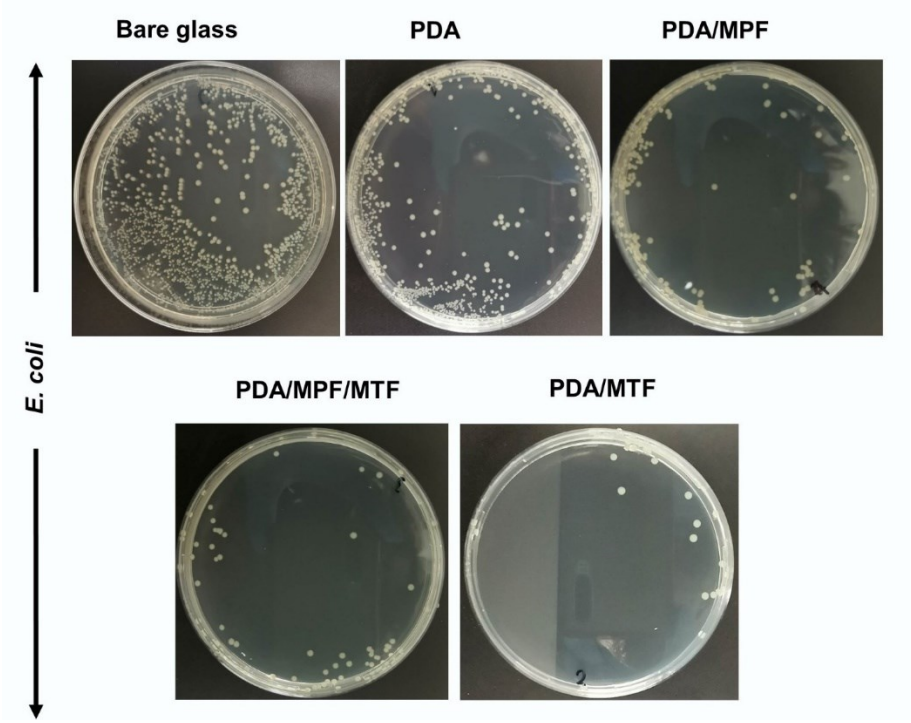
Bare glass
PDA
PDA/MPF
E. coli
PDA/MPF/MTF
PDA/MTF

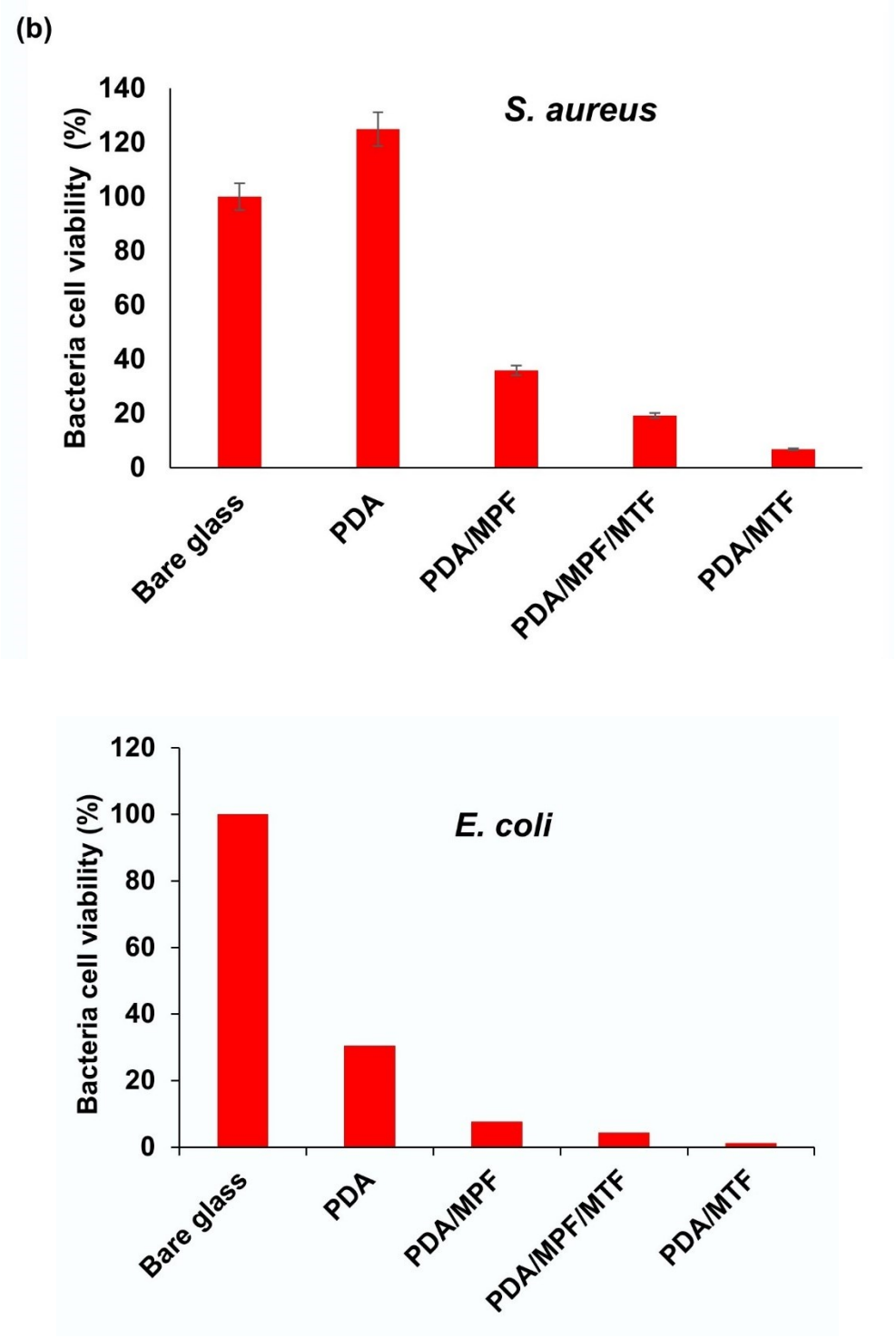

Figure 3.7. The antiadhesion performance of unmodified and modified substrates. (a) CFU images for *S. aureus* (top) and *E.coli* (bottom). (b) survival rates of *S. aureus* (top) and *E. coli* (bottom).

Coating stability in medical devices is essential to ensure their safety, efficacy, and durability. Instability or degradation of coatings can lead to device failure, necessitating device replacement and cost-effectiveness. Therefore, the stability of our coatings was evaluated after aging and shaking for 7 days in a phosphate-buffered saline (PBS) solution by assessing the antibacterial efficacy and comparing it with the freshly coated substrates. As shown in **Figure 3.8** and **Figure 3S5,** only a slight increase in the number of attached bacteria is observed on the aged PDA/MPF/MTF surface (20 and 15.4%) compared to the numbers before aging (19.2 and 4.3%) against *S. aureus* and *E. coli*, respectively, suggesting the stability and durability of this coating which can be attributed to its dual antifouling and bactericidal functionality.[52] Generally, compared to the aged PDA surface, the aged polymer-coated surfaces exhibited enhanced resistance to bacterial adhesion.[53] the PP/PDA/MPF-MTF coating showed better stability than other polymer coatings. This stability could be due to its dual functionality, combining an antibacterial polymer containing quaternary ammonium groups with antifouling zwitterionic polymer, along with an increased count of covalent cross-linking and cation-π interaction between electron-rich π-system and cationic groups.[54]

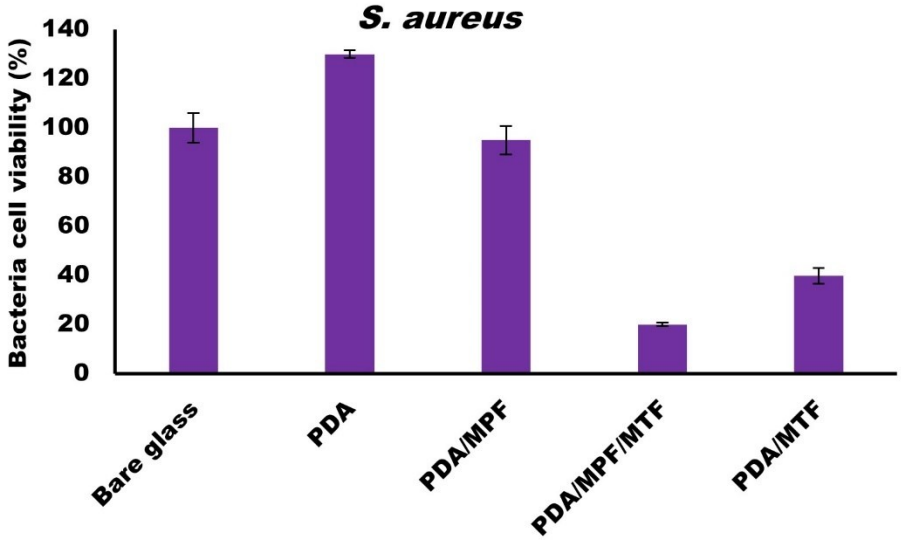

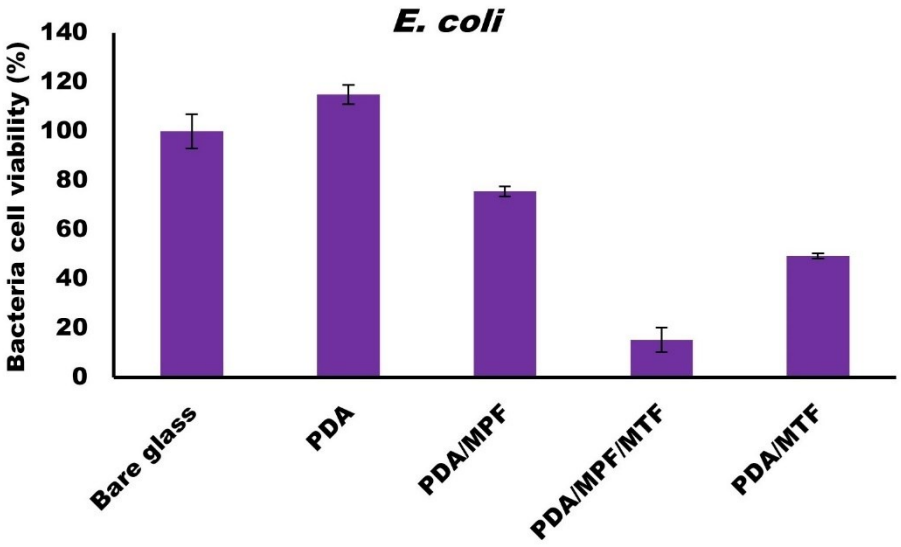

Figure 3.8. survival rates of *S. aureus* (top) and *E. coli* (bottom) on the bare glass, PDA, PDA/MPF, PDA/MPF/MTF, and PDA/MTF after incubation in PBS solution for 7 days.

3.3.5. Cytotoxicity.

A standard MTT assay was conducted to evaluate the cytotoxicity and biocompatibility of the bare glass and modified surfaces. MRC-5 cells were incubated with a culture medium containing extracts from the polymer coatings for 24h. As shown in (**Figure 3.9**), the different coated surfaces showed varying degrees of impact on cell viability. While the cell viability percentage of control was 100%, introducing coatings including DA, PDA/MPF, PDA/MPF/MTF, and PDA/MTF resulted in varying percentages of cell viability. However, their cell viability surpassed 94.3 % of the control, indicating that the coatings did not induce significant cytotoxic effects or adverse reactions in the MRS-5 cells. In the PDA control surface, where no polymer was applied, all cells remained viable, resulting in 105.64 % cell viability compared to the control. Similarly, upon introducing the MPF polymer onto the PDA surface, the cell viability percentage was 104.70 %. This high biocompatibility could be attributed to the increased cell membrane biomimetic phospholipid-based MPF-polymer content in the PDA/MPF sample,

which is responsible for its remarkable biocompatibility. The similarity in structure between the MPC-based polymer and cell membranes allows for a high degree of compatibility and interaction with biological systems, making it an ideal choice for various biomedical applications.[55] The addition of MTF copolymer onto the PDA/MPC surface (PDA/MPC/MTF) resulted in a slight decrease in cell viability to 94.3 %, which could be attributed to the potential cytotoxicity of quaternary ammonium salts in META and AEMA contents.[21] Lastly, the PDA/MTF surface exhibited a ~100% cell viability compared to the control.

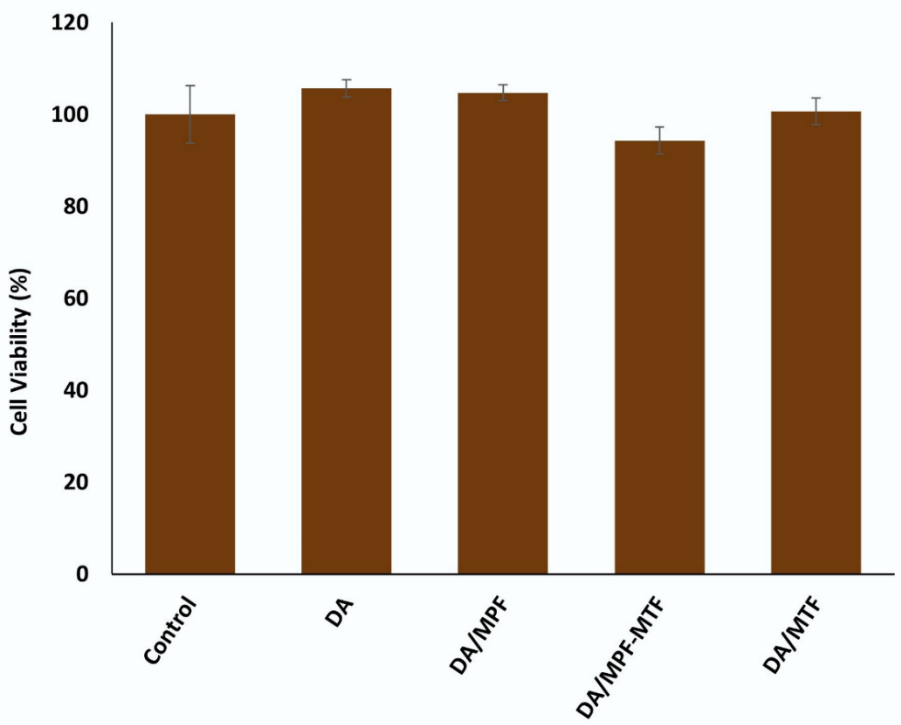

Figure 3.9. The cell viability of MRC-5 cells was cultured for 24 hours on the surfaces (control and coatings of PDA, PDA/MPF, PDA/MPF-MTF, and PDA/MTF modified glass).

3.4. Conclusion. Applying zwitterionic and cationic polymer coatings on surfaces has shown great potential in providing antibacterial and antifouling properties. The morphology of the coated surfaces plays a crucial role in determining their effectiveness. We carefully controlled

the coating process and successfully grafted zwitterionic and cationic polymers to PDA-coated surfaces. It was observed that as the zwitterionic polymer content in the coating increased, the wettability of the surface increased. Similarly, with an increase in the cationic polymer within the coating, there is a gradual enhancement in the bactericidal activity. The coating containing both MPF and MTF demonstrates the ability to repel BSA protein (88.8%) and significantly decreases the cell viability of *S. aureus* to 19.2% and *E. coli* to 7.7%. In addition, the coatings showed a low toxic effect on MRC-5 cells, suggesting a great potential for these antifouling and antibacterial coatings to fulfill biomedical applications.

3.5. Supporting Information.

3.5.1. 2-(1-Carboxy Methylethylsulfanylthiocarbonylsulfanyl)-2-methyl Propionic Acid (CTA) Synthesis.

The RAFT agent was prepared following the methodology outlined in the literature[28] and confirmed by ^{1}H NMR analysis (**Figure S3-1**).

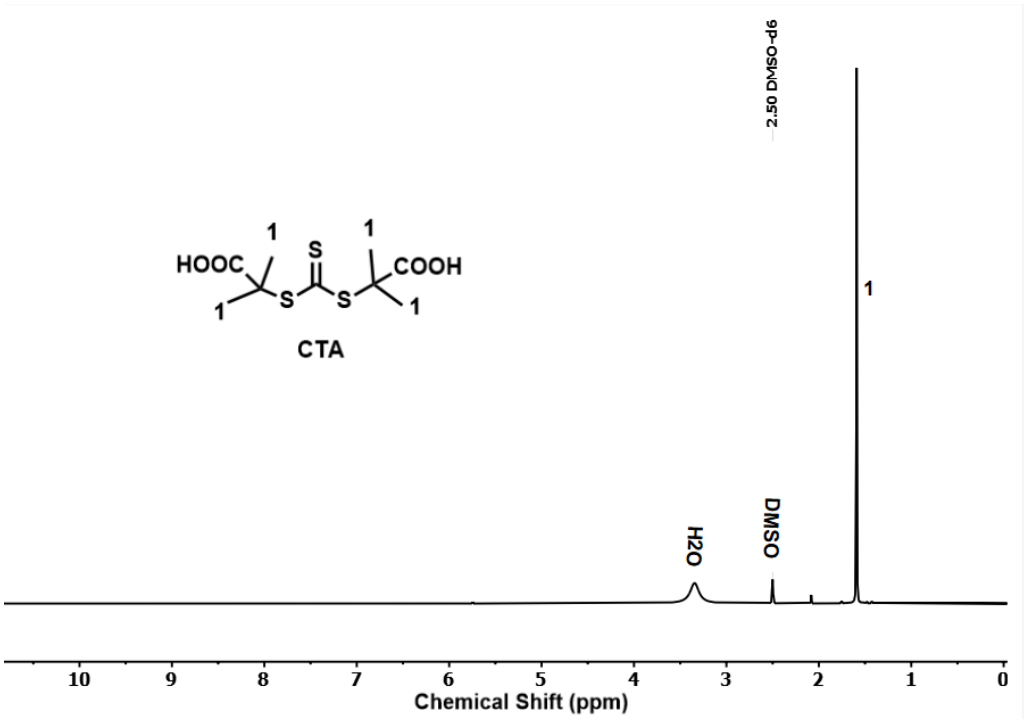

Figure S3-1: ^{1}H NMR spectrum of CTA in DMSO-d6.

3.5.2. 4-Formylphenyl Methacrylate (FPMA) Monomer Synthesis.

FPMA monomer was synthesized according to the procedure mentioned in the literature. 2 g (16.37 mmol) of 4-hydroxybenzaldehyde and 2.54 mL of triethylamine were dissolved in 17 mL of tetrahydrofuran, followed by cooling the mixture to 0°C. Then, 1.92 g (18.37 mmol) of methacryloyl chloride was added dropwise to the mixture at 0°C under continuous stirring. The reaction mixture was left to stir for another 6 h at RT. The reaction solution was filtered thrice and concentrated using a rotary evaporator. The crude product was washed with ethanol and further concentrated using a rotary evaporator, yielding the product as a yellow oil (Yield 76%) **(Figure S3-2 and Figure S3-3).**

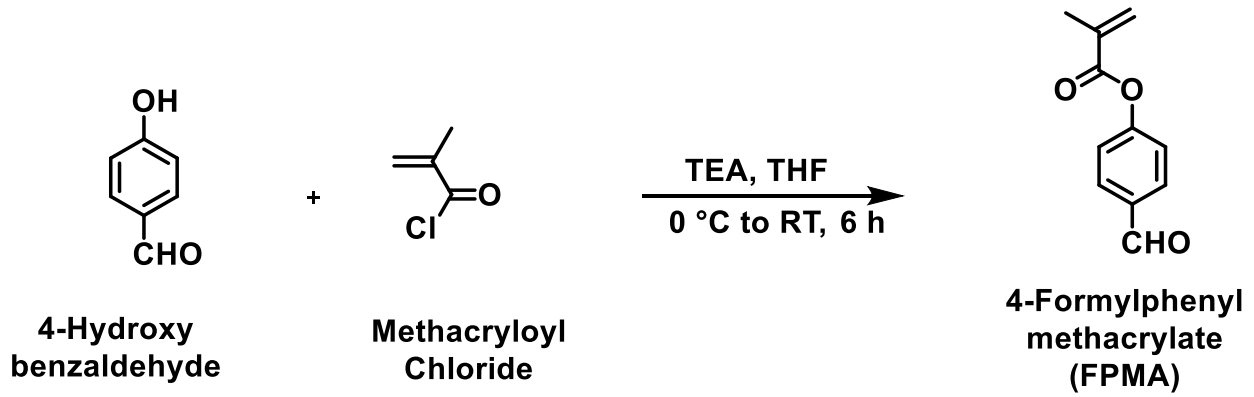

Figure S3-2. Synthesis of 4-Formylphenyl Methacrylate (FPMA) monomer.

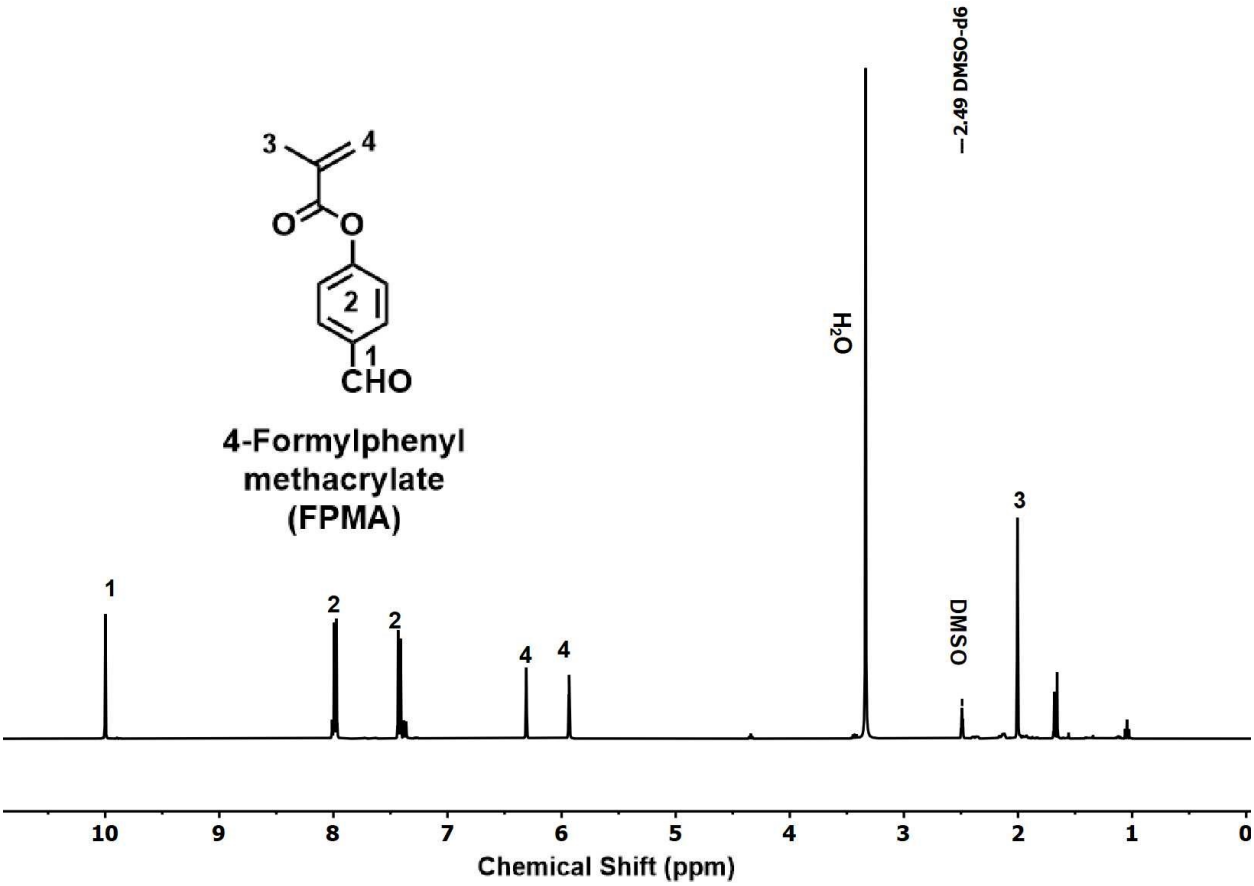

Figure S3-3: ^{1}H NMR spectrum of 4-formylphenyl methacrylate (FPMA) in DMSO-d6.

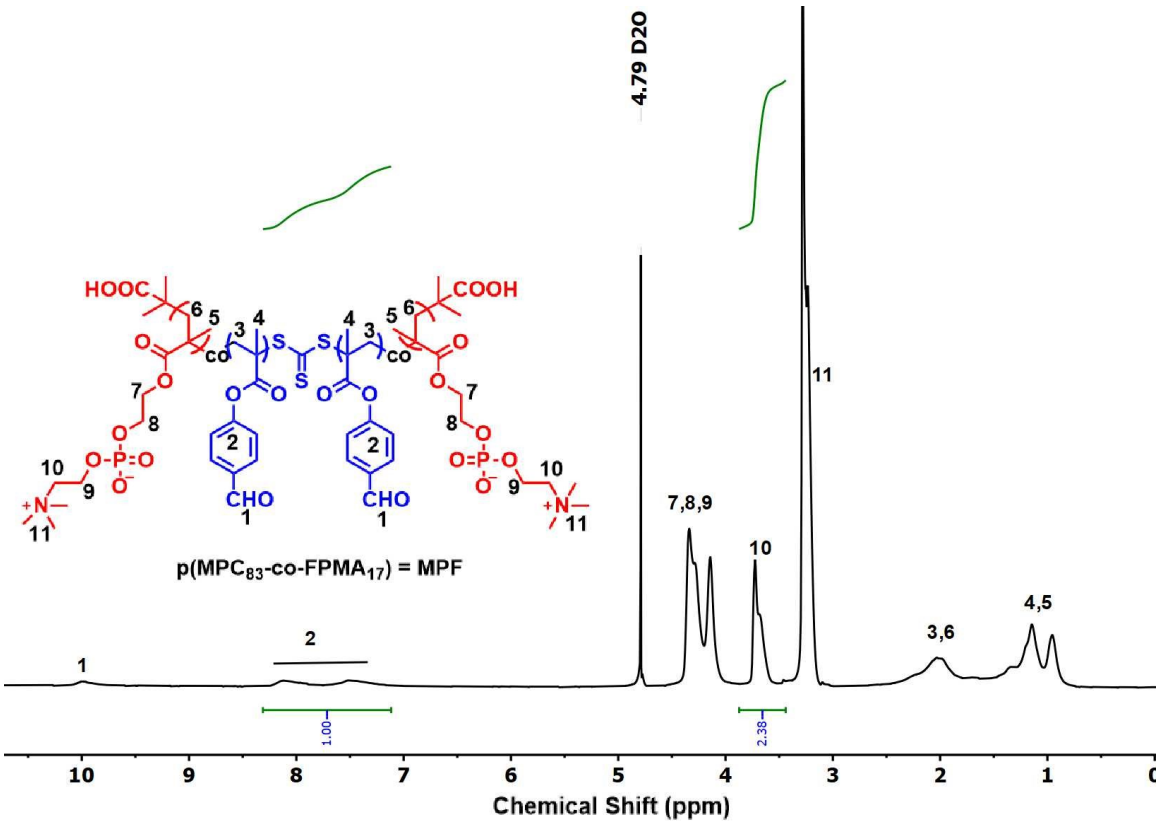

Figure S3-4: ^{1}H NMR spectrum of MPF in D_2O

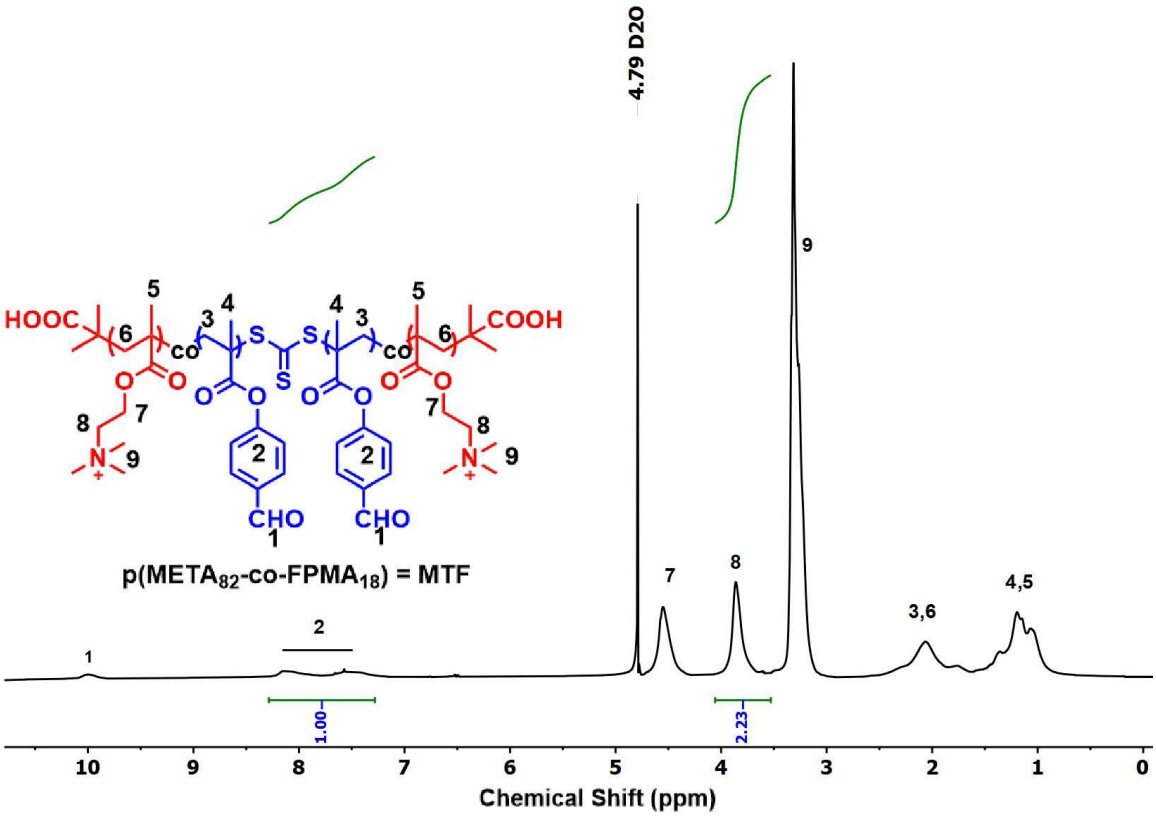

Figure S3-5: ^{1}H NMR spectrum of MTF in D_2O

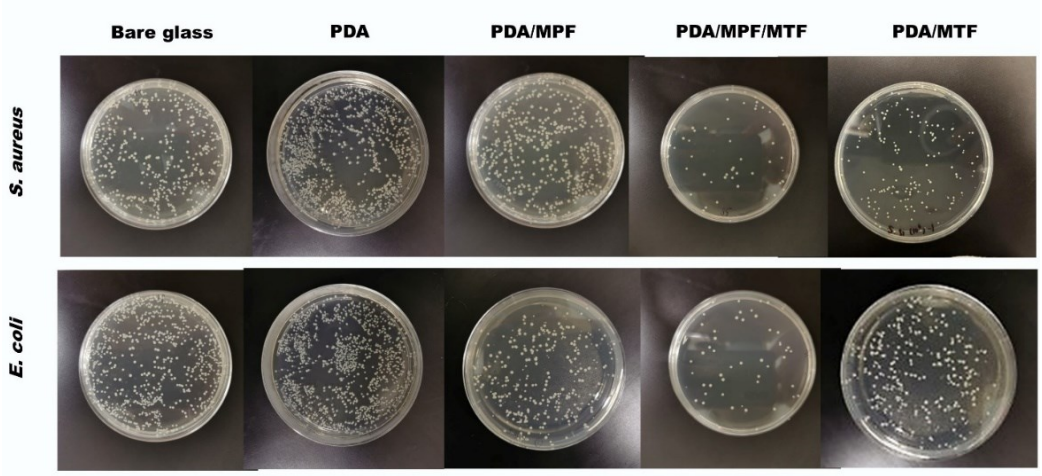

Figure S3-6. TS and LB agar plate photos of *S. aureus* (top) and *E. coli* (bottom) colonies formed by the serially diluted bacterial cells detached from the bare glass and polymer-coated glass slides after being aged in PBS solution for 7 days.

3.6. References.

(1) Neoh, K. G.; Hu, X.; Zheng, D.; Kang, E. T. Balancing Osteoblast Functions and Bacterial Adhesion on Functionalized Titanium Surfaces. *Biomaterials* **2012**, *33* (10), 2813–2822.

(2) Besser, M.; Terberger, J.; Weber, L.; Ghebremedhin, B.; Naumova, E. A.; Arnold, W. H.; Stuermer, E. K. Impact of Probiotics on Pathogen Survival in an Innovative Human Plasma Biofilm Model (HpBIOM). *J. Transl. Med.* **2019**, *17* (1), 1–9.

(3) Xu, L. C.; Siedlecki, C. A. Submicron-Textured Biomaterial Surface Reduces Staphylococcal Bacterial Adhesion and Biofilm Formation. *Acta Biomater.* **2012**, *8* (1), 72–81.

(4) Dai, G.; Ai, X.; Mei, L.; Ma, C.; Zhang, G. Kill-Resist-Renew Trinity: Hyperbranched Polymer with Self-Regenerating Attack and Defense for Antifouling Coatings. *ACS Appl. Mater. Interfaces* **2021**, *13* (11), 13735–13743.

(5) Chen, M.; Qiu, B.; Zhang, Z.; Xie, S.; Liu, Y.; Xia, T.; Li, X. Light-Triggerable and PH/Lipase-Responsive Release of Antibiotics and β-Lactamase Inhibitors from Host-Guest Self-Assembled Micelles to Combat Biofilms and Resistant Bacteria. *Chem. Eng. J.* **2021**, *424* (May), 130330.

(6) Nadell, C. D.; Drescher, K.; Wingreen, N. S.; Bassler, B. L. Extracellular Matrix Structure Governs Invasion Resistance in Bacterial Biofilms. *ISME J.* **2015**, *9* (8), 1700–1709.

(7) Ye, G.; Lee, J.; Perreault, F.; Elimelech, M. Controlled Architecture of Dual-Functional Block Copolymer Brushes on Thin-Film Composite Membranes for Integrated "Defending" and "Attacking" Strategies against Biofouling. *ACS Appl. Mater. Interfaces*

2015, *7* (41), 23069–23079.

(8) Chiang, Y. C.; Chang, Y.; Higuchi, A.; Chen, W. Y.; Ruaan, R. C. Sulfobetaine-Grafted Poly(Vinylidene Fluoride) Ultrafiltration Membranes Exhibit Excellent Antifouling Property. *J. Memb. Sci.* **2009**, *339* (1–2), 151–159.

(9) Fleitas-Salazar, N.; Silva-Campa, E.; Pedroso-Santana, S.; Tanori, J.; Pedroza-Montero, M. R.; Riera, R. Effect of Temperature on the Synthesis of Silver Nanoparticles with Polyethylene Glycol: New Insights into the Reduction Mechanism. *J. Nanoparticle Res.* **2017**, *19* (3).

(10) Arima, Y.; Toda, M.; Iwata, H. Complement Activation on Surfaces Modified with Ethylene Glycol Units. *Biomaterials* **2008**, *29* (5), 551–560.

(11) Zhang, S.; Yang, X.; Tang, B.; Yuan, L.; Wang, K.; Liu, X.; Zhu, X.; Li, J.; Ge, Z.; Chen, S. New Insights into Synergistic Antimicrobial and Antifouling Cotton Fabrics via Dually Finished with Quaternary Ammonium Salt and Zwitterionic Sulfobetaine. *Chem. Eng. J.* **2018**, *336* (August 2017), 123–132.

(12) Wu, C.; Zhou, Y.; Wang, H.; Hu, J. P4VP Modified Zwitterionic Polymer for the Preparation of Antifouling Functionalized Surfaces. *Nanomaterials* **2019**, *9* (5).

(13) Niu, J.; Wang, H.; Chen, J.; Chen, X.; Han, X.; Liu, H. Bio-Inspired Zwitterionic Copolymers for Antifouling Surface and Oil-Water Separation. *Colloids Surfaces A Physicochem. Eng. Asp.* **2021**, *626* (May), 127016.

(14) Zhou, L.; Li, Q. L.; Wong, H. M. A Novel Strategy for Caries Management: Constructing an Antibiofouling and Mineralizing Dual-Bioactive Tooth Surface. *ACS Appl. Mater.*

Interfaces **2021**, *13* (26), 31140–31152.

(15) Yang, X.; Ding, C.; Wu, M.; Xu, X.; Ke, X.; Xu, H.; Li, J.; Lou, F.; Zhou, K.; Jiang, H.; Peng, X.; Wang, X.; Si, L.; Li, J. Biomineral Interface with Superior Cell Adhesive and Antibacterial Properties Based on Enzyme-Triggered Digestion of Saliva Acquired Pellicle-Inspired Polypeptide Coatings. *Chem. Eng. J.* **2021**, *415* (October 2020), 128955.

(16) Cao, J.; Sun, Q.; Shen, A. G.; Fan, B.; Hu, J. M. Nano Au@Cu2-XS with near-Infrared Photothermal and Peroxidase Catalytic Activities Redefines Efficient Antibiofilm-Oriented Root Canal Therapy. *Chem. Eng. J.* **2021**, *422* (December 2020), 130090.

(17) Kang, S.; Herzberg, M.; Rodrigues, D. F.; Elimelech, M. Antibacterial Effects of Carbon Nanotubes: Size Does Matter! *Langmuir* **2008**, *24* (13), 6409–6413.

(18) Ye, M.; Zhao, Y.; Wang, Y.; Zhao, M.; Yodsanit, N.; Xie, R.; Andes, D.; Gong, S. A Dual-Responsive Antibiotic-Loaded Nanoparticle Specifically Binds Pathogens and Overcomes Antimicrobial-Resistant Infections. *Adv. Mater.* **2021**, *33* (9), 1–12.

(19) Lv, C.; Chen, S.; Xie, Y.; Wei, Z.; Chen, L.; Bao, J.; He, C.; Zhao, W.; Sun, S.; Zhao, C. Positively-Charged Polyethersulfone Nanofibrous Membranes for Bacteria and Anionic Dyes Removal. *J. Colloid Interface Sci.* **2019**, *556*, 492–502.

(20) Gottenbos, B.; Van Der Mei, H. C.; Klatter, F.; Nieuwenhuis, P.; Busscher, H. J. In Vitro and in Vivo Antimicrobial Activity of Covalently Coupled Quaternary Ammonium Silane Coatings on Silicone Rubber. *Biomaterials* **2002**, *23* (6), 1417–1423.

(21) Ye, S.; Majumdar, P.; Chisholm, B.; Stafslien, S.; Chen, Z. Antifouling and Antimicrobial Mechanism of Tethered Quaternary Ammonium Salts in a Cross-Linked

Poly(Dimethylsiloxane) Matrix Studied Using Sum Frequency Generation Vibrational Spectroscopy. *Langmuir* **2010**, *26* (21), 16455–16462.

(22) Farah, S.; Aviv, O.; Laout, N.; Ratner, S.; Beyth, N.; Domb, A. J. Quaternary Ammonium Poly(Diethylaminoethyl Methacrylate) Possessing Antimicrobial Activity. *Colloids Surfaces B Biointerfaces* **2015**, *128*, 608–613.

(23) Hong, S.; Na, Y. S.; Choi, S.; Song, I. T.; Kim, W. Y.; Lee, H. Non-Covalent Self-Assembly and Covalent Polymerization Co-Contribute to Polydopamine Formation. *Adv. Funct. Mater.* **2012**, *22* (22), 4711–4717.

(24) Li, S.; Scheiger, J. M.; Wang, Z.; Dong, Z.; Welle, A.; Trouillet, V.; Levkin, P. A. Substrate-Independent and Re-Writable Surface Patterning by Combining Polydopamine Coatings, Silanization, and Thiol-Ene Reaction. *Adv. Funct. Mater.* **2021**, *31* (50).

(25) Qiu, W. Z.; Zhao, Z. S.; Du, Y.; Hu, M. X.; Xu, Z. K. Antimicrobial Membrane Surfaces via Efficient Polyethyleneimine Immobilization and Cationization. *Appl. Surf. Sci.* **2017**, *426*, 972–979.

(26) Shahkaramipour, N.; Lai, C. K.; Venna, S. R.; Sun, H.; Cheng, C.; Lin, H. Membrane Surface Modification Using Thiol-Containing Zwitterionic Polymers via Bioadhesive Polydopamine. *Ind. Eng. Chem. Res.* **2018**, *57* (6), 2336–2345.

(27) Zhang, H.; Luo, J.; Li, S.; Wei, Y.; Wan, Y. Biocatalytic Membrane Based on Polydopamine Coating: A Platform for Studying Immobilization Mechanisms. *Langmuir* **2018**, *34* (8), 2585–2594.

(28) Lai, J. T.; Filla, D.; Shea, R. Functional Polymers from Novel Carboxyl-Terminated

Trithiocarbonates as Highly Efficient RAFT Agents. *Am. Chem. Soc. Polym. Prepr. Div. Polym. Chem.* **2002**, *43* (2), 122–123.

(29) Ovdenko, V.; Kolendo, A. New Bent-Shaped Azomethine Monomers for Optical Applications. *Mol. Cryst. Liq. Cryst.* **2016**, *640* (1), 113–121.

(30) Asha, A. B.; Chen, Y.; Zhang, H.; Ghaemi, S.; Ishihara, K.; Liu, Y.; Narain, R. Rapid Mussel-Inspired Surface Zwitteration for Enhanced Antifouling and Antibacterial Properties. *Langmuir* **2019**, *35* (5), 1621–1630.

(31) Wang, B. L.; Jin, T. W.; Han, Y. M.; Shen, C. H.; Li, Q.; Lin, Q. K.; Chen, H. Bio-Inspired Terpolymers Containing Dopamine, Cations and MPC: A Versatile Platform to Construct a Recycle Antibacterial and Antifouling Surface. *J. Mater. Chem. B* **2015**, *3* (27), 5501–5510.

(32) Cheng, Q.; Guo, X.; Hao, X.; Shi, Z.; Zhu, S.; Cui, Z. Fabrication of Robust Antibacterial Coatings Based on an Organic-Inorganic Hybrid System. *ACS Appl. Mater. Interfaces* **2019**, *11* (45), 42607–42615.

(33) Wang, G.; Weng, D.; Chen, C.; Chen, L.; Wang, J. Influence of TiO2 Nanostructure Size and Surface Modification on Surface Wettability and Bacterial Adhesion. *Colloids Interface Sci. Commun.* **2020**, *34* (November 2019), 100220.

(34) Ma, J.; Zhang, H. Kinetic Investigations of RAFT Polymerization: Difunctional RAFT Agent Mediated Polymerization of Methyl Methacrylate and Styrene. *Macromol. Res.* **2015**, *23* (1), 67–73.

(35) Krylova, V.; Dukštiene, N. Synthesis and Characterization of Ag Layers Formed on

Polypropylene. *J. Chem.* **2013**, *2013*.

(36) Pate, S. G.; Xu, H.; O'Brien, C. P. Operando Observation of CO2transport Intermediates in Polyvinylamine Facilitated Transport Membranes, and the Role of Water in the Formation of Intermediates, Using Transmission FTIR Spectroscopy. *J. Mater. Chem. A* **2022**, *10* (8), 4418–4427.

(37) Kord Forooshani, P.; Polega, E.; Thomson, K.; Bhuiyan, M. S. A.; Pinnaratip, R.; Trought, M.; Kendrick, C.; Gao, Y.; Perrine, K. A.; Pan, L.; Lee, B. P. Antibacterial Properties of Mussel-Inspired Polydopamine Coatings Prepared by a Simple Two-Step Shaking-Assisted Method. *Front. Chem.* **2019**, *7* (September).

(38) Wardani, A. K.; Ariono, D.; Subagjo; Wenten, I. G. Hydrophilic Modification of Polypropylene Ultrafiltration Membrane by Air-Assisted Polydopamine Coating. *Polym. Adv. Technol.* **2019**, *30* (4), 1148–1155.

(39) Hou, C.; Qi, Z.; Zhu, H. Preparation of Core-Shell Magnetic Polydopamine/Alginate Biocomposite for Candida Rugosa Lipase Immobilization. *Colloids Surfaces B Biointerfaces* **2015**, *128*, 544–551.

(40) Morales, D. V.; Rivas, B. L.; Escalona, N. Poly([(2-Methacryloyloxy)Ethyl]Trimethylammonium Chloride): Synthesis, Characterization, and Removal Properties of As(V). *Polym. Bull.* **2016**, *73* (3), 875–890.

(41) Zangmeister, R. A.; Morris, T. A.; Tarlov, M. J. Characterization of Polydopamine Thin Films Deposited at Short Times by Autoxidation of Dopamine. *Langmuir* **2013**, *29* (27), 8619–8628.

(42) Ma, W.; Rajabzadeh, S.; Matsuyama, H. Preparation of Antifouling Poly(Vinylidene Fluoride) Membranes via Different Coating Methods Using a Zwitterionic Copolymer. *Appl. Surf. Sci.* **2015**, *357*, 1388–1395.

(43) Chen, S.; Li, L.; Zhao, C.; Zheng, J. Surface Hydration: Principles and Applications toward Low-Fouling/Nonfouling Biomaterials. *Polymer (Guildf).* **2010**, *51* (23), 5283–5293.

(44) Dang, Y.; Xing, C. M.; Quan, M.; Wang, Y. B.; Zhang, S. P.; Shi, S. Q.; Gong, Y. K. Substrate Independent Coating Formation and Anti-Biofouling Performance Improvement of Mussel Inspired Polydopamine. *J. Mater. Chem. B* **2015**, *3* (20), 4181–4190.

(45) Wang, B. L.; Jin, T. W.; Han, Y. M.; Shen, C. H.; Li, Q.; Lin, Q. K.; Chen, H. Bio-Inspired Terpolymers Containing Dopamine, Cations and MPC: A Versatile Platform to Construct a Recycle Antibacterial and Antifouling Surface. *J. Mater. Chem. B* **2015**, *3* (27), 5501–5510.

(46) Ishihara, K. Bioinspired Phospholipid Polymer Biomaterials for Making High Performance Artificial Organs. *Sci. Technol. Adv. Mater.* **2000**, *1* (3), 131–138.

(47) Zhang, Y.; Zhang, X.; Zhao, Y. Q.; Zhang, X. Y.; Ding, X.; Ding, X.; Yu, B.; Duan, S.; Xu, F. J. Self-Adaptive Antibacterial Surfaces with Bacterium-Triggered Antifouling-Bactericidal Switching Properties. *Biomater. Sci.* **2020**, *8* (3), 997–1006.

(48) Druvari, D.; Koromilas, N. D.; Bekiari, V.; Bokias, G.; Kallitsis, J. K. Polymeric Antimicrobial Coatings Based on Quaternary Ammonium Compounds. *Coatings* **2018**, *8* (1).

(49) Wang, H.; Chen, M.; Jin, C.; Niu, B.; Jiang, S.; Li, X.; Jiang, S. Antibacterial [2-(Methacryloyloxy) Ethyl] Trimethylammonium Chloride Functionalized Reduced Graphene Oxide/Poly(Ethylene-Co-Vinyl Alcohol) Multilayer Barrier Film for Food Packaging. *J. Agric. Food Chem.* **2018**, *66* (3), 732–739.

(50) Asha, A. B.; Peng, Y. Y.; Cheng, Q.; Ishihara, K.; Liu, Y.; Narain, R. Dopamine Assisted Self-Cleaning, Antifouling, and Antibacterial Coating via Dynamic Covalent Interactions. *ACS Appl. Mater. Interfaces* **2022**, *14* (7), 9557–9569.

(51) Mu, M.; Liu, S.; Deflorio, W.; Hao, L.; Wang, X.; Salazar, K. S.; Taylor, M.; Castillo, A.; Cisneros-zevallos, L.; Oh, J. K.; Min, Y. Influence of Surface Roughness, Nanostructure, and Wetting on Bacterial Adhesion. **2023**.

(52) Maan, A. M. C.; Hofman, A. H.; de Vos, W. M.; Kamperman, M. Recent Developments and Practical Feasibility of Polymer-Based Antifouling Coatings. *Adv. Funct. Mater.* **2020**, *30* (32).

(53) Yao, L.; He, C.; Chen, S.; Zhao, W.; Xie, Y.; Sun, S.; Nie, S.; Zhao, C. Codeposition of Polydopamine and Zwitterionic Polymer on Membrane Surface with Enhanced Stability and Antibiofouling Property. *Langmuir* **2019**, *35* (5), 1430–1439.

(54) Burmeister, N.; Zorn, E.; Preuss, L.; Timm, D.; Scharnagl, N.; Rohnke, M.; Wicha, S. G.; Streit, W. R.; Maison, W. Low-Fouling and Antibacterial Polymer Brushes via Surface-Initiated Polymerization of a Mixed Zwitterionic and Cationic Monomer. *Langmuir* **2023**, *39* (49), 17959–17971.

(55) Berrocal, M. J.; Daniel Johnson, R.; Badr, I. H. A.; Liu, M.; Gao, D.; Bachas, L. G.

Improving the Blood Compatibility of Ion-Selective Electrodes by Employing Poly(MPC-Co-BMA), a Copolymer Containing Phosphorylcholine, as a Membrane Coating. *Anal. Chem.* **2002**, *74* (15), 3644–3648.

Chapter 4: Stable Antifouling and Antibacterial Coating Based on Assembly of Copper-Phenolic Networks

4.1. Introduction.

One of the most detrimental consequences of bacterial surface colonization in the medical sector is hospital-associated infections (HAIs), which can be life-threatening.[1] In the United States, HAIs are estimated to infect at least 2 million individuals and result in 23,000 deaths every year, costing USD 55 to 70 billion.[2] When medical devices are inserted into the body, they provide a route for attachment and proliferation of bacteria and protein adsorption, which can develop and become biofilm.[3,4] Therefore, there is a need for antibacterial coatings that can potentially minimize bacterial colonization and consequently reduce the occurrence of HAIs. To address the emerging problem, recent studies demonstrate two major coating strategies: inhibiting the attachment of bacteria and proteins (antifouling coatings) or killing bacteria attached to the surface and in the vicinity (bactericidal coatings). On an antifouling coating, any bacterium that manages to attach will proliferate, while on bactericidal coatings, the accumulation of dead bacteria and debris provides opportunities for other bacteria to colonize the surface. As a result, the integration of antifouling and bactericidal functionalities in a single coating has been investigated to inhibit bacterial colonization.[5,6]

Due to their biocompatibility, renewability, and non-toxicity, polysaccharides are potential candidates to replace synthetic polymers in various biomedical applications, such as wound dressings, regenerative medicine, and drug delivery systems.[7–9] Additionally, polysaccharides, including hyaluronic acid, alginate, chitosan, and heparin, have been used in anti-adhesive coatings for biomedical applications, demonstrating excellent antifouling properties.[10–12] Glycopolymers are another alternative to hydrophilic polymers that exhibit excellent antifouling behavior. They are composed of many hydroxyl groups in their structures; therefore, their complexes with divalent ions exhibit antifouling property that mimics the hydrophilic

polysaccharides by preventing bacterial adhesion and protein adsorption to the materials.[13] For example, a poly(vinylidene difluoride) (PVDF) microporous membrane was modified with poly(D-gluconamidoethyl methacrylate) (PGAMA) by activators generated electron transfer atom transfer radical polymerization (AGET-ATRP) to improve the wettability and antifouling property. With an increase in the PGAMA grafting density, the water contact angle and protein adhesion decreased to as low as 30.4° and 0.19 mg/cm2, respectively, compared to 110° and 0.96 mg/cm^2 for PVDF control.[14] In another study, glycopolymer was copolymerized with DMA, and the resulting copolymer was coated onto different organic and inorganic surfaces (i.e., glass slide, silicon wafer, and polycarbonate) by a simple one-pot process. The authors reported that the DMA monomer provided the adhesive property and the glycopolymer provided the hydrophilic functionality in which their coating reduced the water contact angles to 3.1 and 4.1° compared to 56 and 52° for the glass and silicon wafer controls, respectively.[15]

Recently, metal-phenolic networks (MPNs), consisting of metal ions coordinated with phenolic ligands, are considered versatile materials for simple and stable surface modification of medical devices.[16–18] In 2013, Caruso *et al.* first designed a simple method for fabricating pH-responsive coating based on the coordination complex between Fe^{III} and polyphenols.[19] Since then, many antibacterial coatings have been developed based on metal-phenol chemistry.[20–22] In particular, silver and copper have been used for constructing antimicrobial coatings due to their low cost and antimicrobial properties against a wide range of microorganisms.[23,24] Although copper compounds are less toxic than silver compounds, the instability of CuPNs on bactericidal coatings limited its applications.[25] Therefore, a stable copper-based coating with antibacterial properties and cytocompatibility is needed. Herein, we developed an efficient approach for fabricating antifouling and antibacterial coating based on coordinating copper ions (Cu^{II}) and

GADMA copolymer to form a stable metal-phenolic network on the surface (**Scheme 4.1**). Our MPN coating system demonstrated long-lasting antifouling properties against bovine serum albumin (BSA). The bacteria-killing activity of GADMA-Cu coating against Gram-positive *S. aureus* and Gram-negative *E. coli* and the in vitro cytotoxicity of the coatings were also investigated.

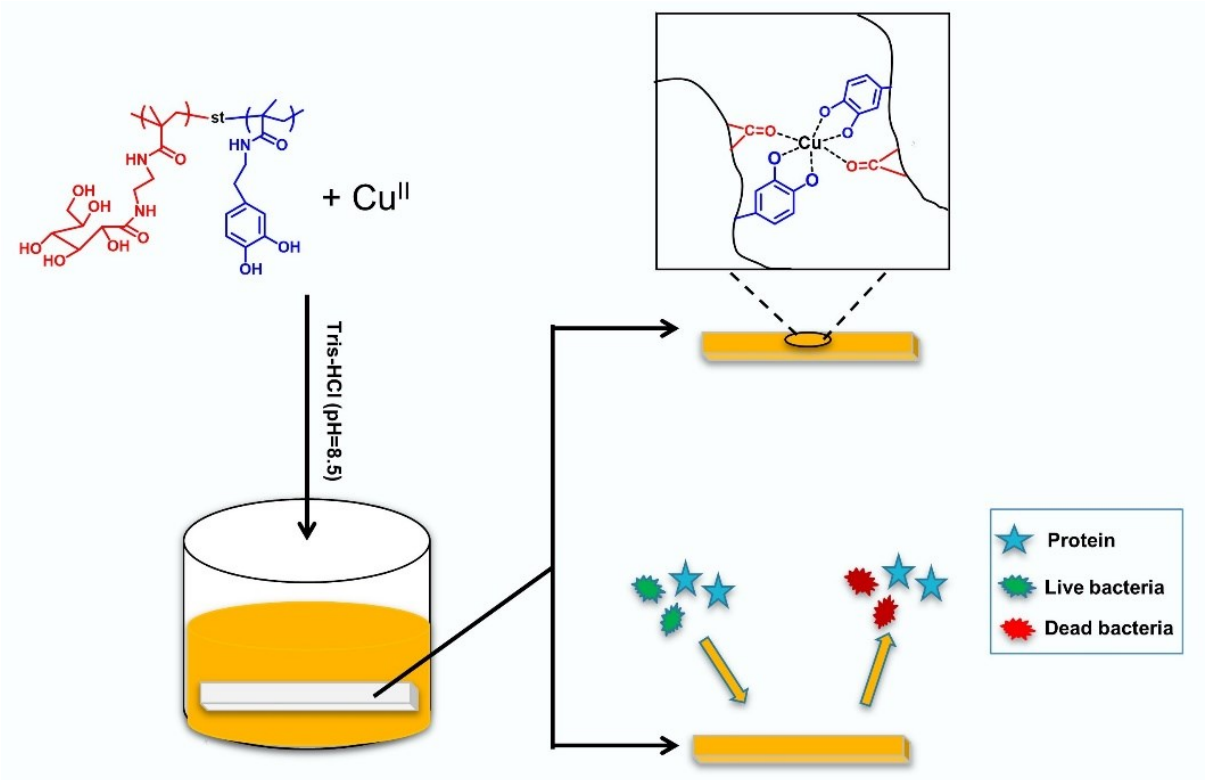

Scheme 4.1. Schematic illustrates one-pot dip-coating on glass slide via metal-catechol networks (MPNs) in the mixture of Cu ions and GADMA copolymer at pH=8.5

4.2. Experimental Section.

4.2.1. Materials. Azo-initiator [4,4′-Azobis(4-cyano valeric acid) (ACVA)], bovine serum albumin (BSA), copper sulfate ($CuSO_4.5H_2O$), methacrylic anhydride, sodium borate, and dopamine hydrochloride were purchased from Sigma-Aldrich. Micro BCA^{TM} Protein Assay Kit was purchased from Fisher Scientific. *N, N*-dimethylformamide (DMF), sodium dodecyl sulfate

(SDS), ethylene diamine (EDA), triethylene amine (TEA), isopropanol, tetrahydro furan (THF) methacrylic anhydride, and dimethyl sulfoxide (DMSO) were obtained from Caledon Laboratories Ltd. (Canada).

4.2.2. Synthesis of p(GAEMA-co-DMA) Copolymer [GADMA]. The monomers [2-gluconamidoethyl methacrylamide (GAEMA) and dopamine mechacrylamide (DMA)] were first synthesized, and their chemical structures were characterized by ^{1}H NMR (see supporting information for more details about protocols and characterization). The GADMA copolymer was synthesized via free radical polymerization and using ACVA as an initiator. Briefly, GAEMA (593 mg, 1.938 mmol), DMA (107 mg, 0.484 mmol), and ACVA (3.39 mg, 0.012 mmol) were dissolved in deionized water and DMF in 50 mL polymerization tube. After degassing by nitrogen for 30 minutes, the polymerization reaction was carried out in an oil bath at 70 °C for 24 hours. The product was then dialyzed against DI water for three days to remove the unreacted monomers, followed by lyophilization to obtain the copolymer. The average molecular weight (M_n) and the polydispersity (PDI) of GADMA were measured by gel permeation chromatography (GPC) as indicated in the literature.[26]

4.2.3. One-step Deposition of GADMA-Cu Coating onto Glass Slides. The glass substrates were rinsed under sonication in DI water for 20 min and then in acetone for 10 min before being dried in air. To prepare MPNs coating, GADMA (8 mg/mL) was dissolved in 10 mM Tris-HCl buffer solution, and the pH was adjusted to pH 8.5 by 1 M NaOH. Then, aqueous solution of $CuSO_4 \cdot 5H_2O$ (5 mg/mL) was mixed with the polymer buffer solution [50:50% (v/v)]. The glass slides were immersed into the mixture solutions and shaken for 10 h at room temperature. The samples were then rinsed with DI water and dried in the air. The GADMA coating (without copper) was also prepared as a control, following the abovementioned steps for MPN coating.

4.2.4. Surface Characterization. To investigate the chemical structures of the bare glass and GADMA coatings, attenuated total reflectance Fourier transform infrared (ATR-FTIR) spectra were recorded using an Agilent Technologies Cary 600 Series FTIR spectrometer. Atomic force microscopy (AFM) in PeakForce tapping mode and under dry conditions was employed to measure the morphology of the modified glass substrates.

4.2.5. Hydrophilicity and Stability of MPNs Coating. The hydrophilicity of bare glass, pristine polypropylene (PP), and the coated substrates [GADMA/glass, GADMA/PP, GADMA-Cu/glass, and GADMA-Cu/PP] was examined by measuring static water contact angles (WCA) using a contact angle goniometer at room temperature. Deionized water (3.0 μL) was dropped on three different spots on each substrate, and the average of contact angles was calculated. WAC was also measured for the glass substrates after incubation in PBS solution for 7 days to investigate the stability of hydrophilic surfaces.

4.2.6. Antifouling Property of Metal-based Coating. To quantify the amount of bovine serum albumin protein (BSA) adsorbed onto the control and GADMA and GADMA-Cu-coated surfaces, the bicinchoninic acid (BCA) technique was performed in triplicate for each sample to ensure the accuracy of results. 0.5 mL of BSA solution (20 mg/mL) was incubated with each sample for 3, 15, and 30 h at 37 °C before rinsing the surfaces with DI water to remove the loose protein. After that, samples were immersed in SDS solution (2 mg/mL) and shaken by ultrasonic bath for 30 min to separate the adsorbed BSA. After incubating the BSA extracts with BCA working reagent for 2 h at 37 °C, the amount of BSA in SDS extracts was determined by measuring the absorbance at 570 nm using a Tecan GENios Pro microplate reader. The adsorbed protein was calculated by comparing the protein concentration on each sample with initial BSA concentrations from the standard curve.

4.2.7. Antibacterial Activity of GADMA-coated Glass and Copper-loaded GADMA-coated Glass Substrates. Two bacterial strains, *E. coli* (Gram-negative) and *S. aureus* (Gram-positive), were used as model bacteria to investigate the antibacterial properties of the bare and modified glass surfaces. In this work, *E. coli* and *S. aureus* were incubated in 25 mL of Luria-Bertani (LB) and 25 mL of tryptic soy (TS) at 37 °C and 5% CO2 for 18 h. Bacteria were centrifuged at 4000 revolutions per minute (rpm) for 5 min and washed with PBS twice. Finally, the harvested bacterial cells were resuspended in 1 mL of PBS solution and diluted to an optical density of 0.15 at 670 (OD670), corresponding to a concentration of 8×10^9 cells/mL. The bacterial suspensions were used for the following bacterial tests.

4.2.7.1. Colony-Forming Units (CFU) Assay. The viability of bacterial cells on bare glass, GADMA surface, and GADMA-Cu surface was assessed using colony-forming units (CFU) assay. *E. coli* and *S. aureus* suspensions with a concentration of 8 x 10^9 cells per mL were adjusted by PBS solution into about 1 x 10^7 cells per mL. 100 μL of each bacterium was dropped on the tops of samples in a 24-well plate and incubated for 24 h at 37 °C. The aliquots of *E. coli* and *S. aureus* were then taken out of the surfaces and serially diluted in PBS solution and spread onto Luria-Bertani (LB) and tryptic soy (TS) agar plates, respectively, in triplicate. After the incubation of agar plates overnight at 37 °C, the viable colonies of bacteria were counted. The bacteriostatic activity of the samples against *E. coli* and *S. aureus* was calculated by comparing the surviving colonies on GADMA and GADMA-Cu coatings with the glass control.

4.2.7.2. Inhibition Zone Test. The non-leaching property of GADMA-Cu-coated glass surfaces was qualitatively examined by performing an inhibition zone test. *E. coli* and *S. aureus* solutions at a concentration of 8 x 10^9 cells/mL were inoculated on LB and TS agar plates and spread using a disposable spreader. The substrates were placed on the agar plates and incubated overnight at

37 °C. The results were then imaged using a digital camera to observe the halo zones.

4.2.8. Cytotoxicity Assessment Using MTT Assay. The MTT [3-(4,5-dimethylthiazol-2-yl)-2,5-diphenyltetrazolium bromide] assay was conducted to evaluate the viability of normal human fibroblast cells (HDFa) in the extracts of bare glass, GADMA, and GADMA-Cu substrates. The extracts were obtained by placing each substrate into the well of a 24-well plate for 24 h, each containing 100 µL of Dulbecco's Modified Eagle Medium (DMEM). The extracts and the control (fresh DMEM medium) were then incubated with HDFa cells for 24 h and tested by MTT assay following the procedure outlined in our previous study.[27]

4.3. Results and Discussion.

4.3.1. GADMA Copolymer Characterization.

The monomer GAEMA [(2,3,4,5,6-Pentahydroxy-N-(2-methacrylamidoethyl) hexanamide] was synthesized from the reaction between 2-aminoethyl methacrylamide hydrochloride (AEMA) and D-gluconolactone and following our previously published report.[28] The route of GAEMA reaction synthesis is illustrated in **Figure S4-1**. Dopamine Methacrylamide Monomer (DMA) was synthesized similarly to the protocol outlined in our previously published research (refer to section 2 and **Figure S4-3** in the supporting information document for the protocol steps).[29] Proton nuclear magnetic resonance spectra (^{1}H NMR) of GAEMA and DMA were recorded with a Varian spectrometer at 500 MHz using D2O and DMSO-*d6* as solvents, respectively (**Figures S4-2 and S4-4**). The GADMA copolymer was synthesized via free radical polymerization of GAEMA and DMA with a targeted degree of polymerization of 220 (**Figure 4.1)**. The mole contents of GAEMA (77%) and DMA (23%) within GADMA copolymer chains were calculated from the ^{1}H NMR spectrum (**Table 4.1** and **Figure S4-5**). These calculations were performed by comparing the proportional integral intensities of CH_2 signals observed at 4.58-3.60 ppm in the

GAEMA backbone and 2.89 ppm in the DMA chain. The number (M_n) and weight (M_w) average molecular weights of GADMA were determined by aqueous GPC and summarized in **Table 4.1**.

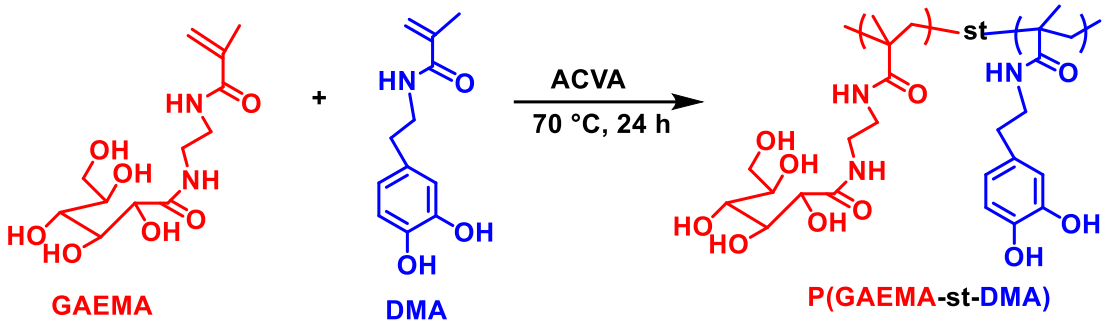

Figure 4.1. Synthetic route of GADMA copolymer.

Table 4.1. Characteristics of the Copolymer GADMA.

Monomer (mole %)					**Molecular weight**	
	Infeed		Calculated from ^{1}H NMR		Calculated from GPC	
Polymer	GAEMA	DMA	GAEMA	DMA	M_n x 10^4 (Da)	PDI
GADMA	80	20	77	23	5.204	2.478

4.3.2. Chemical Structures of Coatings.

ATR-FTIR analysis was carried out to confirm the deposition of GADMA and GADMA-Cu complex on the glass surfaces. The spectra in **Figure 4.2** show the absorption of the uncoated glass surface, GADMA, and GADMA-Cu surfaces. Looking at all spectra, the intensity of characteristic bands at 895 and 748 cm^{-1} on uncoated glass is slightly reduced after the deposition of GADMA and GADMA-Cu coatings, confirming the deposition of polymer coatings onto the glass surfaces. Compared to the control glass, new peaks can be observed on the GADMA-coated glass spectrum. The broad band centered at 3248 cm^{-1} could be attributed to the stretching vibration of −OH groups presented in DMA and GAEMA. The weak signal at 2895 cm^{-1} can be assigned to C−H stretching vibrations. The absorption peak at 1614 cm^{-1}

indicated the stretching vibration of the C=O bond in the amide groups. The peaks observed at 1523 and 1408 cm^{-1} can be attributed to the C−OH in-plane bending and C−N−C stretching, respectively. The metal ions act as electron acceptors to investigate the coordinate interaction between Cu ions and GADMA polymer, while polymer functional groups (e.g., C=O and −OH) work as electron donors. These interactions are expected to weaken the functional groups and shift their peaks to lower wavenumber regions.[30] From the GADMA-Cu spectrum, there is a shift decrease in frequencies of −OH and C=O and groups to 3215 and 1604 cm^{-1}, respectively, compared to the values on the GADMA spectrum. These shifts indicated the coordination complexes involve not only the interaction between copper and phenolic groups but also the bonding of copper with the amide group of glycopolymer. As a result, FTIR data confirmed that GADMA and GADMA-Cu coatings were successfully adhered to the glass substrates.[31]

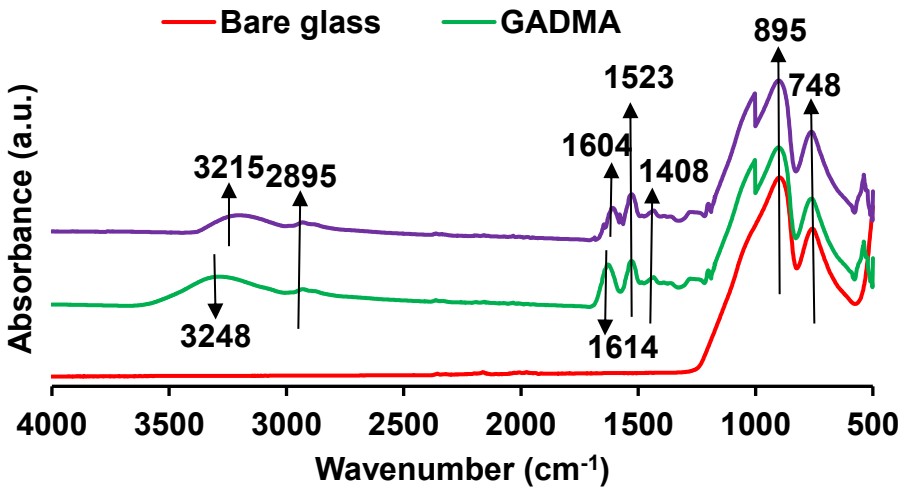

Figure 4.2. FTIR spectra for bare glass, GADMA, and GADMA-Cu-coated glass slides

4.3.3. Surface Morphology.

The morphologies of bare glass, GADMA, and Cu-GADMA-coated surfaces were investigated by AFM, as shown in **Figure 4.3**. The RMS value of the bare glass was small by a value of 0.39

nm, confirming that the bare glass was smooth. In contrast, the RMS roughness increased remarkably to 2.13 nm for the GADMA-deposited surface, where particle-like aggregates were observed due to the deposition of self-polymerized DMA-based copolymer.[32] Further increase in the RMS value was observed after the deposition of Cu-GADMA to reach 3.39 nm, and the surface became rougher with many aggregates. The large number of Cu-GADMA aggregates possibly indicates the successful chelation of Cu^{II} ions with phenolic amide groups of GADMA.[33]

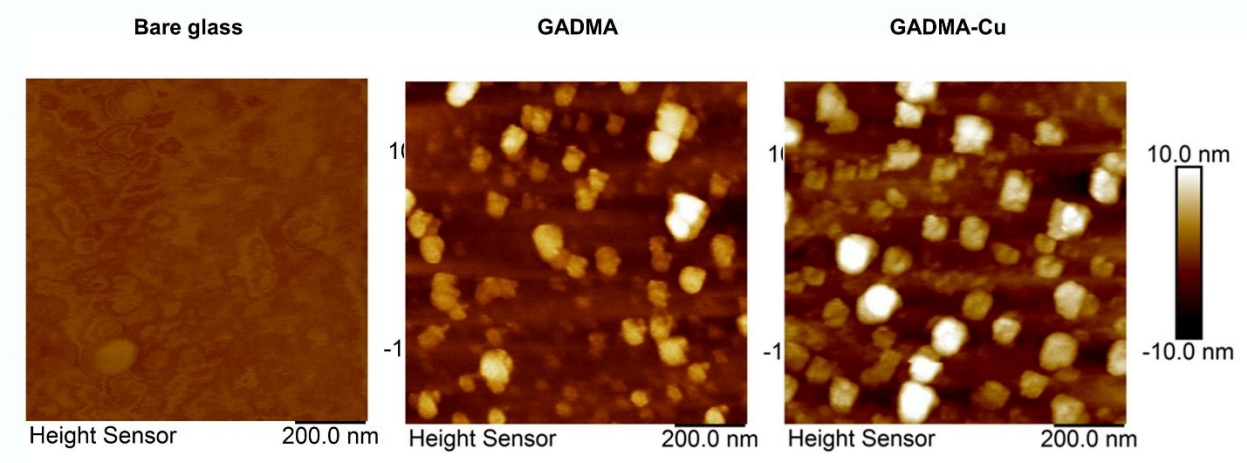

Figure 4.3. AFM images for the bare glass, GADMA, and GADMA-Cu substrates

4.3.4. Wettability and Stability of GADMA-Cu-based Coatings on Glass Surfaces.

The wettability of both pristine (glass and PP) and surfaces coated with GADMA and GADMA-Cu was studied by measuring the WCA in the air and at room temperature using a 3 μL droplet of DI water. As shown in **Figure 4.4a-b,** the coated surfaces significantly reduced WCA values compared to the uncoated control surfaces, suggesting that the glycopolymer layer enhances the hydrophilicity of these surfaces.[34] In **Figure 4.4a,** the WCA value of the pristine PP was significantly high (106.4 ± 1.3°), while the figures for GADMA and Cu-GADMA coatings dropped to 30.9 ± 0.9° and 28.7 ± 1.4°, respectively. Additionally, as shown in **Figure 4.4b (top),** the WCA values for the glass substrates exhibited a similar trend, with a dramatic decrease in

WCA values for the GADMA and GADMA-Cu coatings to 10.5 ± 1.2° and 7 ± 0.9°, respectively, compared to bare glass (44.8 ± 1.8°). This decrease in WCA values indicates the high hydrophilicity of the glycopolymer-based coatings, which could be attributed to hydroxyl and amide groups on glycopolymer units.[35] The Cu^{II} cross-linked catechol groups in the metal-phenolic network structures are expected to impart stability to the coating.[33,36] Therefore, we measured the WCA for the bare glass, GADMA, and GADMA-Cu surfaces after shaking them in PBS solution for 7 days. As shown in **Figure 4.4b (bottom)**, the WCA on the GADMA-coated glass after the shaking recovered to 36.9 ± 0.7° due to the poor stability of the GADMA coating. On the other hand, the GADMA-Cu coating could maintain high hydration at the surface with a WCA of 11.6 ± 0.7° even after immersing in PBS for 7 days due to its strong adhesive ability enhanced by the MPN structure. Such stability of MPNs suggests their biomedical applications in treating chronic wounds.[37]

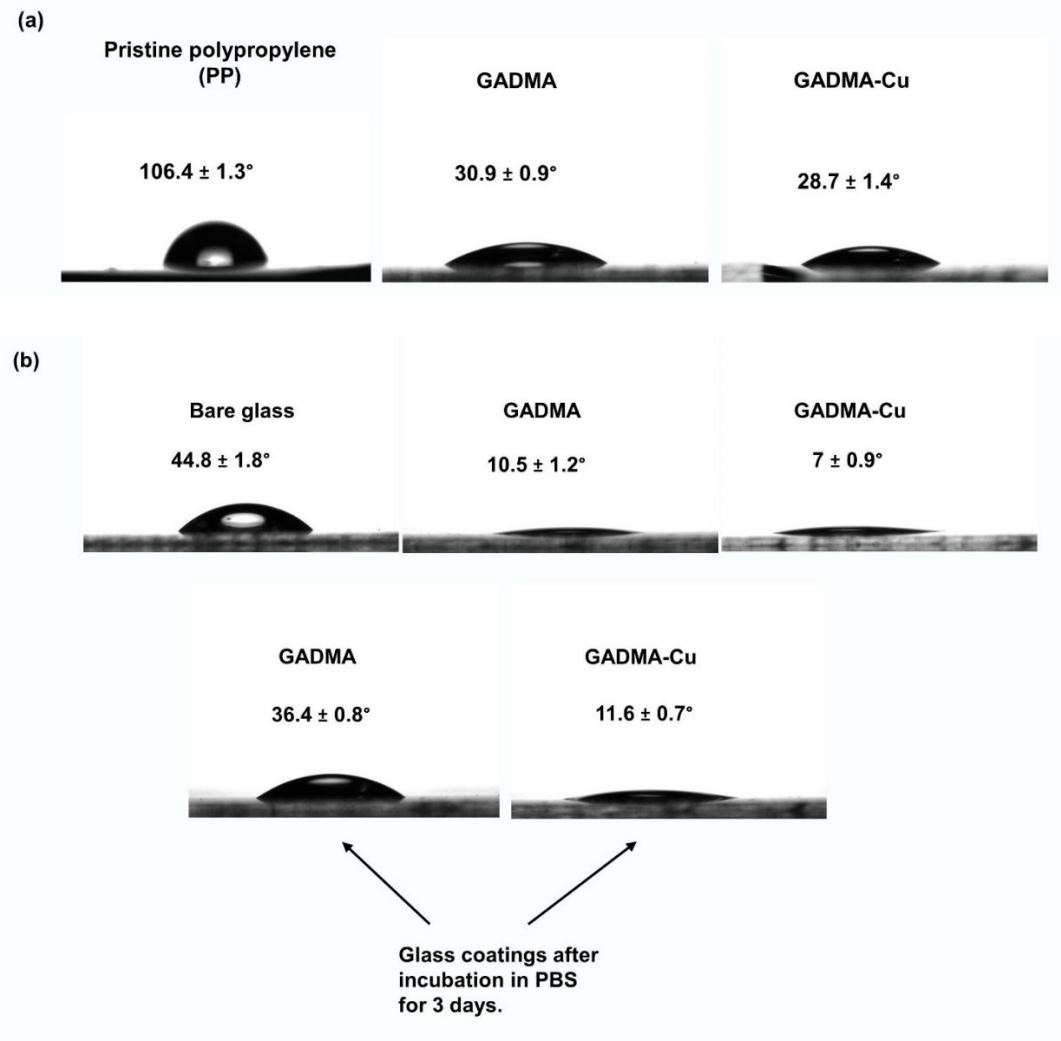

Figure 4.4. WCAs images of (a) pristine PP, GADMA/PP, and GADMA/PP. (b) Fresh bare glass, GADMA/glass, and GADMA-Cu/glass (top) and images after incubation of the coated glass surfaces in PBS for 7 days (bottom).

4.3.5. Antifouling Property of GADMA-Cu-coated Glass Surface.

Understanding and controlling protein adsorption is crucial in the surface interactions to endow biomedical devices with antifouling properties. We selected BSA as a versatile, non-specific adhesive protein because it can bind to positively and negatively charged surfaces.[38] 20 mg/mL of BSA was incubated with bare glass, GADMA, and GADMA-Cu-coated glass surfaces for 3, 15, and 30 h at 37°C. The results shown in **Figure 4.5** reveal that the surface of the bare glass

exhibited the most significant amount of adsorbed BSA by concentrations of 10, 12.2, and 13.9 µg/cm2 after 3, 15, and 30 h of incubation, respectively. The GADMA coating reduced the BSA adsorption to 1.2 µg/cm^2 in the first 3 hours. Then, the amount of protein adsorbed onto the GADMA surface increased with increasing the incubation time, reaching 10.8µg/cm^2 after 30 h of incubation, suggesting that the coating without metal-phenol interaction is unstable. In contrast, the GADMA-Cu coating reduced protein adsorption to 1.1, 1.37, and 1.61 µg/cm2 after incubation at 3, 15, and 30 h, indicating the excellent antifouling effect against the protein. The antifouling property of GADMA-Cu coating is mainly due to the enhanced surface hydration induced by the stability of glycopolymer coating based on a copper-phenolic network.[39,40]

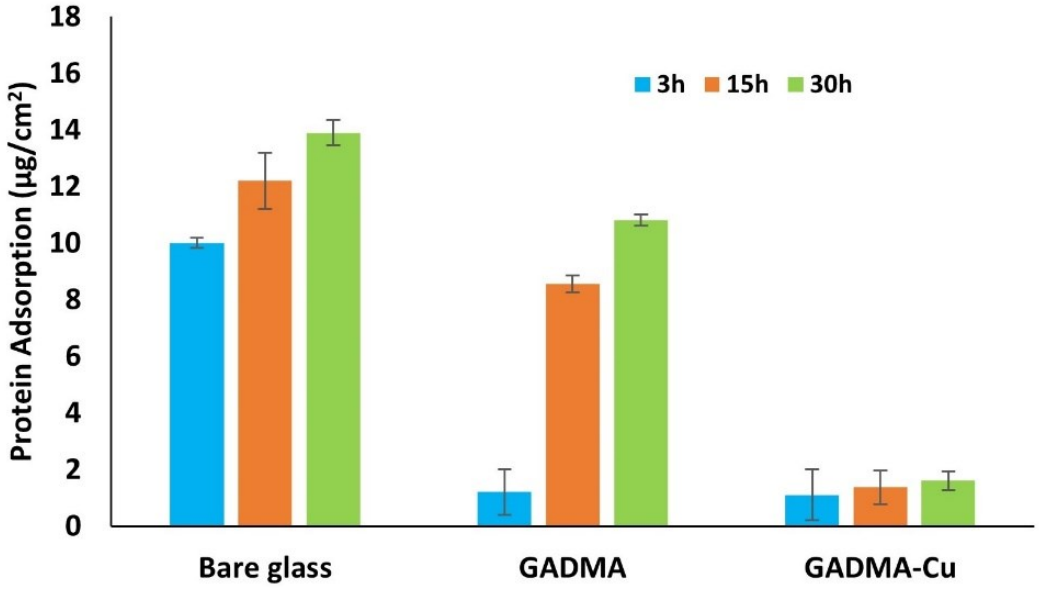

Figure 4.5. Mass of BSA adsorbed onto bare glass, GADMA, and GADMA-Cu-coated glass slides after incubation at 37°C for 3, 15, and 30 h.

4.3.6. Antibacterial Properties.

The CFU assay was carried out to investigate the antibacterial properties of the pristine glass and modified glass surfaces (GADMA and GADMA-Cu) against *E. coli* and *S. aureus*. The number of CFU on each sample was calculated after seeding each bacterium on the surfaces for 24 h at a

concentration of 1 x 10^7 cells/mL. Figure 4.6a-b shows a reduction in the number of viable cells of E. coli and S. aureus on the modified glass slides compared to the control glass surface. The number of viable *E. coli* and *S. aureus* on the pristine glass substrates is about 33 × 10^4 and 29.5 × 10^4 cells/mL, respectively. The number of viable *E. coli* and *S. aureus* on the GADMA surfaces decreases to about 14 X 10^4 and 13 x 10^4. After coordination of Cu^{II}, the GADMA-Cu coating demonstrated the highest antibacterial efficiency of the coating against *E. coli* and *S.* aureus, reducing the number of viable bacteria to zero and 1 x 10^4, respectively, suggesting the synergistic action of the glycopolymer (GAEMA) and the copper. The GAEMA could prevent the adhesion of bacteria on the surface, while the copper could kill the bacteria.[36,41]

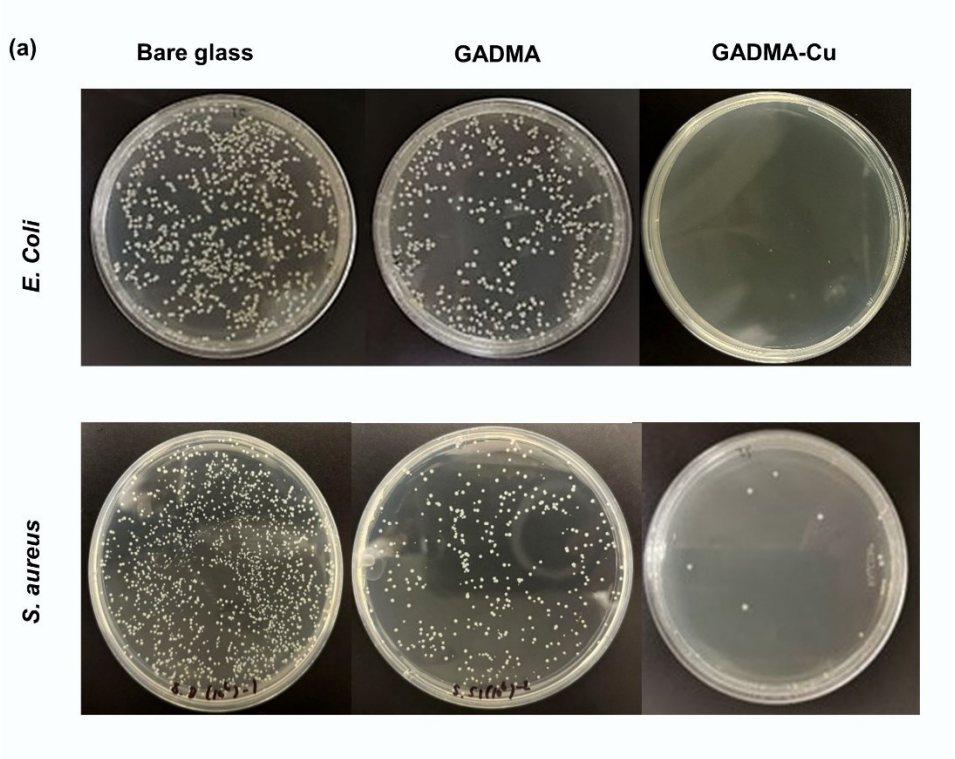

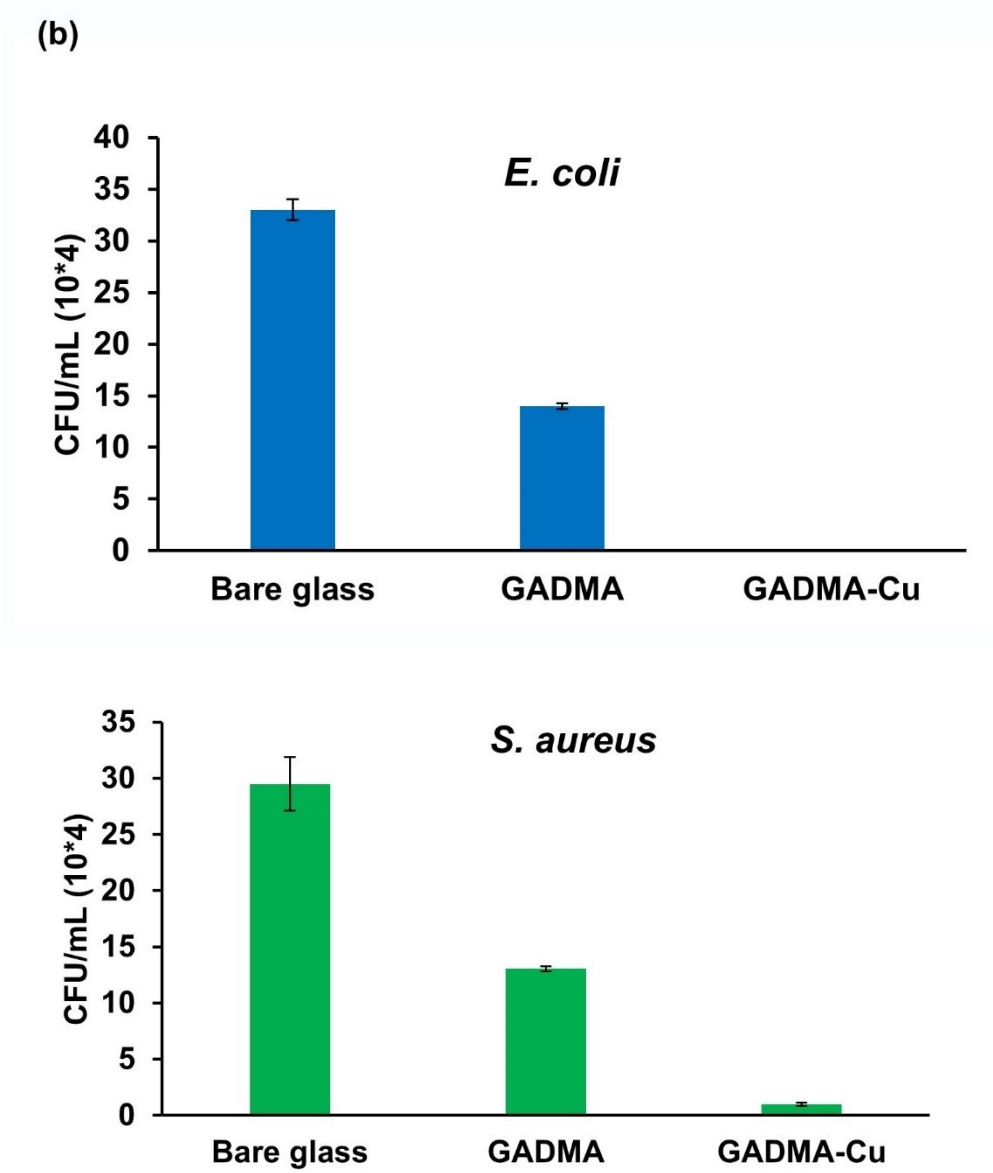

Figure 4.6. images of (a) *E. coli* and *S. aureus* colonies after being cultivated with bare glass, GADMA, and GADMA-Cu substrates. (b) the number of viable bacterial cells on control and modified glass slides.

To examine the release of Cu ions of GADMA-Cu, an inhibition zone test was conducted by placing the bare glass, GADMA, and GADMA-Cu surfaces onto the agar plates containing *E. coli* and *S. aureus* and incubation for 24 h. As shown in **Figure S4-6**, clear zones were observed around GADMA-Cu surfaces against both *E. coli* and *S. aureus*. The presence of inhibition zones

around the GADMA-Cu-coated glass slides confirms that the amount of released copper ions was not high enough to result in the zone of inhibition on the agar plates.[42]

4.3.7. *In Vitro* Cell Cytotoxicity Study.

An MTT assay was carried out to evaluate the biocompatibility of the GADMA and GADMA-Cu coatings to exploit our coatings in biomedical applications. To this end, HDFa cells were incubated with coating extracts for 24 h, and nearly 99% cell viability was observed in all cases compared to 100% cell viability in the presence of the control (see **Figure 4.7**). This phenomenon confirmed that the GADMA polymer mimics natural polysaccharides, enhancing biocompatibility and reducing toxicity.[43] MPNs have also been extensively studied for their biomedical applications and exhibited outstanding cytocompatibility, making them safe for use in biological environments.[44] This fact is consistent with the high cell viability of GADMA-Cu extract, as shown in **Figure 4.7**.

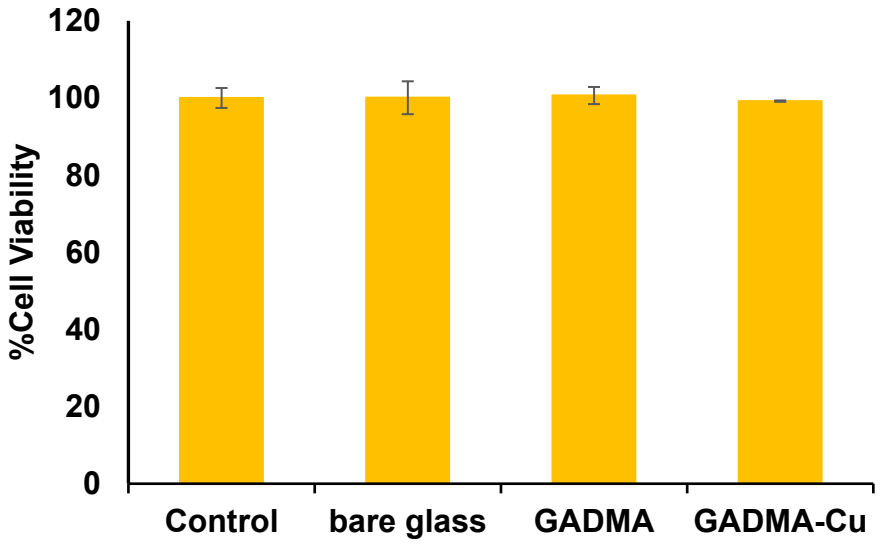

Figure 4.7. The cell viability of HDF cells was cultured for 24 hours with DMEM medium (control), bare glass, GADMA, and GADMA-Cu substrates.

4.4. Conclusion.

A one-step dip-coating method has shown great potential in endowing surfaces with a stable coating for possible antifouling and antibacterial application. *p*(GAEMA-*st*-DMA) and Cu^{II} were simultaneously deposited on glass and PP substrates to form a stable coating based on MPNs chemistry. The open chains of GAEMA glycopolymers facilitated the coordinated interactions with copper ions through its hydroxyl and amide groups, and the residual hydroxyl groups enabled the complex adhesion to the substrates. The GADMA-Cu coating exhibited persistent antifouling properties against BSA protein adsorption and unique antibacterial properties against Gram-negative bacteria (*E. coli*) and Gram-positive bacteria (*S. aureus*). Thus, the resulting coatings may have the potential to be helpful in biomedical applications.

4.5. Supporting Information.

4.5.1. Synthesis of 2-Gluconamidoethyl Methacrylamide (GAEMA).

The monomer GAEMA [(2,3,4,5,6-Pentahydroxy-N-(2-methacrylamidoethyl) hexanamide] was synthesized following our previously published report.[28] The route of GAEMA reaction synthesis is illustrated in Figure S4-1. The chemical structure was characterized by the ^{1}H NMR spectrum recorded on a Varian 500 MHz spectrometer in D_2O (**Figure S4-1**).

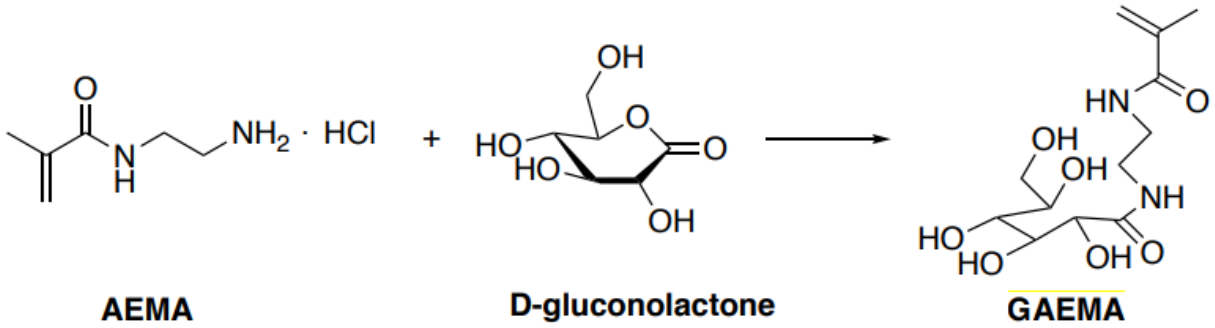

Figure S4-1. Synthesis of 2-gluconamidoethyl methacrylamide (GAEMA). Reaction conditions: TEA, methanol, RT, and overnight.

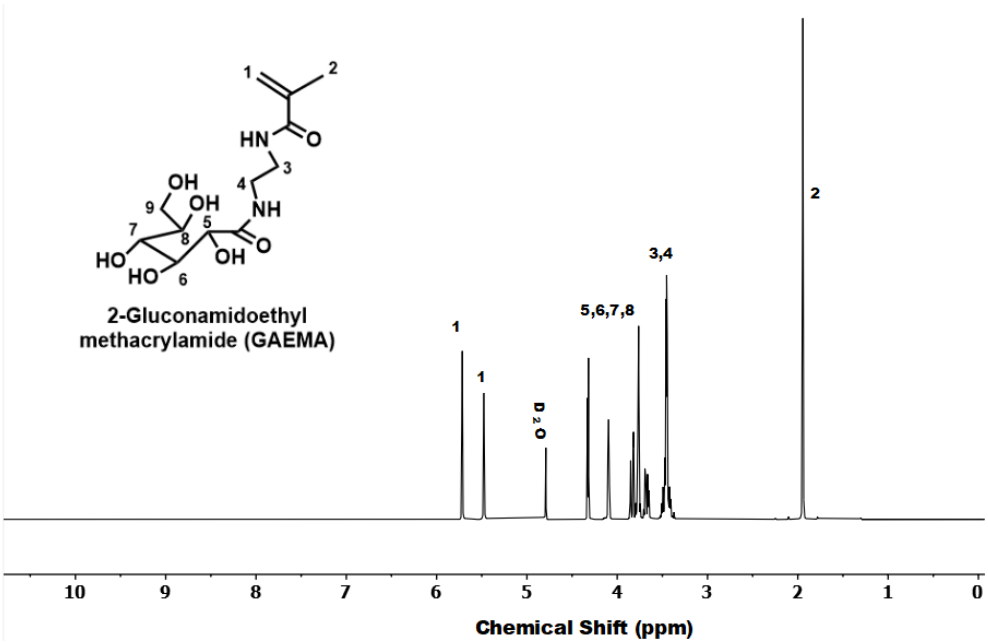

Figure S4-2. ^{1}H NMR spectrum of 2-gluconamidoethyl methacrylamide (GAEMA) in D_2O.

4.5.2. Synthesis of Dopamine Methacrylamide Monomer (DMA).

5 g of sodium borate (13.11 mmol) and 2.0 g of NaHCO3 (23.81 mmol) were dissolved in 50 mL of DI water. After degassing the mixture under nitrogen, 2.5 g (16.32 mmol) of dopamine hydrochloride was added and stirred for another 15 min under nitrogen. Then, a mixture of 2.35 mL (15.85 mmol) methacrylic anhydride and 12.5 mL THF was added dropwise to the above solution in an ice-water bath. The pH of the reaction mixture was monitored, kept in the range of 8 to 9 by adding 1 M NaOH solution, and stirred overnight at room temperature. Then, the reaction mixture was washed twice with ethyl acetate and filtered. After collecting the aqueous layer, the filtrate was acidified to pH 1-2 with 5 M HCl and extracted thrice with a large amount of ethyl acetate. The organic layer was collected, dried with MgSO4, and concentrated under rotavapor. The product was recrystallized in the fridge overnight, filtered, and vacuum dried to obtain DMA monomer. The chemical structure was characterized by ^{1}H NMR spectroscopy using DMSO-d_6 solvent (**Figure S4-3**).

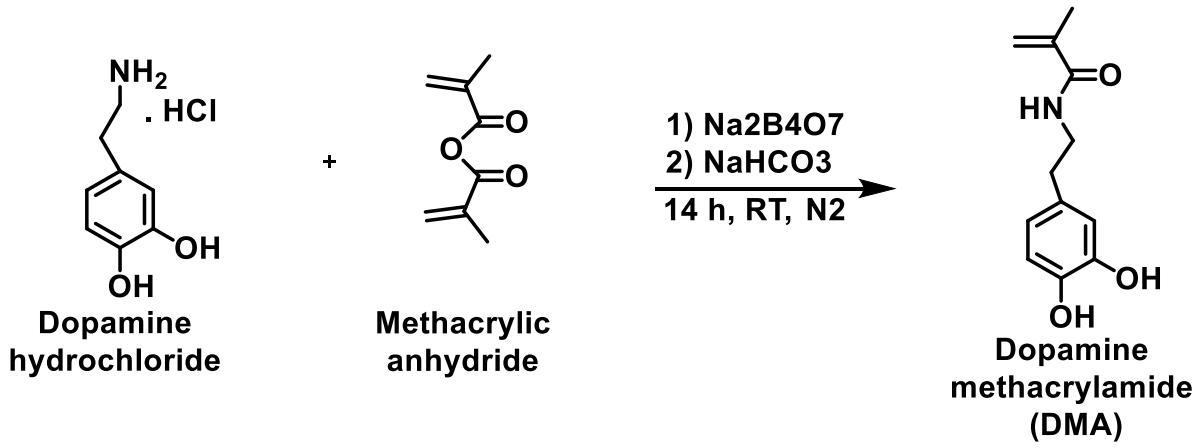

Figure S4-3. Synthetic route of dopamine methacrylamide monomer (DMA).

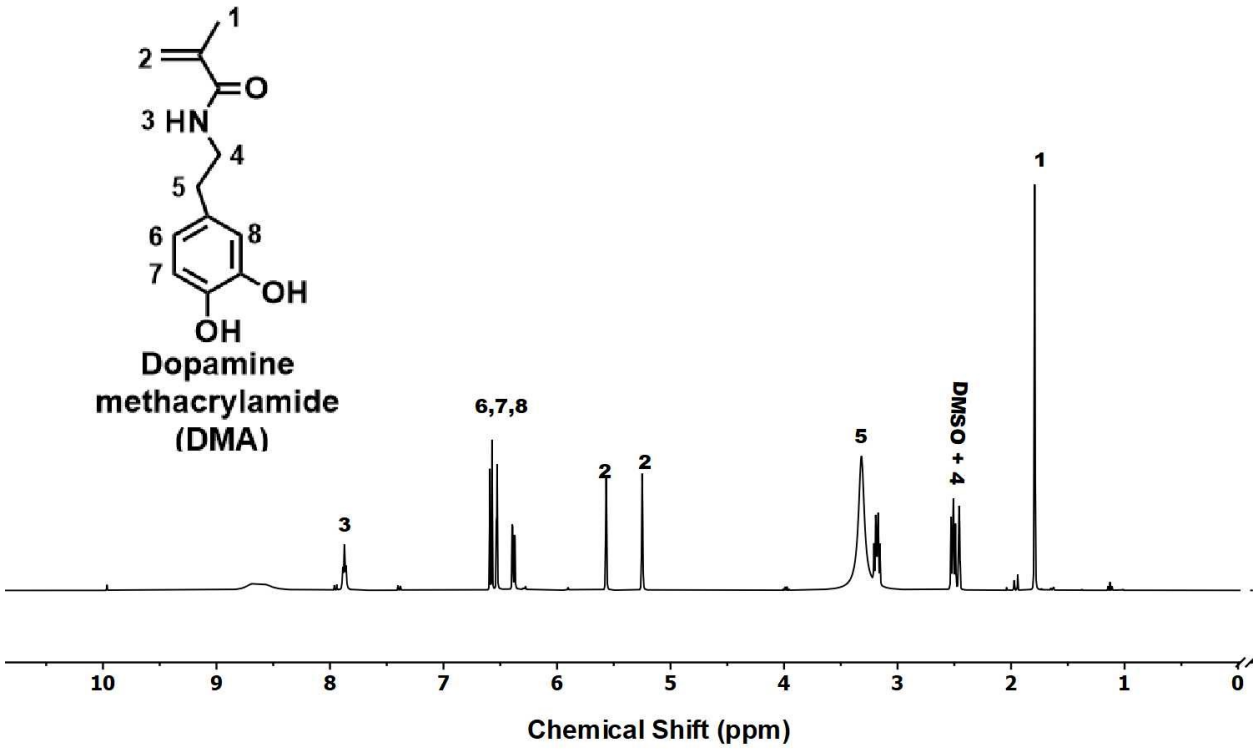

Figure S4-4. ^{1}H NMR spectrum of dopamine methacrylamide monomer (DMA) in DMSO-d_6.

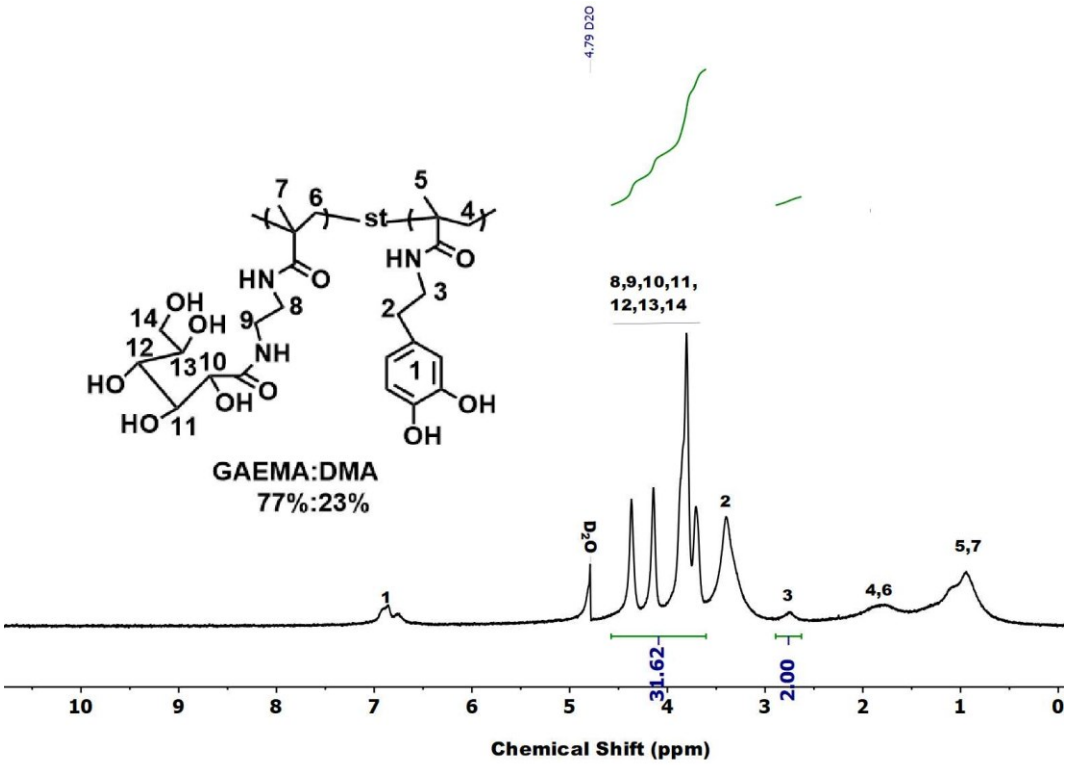

Figure S4-5. ^{1}H NMR spectrum of copolymer *p*(GAEMA-*st*-DMA) using D_2O as a solvent.

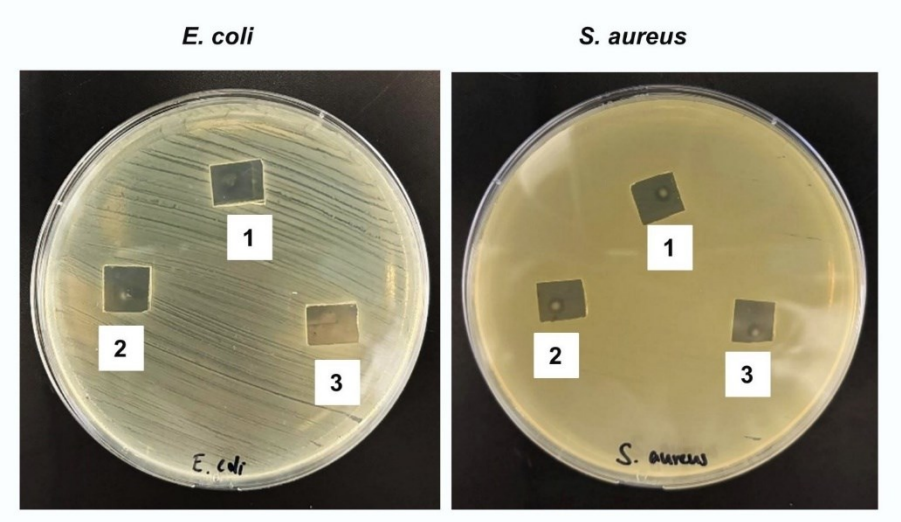

Figure S4-6. Inhibition zones test images against *E. coli and S. aureus*, with a concentration of 8 x 10^9 cells/mL, after incubation of (1) bare glass, (2) GADMA, and (3) GADMA-Cu-coated glass surfaces on LB and TS agar plates for 24 hours at 37°C.

4.6. References.

(1) Leslie, D. C.; Waterhouse, A.; Berthet, J. B.; Valentin, T. M.; Watters, A. L.; Jain, A.; Kim, P.; Hatton, B. D.; Nedder, A.; Donovan, K.; Super, E. H.; Howell, C.; Johnson, C. P.; Vu, T. L.; Bolgen, D. E.; Rifai, S.; Hansen, A. R.; Aizenberg, M.; Super, M.; Aizenberg, J.; Ingber, D. E. A Bioinspired Omniphobic Surface Coating on Medical Devices Prevents Thrombosis and Biofouling. *Nat. Biotechnol.* **2014**, *32* (11), 1134–1140.

(2) Li, B.; Webster, T. J. Bacteria Antibiotic Resistance: New Challenges and Opportunities for Implant-Associated Orthopedic Infections. *J. Orthop. Res.* **2018**, *36* (1), 22–32.

(3) Umscheid, C. A.; Mitchell, M. D.; Doshi, J. A.; Agarwal, R.; Williams, K.; Brennan, P. J. Estimating the Proportion of Healthcare-Associated Infections That Are Reasonably Preventable and the Related Mortality and Costs. *Infect. Control Hosp. Epidemiol.* **2011**, *32* (2), 101–114.

(4) Costerton, J. W.; Stewart, P. S.; Greenberg, E. P. Bacterial Biofilms: A Common Cause of Persistent Infections. *Science (80-.).* **1999**, *284* (5418), 1318–1322.

(5) Zander, Z. K.; Becker, M. L. Antimicrobial and Antifouling Strategies for Polymeric Medical Devices. *ACS Macro Lett.* **2018**, *7* (1), 16–25.

(6) Maan, A. M. C.; Hofman, A. H.; de Vos, W. M.; Kamperman, M. Recent Developments and Practical Feasibility of Polymer-Based Antifouling Coatings. *Adv. Funct. Mater.* **2020**, *30* (32).

(7) Singh, B.; Singh, J.; Dhiman, A.; Mohan, M. Synthesis and Characterization of Arabinoxylan-Bis[2-(Methacryloyloxy)Ethyl] Phosphate Crosslinked Copolymer Network by High Energy Gamma Radiation for Use in Controlled Drug Delivery Applications. *Int. J. Biol. Macromol.* **2022**, *200* (December 2021), 206–217.

(8) Jiang, T.; Nukavarapu, S. P.; Deng, M.; Jabbarzadeh, E.; Kofron, M. D.; Doty, S. B.;

Abdel-Fattah, W. I.; Laurencin, C. T. Chitosan-Poly(Lactide-Co-Glycolide) Microsphere-Based Scaffolds for Bone Tissue Engineering: In Vitro Degradation and in Vivo Bone Regeneration Studies. *Acta Biomater.* **2010**, *6* (9), 3457–3470.

(9) Yang, W.; Kang, X.; Gao, X.; Zhuang, Y.; Fan, C.; Shen, H.; Chen, Y.; Dai, J. Biomimetic Natural Biopolymer-Based Wet-Tissue Adhesive for Tough Adhesion, Seamless Sealed, Emergency/Nonpressing Hemostasis, and Promoted Wound Healing. *Adv. Funct. Mater.* **2023**, *33* (6), 1–16.

(10) Barrantes, A.; Wengenroth, J.; Arnebrant, T.; Haugen, H. J. Poly-L-Lysine/Heparin Multilayer Coatings Prevent Blood Protein Adsorption. *J. Colloid Interface Sci.* **2017**, *485*, 288–295.

(11) Zhou, J.; Romero, G.; Rojas, E.; Ma, L.; Moya, S.; Gao, C. Layer by Layer Chitosan/Alginate Coatings on Poly(Lactide-Co-Glycolide) Nanoparticles for Antifouling Protection and Folic Acid Binding to Achieve Selective Cell Targeting. *J. Colloid Interface Sci.* **2010**, *345* (2), 241–247.

(12) Parfenova, L. V.; Galimshina, Z. R.; Gil'fanova, G. U.; Alibaeva, E. I.; Danilko, K. V.; Pashkova, T. M.; Kartashova, O. L.; Farrakhov, R. G.; Mukaeva, V. R.; Parfenov, E. V.; Nagumothu, R.; Valiev, R. Z. Hyaluronic Acid Bisphosphonates as Antifouling Antimicrobial Coatings for PEO-Modified Titanium Implants. *Surfaces and Interfaces* **2022**, *28* (August 2021), 101678.

(13) Ribeiro, J. P. M.; Mendonça, P. V.; Coelho, J. F. J.; Matyjaszewski, K.; Serra, A. C. Glycopolymer Brushes by Reversible Deactivation Radical Polymerization: Preparation, Applications, and Future Challenges. *Polymers (Basel).* **2020**, *12* (6).

(14) Yuan, J.; Meng, J. Q.; Kang, Y. L.; Du, Q. Y.; Zhang, Y. F. Facile Surface Glycosylation

of PVDF Microporous Membrane via Direct Surface-Initiated AGET ATRP and Improvement of Antifouling Property and Biocompatibility. *Appl. Surf. Sci.* **2012**, *258* (7), 2856–2863.

(15) Feng, K.; Peng, L.; Yu, L.; Zheng, Y.; Chen, R.; Zhang, W.; Chen, G.; Chen, G. Universal Antifogging and Antimicrobial Thin Coating Based on Dopamine-Containing Glycopolymers. *ACS Appl. Mater. Interfaces* **2020**, *12* (24), 27632–27639.

(16) Tu, Q.; Shen, X.; Liu, Y.; Zhang, Q.; Zhao, X.; Maitz, M. F.; Liu, T.; Qiu, H.; Wang, J.; Huang, N.; Yang, Z. A Facile Metal-Phenolic-Amine Strategy for Dual-Functionalization of Blood-Contacting Devices with Antibacterial and Anticoagulant Properties. *Mater. Chem. Front.* **2019**, *3* (2), 265–275.

(17) Yang, Z.; Yang, Y.; Xiong, K.; Wang, J.; Lee, H.; Huang, N. Metal-Phenolic Surfaces for Generating Therapeutic Nitric Oxide Gas. *Chem. Mater.* **2018**, *30* (15), 5220–5226.

(18) Zheng, H. T.; Bui, H. L.; Chakroborty, S.; Wang, Y.; Huang, C. J. Pegylated Metal-Phenolic Networks for Antimicrobial and Antifouling Properties. *Langmuir* **2019**, *35* (26), 8829–8839.

(19) Ejima, H.; Richardson, J. J.; Liang, K.; Best, J. P.; Van Koeverden, M. P.; Such, G. K.; Cui, J.; Caruso, F. One-Step Assembly of Coordination Complexes. *Science (80-.).* **2013**, *341* (6142), 154–157.

(20) Li, X.; Gao, P.; Tan, J.; Xiong, K.; Maitz, M. F.; Pan, C.; Wu, H.; Chen, Y.; Yang, Z.; Huang, N. Assembly of Metal-Phenolic/Catecholamine Networks for Synergistically Anti-Inflammatory, Antimicrobial, and Anticoagulant Coatings. *ACS Appl. Mater. Interfaces* **2018**, *10* (47), 40844–40853.

(21) Meng, L.; Huang, C.; Liu, X.; Qu, H.; Wang, Q. Zwitterionic Coating Assisted by Dopamine with Metal-Phenolic Networks Loaded on Titanium with Improved Biocompatibility

and Antibacterial Property for Artificial Heart. *Front. Bioeng. Biotechnol.* **2023**, *11* (April), 1–12.

(22) Huang, Z.; Zhang, D.; Gu, Q.; Miao, J.; Cen, X.; Golodok, R. P.; Savich, V. V.; Ilyushchenko, A. P.; Zhou, Z.; Wang, R. One-Step Coordination of Metal-Phenolic Networks as Antibacterial Coatings with Sustainable and Controllable Copper Release for Urinary Catheter Applications. *RSC Adv.* **2022**, *12* (25), 15685–15693.

(23) Yang, H.; Li, G.; Stansbury, J. W.; Zhu, X.; Wang, X.; Nie, J. Smart Antibacterial Surface Made by Photopolymerization. *ACS Appl. Mater. Interfaces* **2016**, *8* (41), 28047–28054.

(24) Zhu, Z.; Gao, Q.; Long, Z.; Huo, Q.; Ge, Y.; Vianney, N.; Daliko, N. A.; Meng, Y.; Qu, J.; Chen, H.; Wang, B. Polydopamine/Poly(Sulfobetaine Methacrylate) Co-Deposition Coatings Triggered by CuSO4/H2O2 on Implants for Improved Surface Hemocompatibility and Antibacterial Activity. *Bioact. Mater.* **2021**, *6* (8), 2546–2556.

(25) Mitra, D.; Kang, E. T.; Neoh, K. G. Antimicrobial Copper-Based Materials and Coatings: Potential Multifaceted Biomedical Applications. *ACS Appl. Mater. Interfaces* **2020**, *12* (19), 21159–21182.

(26) Asha, A. B.; Chen, Y.; Zhang, H.; Ghaemi, S.; Ishihara, K.; Liu, Y.; Narain, R. Rapid Mussel-Inspired Surface Zwitteration for Enhanced Antifouling and Antibacterial Properties. *Langmuir* **2019**, *35* (5), 1621–1630.

(27) Asha, A. B.; Ounkaew, A.; Peng, Y. Y.; Gholipour, M. R.; Ishihara, K.; Liu, Y.; Narain, R. Bioinspired Antifouling and Antibacterial Polymer Coating with Intrinsic Self-Healing Property. *Biomater. Sci.* **2022**, *11* (1), 128–139.

(28) Chen, Y.; Tan, Z.; Wang, W.; Peng, Y. Y.; Narain, R. Injectable, Self-Healing, and Multi-Responsive Hydrogels via Dynamic Covalent Bond Formation between Benzoxaborole and Hydroxyl Groups. *Biomacromolecules* **2019**, *20* (2), 1028–1035.

(29) Chen, Y.; Diaz-Dussan, D.; Wu, D.; Wang, W.; Peng, Y. Y.; Asha, A. B.; Hall, D. G.; Ishihara, K.; Narain, R. Bioinspired Self-Healing Hydrogel Based on Benzoxaborole-Catechol Dynamic Covalent Chemistry for 3D Cell Encapsulation. *ACS Macro Lett.* **2018**, *7* (8), 904–908.

(30) Anh, H. T. P.; Huang, C. M.; Huang, C. J. Intelligent Metal-Phenolic Metallogels as Dressings for Infected Wounds. *Sci. Rep.* **2019**, *9* (1), 1–10.

(31) V, A. K.; Veeraiah, M. K.; Hemalatha P. Synthesis and Characterisation of Poly (Vinylpyrrolidone)–Copper (II) Complexes. *Res. J. Chem. Sci.* **2015**, *5* (2), 64–69.

(32) Liu, G.; Xiang, J.; Xia, Q.; Li, K.; Yan, H.; Yu, L. Fabrication of Durably Antibacterial Cotton Fabrics by Robust and Uniform Immobilization of Silver Nanoparticles via Mussel-Inspired Polydopamine/Polyethyleneimine Coating. *Ind. Eng. Chem. Res.* **2020**, *59* (20), 9666–9678.

(33) Zhang, Y.; Jiang, W.; Lei, L.; Wang, Y.; Xu, R.; Qin, L.; Wei, Q. Mussel-Inspired Multicomponent Codeposition Strategy toward Antibacterial and Lubricating Multifunctional Coatings on Bioimplants. *Langmuir* **2022**, *38* (23), 7157–7167.

(34) Xi, Z. Y.; Xu, Y. Y.; Zhu, L. P.; Wang, Y.; Zhu, B. K. A Facile Method of Surface Modification for Hydrophobic Polymer Membranes Based on the Adhesive Behavior of Poly(DOPA) and Poly(Dopamine). *J. Memb. Sci.* **2009**, *327* (1–2), 244–253.

(35) Nuraje, N.; Asmatulu, R.; Cohen, R. E.; Rubner, M. F. Durable Antifog Films from Layer-by-Layer Molecularly Blended Hydrophilic Polysaccharides. *Langmuir* **2011**, *27* (2), 782–791.

(36) Liu, G.; Li, K.; Wang, H.; Ma, L.; Yu, L.; Nie, Y. Stable Fabrication of Zwitterionic Coating Based on Copper-Phenolic Networks on Contact Lens with Improved Surface Wettability and Broad-Spectrum Antimicrobial Activity. *ACS Appl. Mater. Interfaces* **2020**, *12*

(14), 16125–16136.

(37) Wang, D.; Xing, J.; Zhang, Y.; Guo, Z.; Deng, S.; Guan, Z.; He, B.; Ma, R.; Leng, X.; Dong, K.; Dong, Y. Metal–Phenolic Networks for Chronic Wounds Therapy. *Int. J. Nanomedicine* **2023**, *18*, 6425–6448.

(38) Phan, H. T. M.; Bartelt-Hunt, S.; Rodenhausen, K. B.; Schubert, M.; Bartz, J. C. Investigation of Bovine Serum Albumin (BSA) Attachment onto Self-Assembled Monolayers (SAMs) Using Combinatorial Quartz Crystal Microbalance with Dissipation (QCM-D) and Spectroscopic Ellipsometry (SE). *PLoS One* **2015**, *10* (10).

(39) Ejima, H.; Richardson, J. J.; Caruso, F. Metal-Phenolic Networks as a Versatile Platform to Engineer Nanomaterials and Biointerfaces. *Nano Today* **2017**, *12*, 136–148.

(40) Kim, S.; Gim, T.; Kang, S. M. Versatile, Tannic Acid-Mediated Surface PEGylation for Marine Antifouling Applications. *ACS Appl. Mater. Interfaces* **2015**, *7* (12), 6412–6416.

(41) Li, Y.; Milewska, M.; Khine, Y. Y.; Ariotti, N.; Stenzel, M. H. Trehalose Coated Nanocellulose to Inhibit the Infections by S. Aureus. *Polym. Chem.* **2022**, *13* (11), 1502–1509.

(42) Gosau, M.; Bürgers, R.; Vollkommer, T.; Holzmann, T.; Prantl, L. Effectiveness of Antibacterial Copper Additives in Silicone Implants. *J. Biomater. Appl.* **2013**, *28* (2), 187–198.

(43) Muñoz-Bonilla, A.; Fernández-García, M. Glycopolymeric Materials for Advanced Applications. *Materials (Basel).* **2015**, *8* (5), 2276–2296.

(44) Xie, W.; Guo, Z.; Zhao, L.; Wei, Y. Metal-Phenolic Networks: Facile Assembled Complexes for Cancer Theranostics. *Theranostics* **2021**, *11* (13), 6407–6426.

Chapter 5: Conclusions and Future Directions

5.1. Key Findings.

Developing antifouling and antibacterial coatings is becoming increasingly desirable due to the rising number of medical device-associated infections (DAIs). The initial adsorption of proteins on medical device surfaces can act as a platform for subsequent bacterial attachment and biofilm formation, posing a significant challenge in preventing device-related infections. Although antifouling surfaces can inhibit protein adsorption and initial bacterial adhesion, the few bacterial cells that adhere may proliferate and eventually form a biofilm. Conversely, bactericidal surfaces may suffer from the adhesion of dead bacteria and block the bactericidal moieties, leading to eventual biofilm formation. Hence, medical devices with stable, biocompatible, versatile coatings that combine antifouling and antibacterial properties are needed. Since most bacterial cells are hydrophobic, they manage to colonize hydrophobic materials and vice versa preferentially. Constructing hydrophilic coatings is generally applicable for the inhibition of bacterial cell adhesion. Zwitterionic polymers containing zwitterionic groups close to each other can electrostatically form a hydration layer and avoid nonspecific protein and bacteria adhesions. Due to their biocompatibility and non-toxicity, polysaccharides have been demonstrated as promising hydrophilic antifouling agents to replace hydrophilic synthetic polymers. Glycopolymers are also an alternative to hydrophilic polymers and exhibit excellent antifouling behavior. Their structures contain many hydroxyl groups; therefore, their antifouling property mimics the hydrophilic polysaccharides by preventing bacterial adhesion and protein adsorption. They can bind divalent ions and increase the hydration of the polysaccharide films. Metal-phenolic networks (MPNs), consisting of metal ions coordinated with phenolic ligands, are considered versatile materials for fabricating simple and stable coatings on medical device surfaces.

In this thesis, we have taken innovative approaches, developing three distinct bifunctional coatings with excellent cytotoxicity. These coatings are tailored to the chemistry of tannic acid and dopamine, allowing for the covalent deposition of functional polymers using surface-independent, simple, and cost-effective methods. These novel methods open new possibilities for developing advanced medical device coatings.

Chapter 2. A simple one-pot method was employed to endow the glass surface with antifouling and bactericidal properties by simultaneously depositing TA and p(MPC-st-AEMA) via covalent amine-TA interactions, followed by *in situ* generation of AgNPs. The modified glass surfaces had a water contact angle of less than 5°; thus, they are super hydrophilic surfaces and significantly reduced the protein adsorption to as low as 0.21 $\mu g/cm^2$ on the surface coated by copolymer with a molar ratio of MPC: AEMA (9:1). The coatings also demonstrated bactericidal activity by forming zones of inhibition against *E. coli* and *S. aureus* and showed negligible cytotoxicity to normal human lung fibroblast cells (MRC-5). Thus, modified surfaces are potentially helpful as effective and biocompatible antifouling materials for biomedical applications.

Chapter 3. The glass surface was grafted with a self-adhered polydopamine layer via a simple dip-coating method. To functionalize the glass surface with stable bactericidal coating, a combination of quaternary cationic copolymer with fouling-resistant zwitterionic copolymer was successfully grafted by Schiff base linkage between its aldehyde group and the remaining amino groups of self-oxidized PDA. The non-leaching bactericidal quaternary ammonium moieties and covalent bonding rendered excellent stability to the coating against the bacteria adhesion. The coating with an equal weight ratio of copolymers reduced the adherent viable bacteria by 80% even after shaking the sample in PBS for 7 days, compared to 81.8% of bacterial anti-adhesion

for the fresh coating. Compared to uncoated glass, the coating decreased nonspecific BSA protein adsorption by 10 %. Despite its antifouling property, the coating was not cytotoxic to normal human lung fibroblast cells (MRC-5). This suggests the coating may apply to medical devices like contact lenses for wear and loading considerations.

Chapter 4. Using Metal-phenolic networks (MPNs) interactions, a stable coating has been developed based on the complexation of copper ions with phenolic and hydroxyl groups. Glycopolymer poly (GEMA-st-DMA) was successfully grafted to the glass surface based on the adhesive catechol groups of DMA and formed a coordination complex with Cu^{2+}. The copper ions also cross-linked hydroxyl and amide groups on glycopolymer, imparted stability to the coating. Due to the coating hydrophilicity, WCA was reduced to 11.6 ± 0.7° after 7 days of immersion in PBS solution. The antifouling property of the coating was effective in inhibiting BSA adsorption due to the high degree of hydration induced by the binding of copper divalent ions with GAEMA and DMA. The coating also exhibited unique antibacterial properties against Gram-negative bacteria (*E. coli*) and Gram-positive bacteria (*S. aureus*). Such stable MPNs-based coatings suggested their application in the biomedical field.

5.2. Future Directions.

Given the increased number of HAIs, the ongoing development of antibacterial coatings for potential biomedical applications is expected to gain momentum. The coatings must demonstrate resistance to bacterial colonization and biofilm formation to combat these infections. In this regard, significant achievements in the rational design and fabrication of dual-functional antifouling and bactericidal polymeric-based coatings using tannic acid and dopamine chemistries hold great promise. However, there are still challenges for innovation and improvement in these coatings that must be addressed. Transferring the applications of TA and

PDA coatings from the research laboratory into large-scale manufacturing needs to be developed. Long-term stability and toxicity assessments conducted in the laboratory must be replicated in *in vivo* studies, . *In vivo,* assessments should not be conducted solely on small animals to save costs. Tests on large animals are needed as they often provide better predictors of clinical outcomes.

Bibliography

(1) Li, B.; Webster, T. J. Bacteria Antibiotic Resistance: New Challenges and Opportunities for Implant-Associated Orthopedic Infections. *J. Orthop. Res.* **2018**, *36* (1), 22–32.

(2) Sloan, M.; Premkumar, A.; Sheth, N. P. Projected Volume of Primary Total Joint Arthroplasty in the u.s., 2014 to 2030. *J. Bone Jt. Surg. - Am. Vol.* **2018**, *100* (17), 1455–1460.

(3) Besser, M.; Terberger, J.; Weber, L.; Ghebremedhin, B.; Naumova, E. A.; Arnold, W. H.; Stuermer, E. K. Impact of Probiotics on Pathogen Survival in an Innovative Human Plasma Biofilm Model (HpBIOM). *J. Transl. Med.* **2019**, *17* (1), 1–9.

(4) Leslie, D. C.; Waterhouse, A.; Berthet, J. B.; Valentin, T. M.; Watters, A. L.; Jain, A.; Kim, P.; Hatton, B. D.; Nedder, A.; Donovan, K.; Super, E. H.; Howell, C.; Johnson, C. P.; Vu, T. L.; Bolgen, D. E.; Rifai, S.; Hansen, A. R.; Aizenberg, M.; Super, M.; Aizenberg, J.; Ingber, D. E. A Bioinspired Omniphobic Surface Coating on Medical Devices Prevents Thrombosis and Biofouling. *Nat. Biotechnol.* **2014**, *32* (11), 1134–1140.

(5) Wang, B.; Ye, Z.; Xu, Q.; Liu, H.; Lin, Q.; Chen, H.; Nan, K. Construction of a Temperature-Responsive Terpolymer Coating with Recyclable Bactericidal and Self-Cleaning Antimicrobial Properties. *Biomater. Sci.* **2016**, *4* (12), 1731–1741.

(6) Xu, L. C.; Siedlecki, C. A. Submicron-Textured Biomaterial Surface Reduces Staphylococcal Bacterial Adhesion and Biofilm Formation. *Acta Biomater.* **2012**, *8* (1), 72–81.

(7) Bryers, J. D. Medical Biofilms. *Biotechnol. Bioeng.* **2008**, *100* (1), 1–18.

(8) Levin, S. The Crisis in Antibiotic Resistance. *Infect. Dis. Clin. Pract.* **1993**, *2* (1), 53.

(9) Bagge, N.; Schuster, M.; Hentzer, M.; Ciofu, O.; Givskov, M.; Greenberg, E. P.; Høiby,

N. Pseudomonas Aeruginosa Biofilms Exposed to Imipenem Exhibit Changes in Global Gene Expression and β-Lactamase and Alginate Production. *Antimicrob. Agents Chemother.* **2004**, *48* (4), 1175–1187.

(10) Piddock, L. J. V. The Crisis of No New Antibiotics-What Is the Way Forward? *Lancet Infect. Dis.* **2012**, *12* (3), 249–253.

(11) Mitra, D.; Kang, E. T.; Neoh, K. G. Polymer-Based Coatings with Integrated Antifouling and Bactericidal Properties for Targeted Biomedical Applications. *ACS Appl. Polym. Mater.* **2021**, *3* (5), 2233–2263.

(12) Tan, J.; Liang, X.; Yang, J.; Zhou, S. Sol-Gel-Derived Hard Coatings from Tetraethoxysilane and Organoalkoxysilanes Bearing Zwitterionic and Isothiazolinone Groups and Their Antifouling Behaviors. *J. Mater. Chem. B* **2022**, *10* (3), 406–417.

(13) Vaterrodt, A.; Thallinger, B.; Daumann, K.; Koch, D.; Guebitz, G. M.; Ulbricht, M. Antifouling and Antibacterial Multifunctional Polyzwitterion/Enzyme Coating on Silicone Catheter Material Prepared by Electrostatic Layer-by-Layer Assembly. *Langmuir* **2016**, *32* (5), 1347–1359.

(14) Zhang, F.; Yang, L.; Hu, C.; Li, L.; Wang, J.; Luo, R.; Wang, Y. Phosphorylcholine- And Cation-Bearing Copolymer Coating with Superior Antibiofilm and Antithrombotic Properties for Blood-Contacting Devices. *J. Mater. Chem. B* **2020**, *8* (36), 8433–8443.

(15) Zhang, C.; Liu, S.; Tan, L.; Zhu, H.; Wang, Y. Star-Shaped Poly(2-Methyl-2-Oxazoline)-Based Films: Rapid Preparation and Effects of Polymer Architecture on Antifouling Properties. *J. Mater. Chem. B* **2015**, *3* (27), 5615–5628.

(16) Cortez, C.; Quinn, J. F.; Hao, X.; Gudipati, C. S.; Stenzel, M. H.; Davis, T. P.; Caruso, F. Multilayer Buildup and Biofouling Characteristics of PSS-b-PEG Containing Films.

Langmuir **2010**, *26* (12), 9720–9727.

(17) Zhu, X.; Jańczewski, D.; Guo, S.; Lee, S. S. C.; Parra Velandia, F. J.; Teo, S. L. M.; He, T.; Puniredd, S. R.; Julius Vancso, G. Polyion Multilayers with Precise Surface Charge Control for Antifouling. *ACS Appl. Mater. Interfaces* **2015**, *7* (1), 852–861.

(18) Liu, J.; Ye, L.; Sun, Y.; Hu, M.; Chen, F.; Wegner, S.; Mailänder, V.; Steffen, W.; Kappl, M.; Butt, H. J. Elastic Superhydrophobic and Photocatalytic Active Films Used as Blood Repellent Dressing. *Adv. Mater.* **2020**, *32* (11).

(19) Thompson, V. C.; Adamson, P. J.; Dilag, J.; Uswatte Uswatte Liyanage, D. B.; Srikantharajah, K.; Blok, A.; Ellis, A. V.; Gordon, D. L.; Köper, I. Biocompatible Anti-Microbial Coatings for Urinary Catheters. *RSC Adv.* **2016**, *6* (58), 53303–53309.

(20) Ryu, J. H.; Messersmith, P. B.; Lee, H. Polydopamine Surface Chemistry: A Decade of Discovery. *ACS Appl. Mater. Interfaces* **2018**, *10* (9), 7523–7540.

(21) Chandler, D. N T E R F a C E S a N D T H E D R I V I N G F O R C E O F H Y D R O P H O B I C a S S Em B L Y. *Nature* **2005**, *437*, 640–647.

(22) Oh, H.; Hoff, J. E.; Armstrong, G. S.; Haff, L. A. Hydrophobic Interaction in Tannin-Protein Complexes. *J. Agric. Food Chem.* **1980**, *28* (2), 394–398.

(23) Nigg, J. T. 基因的改变NIH Public Access. *Bone* **2008**, *23* (1), 1–7.

(24) Zhao, C.; Nguyen, N. S.; Li, X.; McCarthy, D.; Wang, H. Tannic Acid Coating and in Situ Deposition of Silver Nanoparticles to Improve the Antifouling Properties of an Ultrafiltration Membrane. *J. Appl. Polym. Sci.* **2019**, *136* (14), 1–10.

(25) Li, D.; Li, J.; Wang, S.; Wang, Q.; Teng, W. Dually Crosslinked Copper-Poly(Tannic Acid) Nanoparticles with Microenvironment-Responsiveness for Infected Wound Treatment. *Adv. Healthc. Mater.* **2023**, *12* (17), 1–18.

(26) Zhou, Y.; Wu, S.; Liu, F. High-Performance Polyimide Nanocomposites with Polydopamine-Coated Copper Nanoparticles and Nanowires for Electronic Applications. *Mater. Lett.* **2019**, *237*, 19–21.

(27) Liu, Y.; Han, Y.; Chen, R.; Zhang, H.; Liu, S.; Liang, F. In Situ Immobilization of Copper Nanoparticles on Polydopamine Coated Graphene Oxide for H2O2 Determination. *PLoS One* **2016**, *11* (7), 1–12.

(28) Li, J.; Li, J.; Wei, J.; Zhu, X.; Qiu, S.; Zhao, H. Copper Tannic Acid-Coordinated Metal-Organic Nanosheets for Synergistic Antimicrobial and Antifouling Coatings. *ACS Appl. Mater. Interfaces* **2021**, *13* (8), 10446–10456.

(29) Zhu, Z.; Gao, Q.; Long, Z.; Huo, Q.; Ge, Y.; Vianney, N.; Daliko, N. A.; Meng, Y.; Qu, J.; Chen, H.; Wang, B. Polydopamine/Poly(Sulfobetaine Methacrylate) Co-Deposition Coatings Triggered by CuSO4/H2O2 on Implants for Improved Surface Hemocompatibility and Antibacterial Activity. *Bioact. Mater.* **2021**, *6* (8), 2546–2556.

(30) Shahkaramipour, N.; Lai, C. K.; Venna, S. R.; Sun, H.; Cheng, C.; Lin, H. Membrane Surface Modification Using Thiol-Containing Zwitterionic Polymers via Bioadhesive Polydopamine. *Ind. Eng. Chem. Res.* **2018**, *57* (6), 2336–2345.

(31) Abouelmagd, S. A.; Meng, F.; Kim, B. K.; Hyun, H.; Yeo, Y. Tannic Acid-Mediated Surface Functionalization of Polymeric Nanoparticles. *ACS Biomater. Sci. Eng.* **2016**, *2* (12), 2294–2303.

(32) Zhang, M.; Cheng, C.; Guo, C.; Jin, L.; Liu, L.; Li, M.; Shang, L.; Liu, Y.; Ao, Y. Co-Depositing Bio-Inspired Tannic Acid-Aminopropyltriethoxysilane Coating onto Carbon Fiber for Excellent Interfacial Adhesion of Epoxy Composites. *Compos. Sci. Technol.* **2021**, *204* (October 2020), 108639.

(33) Alfieri, M. L.; Panzella, L.; Oscurato, S. L.; Salvatore, M.; Avolio, R.; Errico, M. E.; Maddalena, P.; Napolitano, A.; d'Ischia, M. The Chemistry of Polydopamine Film Formation: The Amine-Quinone Interplay. *Biomimetics* **2018**, *3* (3).

(34) Chen, S.; Li, L.; Zhao, C.; Zheng, J. Surface Hydration: Principles and Applications toward Low-Fouling/Nonfouling Biomaterials. *Polymer (Guildf).* **2010**, *51* (23), 5283–5293.

(35) Chen, S.; Cao, Z.; Jiang, S. Ultra-Low Fouling Peptide Surfaces Derived from Natural Amino Acids. *Biomaterials* **2009**, *30* (29), 5892–5896.

(36) Nguyen, A. T.; Baggerman, J.; Paulusse, J. M. J.; Zuilhof, H.; Van Rijn, C. J. M. Bioconjugation of Protein-Repellent Zwitterionic Polymer Brushes Grafted from Silicon Nitride. *Langmuir* **2012**, *28* (1), 604–610.

(37) Greene, G. W.; Martin, L. L.; Tabor, R. F.; Michalczyk, A.; Ackland, L. M.; Horn, R. Lubricin: A Versatile, Biological Anti-Adhesive with Properties Comparable to Polyethylene Glycol. *Biomaterials* **2015**, *53*, 127–136.

(38) Yi, L.; Xu, K.; Xia, G.; Li, J.; Li, W.; Cai, Y. New Protein-Resistant Surfaces of Amphiphilic Graft Copolymers Containing Hydrophilic Poly(Ethylene Glycol) and Low Surface Energy Fluorosiloxane Side-Chains. *Appl. Surf. Sci.* **2019**, *480* (February), 923–933.

(39) Leckband, D.; Sheth, S.; Halperin, A. Grafted Poly(Ethylene Oxide) Brushes as Nonfouling Surface Coatings. *J. Biomater. Sci. Polym. Ed.* **1999**, *10* (10), 1125–1147.

(40) Chen, S.; Zheng, J.; Li, L.; Jiang, S. Strong Resistance of Phosphorylcholine Self-Assembled Monolayers to Protein Adsorption: Insights into Nonfouling Properties of Zwitterionic Materials. *J. Am. Chem. Soc.* **2005**, *127* (41), 14473–14478.

(41) Riga, E. K.; Vöhringer, M.; Widyaya, V. T.; Lienkamp, K. Polymer-Based Surfaces Designed to Reduce Biofilm Formation: From Antimicrobial Polymers to Strategies for Long-Term Applications. *Macromol. Rapid Commun.* **2017**, *38* (20), 1–18.

(42) McBain, A. J.; Rickard, A. H.; Gilbert, P. Possible Implications of Biocide Accumulation in the Environment on the Prevalence of Bacterial Antibiotic Resistance. *J. Ind. Microbiol. Biotechnol.* **2002**, *29* (6), 326–330.

(43) Francolini, I.; Donelli, G. Prevention and Control of Biofilm-Based Medical-Device-Related Infections. *FEMS Immunol. Med. Microbiol.* **2010**, *59* (3), 227–238.

(44) Khatoon, Z.; McTiernan, C. D.; Suuronen, E. J.; Mah, T. F.; Alarcon, E. I. Bacterial Biofilm Formation on Implantable Devices and Approaches to Its Treatment and Prevention. *Heliyon* **2018**, *4* (12), e01067.

(45) Li, X.; Sun, L.; Zhang, P.; Wang, Y. Novel Approaches to Combat Medical Device-Associated Biofilms. *Coatings* **2021**, *11* (3), 1–31.

(46) Alotaibi, G. F. Factors Influencing Bacterial Biofilm Formation and Development. *Am. J. Biomed. Sci. Res.* **2021**, *12* (6), 617–626.

(47) Muhammad, M. H.; Idris, A. L.; Fan, X.; Guo, Y.; Yu, Y.; Jin, X.; Qiu, J.; Guan, X.; Huang, T. Beyond Risk: Bacterial Biofilms and Their Regulating Approaches. *Front. Microbiol.* **2020**, *11* (May), 1–20.

(48) Toyofuku, M.; Inaba, T.; Kiyokawa, T.; Obana, N.; Yawata, Y.; Nomura, N. Environmental Factors That Shape Biofilm Formation. *Biosci. Biotechnol. Biochem.* **2016**, *80* (1), 7–12.

(49) Cyanobacteria, C. The Relative Importance of Shear Forces and Surface Hydrophobicity on Biofilm Formation By.

(50) Guo, K.; Freguia, S.; Dennis, P. G.; Chen, X.; Donose, B. C.; Keller, J.; Gooding, J. J.; Rabaey, K. Effects of Surface Charge and Hydrophobicity on Anodic Biofilm Formation, Community Composition, and Current Generation in Bioelectrochemical Systems. *Environ. Sci. Technol.* **2013**, *47* (13), 7563–7570.

(51) Yin, R.; Cheng, J.; Wang, J.; Li, P.; Lin, J. Treatment of Pseudomonas Aeruginosa Infectious Biofilms: Challenges and Strategies. *Front. Microbiol.* **2022**, *13* (August), 1–16.

(52) Magin, C. M.; Cooper, S. P.; Brennan, A. B. Non-Toxic Antifouling Strategies. *Mater. Today* **2010**, *13* (4), 36–44.

(53) Thérien-Aubin, H.; Chen, L.; Ober, C. K. Fouling-Resistant Polymer Brush Coatings. *Polymer (Guildf).* **2011**, *52* (24), 5419–5425.

(54) Sakala, G. P.; Reches, M. Peptide-Based Approaches to Fight Biofouling. *Adv. Mater. Interfaces* **2018**, *5* (18), 1–26.

(55) Okada, A.; Nikaido, T.; Ikeda, M.; Okada, K.; Yamauchi, J.; Foxton, R. M.; Sawadda, H.; Tagami, J.; Matin, K. **疏油**-亲水 **原始**讨论构造文章. *Dent. Mater. J.* **2008**, *27* (4), 565–572.

(56) Lejars, M.; Margaillan, A.; Bressy, C. Fouling Release Coatings: A Nontoxic Alternative to Biocidal Antifouling Coatings. *Chem. Rev.* **2012**, *112* (8), 4347–4390.

(57) Selim, M. S.; Shenashen, M. A.; El-Safty, S. A.; Higazy, S. A.; Selim, M. M.; Isago, H.; Elmarakbi, A. Recent Progress in Marine Foul-Release Polymeric Nanocomposite Coatings. *Prog. Mater. Sci.* **2017**, *87*, 1–32.

(58) Maan, A. M. C.; Hofman, A. H.; de Vos, W. M.; Kamperman, M. Recent Developments and Practical Feasibility of Polymer-Based Antifouling Coatings. *Adv. Funct. Mater.*

2020, *30* (32).

(59) Faustino, C. M. C.; Lemos, S. M. C.; Monge, N.; Ribeiro, I. A. C. A Scope at Antifouling Strategies to Prevent Catheter-Associated Infections. *Adv. Colloid Interface Sci.* **2020**, *284*.

(60) Han, H.; Zhu, J.; Wu, D. Q.; Li, F. X.; Wang, X. L.; Yu, J. Y.; Qin, X. H. Inherent Guanidine Nanogels with Durable Antibacterial and Bacterially Antiadhesive Properties. *Adv. Funct. Mater.* **2019**, *29* (12), 1–17.

(61) Wu, G.; Li, C. C.; Jiang, X. H.; Yu, L. M. Highly Efficient Antifouling Property Based on Self-Generating Hydrogel Layer of Polyacrylamide Coatings. *J. Appl. Polym. Sci.* **2016**, *133* (42), 1–11.

(62) Serhan, M.; Sprowls, M.; Jackemeyer, D.; Long, M.; Perez, I. D.; Maret, W.; Tao, N.; Forzani, E. Total Iron Measurement in Human Serum with a Smartphone. *AIChE Annu. Meet. Conf. Proc.* **2019**, *2019-Novem*.

(63) Jiang, S.; Cao, Z. Ultralow-Fouling, Functionalizable, and Hydrolyzable Zwitterionic Materials and Their Derivatives for Biological Applications. *Adv. Mater.* **2010**, *22* (9), 920–932.

(64) He, M.; Gao, K.; Zhou, L.; Jiao, Z.; Wu, M.; Cao, J.; You, X.; Cai, Z.; Su, Y.; Jiang, Z. Zwitterionic Materials for Antifouling Membrane Surface Construction. *Acta Biomater.* **2016**, *40* (92), 142–152.

(65) Xiao, S.; Ren, B.; Huang, L.; Shen, M.; Zhang, Y.; Zhong, M.; Yang, J.; Zheng, J. Salt-Responsive Zwitterionic Polymer Brushes with Anti-Polyelectrolyte Property. *Curr. Opin. Chem. Eng.* **2018**, *19*, 86–93.

(66) Kawano, S.; Lie, J.; Ohgi, R.; Shizuma, M.; Muraoka, M. Modulating Polymeric

Amphiphiles Using Thermo- And PH-Responsive Copolymers with Cyclodextrin Pendant Groups through Molecular Recognition of the Lipophilic Dye. *Macromolecules* **2021**, *54* (11), 5229–5240.

(67) Quan, X.; Zhao, D.; Li, L.; Zhou, J. Understanding the Cellular Uptake of PH-Responsive Zwitterionic Gold Nanoparticles: A Computer Simulation Study. *Langmuir* **2017**, *33* (50), 14480–14489.

(68) Ueda, T.; Oshida, H.; Kurita, K.; Ishihara, K.; Nakabayashi, N. Preparation of 2-Methacryloyloxyethyl Phosphorylcholine Copolymers with Alkyl Methacrylates and Their Blood Compatibility. *Polym. J.* **1992**, *24* (11), 1259–1269.

(69) Morra, M.; Cassineli, C. Non-Fouling Properties of Polysaccharide-Coated Surfaces. *J. Biomater. Sci. Polym. Ed.* **1999**, *10* (10), 1107–1124.

(70) Wang, R.; Song, X.; Xiang, T.; Liu, Q.; Su, B.; Zhao, W.; Zhao, C. Mussel-Inspired Chitosan-Polyurethane Coatings for Improving the Antifouling and Antibacterial Properties of Polyethersulfone Membranes. *Carbohydr. Polym.* **2017**, *168*, 310–319.

(71) Ribeiro, J. P. M.; Mendonça, P. V.; Coelho, J. F. J.; Matyjaszewski, K.; Serra, A. C. Glycopolymer Brushes by Reversible Deactivation Radical Polymerization: Preparation, Applications, and Future Challenges. *Polymers (Basel).* **2020**, *12* (6).

(72) Yu, K.; Kizhakkedathu, J. N. Synthesis of Functional Polymer Brushes Containing Carbohydrate Residues in the Pyranose Form and Their Specific and Nonspecific Interactions with Proteins. *Biomacromolecules* **2010**, *11* (11), 3073–3085.

(73) Cheng, Q.; Peng, Y. Y.; Asha, A. B.; Zhang, L.; Li, J.; Shi, Z.; Cui, Z.; Narain, R. Construction of Antibacterial Adhesion Surfaces Based on Bioinspired Borneol-Containing Glycopolymers. *Biomater. Sci.* **2022**, *10* (7), 1787–1794.

(74) Feng, K.; Peng, L.; Yu, L.; Zheng, Y.; Chen, R.; Zhang, W.; Chen, G.; Chen, G. Universal Antifogging and Antimicrobial Thin Coating Based on Dopamine-Containing Glycopolymers. *ACS Appl. Mater. Interfaces* **2020**, *12* (24), 27632–27639.

(75) Matsumura, S.; Hlil, A. R.; Lepiller, C.; Gaudet, J.; Guay, D.; Shi, Z.; Holdcroft, S.; Hay, A. S. Stability and Utility of Pyridyl Disulfide Functionality in RAFT and Conventional Radical Polymerizations. *J. Polym. Sci. Part A Polym. Chem.* **2008**, *46* (April), 7207–7224.

(76) C., W. Molecular Mechanisms That Confer Antibacterial Drug Resistance. *Nature* **2000**, *406* (775–781), 775–781.

(77) Kohanski, M. A.; Dwyer, D. J.; Collins, J. J. How Antibiotics Kill Bacteria: From Targets to Networks. *Nat. Rev. Microbiol.* **2010**, *8* (6), 423–435.

(78) Jennings, M. C.; Minbiole, K. P. C.; Wuest, W. M. Quaternary Ammonium Compounds: An Antimicrobial Mainstay and Platform for Innovation to Address Bacterial Resistance. *ACS Infect. Dis.* **2016**, *1* (7), 288–303.

(79) Calabrese, D. R.; Wenning, B.; Finlay, J. A.; Callow, M. E.; Callow, J. A.; Fischer, D.; Ober, C. K. Amphiphilic Oligopeptides Grafted to PDMS-Based Diblock Copolymers for Use in Antifouling and Fouling Release Coatings. *Polym. Adv. Technol.* **2015**, *26* (7), 829–836.

(80) Palermo, E. F.; Vemparala, S.; Kuroda, K. Cationic Spacer Arm Design Strategy for Control of Antimicrobial Activity and Conformation of Amphiphilic Methacrylate Random Copolymers. *Biomacromolecules* **2012**, *13* (5), 1632–1641.

(81) Oda, Y.; Kanaoka, S.; Sato, T.; Aoshima, S.; Kuroda, K. Block versus Random Amphiphilic Copolymers as Antibacterial Agents. *Biomacromolecules* **2011**, *12* (10),

3581–3591.

(82) Yang, Y.; Cai, Z.; Huang, Z.; Tang, X.; Zhang, X. Antimicrobial Cationic Polymers: From Structural Design to Functional Control. *Polym. J.* **2018**, *50* (1), 33–44.

(83) Ganewatta, M. S.; Tang, C. Controlling Macromolecular Structures towards Effective Antimicrobial Polymers. *Polymer (Guildf).* **2015**, *63*, A1–A29.

(84) Narciso, F.; Cardoso, S.; Monge, N.; Lourenço, M.; Martin, V.; Duarte, N.; Santos, C.; Gomes, P.; Bettencourt, A.; Ribeiro, I. A. C. 3D-Printed Biosurfactant-Chitosan Antibacterial Coating for the Prevention of Silicone-Based Associated Infections. *Colloids Surfaces B Biointerfaces* **2023**, *230* (August), 0–2.

(85) Zhou, Y.; Jiang, Y.; Zhang, Y.; Tan, L. Improvement of Antibacterial and Antifouling Properties of a Cellulose Acetate Membrane by Surface Grafting Quaternary Ammonium Salt. *ACS Appl. Mater. Interfaces* **2022**, *14* (33), 38358–38369.

(86) Chang, H. I.; Yang, M. S.; Liang, M. The Synthesis, Characterization and Antibacterial Activity of Quaternized Poly(2,6-Dimethyl-1,4-Phenylene Oxide)s Modified with Ammonium and Phosphonium Salts. *React. Funct. Polym.* **2010**, *70* (12), 944–950.

(87) Xu, X.; Wang, Q.; Chang, Y.; Zhang, Y.; Peng, H.; Whittaker, A. K.; Fu, C. Antifouling and Antibacterial Surfaces Grafted with Sulfur-Containing Copolymers. *ACS Appl. Mater. Interfaces* **2022**, *14* (36), 41400–41411.

(88) Tiller, J. C.; Liao, C. J.; Lewis, K.; Klibanov, A. M. Designing Surfaces That Kill Bacteria on Contact. *Proc. Natl. Acad. Sci. U. S. A.* **2001**, *98* (11), 5981–5985.

(89) Shiga, T.; Mori, H.; Uemura, K.; Moriuchi, R.; Dohra, H.; Yamawaki-Ogata, A.; Narita, Y.; Saito, A.; Kotsuchibashi, Y. Evaluation of the Bactericidal and Fungicidal Activities of Poly([2-(Methacryloyloxy)Ethyl]Trimethyl Ammonium Chloride)(Poly (METAC))-

Based Materials. *Polymers (Basel).* **2018**, *10* (9), 1–9.

(90) Kobayashi, M.; Terada, M.; Terayama, Y.; Kikuchi, M.; Takahara, A. Direct Synthesis of Well-Defined Poly[{2-(Methacryloyloxy)Ethyl} Trimethylammonium Chloride] Brush via Surface-Initiated Atom Transfer Radical Polymerization in Fluoroalcohol. *Macromolecules* **2010**, *43* (20), 8409–8415.

(91) Xu, G.; Liu, P.; Pranantyo, D.; Xu, L.; Neoh, K. G.; Kang, E. T. Antifouling and Antimicrobial Coatings from Zwitterionic and Cationic Binary Polymer Brushes Assembled via "Click" Reactions. *Ind. Eng. Chem. Res.* **2017**, *56* (49), 14479–14488.

(92) Furno, F.; Morley, K. S.; Wong, B.; Sharp, B. L.; Arnold, P. L.; Howdle, S. M.; Bayston, R.; Brown, P. D.; Winship, P. D.; Reid, H. J. Silver Nanoparticles and Polymeric Medical Devices: A New Approach to Prevention of Infection? *J. Antimicrob. Chemother.* **2004**, *54* (6), 1019–1024.

(93) Tagar, S.; Qambrani, N. A. Bacteriological Quality Assessment of Poultry Chicken Meat and Meat Contact Surfaces for the Presence of Targeted Bacteria and Determination of Antibiotic Resistance of Salmonella Spp. in Pakistan. *Food Control* **2023**, *151* (April), 109786.

(94) Lu, Y.; Slomberg, D. L.; Schoenfisch, M. H. Nitric Oxide-Releasing Chitosan Oligosaccharides as Antibacterial Agents. *Biomaterials* **2014**, *35* (5), 1716–1724.

(95) El-Aziz, S. M. A.; Faraag, A. H. I.; Ibrahim, A. M.; Albrakati, A.; Bakkar, M. R. Tyrosinase Enzyme Purification and Immobilization from Pseudomonas Sp. EG22 Using Cellulose Coated Magnetic Nanoparticles: Characterization and Application in Melanin Production. *World J. Microbiol. Biotechnol.* **2024**, *40* (1), 1–18.

(96) Cao, M.; Zhao, W.; Wang, L.; Li, R.; Gong, H.; Zhang, Y.; Xu, H.; Lu, J. R. Graphene

Oxide-Assisted Accumulation and Layer-by-Layer Assembly of Antibacterial Peptide for Sustained Release Applications. *ACS Appl. Mater. Interfaces* **2018**, *10* (29), 24937–24946.

(97) Seil, J. T.; Webster, T. J. Antimicrobial Applications of Nanotechnology: Methods and Literature. *Int. J. Nanomedicine* **2012**, *7*, 2767–2781.

(98) Meng, M.; He, H.; Xiao, J.; Zhao, P.; Xie, J.; Lu, Z. Controllable in Situ Synthesis of Silver Nanoparticles on Multilayered Film-Coated Silk Fibers for Antibacterial Application. *J. Colloid Interface Sci.* **2016**, *461*, 369–375.

(99) Zimmerli, W. Clinical Presentation and Treatment of Orthopaedic Implant-Associated Infection. *J. Intern. Med.* **2014**, *276* (2), 111–119.

(100) Zhang, J.; Zhou, R.; Wang, H.; Jiang, X.; Wang, H.; Yan, S.; Yin, J.; Luan, S. Bacterial Activation of Surface-Tethered Antimicrobial Peptides for the Facile Construction of a Surface with Self-Defense. *Appl. Surf. Sci.* **2019**, *497* (April), 143480.

(101) Yu, Q.; Wu, Z.; Chen, H. Dual-Function Antibacterial Surfaces for Biomedical Applications. *Acta Biomater.* **2015**, *16* (1), 1–13.

(102) Alapján-, V. 済無No Title No Title No Title. **2016**, *318* (OCTOBER), 1–23.

(103) Ejima, H.; Richardson, J. J.; Liang, K.; Best, J. P.; Van Koeverden, M. P.; Such, G. K.; Cui, J.; Caruso, F. One-Step Assembly of Coordination Complexes. *Science (80-.).* **2013**, *341* (6142), 154–157.

(104) Salazar, P.; Martin, M.; Gonzalez, J. L. Polydopamine-Modified Surfaces in Biosensor Applications. *Polym. Sci. Res. Adv. Pract. Appl. Educ. Asp.* **2016**, *1* (July), 385–396.

(105) Li, S.; Scheiger, J. M.; Wang, Z.; Dong, Z.; Welle, A.; Trouillet, V.; Levkin, P. A. Substrate-Independent and Re-Writable Surface Patterning by Combining Polydopamine

Coatings, Silanization, and Thiol-Ene Reaction. *Adv. Funct. Mater.* **2021**, *31* (50).

(106) Asha, A. B.; Chen, Y.; Narain, R. Bioinspired Dopamine and Zwitterionic Polymers for Non-Fouling Surface Engineering. *Chem. Soc. Rev.* **2021**, *50* (20), 11668–11683.

(107) Zhou, C.; Wu, Y.; Thappeta, K. R. V.; Subramanian, J. T. L.; Pranantyo, D.; Kang, E. T.; Duan, H.; Kline, K.; Chan-Park, M. B. In Vivo Anti-Biofilm and Anti-Bacterial Non-Leachable Coating Thermally Polymerized on Cylindrical Catheter. *ACS Appl. Mater. Interfaces* **2017**, *9* (41), 36269–36280.

(108) Li, N.; Li, T.; Qiao, X. Y.; Li, R.; Yao, Y.; Gong, Y. K. Universal Strategy for Efficient Fabrication of Blood Compatible Surfaces via Polydopamine-Assisted Surface-Initiated Activators Regenerated by Electron Transfer Atom-Transfer Radical Polymerization of Zwitterions. *ACS Appl. Mater. Interfaces* **2020**, *12* (10), 12337–12344.

(109) Dalsin, J. L.; Hu, B. H.; Lee, B. P.; Messersmith, P. B. Mussel Adhesive Protein Mimetic Polymers for the Preparation of Nonfouling Surfaces. *J. Am. Chem. Soc.* **2003**, *125* (14), 4253–4258.

(110) Wang, B. L.; Jin, T. W.; Han, Y. M.; Shen, C. H.; Li, Q.; Lin, Q. K.; Chen, H. Bio-Inspired Terpolymers Containing Dopamine, Cations and MPC: A Versatile Platform to Construct a Recycle Antibacterial and Antifouling Surface. *J. Mater. Chem. B* **2015**, *3* (27), 5501–5510.

(111) Liu, G.; Xiang, J.; Xia, Q.; Li, K.; Yan, H.; Yu, L. Fabrication of Durably Antibacterial Cotton Fabrics by Robust and Uniform Immobilization of Silver Nanoparticles via Mussel-Inspired Polydopamine/Polyethyleneimine Coating. *Ind. Eng. Chem. Res.* **2020**, *59* (20), 9666–9678.

(112) Sun, F.; Wu, K.; Hung, H. C.; Zhang, P.; Che, X.; Smith, J.; Lin, X.; Li, B.; Jain, P.; Yu,

Q.; Jiang, S. Paper Sensor Coated with a Poly(Carboxybetaine)-Multiple DOPA Conjugate via Dip-Coating for Biosensing in Complex Media. *Anal. Chem.* **2017**, *89* (20), 10999–11004.

(113) Baldwin, A.; Booth, B. W. Biomedical Applications of Tannic Acid. *J. Biomater. Appl.* **2022**, *36* (8), 1503–1523.

(114) Xu, L. Q.; Pranantyo, D.; Neoh, K. G.; Kang, E. T.; Fu, G. D. Thiol Reactive Maleimido-Containing Tannic Acid for the Bioinspired Surface Anchoring and Post-Functionalization of Antifouling Coatings. *ACS Sustain. Chem. Eng.* **2016**, *4* (8), 4264–4272.

(115) Chen, C.; Yang, H.; Yang, X.; Ma, Q. Tannic Acid: A Crosslinker Leading to Versatile Functional Polymeric Networks: A Review. *RSC Adv.* **2022**, *12* (13), 7689–7711.

(116) Pranantyo, D.; Xu, L. Q.; Neoh, K. G.; Kang, E. T.; Ng, Y. X.; Teo, S. L. M. Tea Stains-Inspired Initiator Primer for Surface Grafting of Antifouling and Antimicrobial Polymer Brush Coatings. *Biomacromolecules* **2015**, *16* (3), 723–732.

(117) Jeong, W.; Kang, H.; Kim, E.; Jeong, J.; Hong, D. Surface-Initiated ARGET ATRP of Antifouling Zwitterionic Brushes Using Versatile and Uniform Initiator Film. *Langmuir* **2019**, *35* (41), 13268–13274.

(118) Xu, G.; Liu, P.; Pranantyo, D.; Neoh, K. G.; Kang, E. T.; Lay-Ming Teo, S. One-Step Anchoring of Tannic Acid-Scaffolded Bifunctional Coatings of Antifouling and Antimicrobial Polymer Brushes. *ACS Sustain. Chem. Eng.* **2019**, *7* (1), 1786–1795.

(119) Xu, G.; Neoh, K. G.; Kang, E. T.; Teo, S. L. M. Switchable Antimicrobial and Antifouling Coatings from Tannic Acid-Scaffolded Binary Polymer Brushes. *ACS Sustain. Chem. Eng.* **2020**, *8* (6), 2586–2595.

(120) Chen, S.; Xie, Y.; Xiao, T.; Zhao, W.; Li, J.; Zhao, C. Tannic Acid-Inspiration and Post-

Crosslinking of Zwitterionic Polymer as a Universal Approach towards Antifouling Surface. *Chem. Eng. J.* **2018**, *337* (October 2017), 122–132.

(121) Xie, Y.; Chen, S.; Zhang, X.; Shi, Z.; Wei, Z.; Bao, J.; Zhao, W.; Zhao, C. Engineering of Tannic Acid Inspired Antifouling and Antibacterial Membranes through Co-Deposition of Zwitterionic Polymers and Ag Nanoparticles. *Ind. Eng. Chem. Res.* **2019**, *58* (27), 11689–11697.

(122) Wang, Y.; Wei, T.; Qu, Y.; Zhou, Y.; Zheng, Y.; Huang, C.; Zhang, Y.; Yu, Q.; Chen, H. Smart, Photothermally Activated, Antibacterial Surfaces with Thermally Triggered Bacteria-Releasing Properties. *ACS Appl. Mater. Interfaces* **2020**, *12* (19), 21283–21291.

(123) Guo, L. L.; Cheng, Y. F.; Ren, X.; Gopinath, K.; Lu, Z. S.; Li, C. M.; Xu, L. Q. Simultaneous Deposition of Tannic Acid and Poly(Ethylene Glycol) to Construct the Antifouling Polymeric Coating on Titanium Surface. *Colloids Surfaces B Biointerfaces* **2021**, *200* (September 2020), 111592.

(124) Liu, Y.; Mao, S.; Zhu, L.; Chen, S.; Wu, C. Based on Tannic Acid and Thermoresponsive Microgels Design a Simple and High-Efficiency Multifunctional Antibacterial Coating. *Eur. Polym. J.* **2021**, *153* (May), 110498.

(125) Zhang, H.; Shen, X.; Fei, Z.; Fan, X.; Ma, L.; Wang, H.; Tian, C.; Zhang, B.; Luo, R.; Wang, Y.; Huang, S. Ag-Incorporated Polydopamine/Tannic Acid Coating on Titanium With Enhanced Cytocompatible and Antibacterial Properties. *Front. Bioeng. Biotechnol.* **2022**, *10* (March), 1–9.

(126) Zhao, J.; Mo, R.; Tian, L. M.; Song, L. J.; Luan, S. F.; Yin, J. H.; Ren, L. Q. Oriented Antibody Immobilization and Immunoassay Based on Boronic Acid-Containing Polymer Brush. *Chinese J. Polym. Sci. (English Ed.* **2018**, *36* (4), 472–478.

(127) Sin, M. C.; Sun, Y. M.; Chang, Y. Zwitterionic-Based Stainless Steel with Well-Defined Polysulfobetaine Brushes for General Bioadhesive Control. *ACS Appl. Mater. Interfaces* **2014**, *6* (2), 861–873.

(128) Ma, W.; Yang, P.; Li, J.; Li, S.; Li, P.; Zhao, Y.; Huang, N. Immobilization of Poly(MPC) Brushes onto Titanium Surface by Combining Dopamine Self-Polymerization and ATRP: Preparation, Characterization and Evaluation of Hemocompatibility in Vitro. *Appl. Surf. Sci.* **2015**, *349*, 445–451.

(129) Peng, B.; Lai, X.; Chen, L.; Lin, X.; Sun, C.; Liu, L.; Qi, S.; Chen, Y.; Leong, K. W. Scarless Wound Closure by a Mussel-Inspired Poly(Amidoamine) Tissue Adhesive with Tunable Degradability. *ACS Omega* **2017**, *2* (9), 6053–6062.

(130) Yang, W.; Sundaram, H. S.; Ella, J. R.; He, N.; Jiang, S. Low-Fouling Electrospun PLLA Films Modified with Zwitterionic Poly(Sulfobetaine Methacrylate)-Catechol Conjugates. *Acta Biomater.* **2016**, *40*, 92–99.

(131) Xiong, F.; Wei, S.; Sheng, H.; Han, X.; Jiang, W.; Zhang, Z.; Li, B.; Xuan, H.; Xue, Y.; Yuan, H. In Situ Polydopamine Functionalized Poly-L-Lactic Acid Nanofibers with near-Infrared-Triggered Antibacterial and Reactive Oxygen Species Scavenging Capability. *Int. J. Biol. Macromol.* **2022**, *201* (December 2021), 338–350.

(132) Ye, G.; Lee, J.; Perreault, F.; Elimelech, M. Controlled Architecture of Dual-Functional Block Copolymer Brushes on Thin-Film Composite Membranes for Integrated "Defending" and "Attacking" Strategies against Biofouling. *ACS Appl. Mater. Interfaces* **2015**, *7* (41), 23069–23079.

(133) Zhao, H.; Huang, Y.; Zhang, W.; Guo, Q.; Cui, W.; Sun, Z.; Eglin, D.; Liu, L.; Pan, G.; Shi, Q. Mussel-Inspired Peptide Coatings on Titanium Implant to Improve

Osseointegration in Osteoporotic Condition. *ACS Biomater. Sci. Eng.* **2018**, *4* (7), 2505–2515.

(134) Carvalho, A. L.; Vale, A. C.; Sousa, M. P.; Barbosa, A. M.; Torrado, E.; Mano, J. F.; Alves, N. M. Antibacterial Bioadhesive Layer-by-Layer Coatings for Orthopedic Applications. *J. Mater. Chem. B* **2016**, *4* (32), 5385–5393.

(135) Zhang, T. Di; Deng, X.; Wang, Y. F.; Wang, X. T.; Zhang, X.; Chen, L. L.; Cao, X.; Zhang, Y. Z.; Zhang, C. Y.; Zheng, X.; Yin, D. C. Layer-by-Layer Coating of Polyvinylamine and Dopamine-Modified Hyaluronic Acid Inhibits the Growth of Bacteria and Tumor Cell Lines on the Surface of Materials. *Appl. Surf. Sci.* **2020**, *530* (July), 147197.

(136) Hegab, H. M.; ElMekawy, A.; Barclay, T. G.; Michelmore, A.; Zou, L.; Saint, C. P.; Ginic-Markovic, M. Single-Step Assembly of Multifunctional Poly(Tannic Acid)-Graphene Oxide Coating to Reduce Biofouling of Forward Osmosis Membranes. *ACS Appl. Mater. Interfaces* **2016**, *8* (27), 17519–17528.

(137) Wang, Z.; Han, M.; Zhang, J.; He, F.; Xu, Z.; Ji, S.; Peng, S.; Li, Y. Designing Preferable Functional Materials Based on the Secondary Reactions of the Hierarchical Tannic Acid (TA)-Aminopropyltriethoxysilane (APTES) Coating. *Chem. Eng. J.* **2019**, *360* (September 2018), 299–312.

(138) Guo, L. L.; Cheng, Y. F.; Ren, X.; Gopinath, K.; Lu, Z. S.; Li, C. M.; Xu, L. Q. Simultaneous Deposition of Tannic Acid and Poly(Ethylene Glycol) to Construct the Antifouling Polymeric Coating on Titanium Surface. *Colloids Surfaces B Biointerfaces* **2021**, *200* (January), 111592.

(139) Liu, L.; Shi, H.; Yu, H.; Zhou, R.; Yin, J.; Luan, S. One-Step Hydrophobization of Tannic

Acid for Antibacterial Coating on Catheters to Prevent Catheter-Associated Infections. *Biomater. Sci.* **2019**, *7* (12), 5035–5043.

(140) Lu, Q.; Zou, F.; Chen, Z.; Gnanasekar, S.; Zhao, D.; Liu, Y.; Liu, H.; Zhang, Y.; Lu, Z.; Kang, E. T.; Xu, L.; Rao, X. A Bioactive Tannic Acid/Vanadium Ions Co-Deposited Coating on Various Surfaces for Antifouling, Photothermal Anti-Bacterial, and Antioxidant Effects. *Prog. Org. Coatings* **2024**, *186* (July 2023), 108010.

(141) Ren, J.; Kong, R.; Gao, Y.; Zhang, L.; Zhu, J. Bioinspired Adhesive Coatings from Polyethylenimine and Tannic Acid Complexes Exhibiting Antifogging, Self-Cleaning, and Antibacterial Capabilities. *J. Colloid Interface Sci.* **2021**, *602*, 406–414.

(142) Liu, J.; Yu, X.; Yang, E.; Li, T.; Yu, H.; Wang, Z.; Dong, B.; Fane, A. G. A Combined Tannic Acid-Copper-Iron Coating of Ultrafiltration Membrane for Enhanced Anti-Bacterial and Algal-Inhibition Performance. *J. Water Process Eng.* **2022**, *50* (September), 103250.

(143) Sagle, A. C.; Ju, H.; Freeman, B. D.; Sharma, M. M. PEG-Based Hydrogel Membrane Coatings. *Polymer (Guildf).* **2009**, *50* (3), 756–766.

(144) Elfarargy, R. G.; Sedki, M.; Samhan, F. A.; Hassan, R. Y. A.; El-Sherbiny, I. M. Surface Grafting of Polymeric Catheters and Stents to Prevent Biofilm Formation of Pathogenic Bacteria. *J. Genet. Eng. Biotechnol.* **2023**, *21* (1).

(145) Dundar Arisoy, F.; Kolewe, K. W.; Homyak, B.; Kurtz, I. S.; Schiffman, J. D.; Watkins, J. J. Bioinspired Photocatalytic Shark-Skin Surfaces with Antibacterial and Antifouling Activity via Nanoimprint Lithography. *ACS Appl. Mater. Interfaces* **2018**, *10* (23), 20055–20063.

(146) Knorr, D. B.; Tran, N. T.; Gaskell, K. J.; Orlicki, J. A.; Woicik, J. C.; Jaye, C.; Fischer, D.

A.; Lenhart, J. L. Synthesis and Characterization of Aminopropyltriethoxysilane-Polydopamine Coatings. *Langmuir* **2016**, *32* (17), 4370–4381.

(147) Clodt, J. I.; Filiz, V.; Rangou, S.; Buhr, K.; Abetz, C.; Höche, D.; Hahn, J.; Jung, A.; Abetz, V. Double Stimuli-Responsive Isoporous Membranes via Post-Modification of Ph-Sensitive Self-Assembled Diblock Copolymer Membranes. *Adv. Funct. Mater.* **2013**, *23* (6), 731–738.

(148) Lu, Z.; Xiao, J.; Wang, Y.; Meng, M. In Situ Synthesis of Silver Nanoparticles Uniformly Distributed on Polydopamine-Coated Silk Fibers for Antibacterial Application. *J. Colloid Interface Sci.* **2015**, *452*, 8–14.

(149) Kim, H. J.; Kim, D.; Yoon, H.; Choi, Y.; Yoon, J.; Lee, J. Polyphenol / Fe III Complex Coated Membranes Having Multifunctional Properties Prepared by a One-Step Fast Assembly. **2015**, 1–8.

(150) Rappold, P. M.; Cui, M.; Grima, J. C.; Fan, R. Z.; Mesy-bentley, K. L. De; Chen, L.; Zhuang, X.; Bowers, W. J.; Tieu, K. Dopamine Release Deficits in Vivo. *Nat. Commun.* **2014**.

(151) Liu, Y.; Mao, S.; Zhu, L.; Chen, S.; Wu, C. Based on Tannic Acid and Thermoresponsive Microgels Design a Simple and High-Efficiency Multifunctional Antibacterial Coating. *Eur. Polym. J.* **2021**, *153* (March), 110498.

(152) Barrett, D. G.; Sileika, T. S.; Messersmith, P. B. Precursors of Tannin-Inspired Nanocoatings †. **2014**, 7265–7268.

(153) Dong, G.; Liu, H.; Yu, X.; Zhang, X.; Lu, H.; Zhou, T. Antimicrobial and Anti-Biofilm Activity of Tannic Acid against Staphylococcus Aureus. *Nat. Prod. Res.* **2018**, *6419*, 1–4.

(154) Wang, P.; Liu, J.; Luo, X.; Xiong, P.; Gao, S.; Yan, J. Mg – Zn – Y – Nd Alloy with

Antioxidant and Platelet-Repellent Functionalities for Vascular. **2019**, 7314–7325.

(155) Ko, M. P.; Huang, C. J. A Versatile Approach to Antimicrobial Coatings via Metal-Phenolic Networks. *Colloids Surfaces B Biointerfaces* **2020**, *187* (November 2019), 110771.

(156) Antifouling, P.; Properties, A.; Xu, K.; Xie, H.; Sun, C.; Lin, W.; You, Z.; Zheng, G.; Zheng, X.; Xu, Y.; Chen, J.; Lin, F. Sustainable Coating Based on Zwitterionic Functionalized. **2023**.

(157) Yeh, S.; Wang, T.; Yusa, S.; Thissen, H.; Tsai, W. Conjugation of Polysulfobetaine via Poly (Pyrogallol) Coatings for Improving the Antifouling E Ffi Cacy of Biomaterials. **2021**, 6–13.

(158) Schleno, J. B. Zwitteration: Coating Surfaces with Zwitterionic Functionality to Reduce Nonspeci Fi c Adsorption. **2014**.

(159) Xu, G.; Pranantyo, D.; Zhang, B.; Xu, L.; Neoh, K.; Kang, E. RSC Advances Deposition of Parasin I Peptide for Antifouling and Antimicrobial Coatings †. **2016**, 14809–14818.

(160) Qiu, W.; Zhao, Z.; Du, Y.; Hu, M.; Xu, Z. Applied Surface Science Antimicrobial Membrane Surfaces via Efficient Polyethyleneimine Immobilization and Cationization. *Appl. Surf. Sci.* **2017**, *426*, 972–979.

(161) Ding, X.; Yang, C.; Lim, T. P.; Hsu, L. Y.; Engler, A. C.; Hedrick, J. L.; Yang, Y. Y. Antibacterial and Antifouling Catheter Coatings Using Surface Grafted PEG-b-Cationic Polycarbonate Diblock Copolymers. *Biomaterials* **2012**, *33* (28), 6593–6603.

(162) Cheng, Y. F.; Pranantyo, D.; Kasi, G.; Lu, Z. S.; Li, C. M.; Xu, L. Q. Amino-Containing Tannic Acid Derivative-Mediated Universal Coatings for Multifunctional Surface Modification. *Biomater. Sci.* **2020**, *8* (8), 2120–2128.

(163) Bu, Y.; Zhang, S.; Cai, Y.; Yang, Y.; Ma, S.; Huang, J.; Yang, H.; Ye, D.; Zhou, Y.; Xu, W.; Gu, S. Fabrication of Durable Antibacterial and Superhydrophobic Textiles via in Situ Synthesis of Silver Nanoparticle on Tannic Acid-Coated Viscose Textiles. *Cellulose* **2019**, *26* (3), 2109–2122.

(164) Zhan, F.; Yan, X.; Sheng, F.; Li, B. Facile in Situ Synthesis of Silver Nanoparticles on Tannic Acid/Zein Electrospun Membranes and Their Antibacterial, Catalytic and Antioxidant Activities. *Food Chem.* **2020**, *330* (June), 127172.

(165) Chen, S.; Yu, F.; Yu, Q.; He, Y.; Jiang, S. Strong Resistance of a Thin Crystalline Layer of Balanced Charged Groups to Protein Adsorption. **2006**, No. 18, 8186–8191.

(166) Jyske, T.; Liimatainen, J.; Tienaho, J.; Brännström, H.; Aoki, D.; Kuroda, K.; Reshamwala, D.; Kunnas, S.; Halmemies, E.; Nakayama, E.; Kilpeläinen, P.; Ora, A.; Kaseva, J.; Hellström, J.; Marjomäki, V. S.; Karonen, M.; Fukushima, K. Inspired by Nature: Fiber Networks Functionalized with Tannic Acid and Condensed Tannin-Rich Extracts of Norway Spruce Bark Show Antimicrobial Efficacy. *Front. Bioeng. Biotechnol.* **2023**, *11* (April), 1–20.

(167) Guo, J.; Sun, W.; Kim, J. P.; Lu, X.; Li, Q.; Lin, M.; Mrowczynski, O.; Rizk, E. B.; Cheng, J.; Qian, G.; Yang, J. Development of Tannin-Inspired Antimicrobial Bioadhesives. *Acta Biomater.* **2018**, *72*, 35–44.

(168) Huang, W.; Wang, J. Q.; Song, H. Y.; Zhang, Q.; Liu, G. F. Chemical Analysis and in Vitro Antimicrobial Effects and Mechanism of Action of Trachyspermum Copticum Essential Oil against Escherichia Coli. *Asian Pac. J. Trop. Med.* **2017**, *10* (7), 663–669.

(169) Asha, A. B.; Ounkaew, A.; Peng, Y. Y.; Gholipour, M. R.; Ishihara, K.; Liu, Y.; Narain, R. Bioinspired Antifouling and Antibacterial Polymer Coating with Intrinsic Self-Healing

Property. *Biomater. Sci.* **2022**, *11* (1), 128–139.

(170) Cumberland, S. L.; Strouse, G. F. Analysis of the Nature of Oxyanion Adsorption on Gold Nanomaterial Surfaces. *Langmuir* **2002**, *18* (1), 269–276.

(171) Oulad, F.; Zinadini, S.; Zinatizadeh, A. A.; Derakhshan, A. A. Fabrication and Characterization of a Novel Tannic Acid Coated Boehmite/PES High Performance Antifouling NF Membrane and Application for Licorice Dye Removal. *Chem. Eng. J.* **2020**, *397* (April), 125105.

(172) Costa, G. G.; Brito, C. C. S. M.; Terezo, A. J.; Cardoso, A. P.; Ionashiro, E. Y.; B. de Siqueira, A. Preparation, Characterization and Antioxidant Evaluation of Cu(II) and Zn(II) Tannates. *Open Chem. J.* **2018**, *5* (1), 158–171.

(173) Liu, C.; Wu, L.; Zhang, C.; Chen, W.; Luo, S. Surface Hydrophilic Modification of PVDF Membranes by Trace Amounts of Tannin and Polyethyleneimine. *Appl. Surf. Sci.* **2018**, *457* (June), 695–704.

(174) Hu, Z.; Berry, R. M.; Pelton, R.; Cranston, E. D. One-Pot Water-Based Hydrophobic Surface Modification of Cellulose Nanocrystals Using Plant Polyphenols. *ACS Sustain. Chem. Eng.* **2017**, *5* (6), 5018–5026.

(175) Hanif, Z.; Khan, Z. A.; Siddiqui, M. F.; Tariq, M. Z.; Park, S.; Park, S. J. Tannic Acid-Mediated Rapid Layer-by-Layer Deposited Non-Leaching Silver Nanoparticles Hybridized Cellulose Membranes for Point-of-Use Water Disinfection. *Carbohydr. Polym.* **2020**, *231* (December 2019), 115746.

(176) Zhao, A.; Zhang, N.; Li, Q.; Zhou, L.; Deng, H.; Li, Z.; Wang, Y.; Lv, E.; Li, Z.; Qiao, M.; Wang, J. Incorporation of Silver-Embedded Carbon Nanotubes Coated with Tannic Acid into Polyamide Reverse Osmosis Membranes toward High Permeability,

Antifouling, and Antibacterial Properties. *ACS Sustain. Chem. Eng.* **2021**, *9* (34), 11388–11402.

(177) Zhao, J.; Shi, Q.; Luan, S.; Song, L.; Yang, H.; Shi, H.; Jin, J.; Li, X.; Yin, J.; Stagnaro, P. Improved Biocompatibility and Antifouling Property of Polypropylene Non-Woven Fabric Membrane by Surface Grafting Zwitterionic Polymer. *J. Memb. Sci.* **2011**, *369* (1–2), 5–12.

(178) Choi, W.; Jin, J.; Park, S.; Kim, J. Y.; Lee, M. J.; Sun, H.; Kwon, J. S.; Lee, H.; Choi, S. H.; Hong, J. Quantitative Interpretation of Hydration Dynamics Enabled the Fabrication of a Zwitterionic Antifouling Surface. *ACS Appl. Mater. Interfaces* **2020**, *12* (7), 7951–7965.

(179) Sabaté del Río, J.; Henry, O. Y. F.; Jolly, P.; Ingber, D. E. An Antifouling Coating That Enables Affinity-Based Electrochemical Biosensing in Complex Biological Fluids. *Nat. Nanotechnol.* **2019**, *14* (12), 1143–1149.

(180) Phan, H. T. M.; Bartelt-Hunt, S.; Rodenhausen, K. B.; Schubert, M.; Bartz, J. C. Investigation of Bovine Serum Albumin (BSA) Attachment onto Self-Assembled Monolayers (SAMs) Using Combinatorial Quartz Crystal Microbalance with Dissipation (QCM-D) and Spectroscopic Ellipsometry (SE). *PLoS One* **2015**, *10* (10).

(181) Chang, C. C.; Kolewe, K. W.; Li, Y.; Kosif, I.; Freeman, B. D.; Carter, K. R.; Schiffman, J. D.; Emrick, T. Underwater Superoleophobic Surfaces Prepared from Polymer Zwitterion/Dopamine Composite Coatings. *Adv. Mater. Interfaces* **2016**, *3* (6), 1–9.

(182) Yeh, S. L.; Wang, T. C.; Yusa, S. I.; Thissen, H.; Tsai, W. B. Conjugation of Polysulfobetaine via Poly(Pyrogallol) Coatings for Improving the Antifouling Efficacy of Biomaterials. *ACS Omega* **2021**, *6* (5), 3517–3524.

(183) Lu, M. M.; Wang, Q. J.; Chang, Z. M.; Wang, Z.; Zheng, X.; Shao, D.; Dong, W. F.;

Zhou, Y. M. Synergistic Bactericidal Activity of Chlorhexidineloaded, Silver-Decorated Mesoporous Silica Nanoparticles. *Int. J. Nanomedicine* **2017**, *12*, 3577–3589.

(184) López-García, J.; Lehocký, M.; Humpolíček, P.; Sáha, P. HaCaT Keratinocytes Response on Antimicrobial Atelocollagen Substrates: Extent of Cytotoxicity, Cell Viability and Proliferation. *J. Funct. Biomater.* **2014**, *5* (2), 43–57.

(185) Wu, D.; Wang, W.; Diaz-Dussan, D.; Peng, Y. Y.; Chen, Y.; Narain, R.; Hall, D. G. In Situ Forming, Dual-Crosslink Network, Self-Healing Hydrogel Enabled by a Bioorthogonal Nopoldiol-Benzoxaborolate Click Reaction with a Wide PH Range. *Chem. Mater.* **2019**.

(186) Neoh, K. G.; Hu, X.; Zheng, D.; Kang, E. T. Balancing Osteoblast Functions and Bacterial Adhesion on Functionalized Titanium Surfaces. *Biomaterials* **2012**, *33* (10), 2813–2822.

(187) Dai, G.; Ai, X.; Mei, L.; Ma, C.; Zhang, G. Kill-Resist-Renew Trinity: Hyperbranched Polymer with Self-Regenerating Attack and Defense for Antifouling Coatings. *ACS Appl. Mater. Interfaces* **2021**, *13* (11), 13735–13743.

(188) Chen, M.; Qiu, B.; Zhang, Z.; Xie, S.; Liu, Y.; Xia, T.; Li, X. Light-Triggerable and PH/Lipase-Responsive Release of Antibiotics and β-Lactamase Inhibitors from Host-Guest Self-Assembled Micelles to Combat Biofilms and Resistant Bacteria. *Chem. Eng. J.* **2021**, *424* (May), 130330.

(189) Nadell, C. D.; Drescher, K.; Wingreen, N. S.; Bassler, B. L. Extracellular Matrix Structure Governs Invasion Resistance in Bacterial Biofilms. *ISME J.* **2015**, *9* (8), 1700–1709.

(190) Chiang, Y. C.; Chang, Y.; Higuchi, A.; Chen, W. Y.; Ruaan, R. C. Sulfobetaine-Grafted Poly(Vinylidene Fluoride) Ultrafiltration Membranes Exhibit Excellent Antifouling Property. *J. Memb. Sci.* **2009**, *339* (1–2), 151–159.

(191) Fleitas-Salazar, N.; Silva-Campa, E.; Pedroso-Santana, S.; Tanori, J.; Pedroza-Montero, M. R.; Riera, R. Effect of Temperature on the Synthesis of Silver Nanoparticles with Polyethylene Glycol: New Insights into the Reduction Mechanism. *J. Nanoparticle Res.* **2017**, *19* (3).

(192) Arima, Y.; Toda, M.; Iwata, H. Complement Activation on Surfaces Modified with Ethylene Glycol Units. *Biomaterials* **2008**, *29* (5), 551–560.

(193) Zhang, S.; Yang, X.; Tang, B.; Yuan, L.; Wang, K.; Liu, X.; Zhu, X.; Li, J.; Ge, Z.; Chen, S. New Insights into Synergistic Antimicrobial and Antifouling Cotton Fabrics via Dually Finished with Quaternary Ammonium Salt and Zwitterionic Sulfobetaine. *Chem. Eng. J.* **2018**, *336* (August 2017), 123–132.

(194) Wu, C.; Zhou, Y.; Wang, H.; Hu, J. P4VP Modified Zwitterionic Polymer for the Preparation of Antifouling Functionalized Surfaces. *Nanomaterials* **2019**, *9* (5).

(195) Niu, J.; Wang, H.; Chen, J.; Chen, X.; Han, X.; Liu, H. Bio-Inspired Zwitterionic Copolymers for Antifouling Surface and Oil-Water Separation. *Colloids Surfaces A Physicochem. Eng. Asp.* **2021**, *626* (May), 127016.

(196) Zhou, L.; Li, Q. L.; Wong, H. M. A Novel Strategy for Caries Management: Constructing an Antibiofouling and Mineralizing Dual-Bioactive Tooth Surface. *ACS Appl. Mater. Interfaces* **2021**, *13* (26), 31140–31152.

(197) Yang, X.; Ding, C.; Wu, M.; Xu, X.; Ke, X.; Xu, H.; Li, J.; Lou, F.; Zhou, K.; Jiang, H.; Peng, X.; Wang, X.; Si, L.; Li, J. Biomineral Interface with Superior Cell Adhesive and Antibacterial Properties Based on Enzyme-Triggered Digestion of Saliva Acquired Pellicle-Inspired Polypeptide Coatings. *Chem. Eng. J.* **2021**, *415* (October 2020), 128955.

(198) Cao, J.; Sun, Q.; Shen, A. G.; Fan, B.; Hu, J. M. Nano Au@Cu2-XS with near-Infrared

Photothermal and Peroxidase Catalytic Activities Redefines Efficient Antibiofilm-Oriented Root Canal Therapy. *Chem. Eng. J.* **2021**, *422* (December 2020), 130090.

(199) Kang, S.; Herzberg, M.; Rodrigues, D. F.; Elimelech, M. Antibacterial Effects of Carbon Nanotubes: Size Does Matter! *Langmuir* **2008**, *24* (13), 6409–6413.

(200) Ye, M.; Zhao, Y.; Wang, Y.; Zhao, M.; Yodsanit, N.; Xie, R.; Andes, D.; Gong, S. A Dual-Responsive Antibiotic-Loaded Nanoparticle Specifically Binds Pathogens and Overcomes Antimicrobial-Resistant Infections. *Adv. Mater.* **2021**, *33* (9), 1–12.

(201) Lv, C.; Chen, S.; Xie, Y.; Wei, Z.; Chen, L.; Bao, J.; He, C.; Zhao, W.; Sun, S.; Zhao, C. Positively-Charged Polyethersulfone Nanofibrous Membranes for Bacteria and Anionic Dyes Removal. *J. Colloid Interface Sci.* **2019**, *556*, 492–502.

(202) Gottenbos, B.; Van Der Mei, H. C.; Klatter, F.; Nieuwenhuis, P.; Busscher, H. J. In Vitro and in Vivo Antimicrobial Activity of Covalently Coupled Quaternary Ammonium Silane Coatings on Silicone Rubber. *Biomaterials* **2002**, *23* (6), 1417–1423.

(203) Ye, S.; Majumdar, P.; Chisholm, B.; Stafslien, S.; Chen, Z. Antifouling and Antimicrobial Mechanism of Tethered Quaternary Ammonium Salts in a Cross-Linked Poly(Dimethylsiloxane) Matrix Studied Using Sum Frequency Generation Vibrational Spectroscopy. *Langmuir* **2010**, *26* (21), 16455–16462.

(204) Farah, S.; Aviv, O.; Laout, N.; Ratner, S.; Beyth, N.; Domb, A. J. Quaternary Ammonium Poly(Diethylaminoethyl Methacrylate) Possessing Antimicrobial Activity. *Colloids Surfaces B Biointerfaces* **2015**, *128*, 608–613.

(205) Hong, S.; Na, Y. S.; Choi, S.; Song, I. T.; Kim, W. Y.; Lee, H. Non-Covalent Self-Assembly and Covalent Polymerization Co-Contribute to Polydopamine Formation. *Adv. Funct. Mater.* **2012**, *22* (22), 4711–4717.

(206) Qiu, W. Z.; Zhao, Z. S.; Du, Y.; Hu, M. X.; Xu, Z. K. Antimicrobial Membrane Surfaces via Efficient Polyethyleneimine Immobilization and Cationization. *Appl. Surf. Sci.* **2017**, *426*, 972–979.

(207) Zhang, H.; Luo, J.; Li, S.; Wei, Y.; Wan, Y. Biocatalytic Membrane Based on Polydopamine Coating: A Platform for Studying Immobilization Mechanisms. *Langmuir* **2018**, *34* (8), 2585–2594.

(208) Lai, J. T.; Filla, D.; Shea, R. Functional Polymers from Novel Carboxyl-Terminated Trithiocarbonates as Highly Efficient RAFT Agents. *Am. Chem. Soc. Polym. Prepr. Div. Polym. Chem.* **2002**, *43* (2), 122–123.

(209) Ovdenko, V.; Kolendo, A. New Bent-Shaped Azomethine Monomers for Optical Applications. *Mol. Cryst. Liq. Cryst.* **2016**, *640* (1), 113–121.

(210) Asha, A. B.; Chen, Y.; Zhang, H.; Ghaemi, S.; Ishihara, K.; Liu, Y.; Narain, R. Rapid Mussel-Inspired Surface Zwitteration for Enhanced Antifouling and Antibacterial Properties. *Langmuir* **2019**, *35* (5), 1621–1630.

(211) Cheng, Q.; Guo, X.; Hao, X.; Shi, Z.; Zhu, S.; Cui, Z. Fabrication of Robust Antibacterial Coatings Based on an Organic-Inorganic Hybrid System. *ACS Appl. Mater. Interfaces* **2019**, *11* (45), 42607–42615.

(212) Wang, G.; Weng, D.; Chen, C.; Chen, L.; Wang, J. Influence of TiO2 Nanostructure Size and Surface Modification on Surface Wettability and Bacterial Adhesion. *Colloids Interface Sci. Commun.* **2020**, *34* (November 2019), 100220.

(213) Ma, J.; Zhang, H. Kinetic Investigations of RAFT Polymerization: Difunctional RAFT Agent Mediated Polymerization of Methyl Methacrylate and Styrene. *Macromol. Res.* **2015**, *23* (1), 67–73.

(214) Krylova, V.; Dukštiene, N. Synthesis and Characterization of Ag Layers Formed on Polypropylene. *J. Chem.* **2013**, *2013*.

(215) Pate, S. G.; Xu, H.; O'Brien, C. P. Operando Observation of CO2transport Intermediates in Polyvinylamine Facilitated Transport Membranes, and the Role of Water in the Formation of Intermediates, Using Transmission FTIR Spectroscopy. *J. Mater. Chem. A* **2022**, *10* (8), 4418–4427.

(216) Kord Forooshani, P.; Polega, E.; Thomson, K.; Bhuiyan, M. S. A.; Pinnaratip, R.; Trought, M.; Kendrick, C.; Gao, Y.; Perrine, K. A.; Pan, L.; Lee, B. P. Antibacterial Properties of Mussel-Inspired Polydopamine Coatings Prepared by a Simple Two-Step Shaking-Assisted Method. *Front. Chem.* **2019**, *7* (September).

(217) Wardani, A. K.; Ariono, D.; Subagjo; Wenten, I. G. Hydrophilic Modification of Polypropylene Ultrafiltration Membrane by Air-Assisted Polydopamine Coating. *Polym. Adv. Technol.* **2019**, *30* (4), 1148–1155.

(218) Hou, C.; Qi, Z.; Zhu, H. Preparation of Core-Shell Magnetic Polydopamine/Alginate Biocomposite for Candida Rugosa Lipase Immobilization. *Colloids Surfaces B Biointerfaces* **2015**, *128*, 544–551.

(219) Morales, D. V.; Rivas, B. L.; Escalona, N. Poly([(2-Methacryloyloxy)Ethyl]Trimethylammonium Chloride): Synthesis, Characterization, and Removal Properties of As(V). *Polym. Bull.* **2016**, *73* (3), 875–890.

(220) Zangmeister, R. A.; Morris, T. A.; Tarlov, M. J. Characterization of Polydopamine Thin Films Deposited at Short Times by Autoxidation of Dopamine. *Langmuir* **2013**, *29* (27), 8619–8628.

(221) Ma, W.; Rajabzadeh, S.; Matsuyama, H. Preparation of Antifouling Poly(Vinylidene

Fluoride) Membranes via Different Coating Methods Using a Zwitterionic Copolymer. *Appl. Surf. Sci.* **2015**, *357*, 1388–1395.

(222) Dang, Y.; Xing, C. M.; Quan, M.; Wang, Y. B.; Zhang, S. P.; Shi, S. Q.; Gong, Y. K. Substrate Independent Coating Formation and Anti-Biofouling Performance Improvement of Mussel Inspired Polydopamine. *J. Mater. Chem. B* **2015**, *3* (20), 4181–4190.

(223) Wang, B. L.; Jin, T. W.; Han, Y. M.; Shen, C. H.; Li, Q.; Lin, Q. K.; Chen, H. Bio-Inspired Terpolymers Containing Dopamine, Cations and MPC: A Versatile Platform to Construct a Recycle Antibacterial and Antifouling Surface. *J. Mater. Chem. B* **2015**, *3* (27), 5501–5510.

(224) Ishihara, K. Bioinspired Phospholipid Polymer Biomaterials for Making High Performance Artificial Organs. *Sci. Technol. Adv. Mater.* **2000**, *1* (3), 131–138.

(225) Zhang, Y.; Zhang, X.; Zhao, Y. Q.; Zhang, X. Y.; Ding, X.; Ding, X.; Yu, B.; Duan, S.; Xu, F. J. Self-Adaptive Antibacterial Surfaces with Bacterium-Triggered Antifouling-Bactericidal Switching Properties. *Biomater. Sci.* **2020**, *8* (3), 997–1006.

(226) Druvari, D.; Koromilas, N. D.; Bekiari, V.; Bokias, G.; Kallitsis, J. K. Polymeric Antimicrobial Coatings Based on Quaternary Ammonium Compounds. *Coatings* **2018**, *8* (1).

(227) Wang, H.; Chen, M.; Jin, C.; Niu, B.; Jiang, S.; Li, X.; Jiang, S. Antibacterial [2-(Methacryloyloxy) Ethyl] Trimethylammonium Chloride Functionalized Reduced Graphene Oxide/Poly(Ethylene-Co-Vinyl Alcohol) Multilayer Barrier Film for Food Packaging. *J. Agric. Food Chem.* **2018**, *66* (3), 732–739.

(228) Asha, A. B.; Peng, Y. Y.; Cheng, Q.; Ishihara, K.; Liu, Y.; Narain, R. Dopamine Assisted Self-Cleaning, Antifouling, and Antibacterial Coating via Dynamic Covalent Interactions.

ACS Appl. Mater. Interfaces **2022**, *14* (7), 9557–9569.

(229) Mu, M.; Liu, S.; Deflorio, W.; Hao, L.; Wang, X.; Salazar, K. S.; Taylor, M.; Castillo, A.; Cisneros-zevallos, L.; Oh, J. K.; Min, Y. Influence of Surface Roughness, Nanostructure, and Wetting on Bacterial Adhesion. **2023**.

(230) Yao, L.; He, C.; Chen, S.; Zhao, W.; Xie, Y.; Sun, S.; Nie, S.; Zhao, C. Codeposition of Polydopamine and Zwitterionic Polymer on Membrane Surface with Enhanced Stability and Antibiofouling Property. *Langmuir* **2019**, *35* (5), 1430–1439.

(231) Burmeister, N.; Zorn, E.; Preuss, L.; Timm, D.; Scharnagl, N.; Rohnke, M.; Wicha, S. G.; Streit, W. R.; Maison, W. Low-Fouling and Antibacterial Polymer Brushes via Surface-Initiated Polymerization of a Mixed Zwitterionic and Cationic Monomer. *Langmuir* **2023**, *39* (49), 17959–17971.

(232) Berrocal, M. J.; Daniel Johnson, R.; Badr, I. H. A.; Liu, M.; Gao, D.; Bachas, L. G. Improving the Blood Compatibility of Ion-Selective Electrodes by Employing Poly(MPC-Co-BMA), a Copolymer Containing Phosphorylcholine, as a Membrane Coating. *Anal. Chem.* **2002**, *74* (15), 3644–3648.

(233) Umscheid, C. A.; Mitchell, M. D.; Doshi, J. A.; Agarwal, R.; Williams, K.; Brennan, P. J. Estimating the Proportion of Healthcare-Associated Infections That Are Reasonably Preventable and the Related Mortality and Costs. *Infect. Control Hosp. Epidemiol.* **2011**, *32* (2), 101–114.

(234) Costerton, J. W.; Stewart, P. S.; Greenberg, E. P. Bacterial Biofilms: A Common Cause of Persistent Infections. *Science (80-.).* **1999**, *284* (5418), 1318–1322.

(235) Zander, Z. K.; Becker, M. L. Antimicrobial and Antifouling Strategies for Polymeric Medical Devices. *ACS Macro Lett.* **2018**, *7* (1), 16–25.

(236) Singh, B.; Singh, J.; Dhiman, A.; Mohan, M. Synthesis and Characterization of Arabinoxylan-Bis[2-(Methacryloyloxy)Ethyl] Phosphate Crosslinked Copolymer Network by High Energy Gamma Radiation for Use in Controlled Drug Delivery Applications. *Int. J. Biol. Macromol.* **2022**, *200* (December 2021), 206–217.

(237) Jiang, T.; Nukavarapu, S. P.; Deng, M.; Jabbarzadeh, E.; Kofron, M. D.; Doty, S. B.; Abdel-Fattah, W. I.; Laurencin, C. T. Chitosan-Poly(Lactide-Co-Glycolide) Microsphere-Based Scaffolds for Bone Tissue Engineering: In Vitro Degradation and in Vivo Bone Regeneration Studies. *Acta Biomater.* **2010**, *6* (9), 3457–3470.

(238) Yang, W.; Kang, X.; Gao, X.; Zhuang, Y.; Fan, C.; Shen, H.; Chen, Y.; Dai, J. Biomimetic Natural Biopolymer-Based Wet-Tissue Adhesive for Tough Adhesion, Seamless Sealed, Emergency/Nonpressing Hemostasis, and Promoted Wound Healing. *Adv. Funct. Mater.* **2023**, *33* (6), 1–16.

(239) Barrantes, A.; Wengenroth, J.; Arnebrant, T.; Haugen, H. J. Poly-L-Lysine/Heparin Multilayer Coatings Prevent Blood Protein Adsorption. *J. Colloid Interface Sci.* **2017**, *485*, 288–295.

(240) Zhou, J.; Romero, G.; Rojas, E.; Ma, L.; Moya, S.; Gao, C. Layer by Layer Chitosan/Alginate Coatings on Poly(Lactide-Co-Glycolide) Nanoparticles for Antifouling Protection and Folic Acid Binding to Achieve Selective Cell Targeting. *J. Colloid Interface Sci.* **2010**, *345* (2), 241–247.

(241) Parfenova, L. V.; Galimshina, Z. R.; Gil'fanova, G. U.; Alibaeva, E. I.; Danilko, K. V.; Pashkova, T. M.; Kartashova, O. L.; Farrakhov, R. G.; Mukaeva, V. R.; Parfenov, E. V.; Nagumothu, R.; Valiev, R. Z. Hyaluronic Acid Bisphosphonates as Antifouling Antimicrobial Coatings for PEO-Modified Titanium Implants. *Surfaces and Interfaces*

2022, *28* (August 2021), 101678.

(242) Yuan, J.; Meng, J. Q.; Kang, Y. L.; Du, Q. Y.; Zhang, Y. F. Facile Surface Glycosylation of PVDF Microporous Membrane via Direct Surface-Initiated AGET ATRP and Improvement of Antifouling Property and Biocompatibility. *Appl. Surf. Sci.* **2012**, *258* (7), 2856–2863.

(243) Tu, Q.; Shen, X.; Liu, Y.; Zhang, Q.; Zhao, X.; Maitz, M. F.; Liu, T.; Qiu, H.; Wang, J.; Huang, N.; Yang, Z. A Facile Metal-Phenolic-Amine Strategy for Dual-Functionalization of Blood-Contacting Devices with Antibacterial and Anticoagulant Properties. *Mater. Chem. Front.* **2019**, *3* (2), 265–275.

(244) Yang, Z.; Yang, Y.; Xiong, K.; Wang, J.; Lee, H.; Huang, N. Metal-Phenolic Surfaces for Generating Therapeutic Nitric Oxide Gas. *Chem. Mater.* **2018**, *30* (15), 5220–5226.

(245) Zheng, H. T.; Bui, H. L.; Chakroborty, S.; Wang, Y.; Huang, C. J. Pegylated Metal-Phenolic Networks for Antimicrobial and Antifouling Properties. *Langmuir* **2019**, *35* (26), 8829–8839.

(246) Li, X.; Gao, P.; Tan, J.; Xiong, K.; Maitz, M. F.; Pan, C.; Wu, H.; Chen, Y.; Yang, Z.; Huang, N. Assembly of Metal-Phenolic/Catecholamine Networks for Synergistically Anti-Inflammatory, Antimicrobial, and Anticoagulant Coatings. *ACS Appl. Mater. Interfaces* **2018**, *10* (47), 40844–40853.

(247) Meng, L.; Huang, C.; Liu, X.; Qu, H.; Wang, Q. Zwitterionic Coating Assisted by Dopamine with Metal-Phenolic Networks Loaded on Titanium with Improved Biocompatibility and Antibacterial Property for Artificial Heart. *Front. Bioeng. Biotechnol.* **2023**, *11* (April), 1–12.

(248) Huang, Z.; Zhang, D.; Gu, Q.; Miao, J.; Cen, X.; Golodok, R. P.; Savich, V. V.;

Ilyushchenko, A. P.; Zhou, Z.; Wang, R. One-Step Coordination of Metal-Phenolic Networks as Antibacterial Coatings with Sustainable and Controllable Copper Release for Urinary Catheter Applications. *RSC Adv.* **2022**, *12* (25), 15685–15693.

(249) Yang, H.; Li, G.; Stansbury, J. W.; Zhu, X.; Wang, X.; Nie, J. Smart Antibacterial Surface Made by Photopolymerization. *ACS Appl. Mater. Interfaces* **2016**, *8* (41), 28047–28054.

(250) Mitra, D.; Kang, E. T.; Neoh, K. G. Antimicrobial Copper-Based Materials and Coatings: Potential Multifaceted Biomedical Applications. *ACS Appl. Mater. Interfaces* **2020**, *12* (19), 21159–21182.

(251) Chen, Y.; Tan, Z.; Wang, W.; Peng, Y. Y.; Narain, R. Injectable, Self-Healing, and Multi-Responsive Hydrogels via Dynamic Covalent Bond Formation between Benzoxaborole and Hydroxyl Groups. *Biomacromolecules* **2019**, *20* (2), 1028–1035.

(252) Chen, Y.; Diaz-Dussan, D.; Wu, D.; Wang, W.; Peng, Y. Y.; Asha, A. B.; Hall, D. G.; Ishihara, K.; Narain, R. Bioinspired Self-Healing Hydrogel Based on Benzoxaborole-Catechol Dynamic Covalent Chemistry for 3D Cell Encapsulation. *ACS Macro Lett.* **2018**, *7* (8), 904–908.

(253) Anh, H. T. P.; Huang, C. M.; Huang, C. J. Intelligent Metal-Phenolic Metallogels as Dressings for Infected Wounds. *Sci. Rep.* **2019**, *9* (1), 1–10.

(254) V, A. K.; Veeraiah, M. K.; Hemalatha P. Synthesis and Characterisation of Poly (Vinylpyrrolidone)–Copper (II) Complexes. *Res. J. Chem. Sci.* **2015**, *5* (2), 64–69.

(255) Zhang, Y.; Jiang, W.; Lei, L.; Wang, Y.; Xu, R.; Qin, L.; Wei, Q. Mussel-Inspired Multicomponent Codeposition Strategy toward Antibacterial and Lubricating Multifunctional Coatings on Bioimplants. *Langmuir* **2022**, *38* (23), 7157–7167.

(256) Xi, Z. Y.; Xu, Y. Y.; Zhu, L. P.; Wang, Y.; Zhu, B. K. A Facile Method of Surface

Modification for Hydrophobic Polymer Membranes Based on the Adhesive Behavior of Poly(DOPA) and Poly(Dopamine). *J. Memb. Sci.* **2009**, *327* (1–2), 244–253.

(257) Nuraje, N.; Asmatulu, R.; Cohen, R. E.; Rubner, M. F. Durable Antifog Films from Layer-by-Layer Molecularly Blended Hydrophilic Polysaccharides. *Langmuir* **2011**, *27* (2), 782–791.

(258) Liu, G.; Li, K.; Wang, H.; Ma, L.; Yu, L.; Nie, Y. Stable Fabrication of Zwitterionic Coating Based on Copper-Phenolic Networks on Contact Lens with Improved Surface Wettability and Broad-Spectrum Antimicrobial Activity. *ACS Appl. Mater. Interfaces* **2020**, *12* (14), 16125–16136.

(259) Wang, D.; Xing, J.; Zhang, Y.; Guo, Z.; Deng, S.; Guan, Z.; He, B.; Ma, R.; Leng, X.; Dong, K.; Dong, Y. Metal–Phenolic Networks for Chronic Wounds Therapy. *Int. J. Nanomedicine* **2023**, *18* (October), 6425–6448.

(260) Ejima, H.; Richardson, J. J.; Caruso, F. Metal-Phenolic Networks as a Versatile Platform to Engineer Nanomaterials and Biointerfaces. *Nano Today* **2017**, *12*, 136–148.

(261) Kim, S.; Gim, T.; Kang, S. M. Versatile, Tannic Acid-Mediated Surface PEGylation for Marine Antifouling Applications. *ACS Appl. Mater. Interfaces* **2015**, *7* (12), 6412–6416.

(262) Li, Y.; Milewska, M.; Khine, Y. Y.; Ariotti, N.; Stenzel, M. H. Trehalose Coated Nanocellulose to Inhibit the Infections by S. Aureus. *Polym. Chem.* **2022**, *13* (11), 1502–1509.

(263) Gosau, M.; Bürgers, R.; Vollkommer, T.; Holzmann, T.; Prantl, L. Effectiveness of Antibacterial Copper Additives in Silicone Implants. *J. Biomater. Appl.* **2013**, *28* (2), 187–198.

(264) Muñoz-Bonilla, A.; Fernández-García, M. Glycopolymeric Materials for Advanced

Applications. *Materials (Basel)*. **2015**, *8* (5), 2276–2296.

(265) Xie, W.; Guo, Z.; Zhao, L.; Wei, Y. Metal-Phenolic Networks: Facile Assembled Complexes for Cancer Theranostics. *Theranostics* **2021**, *11* (13), 6407–6426.